

**BIOCONTROL OF ROOT ROT COMPLEX IN FIELD PEA AND LENTIL AND COMPLETE
GENOME ANALYSIS OF BIOCONTROL BACTERIA**

A Thesis Submitted to the College of Graduate and Postdoctoral Studies
In Partial Fulfillment of the Requirements
For the Degree of Doctor of Philosophy
In the Department of Soil Science
University of Saskatchewan
Saskatoon, Saskatchewan, Canada

By

Ashebir Tsedeke Godebo

PERMISSION TO USE

In presenting this thesis in partial fulfillment of the requirements for a Postgraduate degree from the University of Saskatchewan, I agree that the Libraries of this University may make it freely available for inspection. I further agree that permission for copying of this dissertation in any manner, in whole or in part, for scholarly purposes may be granted by the professor or professors who supervised my thesis work or, in their absence, by the Head of the Department or the Dean of the College in which my thesis work was done. It is understood that any copying or publication or use of this thesis or parts thereof for financial gain shall not be allowed without my written permission. It is also understood that due recognition shall be given to me and to the University of Saskatchewan in any scholarly use which may be made of any material in my thesis. Requests for permission to copy or to make other uses of materials in this thesis in whole or part should be addressed to:

Head of the Department of Soil Science
51 Campus Drive, Room 5D34
University of Saskatchewan
Saskatoon, Saskatchewan, S7N 5A8
Canada

OR

Dean College of Graduate and Postdoctoral Studies
University of Saskatchewan
116 Thorvaldson Building, 110 Science Place
Saskatoon, Saskatchewan, S7N 5C9
Canada

DISCLAIMER

Reference in this dissertation to any specific commercial product, process, or service by trade name, trademark, manufacturer, or otherwise, does not constitute or imply its endorsement, recommendation, or favoring by the University of Saskatchewan. The views and opinions of the author expressed herein do not state or reflect those of the University of Saskatchewan and shall not be used for advertising or product endorsement purposes.

ABSTRACT

Aphanomyces root rot (ARR), caused by the soil-borne oomycete pathogen, *Aphanomyces euteiches*, is a destructive disease of legumes, most notably to field pea (*Pisum sativum* L.) and lentil (*Lens culinaris* L.). It commonly occurs as root rot complex (RRC) along with other soil-borne pathogens, including *Fusarium avenaceum* and *F. oxysporum*, which collectively result in significant crop damage leading to complete loss of productivity. Currently, in Canada, the available management strategies against RRC are inadequate. However, a recent study at the University of Saskatchewan identified soil bacteria, *Lysobacter capsici* K-Hf-H2, *Pseudomonas simiae* K-Hf-L9 and *Pantoea agglomerans* PSV1-7, as potential biocontrol agents against ARR in field pea under controlled growth chamber condition. Therefore, the purpose of this study was to i) investigate the potential for biological control of RRC caused by *A. euteiches*, *F. avenaceum* and *F. oxysporum* and ii) unravel the mechanisms by which biocontrol was achieved. To achieve these objectives, *L. capsici* K-Hf-H2, *P. simiae* K-Hf-L9 and *P. agglomerans* PSV1-7 were evaluated against RRC in field pea and lentil under controlled growth chamber conditions, and the strains' whole genomes were sequenced, annotated, and comparatively analyzed using bioinformatics tools. Also, laboratory-based general functional experiments, siderophores production, proteolytic and cellulolytic capacities, and desiccation tolerance were conducted. Additionally, the current state of the science "biological control of ARR" was determined via a quantitative meta-analysis review using data extracted from published articles investigating the biocontrol of ARR in pea. My meta-analysis findings suggest potential for biological control of ARR and the need for more field trials to demonstrate the higher efficacy level observed under growth chamber conditions. Compared to *P. simiae* K-Hf-L9 and *P. agglomerans* PSV1-7, *L. capsici* K-Hf-H2 demonstrated the highest significant biocontrol efficacy against RRC in field pea and lentil, with higher efficacy in field pea. Moreover, my genome analyses identified several genes and gene clusters encoding various traits potentially involved in the suppression of RRC. Such genetic determinants detected in *L. capsici* K-Hf-H2 genome include genes encoding for Heat Stable Antifungal Factor (HSAF), endoglucanase (cellulase), chitinase, extracellular zinc proteases (metalloendopeptidase), aminopeptidases and siderophores. In *P. simiae* K-Hf-L9 and *P. agglomerans* PSV1-7 genomes, gene and gene clusters encoding iron acquisition, chitin metabolism and protein degradation were detected. I also found evidence that *L. capsici* K-Hf-H2,

P. simiae K-Hf-L9 and *P. agglomerans* PSV1-7 chelate iron through siderophore production and hydrolyze protein via proteolytic activity. Furthermore, *L. capsici* K-Hf-H2 and *P. simiae* K-Hf-L9 were positive for cellulolytic activity. Therefore, my findings indicate the great potential of biological control of RRC in field pea and lentil. Also, the findings in this study represent a significant contribution to the effort of biological control of RRC in field pea and lentil in Canada.

ACKNOWLEDGMENTS

First and foremost, I would like to thank my wife, Mulu Hailu Ayele, for her love, sacrifice and inspiration at all times since high school, also our children, who unconditionally bring happiness and joy to my days. I am incredibly grateful to my supervisors Drs. Jim Germida, Fran Walley and Chris Yost for their mentorship, support, guidance and encouragement during my Ph.D. studies. I would not be here without your support and guidance. I thank you so much: **በጣም አላስግናለሁ!!!** I would like to acknowledge the valuable input from my advisory committee members, Drs. Bobbi Helgason, Sabine Banniza, and Vladimir Vujanovic.

I want to express my gratitude to many friends from the Soil Microbiology Lab 5E25 and University of Saskatchewan students who made this journey with me. Special thanks to Nikki Burnett, Drs. Keith MacKenzie and Kara Loos from the University of Regina, Department of Biology, for their valuable input towards my program. My special thanks also go to Marc St. Arnaud, who always helped me beyond my expectation, including going to the agricultural field and being a great help during soil collection. I would also like to thank Kim Heidinger, Erica Wilchuck, Drs. Ken Van Rees, Tom Yates and Laroque Colin from the Department of Soil Science for their help and support. Thank you, my friends, professors and personnel at the College of Agriculture and Bioresources, for contributing to my academic development.

I am very thankful to Dr. Jeff Schoenau for providing me with his valuable advice and the soil from his farm. I am also grateful for the financial support from the University of Saskatchewan and the University of Regina. This project was possible due to the support of the Agriculture Development Fund grant (Saskatchewan Ministry of Agriculture) and the Discovery Grant Program of the Natural Sciences and Engineering Research Council of Canada (NSERC).

TABLE OF CONTENTS

PERMISSION TO USE	I
DISCLAIMER	II
ABSTRACT.....	III
ACKNOWLEDGMENTS.....	V
TABLE OF CONTENTS	VI
LIST OF TABLES.....	IX
LIST OF FIGURES	XII
LIST OF EQUATIONS	XX
LIST OF ABBREVIATION	XXI
1. GENERAL INTRODUCTION.....	1
1.1 Project description and organization of the thesis	1
2. LITERATURE REVIEW	4
2.1 Root rot in field pea and lentil.....	4
2.2 Root rot symptoms	5
2.3 Microbial biocontrol agents.....	6
2.3.1 Challenges associated with microbial biocontrol agents.....	6
2.3.2 Opportunities to alleviate challenges linked to microbial biocontrol agents.....	9
2.4 The genus <i>Lysobacter</i>.....	10
2.4.1 <i>Lysobacter</i> species as biocontrol agents and mechanisms of action	11
2.5 The genus <i>Pseudomonas</i>.....	14
2.5.1 <i>Pseudomonas simiae</i> as biocontrol agents and mechanisms of action	15
2.6 The genus <i>Pantoea</i>	17
2.6.1 <i>Pantoea agglomerans</i> as biocontrol agents and mechanisms of action	18
2.7 Genome sequencing and assembly	19
2.8 Bacterial genome annotation	20
2.9 Comparative genome analysis.....	22
3. A META-ANALYSIS TO DETERMINE THE STATE OF BIOLOGICAL CONTROL OF APHANOMYCES ROOT ROT	24
3.1 Preface	24
3.2 Abstract	25
3.3 Introduction	25
3.4 Material and methods	27
3.4.1 Literature review and data collection.....	27
3.4.2 Moderator variable and categorical analysis.....	29
3.4.3 Effect size calculation and meta-analysis	30
3.4.4 Test of heterogeneity	30
3.4.5 Publication bias.....	31
3.5 Results.....	31

3.5.1	Measure of efficacy.....	31
3.5.2	Test of heterogeneity	36
3.5.3	Publication bias.....	37
3.6	Discussion.....	39
3.7	Conclusion.....	42
4.	BIOLOGICAL CONTROL OF ROOT ROT COMPLEX OF FIELD PEA AND LENTIL USING APHANOMYCES ROOT ROT BIOCONTROL BACTERIA.....	44
4.1	Preface	44
4.2	Abstract	45
4.3	Introduction	45
4.4	Materials and methods.....	47
4.4.1	<i>In vitro</i> inhibition of <i>Fusarium</i> pathogens.....	47
4.4.2	Evaluation of cell-free supernatant for antimicrobial activity.....	47
4.4.3	Agar-well diffusion assay	48
4.4.4	Biocontrol of root rot complex of field pea and lentil	49
4.4.5	Biocontrol of root rot complex in vermiculite.....	50
4.4.6	Biocontrol of root rot complex in non-sterile soil.....	52
4.4.7	Data collection and analysis for the experiment using both vermiculite and field soil.....	52
4.4.8	Biocontrol of aphanomyces root rot in lentil	53
4.5	Results.....	54
4.5.1	<i>In vitro</i> inhibition of <i>Fusarium</i> pathogens.....	54
4.5.2	Antagonistic activity of cell-free supernatant	56
4.5.3	Autoclave and storage stability of cell-free supernatant	57
4.5.4	Biocontrol of root rot complex in vermiculite.....	59
4.5.5	Biocontrol of root rot complex in non-sterile soil.....	62
4.5.6	Biocontrol of aphanomyces root rot in lentil	69
4.6	Discussion.....	71
4.7	Conclusions	75
5.	WHOLE-GENOME ANALYSIS OF BACTERIAL ISOLATES WITH BIOCONTROL POTENTIAL TOWARDS APHANOMYCES ROOT ROT IN FIELD PEA AND LENTIL CAUSED BY APHANOMYCES EUTEICHES.....	77
5.1	Preface	77
5.2	Abstract	78
5.3	Introduction	79
5.4	Materials and methods.....	80
5.4.1	Strain activation and DNA extraction.....	80
5.4.2	Whole-genome sequencing and assembly.....	81
5.4.3	Whole-genome annotation and comparative analysis.....	82
5.4.4	Detection of antibiotic resistance genes	83
5.4.5	Phylogenetic analysis.....	83
5.4.6	Identification of secondary metabolite regions.....	83
5.4.7	Laboratory investigation of functional activities.....	84
5.5	Results.....	86

5.5.1	Genomic features	86
5.5.2	Genome annotation	88
5.5.3	Genome comparison.....	94
5.5.4	Antibiotics resistance genes	105
5.5.5	Phylogenetic analysis.....	109
5.5.6	Identification of secondary metabolite regions.....	112
5.5.7	Laboratory investigation of functional activities.....	114
5.6	Discussion	121
5.7	Conclusions	130
6.	SYNTHESIS AND CONCLUSIONS	131
6.1	Summary of findings	132
7.	FUTURE RESEARCH.....	136
8.	REFERENCE	138
	APPENDIX A CHAPTER 3 SUPPLEMENTAL INFORMATION	169
	APPENDIX B CHAPTER 4 SUPPLEMENTAL INFORMATION	178
	APPENDIX C CHAPTER 5 SUPPLEMENTAL INFORMATION	185

LIST OF TABLES

Table 3.1. Measures used to quantify dispersion across effect sizes in each moderator variable	37
Table 3.2. Variables used in characterizing publication bias for each moderator effect size	38
Table 4.1. Root rot pathogens combination, pathogens inoculum concentration and application volume.....	49
Table 4.2. Description of visual rating scale used to assess root rot development and suppression (adapted from Chatterton et al., 2019).	53
Table 4.3. Storage and autoclave stability of <i>Lysobacter capsici</i> K-Hf-H2 cell-free supernatant	58
Table 4.4. Effect of biocontrol bacteria <i>L. capsici</i> K-Hf-H2, <i>P. simiae</i> K-Hf-L9 and <i>P. agglomerans</i> PSV1-7 on root rot severity in field pea grown in vermiculite in growth chamber conditions	60
Table 4.5. Effect of biocontrol bacteria <i>L. capsici</i> K-Hf-H2, <i>P. simiae</i> K-Hf-L9 and <i>P. agglomerans</i> PSV1-7 on root rot severity in lentil grown in vermiculite in growth chamber conditions.	61
Table 4.6. Effect of biocontrol bacteria <i>L. capsici</i> K-Hf-H2, <i>P. simiae</i> K-Hf-L9 and <i>P. agglomerans</i> PSV1-7 on root rot severity in field pea grown in non-sterile soil in growth chamber conditions.	64
Table 4.7. Effect of biocontrol bacterial strains on shoot dry weight of field pea grown in non-sterile soil in growth chamber pot trials.....	65
Table 4.8. Effect of biocontrol bacteria <i>L. capsici</i> K-Hf-H2, <i>P. simiae</i> K-Hf-L9 and <i>P. agglomerans</i> PSV1-7 on root rot severity in lentil grown in non-sterile soil in growth chamber conditions.	68
Table 4.9. Effect of biocontrol bacterial strains on shoot dry weight of lentil grown in non-sterile soil in growth chamber pot trials.....	69
Table 4.10. Effect of biocontrol bacteria against aphanomyces root rot severity in lentil grown in vermiculite in growth chamber conditions.....	70
Table 4.11. Effect of biocontrol bacteria against aphanomyces root rot severity in lentil grown in non-sterile soil in growth chamber conditions.	71
Table 5.1. Summary of the <i>Lysobacter capsici</i> K-Hf-H2, <i>Pseudomonas simiae</i> K-Hf-L9, <i>Pantoea agglomerans</i> PSV1-7 and <i>Lysobacter gummosus</i> K-Be-H3 genome characteristics	88

Table 5.2. Summary of genomic features of <i>Lysobacter capsici</i> K-Hf-H2, <i>Lysobacter capsici</i> AZ78, <i>Lysobacter capsici</i> 55, <i>Lysobacter capsici</i> KNU-14 and <i>Lysobacter capsici</i> NF87_2	94
Table 5.3. Summary of genomic features of <i>Pseudomonas simiae</i> K-Hf-L9, <i>Pseudomonas simiae</i> PCL1751 and <i>Pseudomonas simiae</i> WCS417	97
Table 5.4. Summary of genomic features of <i>Pantoea agglomerans</i> PSV1-7, <i>Pantoea agglomerans</i> UAEU18 and <i>Pantoea agglomerans</i> ZJU23.....	100
Table 5.5. Summary of genomic features of <i>Lysobacter. gummosus</i> K-Be-H3, <i>Lysobacter. gummosus</i> 10.1.1 and <i>Lysobacter. gummosus</i> 3.2.11	103
Table 5.6. Antibiotic resistance genes in <i>L. capsici</i> K-Hf-H2 and <i>L. gummosus</i> K-Be-H3 genome using CARD database	106
Table 5.7. Antibiotic resistance genes in <i>P. simiae</i> K-Kf-L9 genome using CARD database. .	107
Table 5.8. Antibiotic resistance genes in <i>P. agglomerans</i> PSV1-7 genome using CARD database.	108
Table 5.9. Secondary metabolites biosynthetic gene clusters in <i>L. capsici</i> K-Hf-H2.....	112
Table 5.10. Secondary metabolites biosynthetic gene clusters in <i>L. gummosus</i> K-Be-H3	112
Table 5.11. Secondary metabolites biosynthetic gene clusters in <i>P. agglomerans</i> PSV1-7	114
Table A. 1 Details on publications used in the meta-analysis (162 studies from 24 publication). Treatment means (Xt), Treatment sample size (nt), Control mean (Xc), Control sample size (nc), Treatment mean natural log (ln(Xt)), Control mean natural log (ln(Xc)), Response ratio natural log (lnR), natural log response ratio variance (Var(lnR)). Five moderator variables: Method of application: ((MoA): Suspension = Sus; Seadcoat = SC; Amendment = Ame; Plate assay = PA); Biocontrol agent richness: ((BAR): Single inoculation = SI; Mixed inoculation = MI), Biocontrol agent type: ((BAT): Bacteria = B; Fungus = F; Plant product = PP; Green Manure = GM; Compost = C; Earthworm = EW); Study scope: ((SS): Growth chamber = GC; Field = Field; Laboratory = Lab); and Reporting system: ((RS): Qualitative = Qual; Quantitative = Quan). Note: Sample size refers to the number of replicates used for the experimental analysis.....	172
Table B. 1 Disease score data for biocontrol assessment of root rot in field pea using vermiculite as a growing media in a growth chamber study	178
Table B. 2 Disease score data for biocontrol assessment of root rot in lentil using vermiculite as a growing media in a growth chamber study	179
Table B. 3 Disease score data for biocontrol assessment of root rot in field pea using non-sterile agricultural soil as a growing media in a growth chamber study.....	180

Table B. 4 Disease score data for biocontrol assessment of root rot in lentil using non-sterile agricultural soil as a growing media in a growth chamber study.....	181
Table B. 5 Disease score data for biocontrol assessment of aphanomyces root rot in lentil using vermiculite as a growing media in a growth chamber study.....	182
Table B. 6 Disease score data for biocontrol assessment of aphanomyces root rot in lentil using non-sterile agricultural soil as a growing media in a growth chamber study.....	183
Table C. 1 Protein encoding genes (pegs) of <i>Lysobacter capsici</i> K-Hf-H2 assigned to the subsystems category of Iron acquisition and metabolism (Siderophores), Carbohydrate metabolism (Chitin and Cellulose), Protein Degradation and according to the RAST version 2.0 server.....	185
Table C. 2 Protein encoding genes (pegs) of <i>Pseudomonas simiae</i> K-Hf-L9 assigned to the subsystems category of Iron acquisition and metabolism (Siderophores), Carbohydrate metabolism (Chitin) and Protein Degradation according to the RAST version 2.0 server.	187
Table C. 3 Protein encoding genes (pegs) of <i>Pantoea agglomerans</i> PSV1-7 assigned to the subsystems category of Iron acquisition and metabolism (Siderophores), Carbohydrate metabolism (Chitin) and Protein Degradation according to the RAST version 2.0 server.	188

LIST OF FIGURES

- Figure 2.1** Genome assembly with Velvet. Reads are assembled into contigs using Velvet and VelvetOptimiser in two steps, (1) velveth converts reads to k-mers using a hash table, and (2) velvetg assembles overlapping k-mers into contigs via a de Bruijn graph (Edwards and Holt, 2013). 20
- Figure 2.2.** Overview of bacterial genome annotation. Structural annotation identifies the location of genes on the contigs of an assembled bacterial genome. Protein-encoding locations are identified, followed by automated assignment of gene function by comparison to existing databases. Non-protein-encoding genes are annotated by identifying key signatures for each type of gene. The resulting annotations are combined with an optional manual curation that can be performed before the final annotated genome is produced (Lynch et al., 2016). 21
- Figure 2.3.** BRIG for multiple genome comparisons. It is easy to see that the Stx2 phage is present in the *E. coli* (EHEC) (purple) and the outbreak genome an *E. coli* (EAEC) (black), but not the EAEC or EPEC chromosomes (Edwards and Holt, 2013)..... 23
- Figure 3.1.** Diagrammatic representation of the steps involved in selecting articles..... 28
- Figure 3.2.** Cumulative analysis of effect size measuring efficacy on biological control of aphanomyces root rot. The analysis detected a significant ($p < .001$) negative summary effect size [-0.411 (CI -0.516 to -0.306)] suggesting suppression of *A. euteiches*. The center of the diamond depicts the overall mean effect size, and the width reflects its confidence interval. CI = confidence interval. 32
- Figure 3.3.** Effect of biocontrol agent application method on aphanomyces root rot suppression. The analysis detected a significant ($p < .05$) negative effect size for amendment, seed coating, and suspension. The center of the horizontal line depicts the effect size, and the width reflects its confidence interval. Number of studies: Amendment 35; Seed coating 79; Suspension 45. CI = confidence interval. 33
- Figure 3.4.** Effect of biocontrol agent richness on aphanomyces root rot suppression. The analysis detected a significant ($p < .001$) negative effect size for mixed and single organism inoculation favoring disease suppression. The center of the horizontal line depicts the effect size, and the width reflects its confidence interval. Number of studies: Mixed organism inoculation 11; Single organism inoculation 151. CI = confidence interval. 33
- Figure 3.5.** Effect of biocontrol agent type on aphanomyces root rot suppression. The analysis detected a significant ($p < .05$) negative effect size for bacterial, compost, fungal and plant product treatments. Number of studies: Bacteria 93; Compost 9; Fungus 26; Green manure 16; Plant product 12. The center of the horizontal line depicts the effect size, and the width reflects its confidence interval. CI = confidence interval. 34
- Figure 3.6.** A separate meta-analysis on the bacterial treatment category indicates bacterial biocontrol agents within the genus *Bacillus* and *Pseudomonas* have a greater efficacy

compared with others in the same category. The center of the diamond depicts the overall mean effect size, and the width reflects its confidence interval. CI = confidence interval. The *Pseudomonas cepacia* tested as a biocontrol agent in the Parke et al., 1991; and King and Parke, 1993 papers were included in the *Burkholderia* analysis, not in the *Pseudomonas* analysis..... 35

Figure 3.7. Study type impact on aphanomyces root rot suppression. The analysis detected a significant ($p < .05$) negative effect size for lab, growth chamber, and field studies. Number of studies: Lab 20; Growth chamber 101; Field 41. The center of the horizontal line depicts the effect size, and the width reflects its confidence interval. . 35

Figure 3.8. Effect of reporting system on aphanomyces root rot suppression. The analysis detected a significant ($p < .001$) negative effect size for the quantitative and qualitative reporting systems. Number of studies: Qualitative 111, and Quantitative 51. CI = confidence interval. 36

Figure 3.9. Trim and fill plot for log response ratio showing asymmetrical distribution of studies about the combined effect size or mean (i.e., the new adjusted effect size). This funnel plot is a measure of study size precision (standard error⁻¹) on the vertical axis as a function of effect size on the horizontal axis. ◦ Observed studies; • imputed studies; ◁ original effect size ▷ recomputed combined effect size. The program suggested 39 studies missing to the left of the mean. The centers of the diamonds depict the overall mean effect sizes, and the widths reflect the confidence interval. 39

Figure 4.1. Diagrammatic representation of the sequence of research activities carried out in the investigation of biological control of aphanomyces root rot (ARR) and root rot complex (RRC) in field pea and lentil. The blue sections indicate previously conducted study (Godebo, 2019), and the green sections represent the current study. 50

Figure 4.2. Inhibition of *Fusarium avenaceum* mycelial growth on PDA plates. Where, A and B were the top and bottom views of the assay plates, respectively. K-Hf-H2: *Lysobacter capsici*; K-Hf-L9: *Pseudomonas simiae*; PSV1-7: *Pantoea agglomerans*.. 55

Figure 4.3. Inhibition of *Fusarium oxysporum* mycelial growth on PDA plates. Where, A and B were the top and bottom views of the assay plates, respectively. K-Hf-H2: *Lysobacter capsici*; K-Hf-L9: *Pseudomonas simiae*; PSV1-7: *Pantoea agglomerans*. 55

Figure 4.4. Inhibition of *F. avenaceum* mycelial growth on PDA plates by *L. gummosis* K-Be-H3. 56

Figure 4.5. Agar-well diffusion assay depicting inhibition of *A. euteiches* mycelia with *L. capsici* K-Hf-H2 cell-free supernatant. A: clearing zone around the wells indicates mycelial growth inhibition. B: negative control plates. The assay was repeated and conducted on a duplicate plate, and data was collected from four inhibition zones each time. 56

Figure 4.6. Growth curve of *L. capsici* K-Hf-H2. The strain was grown in 250 mL half-strength Difco Trypticase soy broth for 14 days at 24°C and 120 rpm. The bacterial suspension was

taken daily, and the optical density at 600 nm was measured. The experiment was repeated, and mean OD values were converted to CFU mL⁻¹, then log CFU mL⁻¹ 57

Figure 4.7. Comparison of the zone of inhibition between cell-free supernatant extracted over the 14 d of *L. capsici* K-Hf-H2 growth phase. The days across the X-axis represent the age of the culture at which time cell-free supernatant was extracted. The cell-free supernatant obtained from the first six-day culture did not produce inhibition; thus, no data was displayed. Error bars indicate the mean standard deviation and means with the same letter are not significantly different. 57

Figure 4.8. Storage and autoclave stability assessment. **Negative control:** wells received 250 µL of filtered half-strength Difco Trypticase soy broth; **Room T⁰, 4°C and -20°C:** wells received 250 µL of cell-free supernatant stored at room temperature; 4°C and -20°C for four months, respectively. **Autoclaved:** wells received autoclaved 250 µL of cell-free supernatant. A plug of *A. euteiches* mycelia (5 mm diameter) was placed in the center of each plate. The assay was repeated and conducted on a duplicate plate, and data was collected from four interaction zones each time. 58

Figure 4.9. Biocontrol assessment of root rot complex in field pea caused by *A. euteiches*. **A:** *A. euteiches*; **B:** *P. simiae* K-Hf-L9 Vs *A. euteiches*; **C:** *P. agglomerans* PSV1-7 Vs *A. euteiches*; **D:** *L. capsici* K-Hf-H2Vs *A. euteiches*; **E:** Un-inoculated. The trials were conducted using a completely randomized design with four replicates..... 62

Figure 4.10. Biocontrol assessment of root rot complex in field pea caused by *A. euteiches*, *F. avenaceum* and *F. oxysporum*. **A:** (*A. euteiches* + *F. avenaceum* + *F. oxysporum*). **B:** *P. simiae* K-Hf-L9 Vs (*A. euteiches* + *F. avenaceum* + *F. oxysporum*); **C:** *P. agglomerans* PSV1-7 Vs (*A. euteiches* + *F. avenaceum* + *F. oxysporum*); **D:** *L. capsici* K-Hf-H2 Vs (*A. euteiches* + *F. avenaceum* + *F. oxysporum*); **E:** Un-inoculated. The trials were conducted using a completely randomized design with four replicates. 62

Figure 4.11. Biological control of root rots in lentils due to *Aphanomyces euteiches* (A. e) by biocontrol bacteria *Lysobacter capsici* K-Hf-H2, *Pseudomonas simiae* K-Hf-L9 and *Pantoea agglomerans* PSV1-7. Negative control: un-inoculated; positive control: (A. e) inoculated. The trials were conducted using a completely randomized design with four replicates. 66

Figure 4.12. Biological control of root rots in lentils due to *Aphanomyces euteiches* (A. e), *Fusarium avenaceum* (F. a) and *Fusarium oxysporum* (F. o) by biocontrol bacteria *Lysobacter capsici* K-Hf-H2, *Pseudomonas simiae* K-Hf-L9 and *Pantoea agglomerans* PSV1-7. Negative control: un-inoculated; positive control: (A. e + F. a + F. o) inoculated. The trials were conducted using a completely randomized design with four replicates... 66

Figure 5.1. Biocontrol bacteria *L. capsici* K-Hf-H2, *P. simiae* K-Hf-L9, and *P. agglomerans* PSV1-7 on Luria Broth (LB) agar plate (Figure 5.1A). Biocontrol bacteria *P. simiae* strain K-Hf-L9 (Figure 5.1B, the middle plate) exhibited fluorescence under UV light. Based on the 16S rRNA sequence, this strain was previously classified and reported as *P. fluorescens*

- K-Hf-L9 (Godebo, 2019). However, average nucleotide identity (ANI) suggested that the strain was more related to *P. simiae* than *P. fluorescens*. 81
- Figure 5.2.** Cell-filtration using Millipore Vacuum Manifold (Millipore Inc., Bedford, MA), Microfil Filtration Funnels and S-Pak 0.45-mm Type HA membranes (Millipore Inc.). An accu-jet ® pro pipette controller was used to remove air through the nozzles of each filter flask and aid the filtration. 86
- Figure 5.3.** Analysis of the protein-encoding genes (pegs) of the *Lysobacter capsici* K-Hf-H2 whole-genome sequence assigned to subsystem categories based on the RAST version 2.0 server. The bar on the left presents the percentage of pegs assigned to subsystems (green) and the pegs that could not be placed into any subsystem (blue). The pie chart in the center depicts the subsystem category distribution. The coloured categories on the right indicate the subsystem feature counts..... 89
- Figure 5.4.** Analysis of the protein-encoding genes (pegs) of the *Pseudomonas simiae* K-Hf-L9 whole-genome sequence assigned to subsystem categories based on the RAST version 2.0 server. The bar on the left presents the percentage of pegs assigned to subsystems (green) and the pegs that could not be placed into any subsystem (blue). The pie chart in the center depicts the subsystem category distribution. The coloured categories on the right indicate the subsystem feature counts..... 89
- Figure 5.5.** Analysis of the protein-encoding genes (pegs) of the *Pantoea agglomerans* PSV1-7 whole-genome sequence assigned to subsystem categories based on the RAST version 2.0 server. The bar on the left presents the percentage of pegs assigned to subsystems (green) and the pegs that could not be placed into any subsystem (blue). The pie chart in the center depicts the subsystem category distribution. The coloured categories on the right indicate the subsystem feature counts..... 90
- Figure 5.6.** Analysis of the protein-encoding genes (pegs) of the *Lysobacter gummosus* K-Be-H3 whole-genome sequence assigned to subsystem categories based on the RAST version 2.0 server. The bar on the left presents the percentage of pegs assigned to subsystems (green) and the pegs that could not be placed into any subsystem (blue). The pie chart in the center depicts the subsystem category distribution. The coloured categories on the right indicate the subsystem feature counts..... 90
- Figure 5.7.** Annotation overview for K-Hf-H2.peg.1000 in *L. capsici* K-HF-H2 encoding for extracellular zinc protease (EC 3.4.24.25) and (EC 3.4.24.26). The chromosomal region of the focus gene (top) was compared with three organisms. The graphic is centred on the focus gene, which is red and numbered 1. Sets of genes with a similar sequence are grouped with the same number and colour. The figure shows a cluster of extracellular zinc proteases in the K-HF-H2 genome..... 91
- Figure 5.8.** Annotation overview for K-Hf-H2.peg.3466 in *L. capsici* K-HF-H2 encoding for chitinase EC 3.2.1.14. The chromosomal region of the focus gene (top) was compared with three organisms. The graphic is centered on the focus gene, which is red and numbered 1. Sets of genes with similar sequence are grouped with the same number and color. 92

Figure 5.9. Annotation overview for K-Hf-H2.peg.855 in *L. capsici* K-HF-H2 encoding for endoglucanase EC 3.2.1.4. The chromosomal region of the focus gene (top) was compared with four organisms. The graphic is centred on the focus gene, which is red and numbered 1. Sets of genes with a similar sequence are grouped with the same number and colour. 92

Figure 5.10. Annotation overview for K-Hf-L9.peg.4600 in *P. simiae* K-Hf-L9 encoding for N-acetylglucosamine utilizing genes: EC 3.5.1.25, EC 2.7.1.69 and EC 3.5.99.6. The chromosomal region of the focus gene (top) was compared with three organisms. The graphic is centred on the focus gene, which is red and numbered 1. Sets of genes with a similar sequence are grouped with the same number and colour. 93

Figure 5.11. Annotation overview for K-Hf-L9.peg.846 and K-Hf-L9.peg.848 in *P. simiae* K-Hf-L9 encoding for TldE-TldD proteolytic complex genes. The chromosomal region of the focus gene (top) was compared with *P. fluorescens* SBW25. The graphic is centred on the focus gene, which is red and numbered 1. Sets of genes with a similar sequence are grouped with the same number and colour. 93

Figure 5.12. Annotation overview for PSV1.peg.969 in *P. agglomerans* PSV 1-7 encoding for TldD protein, part of TldE/TldD proteolytic complex. The chromosomal region of the focus gene (top) was compared with *Escherichia Coli* K 12. The graphic is centred on the focus gene, which is red and numbered 1. Sets of genes with a similar sequence are grouped with the same number and colour. 93

Figure 5.13. Graphical visualization of the BLAST comparisons of the *Lysobacter capsici* K-Hf-H2 genome with genomes of four type strains, *L. capsici* 55, *L. capsici* AZ78, *L. capsici* KNU-14 and *L. capsici* NF87_2. The order of the rings: Ring 1. *L. capsici* K-Hf-H2; Ring 2. GC Content; Ring 3. GC Skew; Ring 4. *L. capsici* 55, Ring 5. *L. capsici* AZ78, Ring 6. *L. capsici* KNU-14 and Ring 7. *L. capsici* NF87_2. The darker regions indicate the presence of multiple hits corresponding to the portion of the *L. capsici* K-Hf-H2 genome sequence. In contrast, gaps indicate the absence of sequences with less than a 50% identity ratio to the *L. capsici* K-Hf-H2 genome sequence. The graph was generated by BRIG 0.95..... 95

Figure 5.14. Venn Diagram showing the number of shared and genome-specific gene families among *Lysobacter capsici* K-Hf-H2 and the four type strains *L. capsici* 55, *L. capsici* AZ78, *L. capsici* KNU-14 and *L. capsici* NF87_2. The diagram was generated using EDGAR version 3.0. 96

Figure 5.15. Graphical visualization of the BLAST comparisons of the *Pseudomonas simiae* K-Hf-L9 genome with genomes of two type strains, *Pseudomonas simiae* PCL1751 and *Pseudomonas simiae* WCS417. The order of the rings: Ring 1. *P. simiae* K-Hf-L9; Ring 2. GC Content; Ring 3. GC Skew; Ring 4. *P. simiae* PCL1751 and Ring 5. *P. simiae* WCS417. The darker regions indicate the presence of multiple hits corresponding to the portion of the *P. simiae* K-Hf-L9 genome sequence. In contrast, gaps indicate the absence of sequences with less than a 50% identity ratio to the *P. simiae* K-Hf-L9 genome sequence. The graph was generating by BRIG 0.95..... 98

Figure 5.16. Venn Diagram showing the number of shared and genome-specific gene families among *Pseudomonas simiae* K-Hf-L9, *Pseudomonas simiae* PCL1751 and *Pseudomonas simiae* WCS417. The diagram was generated using EDGAR version 3.0. 99

Figure 5.17. Graphical visualization of the BLAST comparisons of the *Pantoea agglomerans* PSV1-7 chromosome with chromosomes of two type strains, *Pantoea agglomerans* UAEU18 and *Pantoea agglomerans* ZJU23. The order of the rings: Ring 1. *P. agglomerans* PSV1-7; Ring 2. GC Content; Ring 3. GC Skew; Ring 4. *P. agglomerans* UAEU18 and Ring 5 *P. agglomerans* ZJU23. The darker regions indicate the presence of multiple hits corresponding to the portion of the *P. agglomerans* PSV1-7 genome sequence. In contrast, gaps indicate the absence of sequences with less than a 50% identity ratio to the *P. agglomerans* PSV1-7 genome sequence. The graph was generating by BRIG 0.95..... 101

Figure 5.18. Venn Diagram showing the number of shared and genome-specific gene families among *Pantoea agglomerans* PSV1-7, *Pantoea agglomerans* UAEU18 and *Pantoea agglomerans* ZJU23. The diagram was generated using EDGAR version 3.0..... 102

Figure 5.19. Graphical visualization of the BLAST comparisons of the *Lysobacter gummosus* K-Be-H3 genome with genomes of two type strains, *Lysobacter gummosus* 10.1.1 and *Lysobacter gummosus* 3.2.11. The order of the rings: Ring 1. *Lysobacter gummosus* K-Be-H3; Ring 2. GC Content; Ring 3. GC Skew; Ring 4. *Lysobacter gummosus* 10.1.1 and Ring 5. *Lysobacter gummosus* 3.2.11. The darker regions indicate the presence of multiple hits corresponding to the portion of the *Lysobacter gummosus* K-Be-H3 genome sequence. In contrast, gaps indicate the absence of sequences with less than a 50% identity ratio to the *Lysobacter gummosus* K-Be-H3 genome sequence. The graph was generating by BRIG 0.95..... 104

Figure 5.20. Venn Diagram showing the number of shared and genome-specific gene families among *Lysobacter gummosus* K-Be-H3, *Lysobacter gummosus* 10.1.1, and *Lysobacter gummosus* 3.2.11. The diagram was generated using EDGAR version 3.0. 105

Figure 5.21. Phylogenetic tree showing the relationships among *L. capsici* K-Hf-H2, *L. gummosus* K-Be-H3 and members of the genus *Lysobacter*. The tree was inferred based on their 16S rRNA gene sequences data collected from the GenBank database. The sequences were aligned by ClustalW, and the product was used to generate a phylogenetic tree using the Neighbor-Joining method (Saitou and Nei, 1987). The evolutionary distances were computed using Kimura's two-parameter model (Kimura, 1980). The sequences' accession numbers are provided in parentheses. Numbers at the nodes indicate bootstrap values, >70%, from 1000 data replication (Felsenstein, 1985). The phylogenetic analyses were performed using MEGAX (Kumar et al., 2018). 110

Figure 5.22. Phylogenetic tree showing the relationships between *Pseudomonas simiae* K-Hf-L9 and members of the genus *Pseudomonas*. The tree was inferred based on their 16S rRNA gene sequences data collected from the GenBank database. The sequences were aligned by ClustalW, and the product was used to generate a phylogenetic tree using the Neighbor-Joining method (Saitou and Nei, 1987). The evolutionary distances were computed using Kimura's two-parameter model (Kimura, 1980). The sequences' accession numbers are

provided in parentheses. Numbers at the nodes indicate bootstrap values, >70%, from 1000 replication of the data (Felsenstein, 1985). The phylogenetic analyses were carried out using MEGAX (Kumar et al., 2018)..... 111

Figure 5.23. Phylogenetic tree showing the relationships between *Pantoea agglomerans* PSV1-7 and members of the genus *Pantoea*. The tree was inferred based on their 16S rRNA gene sequences data collected from the GenBank database. The sequences were aligned by ClustalW, and the product was used to generate a phylogenetic tree using the Neighbor-Joining method (Saitou and Nei, 1987). The evolutionary distances were computed using Kimura's two-parameter model (Kimura, 1980). The sequences' accession numbers are provided in parentheses. Numbers at the nodes indicate bootstrap values, >70%, from 1000 replication of the data (Felsenstein, 1985). The phylogenetic analyses were carried out using MEGAX (Kumar et al., 2018)..... 111

Figure 5.24. KEGG map showing sphingolipid synthesis for fungi. *Lysobacter capsici* K-Hf-H2 interfere with the biosynthesis of sphingolipid via eight genes at three targets indicated by green background in the synthesis pathway. These eight genes are three beta-galactosidase (EC 3.2.1.23) K-Hf-H2.peg.2824, K-Hf-H2.peg.2826 and K-Hf-H2.peg.4307; four alpha-galactosidase (EC 3.2.1.22) K-Hf-H2.peg.2151, K-Hf-H2.peg.2815, K-Hf-H2.peg.4298 and K-Hf-H2.peg.4300 and one exo-alpha-sialidase (EC 3.2.1.18) K-Hf-H2.peg.3941.113

Figure 5.25. Siderophore production by *Pantoea agglomerans* PSV1-7, *Lysobacter capsici* K-Hf-H2 and *Pseudomonas simiae* K-Hf-L9 on Chrome Azurol S (CAS). The orange halo zones around the colony indicate siderophore production. The plates were incubated at 25 °C for 7 d..... 115

Figure 5.26. Protein hydrolysis by *Lysobacter capsici* K-Hf-H2. Clearing zones around the colonies (A) and wells (B) indicate protein hydrolysis on skimmed milk agar (SMA) plates. The plates were incubated at 25 °C for 7 d. 116

Figure 5.27. Protein hydrolysis by *Pseudomonas simiae* K-Hf-L9. Clearing zones around the colonies (A) indicate protein hydrolysis on skimmed milk agar (SMA) plates. However, the cell-free supernatant of *P. simiae* K-Hf-L9 did not produce visually detectable protein hydrolysis around the wells (B) within 7 d of incubation at 25 °C..... 117

Figure 5.28. Protein hydrolysis by *Pantoea agglomerans* PSV1-7. Clearing zones around the colonies (A) indicate protein hydrolysis on skimmed milk agar (SMA) plates. However, the cell-free supernatant of *Pantoea agglomerans* PSV1-7 did not produce visually detectable protein hydrolysis around the wells (B) within 7 d of incubation at 25 °C. .. 118

Figure 5.29. Protein hydrolysis positive controls. (A): skimmed milk agar plates that received 20 µL of filter-sterilized Trypsin (150 USP units mg⁻¹) enzyme solution; (B): skimmed milk agar plates with wells that received filter-sterilized 50 µL of the trypsin enzyme solution. The clearing zones in the center of the plates indicate protein hydrolysis by the enzyme trypsin. The plates were incubated at 25 °C for 5 d. 119

Figure 5.30. Cellulose hydrolysis capacity of <i>Lysobacter capsici</i> K-Hf-H2 on cellulose-Congo-red agar media. Clearing zones around the colony indicate hydrolysis of cellulose. The plates were incubated at 25 °C for 5 d..	120
Figure 5.31. Cellulose hydrolysis capacity of <i>Pseudomonas simiae</i> K-Hf-L9 on cellulose-Congo-red agar media. Clearing zones around the colony indicate hydrolysis of cellulose. The plates were incubated at 25 °C for 5 d..	120
Figure 5.32. Desiccation tolerance of biocontrol bacteria. The reported values are mean percent survival obtained from three independent experiments. Membranes were cut in half and transferred to an empty Petri dish (dry) and a water-agar plate (12.5 g agar L-1) (wet) and stored at room temperature and humidity for 24 h. Error bars indicate standard deviation. The percent survival of the biocontrol bacteria was significantly different and means represented with a different letter indicate significant difference.	121
Figure 5.33. Chemical structure of HSAF (Yu et al., 2007).....	125
Figure F. 1. SAS code used to run non-parametric analysis on disease rating scale.....	184

LIST OF EQUATIONS

Equation 3.1. Effect size calculation.....	30
Equation 3.2. Non-parametric variance calculation.....	30
Equation 3.3. Test of heterogeneity	31
Equation 5.1. Desiccation tolerance	86

LIST OF ABBREVIATION

ACC: 1-aminocyclopropane-1-carboxylate

ANOVA: analysis of variance

ARR: aphanomyces root rot

BGCs: biosynthetic gene clusters

BRIG: BLAST Ring Image Generator

CDS: protein-coding genes

DNA: deoxyribonucleic acid

EAEC: enteroaggregative *E. coli*

EHEC: enterohaemorrhagic *E. coli*

EPEC: enteropathogenic *E. coli*

HSAF: heat-stable antifungal factor

mRNA: messenger RNA

NCG: non-coding genes

nrps: nonribosomal peptide synthetase

PacBio: Pacific Biosciences

PGPR: plant growth-promoting rhizobacteria

pks: polyketide synthase

PTM: polycyclic tetramate macrolactam

RAST: rapid annotations subsystems technology

RNA: ribonucleic acid

rRNA: ribosomal RNA

tRNA: transfer RNA

SMRT: single-molecule real-time

1. GENERAL INTRODUCTION

1.1 Project description and organization of the thesis

Aphanomyces root rot poses a significant threat to the sustainable production of field pea and lentil crops in western Canada (Wu et al., 2018). Currently, the available disease management options are limited. Furthermore, none provide adequate control (Hughes and Grau, 2013), indicating the need to develop alternative methods to control the severe yield and economic losses caused by this disease. Due to this, the potential for biological control of ARR was investigated using naturally occurring antagonistic bacterial isolates obtained from agricultural soil including isolates *Lysobacter capsici* K-Hf-H2, *Pseudomonas simiae* K-Hf-L9 and *Pantoea agglomerans* PSV1-7 previously identified as having significant biocontrol potential (Godebo, 2019). Others have examined biocontrol methods to evaluate ARR suppression using multi-step processes, including isolation of inhibitory organisms, lab assays, growth chambers and field trials (Chapter 3). Such studies are essential for critical review studies, understanding the current state of the science "biological control of ARR" and drawing robust conclusions that will direct future research.

Even though *L. capsici* K-Hf-H2, *P. simiae* K-Hf-L and *P. agglomerans* PSV1-7 were previously identified as having significant biocontrol potential (Godebo, 2019), the activity of these strains towards fungal pathogens causing root rot in field pea and lentil and the mechanism(s) by which biocontrol was achieved were unknown. Screening bacterial isolates for biocontrol potential often begins by assessing the efficacy of a single strain against one plant pathogen *in vitro* (Liu et al., 2017). This is followed by *in vivo* assessments against a single plant disease (Li et al., 2011). However, under field conditions, more than one pathogen is usually part of a complex that causes the disease to develop in a crop. For example, ARR in field pea and lentil often occurs in a complex with other pathogens (Hughes and Grau, 2013). As a result, it is advantageous to investigate whether the biocontrol bacteria that suppresses ARR (Godebo et al., 2020) also exhibits antagonistic and disease suppression potential towards fungal pathogens such as *Fusarium avenaceum* and *Fusarium oxysporum*, which individually or collectively cause root rot in pea and lentil.

Biological control agents inhibit plant pathogens through several antagonistic mechanisms, including the production and secretion of secondary bioactive metabolites directed by gene and gene clusters with known and unknown functions (Pal et al., 2000; Nguyen et al., 2017). Therefore, understanding the genes and gene clusters involved in suppressing plant diseases like ARR is an essential component of elucidating mechanisms of disease suppression. In this context, genome annotation, identifying functional elements along a genome sequence, provides an opportunity to link genomic information with biological functions.

The development of DNA sequencing technologies has transformed many aspects of biology, including the whole genome sequencing of biocontrol bacteria (Kim et al., 2017). Whole-genome sequences enable comparative genomic analyses among closely related bacterial species that differ in a specific aspect (Hossain et al., 2015); for example, comparative genomic analysis among bacterial species differing in inhibitory potential towards *A. euteiches* (i.e., those that do and do not have inhibitory activity). Thus, comparative genomics analyses play a significant role in shedding light on the genetic basis underlying the ability of a bacterium to inhibit *A. euteiches*, *F. avenaceum* and *F. oxysporum* growth and suppress disease development.

The overall objectives of this study were to: (i) understand the current state of the science "biological control of ARR" using a quantitative meta-analysis review; (ii) investigate the biocontrol potential of *L. capsici* K-Hf-H2, *P. simiae* K-Hf-L9 and *P. agglomerans* PSV1-7 against *Fusarium* pathogens involved in the root rot of field pea and lentil; and (iii) predict the mechanisms by which biocontrol is achieved by these organisms. To accomplish these objectives, studies were conducted based on the following hypotheses: (1) The ARR biocontrol bacteria *L. capsici* K-Hf-H2, *P. simiae* K-Hf-L9 and *P. agglomerans* PSV1-7 can be used to suppress root rot complex in field pea and lentil due to *A. euteiches*, *F. avenaceum* and *F. oxysporum*; (2) Biocontrol bacteria, *L. capsici* K-Hf-H2, *P. simiae* K-Hf-L9 and *P. agglomerans* PSV1-7, harbour specific sets of genes responsible for their antagonistic activity towards *A. euteiches*, *F. avenaceum* and *F. oxysporum* and suppression of disease symptoms. Additionally, the state of biological control of ARR was reviewed using a comprehensive meta-analysis review.

This research thesis is presented in manuscript-style format. The thesis consists of a literature review (Chapter 2) followed by three studies (Chapter 3: a meta-analysis review and research studies: Chapter 4 and 5), a general discussion (Chapter 6), and future research directions (Chapter

7). Chapter 3 describes the state of biological control of ARR based on a comprehensive meta-analysis review in reference to previously published articles. Chapter 4 describes the biocontrol of RRC in field pea and lentil using *in vitro* and *in vivo* trials. Chapter 5 begins with the characterization of biocontrol bacteria using a genomic approach including sequencing, annotation and comparative genomics and provides insights on genes and gene clusters encoding for traits potentially involved in the biological control of RRC in field pea and lentil. Chapter 6 is a synthesis chapter that ties the research chapters together by discussing the results of the current study using relevant literature. Finally, Chapter 7 offers concepts for future studies by identifying potential research gaps. The individual chapters are organized and presented as a stand-alone and are suited for submission to peer-reviewed journals. Before each chapter, a preface is provided to preserve the flow of the research story and connect one chapter to the next. Since the thesis is organized using a manuscript style, some repetition of materials previously reported occurs.

2. LITERATURE REVIEW

2.1 Root rot in field pea and lentil

Canada is the primary field pea (*Pisum sativum* L.) and lentil (*Lens culinaris* L.) producing country globally, mainly for export. Within Canada, the production of these legume crops is concentrated in Saskatchewan and Alberta, with a smaller area of pea production in Manitoba (Chatterton et al., 2019). However, in recent years, the root rot of field pea and lentil has been increasing in western Canada (Gossen et al., 2016). Although it is challenging to quantify yield loss caused by root rot, complete loss of productivity has been observed in heavily infested pea fields in Alberta and Saskatchewan (Banniza et al., 2013; Chatterton et al., 2015; Gossen et al., 2016).

Root rot in pea and lentil is caused by a complex of pathogens, including *A. euteiches*, which affects the developing below-ground portion of the plant, leading to poor-performing pulse crops (Saskatchewan Pulse Grower, 2017). Although *A. euteiches* can be isolated from alfalfa (*Medicago sativa* L.), snap bean (*Phaseolus vulgaris* L.) and red kidney bean (*Proteus vulgaris* L.), faba bean (*Vicia faba* L.), red clover (*Trifolium pratense* L.), white clover (*Trifolium repens* L.), and several weed species, it causes the most significant economic impact to pea and lentil crops (Wu et al., 2018). The broad host range of *A. euteiches*, combined with its long-lived oospores, makes the management of ARR with traditional methods difficult (Xue, 2003; Wu et al., 2018). Moreover, *A. euteiches* occurs as a complex under field conditions with other pathogens that individually or synergistically cause root rot complex (RRC) in field pea and lentil (Xue, 2003).

The RRC of pea and lentil is a disease caused by various fungal and fungus-like organisms that collectively affect the root of a developing plant leading to a loss of productivity that can extend up to 100% (Gaulin et al., 2007). Pathogens involved in the causation of RRC in western Canada include *A. euteiches*, *Pythium* spp., *Fusarium* spp. and *Rhizoctonia solani* (Wu et al., 2018). These are soilborne pathogens that cause disease at any developmental stage of the crop. *Pythium* spp. and *A. euteiches* are water-loving oomycetes commonly referred to as "water moulds" (Robideau, 2013). *Pythium* spp. can be controlled with seed treatments (Scott et al., 2020). However, effective control methods are not available for *A. euteiches* in Canada, apart from the fungicide INTEGO™ Solo (ethaboxam) and Vibrance® Maxx RFC, which are registered for use against early-season ARR (Guide to Crop Protection, 2021). *Aphanomyces euteiches* is the most

destructive pathogen due to the lack of effective treatment methods and the presence of oospores can persist in the soil for more than ten years (Gaulin et al., 2007). These oospores can accumulate quickly when a susceptible crop is planted (Hughes and Grau, 2013).

The available RRC management options in Canada are limited, and none provide adequate control (Hughes and Grau, 2013), thus, there is a need for alternative control methods against the RRC of field pea and lentil. Consequently, developing biological control agents capable of surviving and propagating in target locations and ultimately establishing a rhizosphere presence that suppresses root rot symptoms in pea and lentil, is desirable.

2.2 Root rot symptoms

The root rot symptoms of pulse crops can be classified as below-ground and above-ground symptoms (Wakelin et al., 2002). The below-ground symptoms are early-stage symptoms, including reduced root biomass, decay and brown discolouration of roots; nodules are often absent or pale in colour. Pulse crops affected with root rot pathogens usually appear in patches that can expand if the condition is conducive to the pathogen over several growing seasons (Hughes and Grau, 2013). The above-ground symptoms include poor emergence, yellowing and wilting of lower leaves, dwarfing and stunting of plants, and even death of the entire plant (Wakelin et al., 2002; Hughes and Grau, 2013; Godebo et al., 2020).

Root rot of pea and lentil that occurs due to the collective action of *A. euteiches*, *Pythium* spp., *Fusarium* spp., and *R. solani* poses an increased risk of yield loss. In these situations, identifying the primary pathogen, the role of each pathogen, and the nature of the interrelationships among pathogens is difficult to ascertain. Furthermore, once the plants are profoundly affected, the root is decayed, or the plant is dead, making the identification of root rot pathogens difficult because other organisms feed on the decaying plant tissue (Hughes and Grau, 2013). Moreover, under field conditions, root rot symptoms are often associated with areas of flooding or waterlogging. Therefore, the search for an effective biocontrol agent capable of suppressing root rot symptoms needs to consider these biotic and environmental conditions. Also, effective microbial biocontrol agents are those that can survive and proliferate under conditions conducive to the disease-causing agent.

2.3 Microbial biocontrol agents

Biocontrol of plant diseases is the inhibition of plant pathogens and the suppression of disease symptoms *via* living organisms (Heimpel and Mills, 2017). Using biocontrol is a natural and environmentally acceptable method that has become an integral component of pest and pathogen management strategies (Xue et al., 2003). Initial screening of microbes for biocontrol activity involves detecting, isolating and identifying an isolate that exhibits antagonistic activities against a known plant pathogen (Godebo et al., 2020). Then, investigating biocontrol efficacy *in planta* indicates the likelihood of being developed as a commercial biocontrol agent. Typically, microbes that are effective against pathogens are multiplied on artificial media and applied in various formulations as one-time or multiple applications during the plant growth period. Such biocontrol agents are generally referred to as "augmentative biocontrol" (Eilenberg et al., 2001; Heimpel and Mills, 2017; van Lenteren et al., 2018). From the commercial perspective, companies producing biocontrol agents use living microorganisms registered as plant protection products (Glare et al., 2012). Moreover, in some instances, the active metabolite secreted by the antagonist is used as the biocontrol product for commercial augmentative biocontrol. However, such active metabolites are considered "chemical" in the European Union (Köhl et al., 2019).

Microbial biological control agents protect crops through various modes of action. These modes of action include direct antibiosis *via* the production of antimicrobial secondary metabolites (Raaijmakers and Mazzola, 2012; Ghorbanpour et al., 2018), induction of resistance (Pieterse et al., 2014; Conrath et al., 2015) and competition for root colonization and nutrients (Spadaro and Droby, 2016). In addition to being used as biocontrol agents, some microbial agents play a significant role as biofertilizers and promote plant growth (Márquez et al., 2020). These roles include fixing N, solubilizing P, chelating Fe, producing hormone-like substances, degrading 1-aminocyclopropane-1-carboxylate (ACC) deaminase, and degrading organic matter and releasing nutrients in the soil (Pertot et al., 2015). Since biocontrol agents limit pathogen populations by various direct and indirect mechanisms, understanding the nature of the mode of action determines the characteristics of the biocontrol agent and how a pathogen population is affected (Köhl et al., 2019).

2.3.1 Challenges associated with microbial biocontrol agents

The use of biocontrol agents has been demonstrated to be a potential method for controlling plant diseases caused by various pathogens; thus, the search for novel strains capable of preventing

or suppressing plant diseases is under investigation in multiple parts of the world (Wu et al., 2018; Kaewsalong et al., 2019). However, the success of these investigations is primarily limited to controlled conditions and organisms that have biocontrol properties under controlled conditions often are not effective under field conditions. For example, several studies (e.g., Mark et al., 2006; Nicot et al., 2011), indicated the irregularity of effectiveness of several biological control agents when introduced under field conditions ranging from being less effective to completely ineffective even if significant efficacy was observed under controlled conditions.

The irregularity in biocontrol efficacy in the field conditions is attributed to various factors, including soil type and soil conditions, and climatic variations such as temperature, humidity, and UV irradiation encountered in field conditions (Smolinska and Kowalska, 2018). Another reason for irregular biocontrol efficacy is the lack of ecological competence that can reduce the survival and colonization ability of the biocontrol (Bardin et al., 2015). Also, the biocontrol agent's intrinsic traits result in inconsistent production of bioactive metabolites required to suppress the pathogen (Li et al., 2019), and inadequate formulation and application methods can contribute to inconsistent biocontrol efficacy (Ruocco et al., 2011). Moreover, field conditions are so complex that more than one disease-causing agent can usually exist (Williamson-Benavides and Dhingra, 2021). A putative biocontrol agent effective in controlled conditions faces challenges from pathogens that individually or synergistically cause disease to the plant. For example, pathogens causing root rot in legumes usually occur as a complex (Hughes and Grau, 2013), and a putative biocontrol agent found to be effective against one of the pathogens can face challenges that diminish its efficacy under field conditions.

The reduced efficacy under field conditions can also relate to the diversity of sensitivity of the plant pathogens to the biological control agents, with the possible existence of less sensitive isolates in natural populations of plant pathogens (Bardin et al., 2015; Lahlali et al., 2022). Moreover, maintaining the population of biocontrol agents above a certain level in the soil is an essential factor that affects biocontrol efficacy in controlled and field conditions (Yuan et al., 2014). Controlled conditions such as those present in growth chambers offer a better opportunity to manipulate experimental conditions to maintain the population of biocontrol agents above a certain level; thus, higher efficacy can be observed. Another factor could be the biocontrol agent application method (Marian and Shimizu, 2019). Developing a biocontrol agent application method giving high performance under field conditions is challenging due to several factors related

to the biocontrol agent and the plant pathogens' intrinsic nature discussed in the following paragraph (Palmieri et al., 2022).

From the biocontrol agent perspective, our limited knowledge about its physiological needs and requirements determines the ability to formulate application methods that result in higher efficacy (Niu et al., 2020). This, in turn, affects its resilience under natural conditions (Bardin et al., 2015). The effectiveness of biocontrol agents toward plant pathogens relates to the selection pressure coming from the biocontrol agent (Köhl et al., 2019). This selection pressure can be affected by factors like application method, including doses of application and mode of action of the biocontrol agents (Ghorbanpour et al., 2018; Mishra et al., 2018; Lahlali et al., 2022). For example, in a study by Mishra et al. (2018) several mechanisms of action, such as antibiosis, competition for nutrients and space, parasitism, interfering with the mechanisms of pathogenesis and induction of local or systemic resistance were identified but our understanding of the precise biological control mechanisms is still incomplete (Bardin et al., 2015; Niu et al., 2020). Moreover, it is unknown if biological control agents have a dominant mechanism that may be affected by external conditions nor is it clear what conditions make them switch from one mechanism to another (Bardin et al., 2015).

From the plant pathogen perspective, for example, the efficacy of biocontrol agents toward plant pathogens can be linked to characteristics of the plant pathogen, including the genetic diversity and ability to evolve due to selection pressure (Köhl et al., 2019). These factors are controlled by population genetic processes such as population size, mutation, and gene flow (McDonald and Linde 2002). According to McDonald and Linde (2002), plant pathogen populations with increased evolutionary attributes have a better chance of overcoming varietal pressure.

Therefore, there is a need to identify microbes offering higher efficacy under field conditions and improve our ability to identify microbes that are more likely to exhibit biocontrol properties. In this regard, molecular science, which is continuously advancing, particularly whole-genome sequencing and bioinformatics tools, are valuable assets to improve our ability to identify microbes that are more likely to exhibit biocontrol properties under field conditions.

2.3.2 Opportunities to alleviate challenges linked to microbial biocontrol agents

The development of DNA sequencing technologies has transformed many aspects of biology, including whole-genome sequencing, annotation and comparative genomics (Kim et al., 2017). Microbial whole-genome sequencing is an excellent tool for analyzing and characterizing the sequences with biocontrol-related genes and gene clusters with known and unknown functions (Sui et al., 2020). Genome annotation allows one to link genomic information with biological processes (Ejigu and Jung, 2015). The benefits of understanding the whole-genome sequence of a biocontrol agent include knowing the specific locations of the gene and gene clusters that have significance in controlling plant disease and the general genomic profile of the biocontrol agent (Thiruvengadam et al., 2022).

Currently, whole-genome sequencing technology is becoming accessible due to decreased costs associated with DNA sequencing instruments and consumables (Quainoo et al., 2017; Adewale, 2020). Thus, DNA sequencing instruments like the MinION (Oxford Nanopore Technologies), the size of a typical smartphone, are now available in many laboratories to execute their genome sequencing projects (Lu et al., 2016; Wang et al., 2021). Furthermore, Oxford Nanopore sequencing generates reads sufficiently long enough to be of great use in *de novo* assembly (Koren and Phillippy, 2015). Therefore, the long-read data from the Oxford Nanopore MinION is commonly used to assemble complete bacterial genomes to accurately reconstruct gene order and orientation without using data from other sequencing technologies (Loman et al., 2015). In addition, the assembled genome provides an opportunity to give descriptive information to the gene and gene clusters using bioinformatics tools that perform annotation and comparative genomics (Wang et al., 2021).

Predicting the biological function and understanding the genetic determinates directing the biocontrol mechanisms helps understand the biotic and abiotic factors affecting the expression of the trait encoded by the gene responsible for suppressing the plant disease (Loper et al., 2012). This insight helps consider these factors before applying the biocontrol agent for field trials. Moreover, whole-genome sequencing and bioinformatics tools enable us to understand the natural cellular requirements to survive, colonize and exhibit disease suppression under conditions conducive to the pathogen (Scherlach and Hertweck, 2021). These tools give us insight into the type of carbon source a given biocontrol organism can metabolize. This information is essential during the inoculum development stage and after application. Whole-genome sequencing and

bioinformatics tools also enable us to understand the natural fitness of the biocontrol agent in colonizing and forming a biofilm to dominate the space shared by the pathogen and the biocontrol agent (Muhammad et al., 2020). Whole-genome sequencing and bioinformatics tools enable us to understand gene and gene clusters that have special significance depending on environmental conditioning, including UV, light intensity, salinity, oxygen and water (Fischbach and Voigt, 2011)

Apart from genome annotation, whole-genome sequence enables us to perform comparative genome analysis (Ejigu and Jung, 2015). Comparative genome analysis is a powerful bioinformatics tool that allows us to visualize differences and similarities among closely related bacterial species that differ in biocontrol potential towards plant pathogens (Zaid et al., 2022). Furthermore, this comparison sheds light on the genetic basis underlying the biocontrol ability of a biocontrol agent (Hossain et al., 2015).

To summarize, there is an excellent opportunity to alleviate challenges linked to microbial biocontrol agents' efficacy under field conditions. Furthermore, when coupled with functional experiments in plant systems and under laboratory conditions, genome analysis is an excellent tool to identify microbes offering higher efficacy under field conditions. Thus, it ultimately improves our ability to identify microbes more likely to exhibit biocontrol properties under field conditions.

2.4 The genus *Lysobacter*

The genus *Lysobacter* was first defined by Christensen and Cook (1978). Until then, species belonging to *Lysobacter* were assigned or misidentified as *Stenotrophomonas* and *Xanthomonas* (Sullivan et al., 2003; Puopolo et al., 2018). *Stenotrophomonas*, *Xanthomonas* and *Lysobacter* are genera within the Xanthomonaceae family. The *Lysobacter* species are now documented in the phylum Proteobacteria and are found in soil and water habitats. They are recognized by gliding motility, a high G+C content (65.4% to 70.1%), lytic activity against other microorganisms including fungi and oomycetes, and optimum growth temperature of 28 °C (Christensen and Cook, 1978; Reichenbach, 2006).

Currently, there are 88 species within the genus *Lysobacter* and two subspecies (genus *Lysobacter*, <https://lpsn.dsmz.de/search?word=lysobacter>). Their diversity is constantly increasing partly due to the reclassification of previously misidentified bacterial species (Miess et al., 2016; Margesin et al., 2018) and the increasing proposal of new *Lysobacter* species due to genome

sequencing. The majority of *Lysobacter* genomes that are publicly available are strains belonging to *L. antibioticus*, *L. capsici*, and *L. enzymogenes* species which are reported as biocontrol agents against phytopathogenic microorganisms (Brescia et al., 2020). The availability of sequenced genomes allows for conducting genome comparison studies that aim to answer a specific research question (de Bruijn et al., 2015; Liu et al., 2015; Puopolo et al., 2016). For example, Liu et al. (2015) conducted a genome comparison study to find orthologues representing the core genome of *Lysobacter* spp. Their findings indicated that *L. arseniciresistens* ZS79T, *L. concretionis* Ko07T, *L. daejeonensis* GH1-9T, *L. defluvii* IMMIB APB-9T and the biocontrol agent *L. capsici* AZ78 shared 1207 genes. Another study by Puopolo et al. (2016) indicated that a biocontrol agent *L. capsici* AZ78 lacks genes involved in causing infection in humans and plants compared to the genome of phylogenetically related strains, *Xanthomonas campestris* pv. *campestris* ATCC 33913 (plant pathogen) and *Stenotrophomonas maltophilia* K729a (human pathogen). Therefore, Puopolo et al. (2016) concluded that *Lysobacter* strains are not virulent and can be developed as safe biocontrol agents of plant pathogens.

2.4.1 *Lysobacter* species as biocontrol agents and mechanisms of action

The *Lysobacter* species have gained the research community's attention due to their promising potential as biocontrol agents against many plant diseases (Lin et al., 2021). Several research findings indicated that *Lysobacter* strains utilize multiple mechanisms, including the production of antibiotics, lytic enzymes, toxic compounds, competition for colonization, predation, and induction of plant resistance (de Bruijn et al., 2015; Puopolo et al., 2016). Such a multiple-mechanism mode of action is essential for a biological control agent as it diminishes the occurrence of resistant populations of plant pathogenic microorganisms (Puopolo et al., 2018). Furthermore, genome mining, annotation and bioinformatics studies confirmed that the *Lysobacter* genome has an incredible array of genes encoding lytic enzymes capable of degrading complex molecules in soil and the cell wall of plant pathogenic microorganisms (de Bruijn et al., 2015; Puopolo et al., 2016).

The lytic enzymes produced by members of *Lysobacter* include proteases, which catalyze the hydrolysis of peptide bonds (Vasilyeva et al., 2014). Proteases are the most studied enzymes produced by *Lysobacter* strains due to their biotechnological application, controlling plant pathogenic microorganisms, and cleaning medical and industrial equipment from pathogenic bacteria (Joshi and Satyanarayana, 2013; Gökçen et al., 2014). Chitinases are another group of

enzymes produced by the *Lysobacter* strains active against chitin, the cell wall components of fungi and insects (Zhang et al., 2001). Also, *Lysobacter* strains produce glucanases (β -1,3-glucanases) that degrade and lyse the mycelial structure and display biocontrol activity against root rot pathogens such as *Rhizoctonia solani*, *Sclerotium rolfsii*, *Bipolaris sorokiniana* and *Pythium ultimum* (Siddique, 2005; Palumbo et al., 2005). Furthermore, the glucanases produced by *L. enzymogenes* C3 and N4-7 were purified and characterized, and *gluA*, *gluB*, and *gluC* were identified as genes involved in their production (Palumbo et al., 2005). Other enzymes of great significance that the members of *Lysobacter* species produce include elastases, endonucleases, endoamylases, esterases, keratinases and phosphatases (Reichenbach, 2006) and lipases (Ko et al., 2009).

2.4.1.1 Heat stable antifungal factor (HSAF)

Another antimicrobial compound considered novel in its nature and mode of action and regarded as the forerunner of future biological pesticides is the heat-stable antifungal factor (HSAF) (Luo et al., 2013; Yuen et al., 2018). Structurally, the HSAF is a polycyclic tetramate macrolactam (PTM) that is identical to dihydromaltophilin (Xie et al., 2012), which is a secondary metabolite isolated from *Streptomyces* sp. (Graupner et al., 1997). It is insoluble in virtually all organic solvents, sparingly soluble in methanol, and slightly more soluble in pyridine; it is acidic with a chemical formula $C_{29}H_{40}N_2O_6$ and readily forms salts with amines and other cations (Graupner et al., 1997; Yu et al., 2007).

The HSAF is regarded as the forerunner of future biological pesticides due to two significant benefits over other antifungal agents. Firstly, it is non-toxic to animals and plants due to its specific inhibition mechanism (Li et al., 2006); and secondly it is heat stable (Kobayashi and Yuen, 2005), which is an excellent attribute that can ease its production, extraction, transportation, and long-term storage. The mechanism by which HSAF exhibits inhibitory activity is by disrupting the biosynthesis of sphingolipids required for polarized mycelial growth. Although sphingolipids are abundant components of eukaryotic cell membranes and signalling molecules involved in numerous cellular processes (Rollin-Pinheiro et al., 2016), the type of sphingolipids targeted by HSAF are absent in animals and plants (Yu et al., 2007). As a result, it is believed that this unique antagonistic mechanism may lead to developing a novel agent with a broad spectrum of action (Tang et al., 2018).

Currently, detailed information regarding the factors that affect HSAF is not available and studies focusing on HSAF were conducted on two strains of *L. enzymogenes*: strain C3 and OH11 (Yu et al., 2007; Meers et al., 2018; Zhao et al., 2019). *Lysobacter enzymogenes* that produce HSAF are not commonly used in the fermentation industry; thus, its optimum culture conditions, including pH, temperature, aeration, fermentation, and others, are not well described (Tang et al., 2018). However, research articles have reported findings such as: (1) HSAF was produced under nutrient-limited conditions; (2) HSAF is a colourless powder with a melting point of greater than 300°C when crystallized from methanol; (3) boiled culture broth of *L. enzymogenes* (i.e., 10 min in a water bath) inhibited fungal spore germination but the boiled culture broth from polyketide synthase (pks) disrupted mutants failed to inhibit fungal spore germination (pks: genes for the biosynthesis of HSAF) (Yu et al., 2007; Tang et al., 2018); (4) boiled cell-free culture filtrates of *L. enzymogenes* (i.e., boiled for 5 min) retained inhibitory activity towards fungal growth (Kobayashi and Yuen, 2005); and (5) medium composition, culture temperature, and fermentation time was identified as being the most significant factors affecting the production of HSAF (Tang et al., 2018)

Genome analysis identified pks/nrps as the critical genes involved in the biosynthesis of HSAF in *L. enzymogenes* C3 (Yu et al., 2007). Initially, two polyketide precursors are synthesized synchronously by a single polyketide synthase (pks) and then assembled with one amino acid (ornithine) to form a macrocyclic lactam *via* cycloaddition reactions by a nonribosomal peptide synthetase (nrps) (Lou et al., 2011; Su et al., 2018). Also, other positive and negative regulatory factors may influence the biosynthesis of HSAF (Tang et al., 2018). Recent molecular studies (de Bruijn et al., 2015; Takami et al., 2017; Zhang et al., 2014) showed the presence of genes involved in the biosynthesis of unidentified bioactive secondary metabolites, indicating the need for more studies that aim to unravel their role in the control of plant diseases.

Besides their biocontrol potential, *Lysobacter* strains are also reported to play a significant role in the bioremediation of sites polluted with heavy metals and petroleum derivatives (Caliz et al., 2011; Luo et al., 2012; Yang et al., 2015; An et al., 2019). Thus, the genus *Lysobacter* holds excellent potential for a broad spectrum of applications.

2.5 The genus *Pseudomonas*

Pseudomonas is one of the most complex genera with the most significant number of Gram-negative bacterial species (Silby et al., 2011). Since its first description, the introduction of isolates to the genus has been contentious (Stanier et al., 1966), and currently, there are 255 species and 18 subspecies (Samarzija and Zamberlin, 2022). Bacterial species in this genus show remarkable versatility in physiological and metabolic profiles (Palleroni, 1992). This versatility enables the species to colonize diverse terrestrial and aquatic habitats; thus, they are of great interest and importance in plant health and development, human disease and biotechnological applications (Silby et al., 2011).

Pseudomonas species have been extensively studied in plant health and development through their interactions with host plants, and several of them are regarded as plant growth-promoting rhizobacteria (PGPR) (Lamers et al., 1988; Pieterse et al., 2021). Moreover, they are abundant in the rhizosphere of plants and are known for the biocontrol of plant pathogens, including fungi and oomycetes (Loper and Gross, 2007; Narayanasamy, 2013). For example, Ghirardi et al. (2012) studied the colonization of the tomato rhizosphere by 23 *P. fluorescens* strains and identified two main traits responsible for rhizosphere competitiveness. The first trait was utilizing various organic compounds such as nitrogen oxides and oxygen as electron donors and acceptors. The second trait was the ability to produce antibiotic compounds such as phenazines and diphloroglucinol.

Similarly, Cole et al. (2017), via genome-wide mapping of the root colonizer *P. simiae* strain, identified more than 100 genes encoding traits that have significance in competitive root colonization of *Arabidopsis thaliana* roots. Of the traits, defence-related genes, sugar metabolism and motility were found to be the most important for root colonization. Thus, *P. simiae* species are now considered model root-colonizing bacteria (Samad et al., 2019; Pieterse et al., 2021). The *P. simiae* strains were previously identified as *P. fluorescens* due to physiological, morphological, and phenotypic similarities (Martinez-Garcia et al., 2015; Godebo et al., 2020; Pieterse et al., 2021). However, based on nucleotide identity, these strains are now recognized as *P. simiae* (Godebo et al., 2021; Pieterse et al., 2021). *Pseudomonas simiae* WCS417, previously identified as *P. fluorescens* WCS417, is one of the best-studied plant growth promoters and a biocontrol agent of take-all disease in field-grown wheat (Pieterse et al., 2021).

Pseudomonas simiae WCS417 has been under scientific study for over three decades since its first isolation in 1988 from lesions of wheat roots growing in a take-all disease-suppressive soil (Lamers et al., 1988; Yu et al., 2021; Verbon et al., 2022). This strain was also reported to suppress Panama disease incidence caused by *F. oxysporum* f. sp. cubense by 87.4% (Nel et al., 2006). Moreover, Ton et al. (2002) and Van der Ent et al. (2008) indicated that WCS417 also suppressed the oomycete pathogen *Hyaloperonospora arabidopsidis*. Gómez-Lama et al. (2022) studied the impact of *P. simiae* PICF7 and labelled the strain as a versatile biocontrol and plant-growth-promoting rhizobacteria on banana holobiont and identified induced systemic resistance (ISR) markers. Moreover, following its introduction into the soil under controlled conditions, a significant shift in microbial community interactions through co-occurrence network analysis was observed; however, there was no alteration in the composition and structure of the root microbiota (Gómez-Lama et al., 2022). A study by Martínez-García et al. (2015) indicated that *P. simiae* PICF7 is an effective biocontrol agent against the soil-borne fungus *Verticillium dahliae*, the causal agent of one of the most devastating diseases of olive (*Olea europaea* L.). Therefore, based on these review findings, *P. simiae* strains, including *P. simiae* K-Hf-L9 (Godebo et al., 2020) that suppressed ARR and one of the main strains in the current study have potential promise for biotechnological development as a biological control agent.

2.5.1 *Pseudomonas simiae* as biocontrol agents and mechanisms of action

Several *Pseudomonas* species, including *P. simiae* strains, are named PGPR, because of their capacity to promote plant growth through direct and indirect mechanisms (Glick, 2012; Pieterse et al., 2021). Direct mechanisms refer to promoting plant growth in a pathogen-free system by providing plants with resources and nutrients they lack, such as iron, phosphorus and fixed nitrogen (Glick, 2012; Olanrewaju et al., 2017). The indirect mechanisms refer to bacterial traits that inhibit the functioning of soil-borne pathogens, thus, reducing disease incidence in the host plant (Olanrewaju et al., 2017). Such traits common in *Pseudomonas* species include the occurrence of ACC deaminase, antibiotics, cell wall degrading enzymes, competition, hydrogen cyanide, induced systemic resistance, quorum quenching and siderophores (Singh et al., 1999; Frankowski et al., 2001; Ma et al., 2002; Ma et al., 2002; Mazurier et al., 2009; Cornforth et al., 2014).

Biological mechanisms can have either a direct or indirect impact on the plant pathogen. For instance, direct effects on the pathogen can occur via antibiosis, parasitism, or competition for

space and nutrients, whereas indirect effects include stimulating host defence mechanisms like induced systemic resistance (ISR), systemic acquired resistance and local responses (Bubici et al., 2019). Research findings indicated that *P. simiae* strains also play a significant role via direct and indirect mechanisms. For example, studies comparing *P. simiae* WCS417 (wild-type) and mutant strains lacking the iron-chelating siderophore known as pyoverdine demonstrated that a wild-type was capable of promoting plant growth by suppressing fusarium wilt pathogens in carnation (*Dianthus caryophyllus*) through competition for iron in the soil (Duijff et al., 1993; Van Peer et al., 1990). In a related study, in a pathogen-free system the wild-type was able to promote plant growth in Arabidopsis (Pieterse and Van Loon, 1999). Similarly, different strains of *P. fluorescens* isolated from paddy field soil inhibited mycelial growth of the root rot pathogen *F. oxysporum* via producing siderophore-mediated antagonistic activity (Chaiharn et al., 2009).

For root-associated bacteria with attributes of biocontrol capacity and plant growth promotion like *Pseudomonas* spp., colonization of the rhizosphere is an essential step (Bakker et al., 2013). In line with this, Pieterse et al. (2014) and Gao et al. (2018) demonstrated that a fluorescent labelled *P. simiae* WCS417 was able to colonize the roots exterior of Arabidopsis and the grass species *Brachypodium distachyon*, respectively. However, no entophytic growth was detected in both plants. In contrast, an earlier report indicated that the strain was able to colonize the tomato root interior and grow endophytically (Duijff et al., 1997), suggesting strain and plant root specificity.

Complete genome sequencing and analysis of *P. simiae* strain WCS417 identified 11 secondary metabolite biosynthetic gene clusters (BGCs), which affect neighboring microbes or processes in the host plant and enable the strain to outcompete microbes that share the same niches in the rhizosphere (Berendsen et al., 2015; Stringlis et al., 2018). In addition, several root-associated *Pseudomonas* species were reported to possess BGCs encoding for the production of antimicrobial compounds like 2, 4-diacetylphloroglucinol, cyclic lipopeptide biosurfactants, phenazines, pyrrolnitrin and hydrogen cyanide; however, these were reported to be absent in the *P. simiae* strain WCS417 genome (Loper et al., 2012). Therefore, Pieterse et al. (2021) concluded that although the presence of a betalactone with putative antibacterial activity, bactericidal proteins with a narrow taxonomic range of effectiveness, and a few bacteriocins were detected in *P. simiae* WCS417, it has limited potential to produce known anti-microbial agents. Thus, the antagonistic

and biocontrol potential of the *P. simiae* is believed to be mainly through siderophore-mediated competition for iron (Berendsen et al., 2015).

2.6 The genus *Pantoea*

The genus *Pantoea* constitutes bacterial species characterized as non-spore-forming, non-encapsulated, Gram-negative bacteria belonging to the family of Enterobacteriaceae. The genus contains 40 described species and two subspecies which commonly occur in habitats like water, soil, human, animals, and plants (genus *Pantoea*, <https://www.bacterio.net/genus/pantoea>). The taxonomy of the genus is continuously evolving due to improved taxonomic methodologies; for example, bacterial species such as *P. terrea*, *P. punctate* and *P. citrea* which were once in *Pantoea* were moved to a new genus *Tatumella* (Brady et al., 2010). Other *Pantoea* species like *P. gaviniae*, *P. calida*, *P. intestinalis* and *P. theicola* were transferred to a new genus *Mixta* (Palmer et al., 2018).

The *P. agglomerans* belonging to *Pantoea* are primarily epiphytic (Andrews and Harris, 2000; Lindow and Brandl, 2003; Grimont and Grimont, 2005). However, like the rest of the *Pantoea*, they are commonly found in diverse ecological niches (Brown and Leff, 1996; Laitinen et al., 1999; Francis et al., 2000), and several of them have been reported as biocontrol agents. For example, strains of *P. agglomerans* are sold as commercial biological control agents against various plant diseases such as fire blight of apple and pear trees (Johnson and Stockwell, 1988; Wodzinski et al., 1994), basal kernel blight of barley (Braun-Kiewnick et al., 2000) and post-harvest fungal diseases of pome fruits (Bonaterra et al., 2003; Bonaterra et al., 2005; Frances et al., 2006). Moreover, here in Canada, the United States and New Zealand strains of *P. agglomerans* are registered for biocontrol of fire blight under the product name BlightBan C9-1™ and Bloomtime™ in Canada and the United States and BlossomBless™ in New Zealand (Ishimaru et al., 1988; Vanneste et al., 2002; Pusey et al., 2008).

Although *P. agglomerans* have been used as commercial biocontrol agents in Canada, the United States and New Zealand and approved by their respective Pest Management Regulatory Agencies (Health Canada PMRA, 2009), their registration efforts in Europe are not successful due to biosafety concerns. This concern was due to the presence of clinical reports that identified strains of *P. agglomerans* as opportunistic human pathogens and thus classified the species as a biosafety level 2 organism in Europe (Geere, 1997; Kratz et al., 2003; Van Rostenberghe et al., 2006;

Bergman et al., 2007; Cruz et al., 2007). However, ascertaining its pathogenicity is challenging because the clinical reports are always polymicrobial, meaning the report often involves patients already affected by diseases of other origins (Cruz et al., 2007). This suggests the need for more investigations that clarify whether agriculturally beneficial isolates of the *P. agglomerans* are different from their clinical counterpart or harbour potential pathogenic traits that would justify their current biosafety limits in Europe. In this regard, comparative genome analysis becomes a valuable tool.

2.6.1 *Pantoea agglomerans* as biocontrol agents and mechanisms of action

The *P. agglomerans* have been identified as an antagonist of many plant pathogens belonging to bacteria and fungi through competitive exclusion, which involves the occupation of sites otherwise colonized by the pathogen and/or the production of antibiotics which target amino acid biosynthesis in the pathogen (Wright et al., 2001; Vanneste et al., 2001; Pusey et al., 2011; Sammer et al., 2012; Kamber et al., 2012; Smith et al., 2013). However, in addition to antibiosis and competition, the other mechanisms of the antagonistic properties of *P. agglomerans* are less known and are often related to the induction of plant resistance to disease development (Han et al., 2000; Ortmann and Moerschbacher, 2006; Ortmann et al., 2006). Moreover, Chernin et al. (1995) demonstrated that strains of *P. agglomerans* exhibit strong anti-fungal activity via the chitinolytic mechanism. Therefore, the biocontrol activity of the *P. agglomerans* strain towards the fungal pathogens is likely through the production of antimicrobial compounds, including antibiotic and chitinolytic enzymes, and competitive exclusion.

Strains of *P. agglomerans* were reported to be effective against several important fungal plant pathogens, including the ones that cause root rot in peas and lentils. For instance, *P. agglomerans* are reportedly effective against wheat pathogens such as *Puccinia recondite* f. sp. *Tritici*, which causes brown rust; and *Fusarium culmorum*, which causes seedling and head blight, and root rot (Kempf and Wolf, 1989). Additionally, *P. agglomerans* is effective against the pathogen *F. avenaceum* and *F. oxysporum*, which are commonly part of the RRC in peas and lentils (Romanenko and Alimov, 2000). Also, the *P. agglomerans* strains have been reported to be effective against *F. graminearum*, which causes fusarium head blight and results in a significant loss of productivity in oats, maize, wheat, and barley (Pandolfi et al., 2010). Moreover, *P. agglomerans* were reported to be effective against the plant pathogenic fungus *Rhizoctonia solani*, which has a wide host range also causes root rot in pea and lentil (Rosales et al., 1993).

2.7 Genome sequencing and assembly

The evolution of second-generation sequencing technology advanced the traditional Sanger sequencing standard, first developed and introduced by Sanger et al. (1977). Second-generation sequencing technology, also known as high-throughput DNA sequencing, is now broadly accessible due to a decrease in instrument and consumables costs, and it is now available in many laboratories to execute their internal genome sequencing projects (Hu et al., 2021). However, generating a complete microbial genome assembly using second-generation sequencing technologies remained a challenge for many years due to the complex nature of genomes (Altermann et al., 2022). Rapid technological advances continue to improve genome sequencing. For example, Pacific Biosciences (PacBio) uses a single-molecule real-time (SMRT) sequencing approach, which produces a significantly longer read length compared to second-generation technologies (Ben Khedher et al., 2022). Although PacBio reads from the third generation PacBio sequencing platform contain low accuracy (error rate of about 15%), the data generated is expected to resolve complex repeats (Ben Khedher et al., 2022). The MinION (Oxford Nanopore Technologies) is another long-read single-molecule genome sequencing instrument that is the size of a typical smartphone (Lu et al., 2016; Wang et al., 2021; Ben Khedher et al., 2022). The technology directly senses native, individual DNA fragments without the need for amplification, and it can sequence extremely long fragments (>10 kb) of DNA without a reduction in sequence quality (Giguere, 2022). Various hybrid strategies such as ALLPATHS-LG6, PacBio corrected reads (PbCR) pipeline, SPAdes and SSPACE-LongRead were proposed to overcome the issue of high repetitiveness and low accuracy and construct a complete microbial genome (Miller et al., 2017; Kammonen et al., 2019; Hackl et al., 2022). As opposed to hybrid approaches and PacBio long reads that introduce random errors, nonhybrid strategies that entirely use long reads to produce *de novo* microbial genome assemblies were developed (Gonzalez-Garcia et al., 2022).

De novo assembly is the reconstruction of a genome sequence without the aid of any other information aside from the reads produced by the sequencing process (Edwards and Holt, 2013; Zhang et al., 2021; Gonzalez-Garcia et al., 2022). It is accomplished by similarity alignments made among the reads themselves or through the overlap of k-mers. The final output of the algorithm is contiguous sequences (contigs), as shown in Fig. 2.1 (Edwards and Holt, 2013; Lynch et al., 2016). The construction of the initial contigs requires determining the longest overlap, and optimal placement of shorter reads results in a draft genome. This draft genome can progress into a "high-

quality draft genome" with the addition of information such as optical mapping data, mate-pair or long-read sequences (Yuan et al., 2020). The draft genome also can progress to "closed genome" when gaps between contigs scaffolds are resolved or "finished genome" when any misassemblies or other sequencing anomalies and uncertainties are resolved (Lynch et al., 2016; Lood et al., 2022).

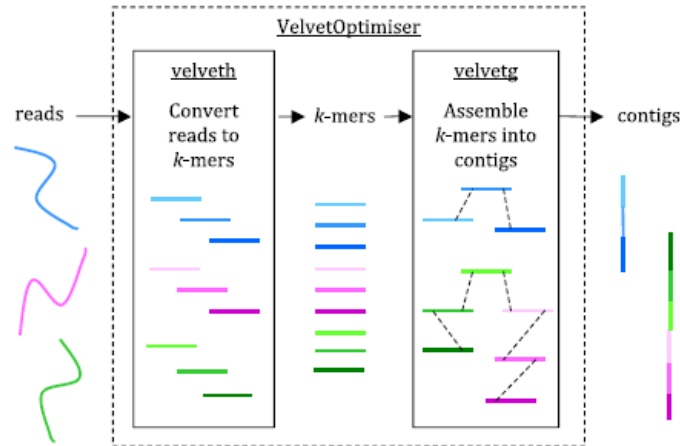


Figure 2.1 Genome assembly with Velvet. Reads are assembled into contigs using Velvet and VelvetOptimiser in two steps, (1) velveth converts reads to k-mers using a hash table, and (2) velvetg assembles overlapping k-mers into contigs via a de Bruijn graph (Edwards and Holt, 2013).

2.8 Bacterial genome annotation

Once the contigs assembly is complete and the draft genome is obtained, the next step is genome annotation. Genome annotation is the process of identifying gene and gene clusters, including ribosomal and tRNAs encoded in the genome, and assigning descriptive information to these features (Edwards and Holt 2013; Lynch et al., 2016; Abril and Castellano, 2019; Peter et al., 2019). The protein-coding genes, known as coding sequences (CDS), and the noncoding genes, such as the rRNA and tRNA, are typically annotated in bacterial genomes (Richardson and Watson, 2013; Thibaud-Nissen, 2022).

Genome annotation is either structural or functional (Harbola et al., 2022). Structural annotation, also known as gene finding or gene prediction, identifies the location of the protein-coding genes (CDS) and the non-coding genes (tRNA and rRNA) (De Sa et al., 2018; Peter et al., 2019; Harbola et al., 2022). Functional annotation assigns descriptive information to these features (Lynch et al., 2016; Lueder et al., 2021). Although the functions of the non-coding genes are

apparent, the protein-coding sequences have a diverse role that is not easily understood. Therefore, the protein-coding sequences usually undergo functional annotation to deduce their predictive biological function (Ejigu and Jung, 2015; Song et al., 2018; Zhao et al., 2020). The schematic representation of the bacterial genome annotation process is presented in Fig. 2.2 (Lynch et al., 2016).

Bacterial genome annotation can be accomplished by uploading the assembled genome file to a fully automated web-based tool, like the rapid annotations subsystems technology (RAST) (Aziz et al., 2008) or by using command-line annotation tools including the methods based on *de novo* discovery of genes, like Prokka (Seemann, 2014) and DIYA (Do-It-Yourself Annotator) (Stewart et al., 2009). The RAST pipeline is an easy-to-use online *de novo* annotation tool that uses a series of subsystem techniques to compare sequence reads that are likely to be genes with a sophisticated database of genes and RNA sequences. The RAST generates high-quality annotation output that is downloadable in a variety of formats, including in GenBank format (Aziz et al., 2008).

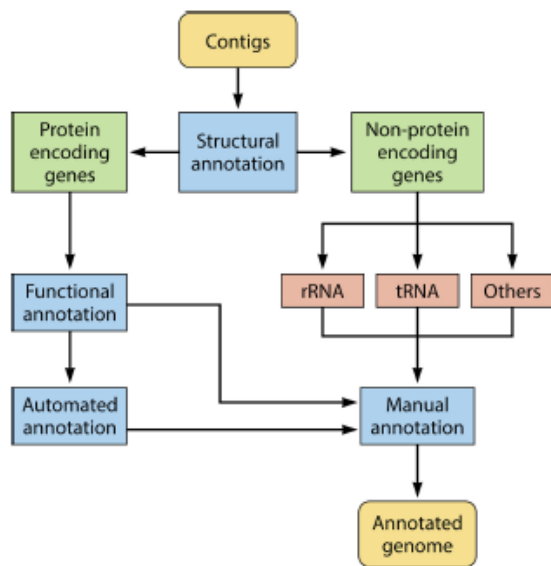


Figure 2.2. Overview of bacterial genome annotation. Structural annotation identifies the location of genes on the contigs of an assembled bacterial genome. Protein-encoding locations are identified, followed by automated assignment of gene function by comparison to existing databases. Non-protein-encoding genes are annotated by identifying key signatures for each type of gene. The resulting annotations are combined with an optional manual curation that can be performed before the final annotated genome is produced (Lynch et al., 2016).

2.9 Comparative genome analysis

Genome comparison to other genomes or DNA sequences is an integral part of functional genomics experiments that answers questions like "which genes do these genomes share and which are unique to particular genomes?" Researchers interested in searching for specific genes that are responsible for the biocontrol activity of plant pathogens are likely to ask questions of this nature. Different software tools are used for genome comparison, and most users utilize tools that generate figures. These figures are not only essential to visualize the comparisons and aid interpretation of the data but also facilitate the communication of results. The Java-based software tool called BLAST Ring Image Generator (BRIG) visualizes the comparison of a reference sequence to a set of query sequences (Alikhan et al., 2011). The comparative analysis outputs are plotted as a series of rings with each ring denoting a query sequence that is differentiated with colour to indicate the presence of hits to the reference sequence.

It is essential to bear in mind that genome comparison using BRIG is reference-based and reveals the regions of the reference sequence that are present or absent in query sequences. However, it cannot show the area of the query sequences that are missing from the reference sequence. Thus, the reference sequence that is chosen for comparative purpose plays a significant role in the understanding of the output. For example, in Fig. 2.3 below an enterohaemorrhagic *E. coli* (EHEC) genome is used as the reference sequence and the *E. coli* O104:H4 outbreak genome assembly, together with other pathogenic *E. coli* genomes, which are used as queries (Edwards and Holt, 2013). The generated figure indicated that the outbreak strain differs from the other EHEC in terms of gene content but shares with it the Stx2 phage sequence, which is missing from enteroaggregative *E. coli* (EAEC) and enteropathogenic *E. coli* (EPEC). This concept can be applied to compare aphanomyces biocontrol bacterial genomes with phylogenetically related bacteria differing in a specific aspect. This comparison can encompass those bacteria, for example, lacking biocontrol activity and harbouring gene/gene cluster encoding virulence to humans and plants.

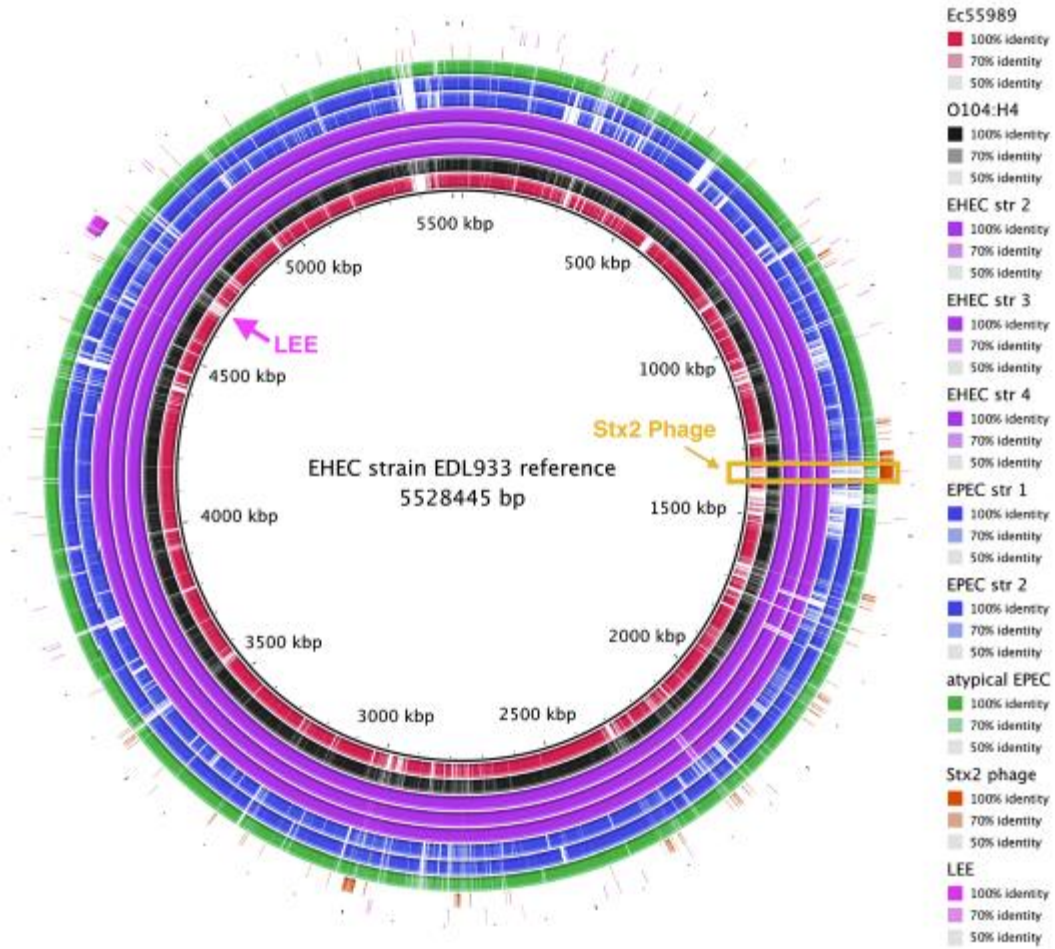


Figure 2.3. BRIG for multiple genome comparisons. It is easy to see that the Stx2 phage is present in the *E. coli* (EHEC) (purple) and the outbreak genome an *E. coli* (EAEC) (black), but not the EAEC or EPEC chromosomes (Edwards and Holt, 2013).

3. A META-ANALYSIS TO DETERMINE THE STATE OF BIOLOGICAL CONTROL OF APHANOMYCES ROOT ROT¹

3.1 Preface

Aphanomyces root rot is a destructive disease of legumes, most notably in peas and lentils worldwide. Hence, to control this disease, several scientists have conducted research assessing effects of microbial biocontrol agents on aphanomyces on artificial culture media, *in vivo* (*in planta*) biocontrol assays in controlled growth chamber conditions, and in agricultural field experiments. However, despite these studies, a systematic review reflecting the current state of the science of biological control of ARR is unavailable. Therefore, the goal of this chapter was to conduct a meta-analysis using previously published articles investigating the biological control of ARR and provide insight into its current state. This study identified the potential promise for biological control of ARR using biocontrol agents and the need for more field-based trials to replicate the findings of the lab and growth chamber trials.

¹This chapter is published in Frontiers Journal (Frontiers in Molecular Biosciences) as Godebo, A. T., Wee, N. M. J., Yost, C. K., Walley, F. L., & Germida, J. J. (2021). A Meta-Analysis to Determine the State of Biological Control of Aphanomyces Root Rot. Frontiers in molecular biosciences, 8. DOI: [10.3389/fmolb.2021.777042](https://doi.org/10.3389/fmolb.2021.777042)

3.2 Abstract

The increasing incidence and prevalence of the pathogen *Aphanomyces euteiches* in various pulse-growing regions worldwide necessitates the development of effective management strategies, including biological control agents. Numerous labs have undertaken research examining biological control methods to evaluate ARR suppression in multi-step processes that include isolation of inhibitory organisms, lab assays, growth chamber assays, and field trials. Given the emergence of various biocontrol agents and the need to mitigate aphanomyces yield losses, a meta-analysis approach was undertaken to analyze the effectiveness of biocontrol agents in relation to application method, biocontrol agent richness, biocontrol agent type, the type of study, and reporting system-oriented moderator variables. An effect size, calculated as a natural log response ratio, resulted in a summary weighted mean of -0.411, suggesting the overall effectiveness of biocontrol agents ($P < 0.001$). *Aphanomyces* root rot suppression using biological treatments showed significant heterogeneity for all moderator variables, confirming that the studies do not share a common effect size and the use of a random effect model was appropriate. Across studies, meta-analyses revealed that soil amendments, biocontrol agent application as a seed coating and suspension, bacterial and fungal biocontrol agents, mixed applications, growth chamber and field studies, qualitative and quantitative reporting systems were all associated with significantly positive outcomes for ARR suppression. The findings suggest that there is a potential promise for biological control of ARR, and more field trials need to be conducted to demonstrate the efficacy level observed under growth chamber conditions. Moreover, this study identified a lack of detailed understanding of the mechanism(s) of biological control of ARR as a research priority.

3.3 Introduction

Aphanomyces root rot caused by the soil-borne oomycete pathogen *Aphanomyces euteiches* affects the belowground portion of the developing plant, leading to poor yields in pulse crops (Saskatchewan Pulse Growers, 2017). Although *A. euteiches* can be isolated from alfalfa (*Medicago sativa* L.), snap bean (*Phaseolus vulgaris* L.) and red kidney bean (*Proteus vulgaris* L.), faba bean (*Vicia faba* L.), red clover (*Trifolium pratense* L.), white clover (*Trifolium repens* L.), and several weed species, it causes the greatest economic impacts to pea (*Pisum sativum* L.) and lentil (*Lens culinaris* Medik.) crops (Wu et al., 2018). The genus *Aphanomyces* comprises three subgroups: *Aphanomyces* plant pathogens; *Aphanomyces* aquatic animal pathogens; and *Aphanomyces* saprophytic species (Gaulin et al., 2018). Among the plant pathogens, *A. euteiches*

is the most destructive pathogen (Wu et al., 2018). Moreover, although the oomycete pathogen *Pythium* can be controlled by seed treatments (Chatterton et al., 2016) and fungicides that control root rot causing pathogens like *Fusarium* are available, they are not providing adequate protection against ARR (Top Crop Manager, 2021).

Currently, no successful management method exists for control of ARR. Crop rotation, disease avoidance and host resistance are reported to offer limited success (Wakelin et al., 2002; Sauvage et al., 2007; Hughes and Grau, 2013; Conner et al., 2013). At present, INTEGOTOTM Solo (ethaboxam) and Vibrance[®] Maxx RFC are two registered fungicides for suppressing an early season ARR in field pea and lentil in Canada (Guide to Crop Protection, 2021). Due to the lack of effective control methods and the growing demand for sustainable production practices, biological control methods are proposed to offer an effective, safe, and environmentally favourable alternative (Godebo et al., 2020). Xue et al. (2003) and Godebo et al. (2020) reported that biocontrol of ARR could be achieved using antagonistic microbes. Several biocontrol agents with varying levels of biocontrol efficacy are commercialized as biocontrol agents for other plant pathogens. Some examples of these products include Integral (*B. subtilis* MBI 600) for *Rhizoctonia* spp. and *Fusarium* spp.; Kodiak (*Bacillus subtilis* GB03) for *Rhizoctonia* spp., *Fusarium* spp., and *Aspergillus* spp.; and Serenade (*B. subtilis* QST 713) for *Botrytis* spp., *Sclerotinia* spp., *Xanthomonas* spp., and *Erwinia* spp. (Liu et al., 2017). The nomenclature of these *Bacillus subtilis* species is now changed to *Bacillus velezensis* (Dunlap et al., 2016).

Several factors, including the type of the biocontrol agent, biocontrol agent richness, method of application, and study type, influence the effectiveness of a biocontrol agent in controlling plant pathogens (Chandrasekaran et al., 2016). For instance, mixed application of biocontrol agents may be assumed to offer more significant suppression of plant pathogens. However, a study by Dandurand and Knudsen (1992) reported that ARR suppression was not significantly different when pea seeds were treated with a combination of *Trichoderma harzianum* and *Pseudomonas fluorescens* strains compared to treatment with *T. harzianum* alone. Thus, due to these and other factors, biocontrol research reports indicate the level of plant disease suppression is inconsistent among and between studies investigating similar biocontrol agents. Moreover, an increasing number of studies report several biocontrol agents demonstrate variable efficacy in controlling ARR. Because of these apparent contradictory observations, there is a need to conduct a meta-

analysis study to determine the state of the biological control of ARR and draw conclusions that will direct future research.

Meta-analysis provides a critical and quantitative review of research data extracted from various studies to determine the influence of treatment (experimental) factors on effect sizes and evaluate possible publication bias (Rosenberg et al., 2004). Meta-analysis offers the opportunity to draw a holistic conclusion based on primary experimental findings from several studies (Nelson et al., 2015). Others have used this approach to examine biocontrol agents. For example, Chandrasekaran et al. (2016) performed a meta-analysis to quantify the overall efficacy of biocontrol agents in reducing *Ralstonia* wilt and their effect on growth promotion and crop yield. Shrestha et al. (2016) conducted a meta-analysis to understand the efficacy of the non-chemical practice anaerobic soil disinfestation on a range of soil-borne pathogens, nematodes and weeds. In this review, meta-analysis was used to quantitatively analyze the findings of 24 published studies (Appendix A) on the biological control of ARR.

3.4 Material and methods

3.4.1 Literature review and data collection

A database of research articles investigating the potential for biological control of *A. euteiches* was assembled using Web of Science (<https://www.webofscience.com>) in April 2021. The keyword used for the initial search, "*Aphanomyces*," returned 1285 search results. These search results were filtered to 449 articles using the keyword "*Aphanomyces euteiches*" and to 41 using the keyword "biological control." Articles were also searched in other sources, namely Science, (<https://www.sciencemag.org>), Nature (<https://www.nature.com>), Elsevier-Science Direct (<https://www.sciencedirect.com>), Springer (<https://www.springer.com>), Wiley & Sons (<https://onlinelibrary.wiley.com>), Scopus (<https://www.scopus.com>) and Google Scholar (<https://scholar.google.com>). The articles were further screened for meeting inclusion criteria. These criteria for including a study were: 1) a treatment with at least one biocontrol agent; 2) reporting a measure of disease intensity (disease incidence or disease severity); and 3) employing statistical methods for data analysis. This meta-analysis did not include studies solely investigating chemical control agents. Based on these inclusion criteria, the meta-analysis included 24 published articles spanning 1990 to 2020 (Fig. 3.1 and Appendix A).

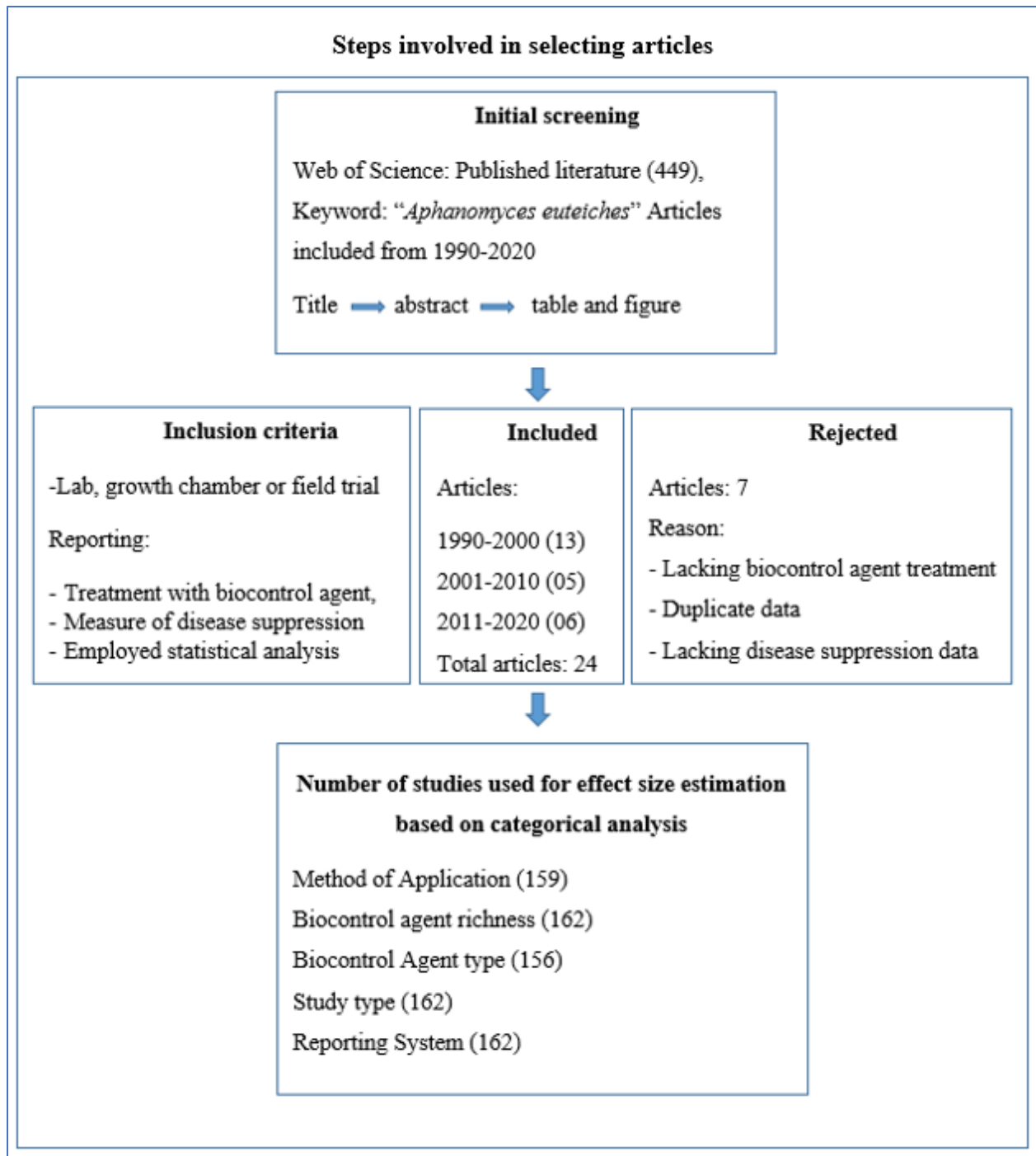


Figure 3.1. Diagrammatic representation of the steps involved in selecting articles.

Treatment means and sample sizes were collected for each study to investigate the impact of biocontrol agents on suppressing ARR in relation to five factors determined as moderator variables. Biocontrol agent treatment means were those that were evaluated for biocontrol activities in the respective studies. In contrast, positive controls that only received the pathogen

were considered control means (i.e., positive controls in each study). Multiple biocontrol agents studied in an article were treated as independent studies commonly regarded as paired observations in meta-analysis literature. Hence, each biocontrol agent represented individual units in this meta-analysis. For instance, Godebo et al. (2020) reported biocontrol efficacy data for 20 strains from two growth chamber studies. Each trial evaluated ten different bacteria; accordingly, that article resulted in 20 studies, and this approach is consistent with that used by Shrestha et al. (2016). Thus, the entire data set consisted of "162 studies" from 24 published articles (Appendices A and B).

3.4.2 Moderator variable and categorical analysis

A moderator variable is a variable that can alter the association between the study factors (independent variables: for example, biocontrol agent application method) and the outcome (the dependent variables: for example, response ratio) (Allen, 2017). Various moderator variables affecting ARR suppression were identified, categorized, and categorical moderator analysis was conducted using Comprehensive Meta-Analysis Version 3 software (Borenstein et al., 2013). The first moderator variable was the application method, and it was categorized into three levels: seed coating, suspension, and amendment. Seed coating and suspension refer to biocontrol inoculants applied *via* seed coating and liquid formulations, respectively. The amendment describes plant growing media amended with compost, green manure, and other plant products for the purpose of suppressing ARR. The second variable was biocontrol agent richness, and it describes the number of biocontrol agents inoculated for the biocontrol assessment of *A. euteiches* in a single inoculation. It was evaluated into two levels as single and mixed organism inoculation. Single organism inoculation refers to the inoculation of a single biocontrol agent. In contrast, mixed organism inoculation is the application of two or more biocontrol agents as a co-inoculation. The third variable was biocontrol agent type, which represented studies that reported the taxonomical identity and type of the biocontrol agents. This was divided into five levels: bacteria, fungi, green manure, compost, and plant product that did not incorporate synthetic chemical products. The fourth variable was the type of the study, which denotes the studies that investigated the inhibition of *A. euteiches* growth and suppression of root rot symptom development. This was categorized into three levels: lab, growth chamber, and field studies. The lab study refers to studies conducted under laboratory conditions, including culture media-based *A. euteiches* growth inhibition and other inhibition assays undertaken in laboratory settings. The last moderator variable was the pathogen suppression reporting system analyzed in two groups as qualitative or quantitative. The

qualitative reporting system represented experimental data collected using a disease rating scale. In contrast, the quantitative reporting system included experimental data that measured pathogen infestation levels, for example, quantifying *A. euteiches* level in roots and measuring oogonia (*A. euteiches* developmental stage) production and plant dry weight. The host plant species (example: field pea versus lentil) and mechanism of action were not investigated as moderator variables due to the lack of sufficient data representing these two variables.

3.4.3 Effect size calculation and meta-analysis

The effect size of investigated biocontrol agents was estimated as a natural log of the response ratio ($\ln R$) as a measuring standard to assess the effectiveness of the treatments covered in each study. A response ratio is the ratio of measured outcome in the treated (treatment) group relative to measured outcomes in the treatments that received the pathogen only (i.e., positive controls in each study), as stated by Rosenberg et al. (2000). This meta-analysis used a random-effect model that assumes true effects varied across studies instead of a fixed model that considers the same value for all studies. Therefore, the effect size for each study was calculated according to the following formula: (Chandrasekaran et al., 2016)

$$\ln R = \ln(\mathbf{X}_t/\mathbf{X}_c) = \ln(\mathbf{X}_t) - \ln(\mathbf{X}_c) \quad (\text{Eq. 3.1})$$

R is the response ratio, \mathbf{X}_t is the biocontrol agent treatment mean, and \mathbf{X}_c is the control mean. Since the majority of the studies did not report a measure of dispersion, a non-parametric variance was calculated as stated in Shrestha et al. (2016) as:

$$V_{\ln R} = (\mathbf{n}_t + \mathbf{n}_c) / (\mathbf{n}_t * \mathbf{n}_c) \quad (\text{Eq. 3.2})$$

$V_{\ln R}$ is variance of the natural log of response ratios, \mathbf{n}_t is the treatment mean sample size, whereas \mathbf{n}_c is the sample size of the control mean.

3.4.4 Test of heterogeneity

During the moderator variable analysis, three \mathbf{Q} statistics were generated per factor, a measure of weighted squared deviation used to assess heterogeneity. The first \mathbf{Q} was the variation within categories, the second was the variation between categories, and the last was the total heterogeneity (\mathbf{Q}_t) which is composed of the within-study and between-study variation. The \mathbf{Q}

statistic is distributed as Chi-square and it shows the observed dispersion under the null hypothesis, and its anticipated value is equal to the degrees of freedom (**Df**). In addition, heterogeneity was measured using a descriptive index designated as I^2 , and it measures the ratio of true variation (Heterogeneity) to total variation across studies as described by Shrestha et al. (2016):

$$I^2 = ((Q_t - Df) / Q_t) * 100 \quad (\text{Eq. 3.3})$$

where **Df** represents the degree of freedom. When **Df** is larger than **Q_t**, negative value of I^2 is set to zero, so that I^2 lies between 0% and 100% and a value of zero means no true heterogeneity. A positive value indicates true heterogeneity, and large values represent a more significant proportion of the observed variation due to true heterogeneity among studies. Thus, much of the total heterogeneity can be addressed by subdividing studies into groups of interest. Homogeneity was considered invalid when the *P*-value for the Q-test (P_{hetero}) for heterogeneity was less than 0.1 (Bristow et al., 2013; Iacovelli et al., 2014; Shrestha et al., 2016).

3.4.5 Publication bias

Since meta-analysis is accepted as comprehensive, publication bias (i.e., systematic unrepresentativeness) is often raised as a concern with such analyses. This is due to the trend that significant treatment differences get published more than non-significant findings. Although it is difficult to find direct evidence of publication bias, it can be estimated using a statistical approach (Madden and Paul, 2011; Koricheva and Gurevitch, 2014). The concept behind publication bias analysis is that studies with smaller sample sizes and/or higher variance usually have greater effect sizes than large studies which have much more precision. Therefore, the publication bias analysis method involves understanding the relationship between study effect size and precision. In this meta-analysis publication bias was investigated statistically with Egger's regression test (Egger et al., 1997). The analysis output is presented graphically with funnel plots of effect sizes versus precision (standard error⁻¹). In addition, the iterative trim and fill method was used to visualize how the summary effect size would shift when significant bias was discarded.

3.5 Results

3.5.1 Measure of efficacy

In this meta-analysis, a natural log response ratio ($\ln R$) value less than zero represents inhibition of *A. euteiches* growth and suppression of root rot symptoms. In contrast, a $\ln R$ value

greater than zero shows no inhibition of the pathogen, no suppression of disease symptoms and more severe disease. Thus, a value of zero suggests no treatment effect on *A. euteiches* and disease incidence. The meta-analysis on cumulative efficacy detected a significant ($P < 0.001$) negative effect size (-0.411 [CI -0.516 to -0.306]) favouring inhibition of *A. euteiches* and suppression of disease symptoms (Fig. 3.2).

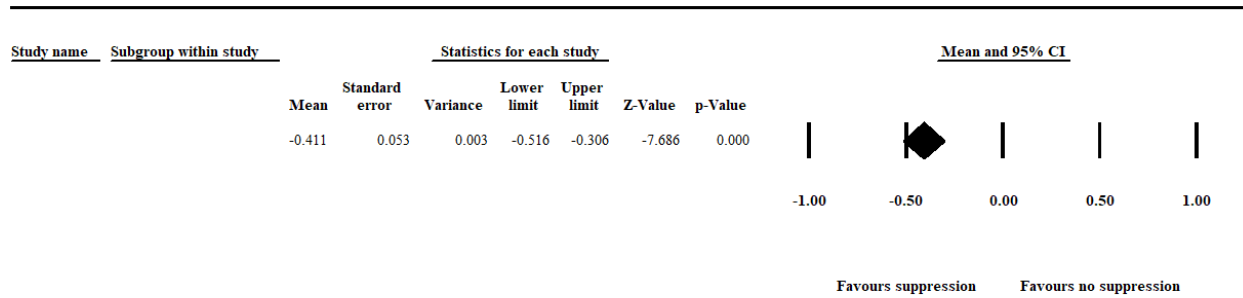


Figure 3.2. Cumulative analysis of effect size measuring efficacy on biological control of aphanomyces root rot. The analysis detected a significant ($p < .001$) negative summary effect size [-0.411 (CI -0.516 to -0.306)] suggesting suppression of *A. euteiches*. The center of the diamond depicts the overall mean effect size, and the width reflects its confidence interval. CI = confidence interval.

The subgroups under the respective moderator variables were considered significantly different from each other and the overall mean when there was no confidence interval overlap. Also, the true difference that is heterogeneity among studies within each moderator variable was determined based on I^2 and P_{hetero} . Results are grouped according to moderator variables as application method, biocontrol agent richness, biocontrol agent type, study type and reporting system. A random-effects model is used to combine studies within each subgroup, and the subgroups were further combined using the same model. Then, the resulting overall effect size was used to determine the moderator variable's impact on *A. euteiches* inhibition or suppression of disease symptoms.

3.5.1.1 Method of application

The analysis detected a significant ($P < 0.05$) negative effect size (-0.492 [CI -0.803 to -0.181]), favouring disease suppression when the application method was analyzed in relation to amendments (i.e., plant growing media amended with compost, green manure and other plant products). Also, application as seed coating and liquid suspension showed a significant ($P < 0.001$)

negative effect size (-0.329 [CI -0.445 to -0.213]) and (-0.367 [CI -0.505 to -0.229]), favouring disease suppression, respectively (Figs. 3.3).

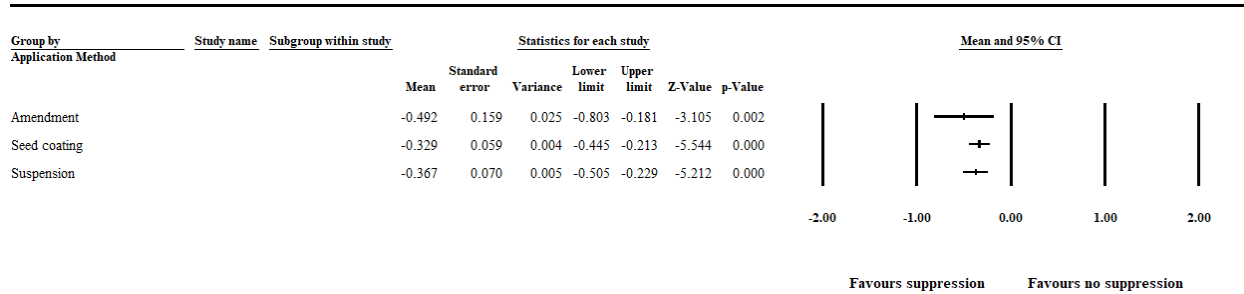


Figure 3.3. Effect of biocontrol agent application method on aphanomyces root rot suppression. The analysis detected a significant ($p < .05$) negative effect size for amendment, seed coating, and suspension. The center of the horizontal line depicts the effect size, and the width reflects its confidence interval. Number of studies: Amendment 35; Seed coating 79; Suspension 45. CI = confidence interval.

3.5.1.2 Biocontrol agent richness

The analysis of biocontrol agent richness effect on suppression of *A. euteiches* was categorized as single and mixed organism inoculation. The result showed a significant ($P < 0.001$) negative effect size (-0.899 [CI -1.292 to -0.507]) and (-0.374 [CI -0.481 to -0.267]) for mixed and single organism inoculation, respectively (Fig. 3.4).

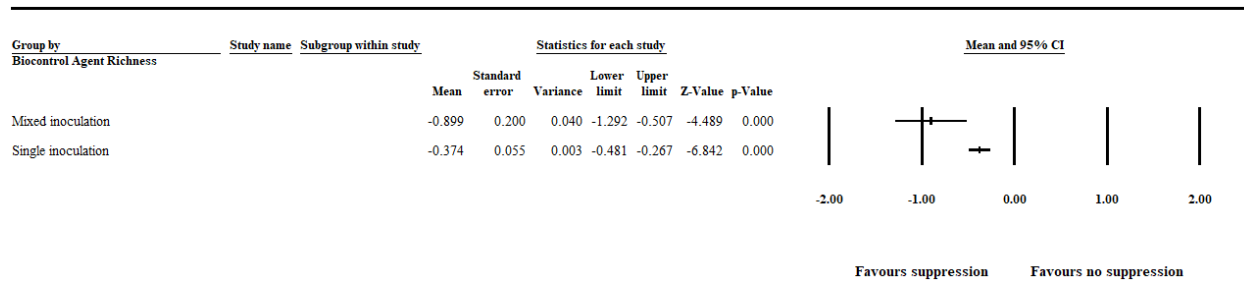


Figure 3.4. Effect of biocontrol agent richness on aphanomyces root rot suppression. The analysis detected a significant ($p < .001$) negative effect size for mixed and single organism inoculation favoring disease suppression. The center of the horizontal line depicts the effect size, and the width reflects its confidence interval. Number of studies: Mixed organism inoculation 11; Single organism inoculation 151. CI = confidence interval.

3.5.1.3 Biocontrol agent type

In this meta-analysis, in addition to bacterial and fungal agents, other treatments such as compost, green manure, and plant products (e.g., seed powder) used to suppress ARR were considered as biological treatments. Hence, bacteria, fungi, compost, green manure, and plant products were deemed individual levels in this category. The meta-analysis detected a significant negative effect size for bacteria (-0.225 [CI -0.311 to -0.138]), compost (-0.291 [CI -0.519 to -0.063]), fungi (-0.671 [CI -1.058 to -0.285]) and plant product (-0.907 [CI -1.578 to -0.236]) treatments. However, the summary effect size for green manure treatments was not significant (Fig. 3.5).

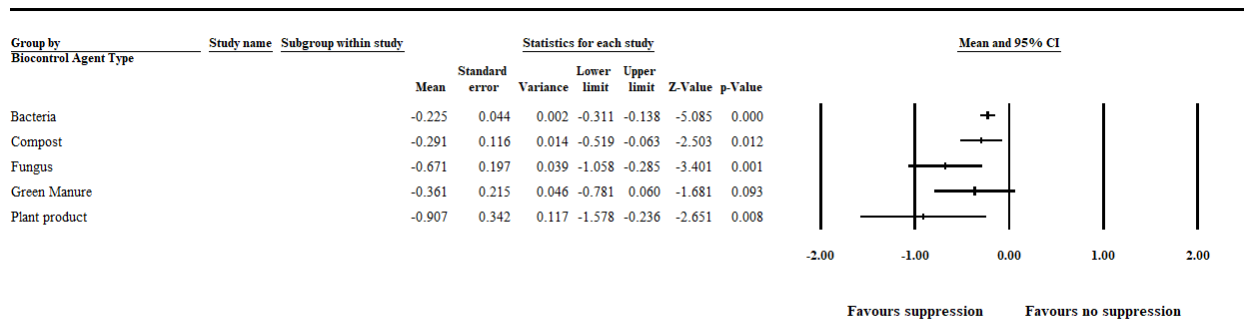


Figure 3.5. Effect of biocontrol agent type on aphanomyces root rot suppression. The analysis detected a significant ($p < .05$) negative effect size for bacterial, compost, fungal and plant product treatments. Number of studies: Bacteria 93; Compost 9; Fungus 26; Green manure 16; Plant product 12. The center of the horizontal line depicts the effect size, and the width reflects its confidence interval. CI = confidence interval.

Due to the relatively high number of treatments within the bacterial category, a separate analysis based on genus level grouping was performed to detect bacterial biocontrol agents (genus level) exhibiting greater efficacy compared to others in the same category. The meta-analysis detected bacterial biocontrol agents within the genus *Bacillus* and *Pseudomonas* as having a significant efficacy with both the lower and upper limits of the 95% CI laying in the region favouring ARR suppression (Fig. 3.6).

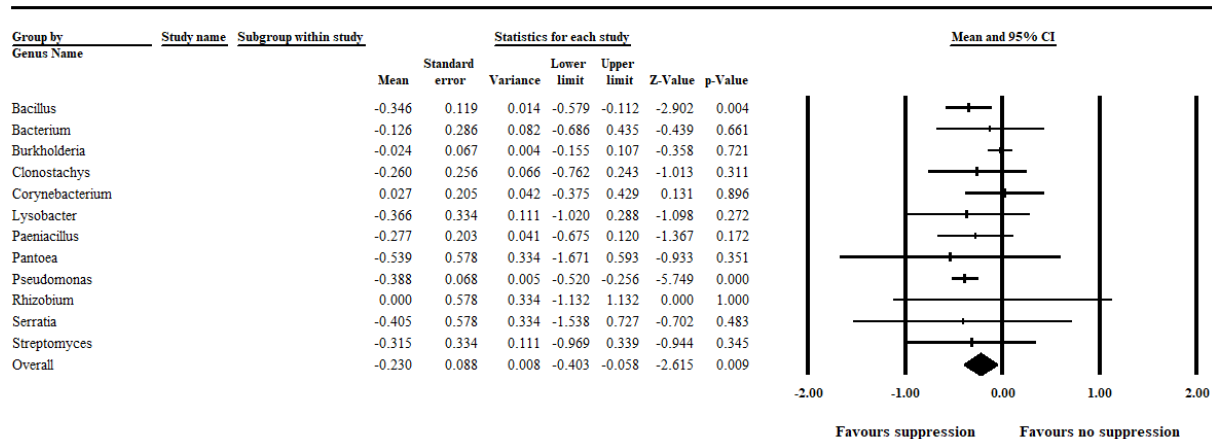


Figure 3.6. A separate meta-analysis on the bacterial treatment category indicates bacterial biocontrol agents within the genus *Bacillus* and *Pseudomonas* have a greater efficacy compared with others in the same category. The center of the diamond depicts the overall mean effect size, and the width reflects its confidence interval. CI = confidence interval. The *Pseudomonas cepacia* tested as a biocontrol agent in the Parke et al., 1991; and King and Parke, 1993 papers were included in the *Burkholderia* analysis, not in the *Pseudomonas* analysis.

3.5.1.4 Study type

The analysis detected a significant ($P < 0.05$) negative effect size (-0.301 [CI -0.591 to -0.011]), (-0.542 [CI -0.672 to -0.411]) and (-0.192 [CI -0.374 to -0.009]), favouring disease suppression when study type was assessed in relation to lab, growth chamber and field studies, respectively (Figs. 3.7).

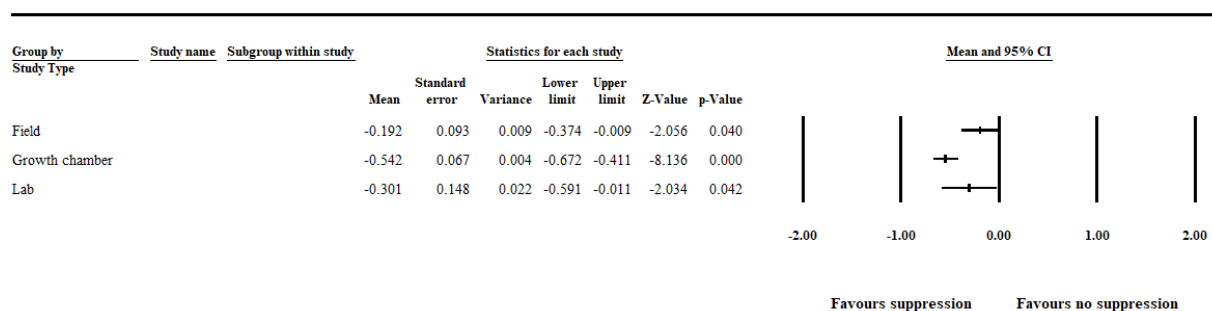


Figure 3.7. Study type impact on aphanomyces root rot suppression. The analysis detected a significant ($p < .05$) negative effect size for lab, growth chamber, and field studies. Number of studies: Lab 20; Growth chamber 101; Field 41. The center of the horizontal line depicts the effect size, and the width reflects its confidence interval. CI = confidence interval.

3.5.1.5 Reporting system

The analysis detected a significant ($P < 0.001$) negative effect size (-0.407 [CI -0.533 to -0.281]) and (-0.420 [CI -0.609 to -0.231]) for the quantitative and qualitative reporting systems (Fig. 3.8).

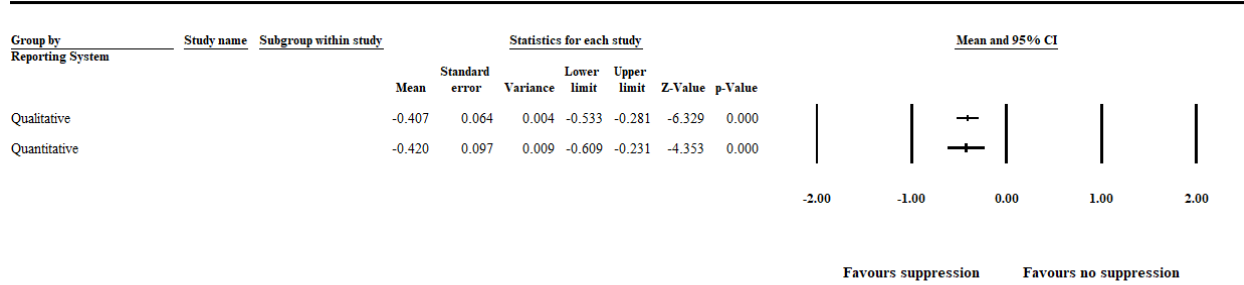


Figure 3.8. Effect of reporting system on aphanomyces root rot suppression. The analysis detected a significant ($p < .001$) negative effect size for the quantitative and qualitative reporting systems. Number of studies: Qualitative 111, and Quantitative 51. CI = confidence interval.

3.5.2 Test of heterogeneity

The null hypothesis for heterogeneity is that the studies share a common effect size. The test of heterogeneity addresses whether the observed dispersion among effects exceeds the amount that would be expected by chance. As indicated in Section 3.3.4, the Q statistic distributed as Chi-square shows the observed dispersion under the null hypothesis, and its anticipated value is equal to the degrees of freedom. Since Q tests the null hypothesis and assumes no dispersion across effect sizes, it is essential to quantify this dispersion. Hence, the dispersion is quantified based on the I^2 value. The heterogeneity analysis quantified that the overall I^2 is greater than 84 for each effect variable, which means that more than 84% of the observed variance between studies is due to real differences in the effect size. Thus, less than 16% of the observed variance would have been expected based on a random error (Table 3.1).

Table 3.1. Measures used to quantify dispersion across effect sizes in each moderator variable

Moderator variable	Levels	Heterogeneity				
		N	Q _i -value	Df (Q)	P-value	I ²
Application method	Amendment	35	422	34	<0.001	91.93
	Seed coating	79	618	78	<0.001	87.37
	Suspension	45	21	44	0.999	0.00
	Overall	159	1 128	158	<0.001	86.00
Biocontrol agent richness	Mixed inoculation	11	81	10	<0.001	87.68
	Single inoculation	151	1 165	150	<0.001	87.13
	Overall	162	1 291	161	<0.001	87.53
Biocontrol agent type	Bacteria	93	365	92	<0.001	74.81
	Compost	9	10	8	0.283	17.95
	Fungus	26	108	25	<0.001	76.81
	Green Manure	16	221	15	<0.001	93.21
	Plant product	12	130	11	<0.001	91.52
	Overall	156	1 018	155	<0.001	84.77
Study type	Field	41	266	40	<0.001	85.06
	Growth chamber	101	838	100	<0.001	88.07
	Lab	20	26	19	0.119	28.04
	Overall	162	1 291	161	<0.001	87.53
Reporting system	Qualitative	111	860	110	<0.001	87.22
	Quantitative	51	421	50	<0.001	88.13
	Overall	162	1 290	161	<0.001	87.53

A random-effects model was used to combine studies within each subgroup, and the same model was used to combine subgroups and yield the overall heterogeneity measures.

3.5.3 Publication bias

The comprehensive meta-analysis detected evidence of publication bias. Both large and small studies included in this meta-analysis did not have the expected variability around the overall effect size across the range of standard errors (precision) (Table 3.2). Also, the presence/absence of publication bias was checked by graphical representation using a funnel plot (Fig. 3.9). Within the Egger regression test, each summary effect had a *P*-value less than 0.05, indicating the presence of publication bias (i.e., there was a tendency for effect size to increase as study size decreased; Table 3.3). The Duval and Tweedie (2000) trim and fill method based on a random-effects model initially trimmed the most extreme small studies, looked for missing studies, and located the

unbiased effect in an iterative procedure. The method then populated the plot by re-inserting the trimmed studies until the funnel plot established symmetry on the adjusted (new) summary effect. Finally, the original studies were added back to the analysis along with their imputed counterparts to obtain an appropriate variance. In cases where between-study heterogeneity exists (as it was in this meta-analysis) Duval and Tweedie's Trim and Fill may incorrectly adjust for publication bias and result in a wrongly adjusted summary effect (Terrin et al., 2003). The issue associated with missing studies is that their absence in the analysis may lead to an exaggerated summary effect. In this meta-analysis, however, the new summary effect value adjusted for missing studies was further from the point of no impact (value = 0) than the biocontrol treatments' original overall effect size value (Fig. 3.9). Actually, if the new summary effect and suggested adjustments are legitimate for the biological control of ARR (i.e., the missing studies are valid), then Duval and Tweedie's Trim and Fill analysis indicated an even more significant impact of the biocontrol agent treatments in suppressing ARR. Therefore, this publication bias must be acknowledged in the interpretation of the analyses.

Table 3.2. Variables used in characterizing publication bias for each moderator effect size

Moderator variable	Summary Effect ¹			Funnel plot ²	Egger's regression intercept ³		Duval and Tweedie trim and fill ⁴	
	N	<i>lnR</i>	<i>P</i>		Yes	Intercept	<i>P</i>	adjusted
Application method	159	-0.36	<0.001	Yes	-1.53	<0.001	-0.57	37
Biocontrol agent richness	162	-0.41	<0.001	Yes	-1.64	<0.001	-0.62	39
Biocontrol agent type	156	-0.26	<0.001	Yes	-1.41	<0.001	-0.51	29
Study Type	162	-0.41	<0.001	Yes	-1.64	<0.001	-0.62	39
Reporting system	162	-0.41	<0.001	Yes	-1.64	<0.001	-0.62	39

¹Summary effect: N, number of studies; *lnR*, natural log of overall summary effect; *P*, the probability that summary effect is 0; ²Funnel plot appears asymmetrical. ³Egger's regression intercept: Intercept, This is a test for the Y-intercept = 0, *P* probability that the intercept is 0. ⁴Duval and Tweedie trim and fill: adjusted, new summary effect after imputing missing studies using an iterative trim and fill procedure. No. impute, number of studies imputed in the trim and fill analysis.

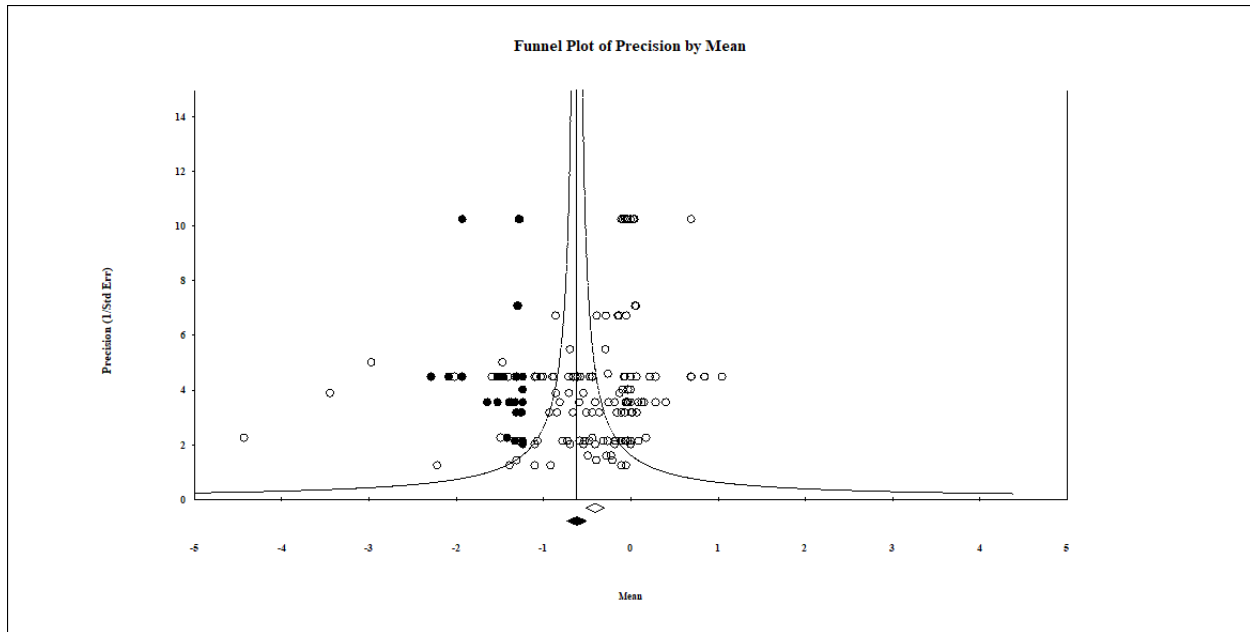


Figure 3.9. Trim and fill plot for log response ratio showing asymmetrical distribution of studies about the combined effect size or mean (i.e., the new adjusted effect size). This funnel plot is a measure of study size precision (standard error⁻¹) on the vertical axis as a function of effect size on the horizontal axis. ○ Observed studies; ● imputed studies; ◇ original effect size ◆ recomputed combined effect size. The program suggested 39 studies missing to the left of the mean. The centers of the diamonds depict the overall mean effect sizes, and the widths reflect the confidence interval.

3.6 Discussion

This meta-analysis provided strong evidence of an overall ARR suppression by biological control agents even when the summary effect value was adjusted for missing studies assumed to represent publication bias. These agents played an essential role in reducing ARR severity. The investigation also confirmed that the extent of disease suppression varied widely among experiments with the natural log response ratio ranging from -4.43 (i.e., strong disease suppression) to $+1.05$ (displaying no suppression relative to the control). Although the cumulative analysis effect size suggested disease suppression, this was not uniform across the various moderator variables and levels.

Once a potential biocontrol agent is identified, it is essential to understand the method of application that offers the highest efficacy. This is because, for effective biocontrol of soil-borne plant diseases like ARR, the proliferation of the biocontrol agent after introduction into the soil is one of the significant considerations. Therefore, an efficient application method needs to promote the biocontrol agent's rhizosphere competence, which includes producing an inoculum which survives, grows, and colonizes the rhizosphere and the plant roots over a considerable period (Yigit

and Dikilitas, 2007; Compant et al., 2005; El-Mougy and Abdel-Kader, 2019). In this regard, this meta-analysis analysis indicated that the different types of application methods significantly influenced ARR suppression. For example, significant disease suppression was obtained when biological treatments were applied as a seed coating and liquid suspension.

Several biocontrol agents were reported to be effective when applied as a seed coating and liquid suspension. For example, Abdel-Kader et al. (2012) investigated different application methods of biocontrol agents for controlling oomycete and fungal root rot incidence of some vegetables under greenhouse conditions. Their results indicated that although seed coating application was significant in reducing root rot incidence, soil drenched with different bio-agents showed more efficacy against root rot in cucumber, cantaloupe, tomato and pepper in the post-emergence growth stage. Furthermore, a review study by Rocha et al. (2019) described seed coating as an essential tool for delivering beneficial microbes to agricultural crops to promote crop growth, yield, and crop protection against pathogens. Therefore, as detected in this meta-analysis, liquid suspension and seed coating application are efficient methods to obtain a significant level of ARR suppression. Moreover, choosing the method of application that offers the highest efficacy relies on a better understanding of the biological and application-oriented factors influencing the disease suppression potential of the biocontrol agent (Ojiambo and Scherm, 2006).

The meta-analysis investigated the impact of single and mixed organism inoculation of biocontrol agents on ARR suppression. Although it is challenging to draw a strong common conclusion due to the small sample size ($n = 11$), the analysis indicated that mixed organism inoculation had greater disease suppression efficacy than a single organism inoculation. Such a phenomenon could be attributed to the notion that mixed inoculation of biocontrol agents can provide a more significant disease suppression effect than a single organism inoculation due to synergistic or additive effects. This finding is consistent with studies by Stiling and Cornelissen (2005) and Chandrasekaran et al. (2016), who conducted a meta-analysis review on biological control agents' performance and the genus *Pseudomonas* as a biological control agent against bacterial wilt, respectively. However, this study results contradict a study finding by Dandurand and Knudsen (1992) in which they reported ARR suppression was not significantly different when pea seeds were treated with a combination of *T. harzianum* and *Pseudomonas fluorescens* strains compared to treatment with *T. harzianum* alone. Furthermore, among the biocontrol agent types,

compost, plant products, fungal, and bacterial biocontrol agents were effective biocontrol treatments for suppressing ARR.

In this meta-analysis study, multiple biocontrol agents studied in an article were treated as independent studies, and each represented individual units. Therefore, owing to the relatively high total number of bacterial biocontrol agents ($n = 93$) evaluated for biocontrol efficacy, it is possible that a bacterial biocontrol agent with high efficacy could be hidden in such groupings. Therefore, care needs to be given when interpreting grouping results. In this regard, a separate analysis on the bacterial biocontrol agents at a genus level grouping detected bacterial strains in the genus *Bacillus* and *Pseudomonas* significantly favouring disease suppression (Fig. 3.6). This finding was consistent with those of Wakelin et al. (2002), who investigated *A. euteiches* growth inhibition and suppression of pea root rot using spore-forming bacteria, including *Bacillus* species. Similarly, several *Pseudomonas* species that exhibited biocontrol efficacy against ARR and other oomycete diseases, such as *Pythium* damping-off, were reported (Parke et al., 1991; King and Parke, 1993; Reddy, 2002).

The meta-analysis detected that disease suppression was favoured in both growth chamber and field studies, indicating the potential for biological control of ARR. However, more significant suppression was achieved in growth chamber trials (Fig. 3.7). Others have similarly indicated that biological control agents produce better consistency and higher efficacy against various plant pathogens under controlled growth chamber conditions than field trials (Guetsky et al., 2001; Mark et al., 2006; Nicot, 2011). For the most part, the irregularity in biocontrol efficacy in the field could be attributed to various factors, including soil type and soil conditions, climatic variations such as temperature, humidity, and UV irradiation encountered in field conditions. Another reason could be the lack of ecological competence that reduces the survival and colonization ability of the biocontrol agents. Also, inconsistent production of bioactive metabolites required to suppress the pathogen and inadequate formulation and application methods can contribute to inconsistent biocontrol efficacy (Elad and Stewart, 2007; Mark et al., 2006; Ruocco et al., 2011). Moreover, under field conditions, usually more than one pathogen is part of a complex that causes the disease to a crop. For example, ARR often occurs in a complex with other root rot causing pathogens (Parke et al., 1991; Xue 2003; Hughes and Grau, 2013). Finally, maintaining the population of biocontrol agents above a certain level in the soil is an essential factor that affects biocontrol efficacy in both growth chamber and field conditions (Yuan et al., 2014). Since growth chamber

studies offer a better opportunity to control experimental conditions, maintaining the population of biocontrol agents above a certain level is more feasible in growth chamber studies.

One of the challenges in plant pathology studies is to develop standardized qualitative and quantitative disease incidence and severity measures that integrate numerical and observational data. Another challenge is the severity of the disease in relation to a biocontrol agent's capability to control it. Biocontrol agents have their limitations in terms of the severity of the disease that they can control. Furthermore, moving from a controlled environment to the field, a biocontrol agent will very likely encounter populations of the target pathogen that are genetically different, with different virulence than the populations it was exposed to during screening procedures. In this meta-analysis between data entries used to analyze the impact of reporting systems, both qualitative and quantitative reporting systems favoured the detection of ARR suppression. Qualitative reporting systems like the "disease rating scale" are more common in plant pathological studies such as biological control of ARR. However, it is prone to bias compared to quantitative reporting systems due to its subjective nature and lack of standardized measuring tools. Therefore, to increase precision and minimize error, there is a need to establish an agreed-upon standardized system for assessing biocontrol agent performance that integrates direct and indirect quantitative disease incidence measuring reports. For example, quantifying pathogen infestation levels and measuring plant health and growth monitoring parameters like plant dry weight and plant height.

3.7 Conclusion

This meta-analysis detected factors such as biocontrol application method, biocontrol agent type and richness, study type, and reporting system as affecting the measured efficacy of biological control of ARR. In addition, some of the findings strengthened the prevailing view that most biocontrol agents display higher efficacy under controlled plant growing conditions than field trials. Also, strains within the genera *Bacillus* and *Pseudomonas* favoured more significant suppression among bacterial biocontrol agents. Moreover, biocontrol of ARR was significantly suppressed when an inoculant consisting of mixed organisms was used compared to one biocontrol agent alone. Therefore, this meta-analysis demonstrated there is very good potential for biological control of ARR.

Initially, aphanomyces biocontrol mechanism and plant type were considered as moderator variables; however, these two potential categorical variables were not included due to insufficient

data. Therefore, future studies to elucidate the mechanism(s) of biological control of ARR need to be a priority. These include understanding the biology of the biocontrol agents and their natural fitness that play a crucial role in colonizing and successfully establishing in soils conducive to *A. euteiches*, including warm (23 °C) moist soil conditions. Also, identifying a biocontrol agent that naturally forms a symbiotic association with pea plants (for example, *Rhizobium* spp) could play an essential role in clearly determining the "best and most effective" biocontrol agents for ARR. Moreover, identification and characterization of the mechanistic nature of disease suppression offer an additional insight into whether it is beneficial to utilize an active metabolite to control ARR than the biocontrol agent itself.

4. BIOLOGICAL CONTROL OF ROOT ROT COMPLEX OF FIELD PEA AND LENTIL USING APHANOMYCES ROOT ROT BIOCONTROL BACTERIA

4.1 Preface

Effective management strategies against ARR are unavailable in Canada. Therefore, biological control methods, which represents a sustainable agriculture technology, are considered an alternative approach. Previously I identified bacterial strains *L. capsici* K-Hf-H2, *P. simiae* K-Hf-L9 and *P. agglomerans* PSV1-7 as potential biocontrol agents of ARR in field pea in growth chamber trials (Godebo et al., 2020). However, ARR occurs as a complex with other root rot pathogens under field conditions. Thus, the goal of this chapter was to investigate the potential for biological control of RRC in field pea and lentil using *L. capsici* K-Hf-H2, *P. simiae* K-Hf-L9 and *P. agglomerans* PSV1-7 under controlled growth chamber conditions.

4.2 Abstract

Root rot in field pea and lentil initially affects the belowground portion of the developing plant, leading to poor growth and loss of productivity. Among root rot diseases, ARR caused by *A. euteiches* is the most destructive, and currently, there are no effective management strategies. Under field conditions, *A. euteiches* typically occurs with other pathogens, including *Fusarium avenaceum* and *Fusarium oxysporum*, that individually and collectively cause root rot. Previously I identified ARR several biocontrol bacteria: *L. capsici* K-Hf-H2, *P. simiae* K-Hf-L9 and *P. agglomerans* PSV1-7. In this study biocontrol activity of these bacteria was investigated against the RRC caused by *A. euteiches*, *F. avenaceum* and *F. oxysporum* in field pea and lentil under growth chamber conditions. During *in vitro* dual plate screening, the three biocontrol bacteria and *L. gummosis* K-Be-H3 (a culture collection strain with strong antagonistic properties against *A. euteiches*) inhibited the mycelial growth of all three pathogens. Comparatively, the strains exhibited higher efficacy against *F. avenaceum* than against *F. oxysporum*. Of the four biocontrol bacteria, *L. gummosis* K-Be-H3 showed the greatest antagonistic activity, including lysing the fresh and well-grown mycelia structure of *F. avenaceum* with an apparent loss of mycelia integrity and alteration of the mycelia morphology. The cell-free supernatant of *L. capsici* K-Hf-H2 inhibited *A. euteiches* mycelial growth with a mean zone of inhibition ranging from 2 to 8.25 mm, and the inhibition activity of the supernatant was stable for four months when stored at 4°C. In a growth chamber study using non-sterile agricultural soil as a growing media, the biocontrol bacteria significantly suppressed ARR and RRC in both field pea and lentil. Compared to *P. simiae* K-Hf-L9 and *P. agglomerans* PSV1-7, *L. capsici* K-Hf-H2 produced the highest significant biocontrol efficacy in all treatment combinations in both crops, but with a higher efficacy in field pea. In addition, *L. capsici* K-Hf-H2 was identified as capable of promoting growth in field pea compared with untreated negative control plants. This lead to a significant increase in shoot dry weight, with a maximum increase of 56.5% in field pea treated with *L. capsici* K-Hf-H2 and challenged by the pathogen *A. euteiches*. These results demonstrate *L. capsici* K-Hf-H2 potential as a biocontrol agent against the RRC caused by *A. euteiches*, *F. avenaceum* and *F. oxysporum*.

4.3 Introduction

Pulse crops are essential components of cropping rotations common across the Canadian prairies (Li et al., 2018). These legumes fix atmospheric nitrogen (N₂) through symbiotic associations with *Rhizobium*. This symbiotic relationship positively impacts the yield of the following crop by naturally changing the soil microbial community and nutrient levels (Hossain et al., 2016). Field pea (*Pisum sativum* L.) and lentil (*Lens culinaris* Medikus) are among the significant pulse crops cultivated in the Canadian prairies (Gossen et al., 2016; Hossain et al., 2016), and Canada is the world's largest exporter of field pea and lentil (Risula, 2017; ECODA:

Eastern Canada Oilseeds Development Alliance, 2022). However, *Aphanomyces euteiches* and other root rot-causing pathogens collectively termed the RRC pose a significant threat to the sustainability and productivity of these crops.

The RRC of field pea and lentil consists of *Fusarium* spp., *Pythium* spp., *Rhizoctonia solani* Kuhn (teleomorph: *Thanatephorus cucumeris* (Frank) Donk), and *A. euteiches* Drechs (Xue 2003; Bodah 2017). These pathogens cause various diseases in field pea and lentil at various growth stages. These include root rot, and reduction of stand establishment, nitrogen fixation, root distribution, and root vigour (Gossen et al., 2016). In the past, root rot symptoms were overlooked as affected plants were unevenly distributed within a field, and symptoms were underestimated unless there was a substantial impact on the above-ground part of the plant (Moussart et al., 2009; Navarro et al., 2008). Recently, however, the abundance of root rot across western Canada is at a destructive level (McLaren et al., 2015). Unfortunately, management strategies for the RRC components are inadequate. Therefore, given the increased risk of yield loss in field pea and lentil due to RRC and the focus on sustainable field pea and lentil production in Canada, research into the control of pathogens involved in this disease complex is essential.

A recent study by Godebo et al. (2020) identified three soil bacteria: *L. capsici* K-Hf-H2, *P. simiae* K-Hf-L9 and *P. agglomerans* PSV1-7, as having biocontrol potential against ARR in field pea. Although *A. euteiches* often causes disease in a complex involving other pathogens, symptoms are usually quite similar (Willsey et al., 2018). In such cases, identifying the primary pathogen, the role played by each pathogen, and the nature of the interrelationships is difficult to ascertain (Hughes and Grau, 2013). Of all the pathogens that contribute to the RRC in pulse crops in Saskatchewan, Canada, *Fusarium* species such as *Fusarium avenaceum* and *Fusarium oxysporum* are the most predominant (Bogdan, 2019; Safarieskandari et al., 2021). Of the *Fusarium* species, *Fusarium avenaceum* is the most common and aggressive species in pea, lentil, and chickpea, with lentil being more susceptible than pea (Bogdan, 2019; Saskatchewan Pulse Growers, 2019; Safarieskandari et al., 2021). A survey from 2015 to 2018 found that *F. avenaceum* was present in over 98% of pea and lentil fields sampled across the Prairies (Bogdan, 2019; Safarieskandari et al., 2021). Therefore, identifying biocontrol bacteria with a broad spectrum of activities against members of the RRC can provide a multifaceted advantage that encompasses both sustainability and economic benefits to growers. The main objective of this study was to investigate the potential

for the biological control of the RRC of field pea and lentil caused by strains of *A. euteiches*, *F. avenaceum* and *F. oxysporum* under growth chamber conditions using ARR biocontrol bacteria.

4.4 Materials and methods

4.4.1 *In vitro* inhibition of *Fusarium* pathogens

For this study, two strains of *Fusarium* pathogen, SMCD 2241 *F. avenaceum* (Fr.) Sacc and SMCD 2242 *F. oxysporum* Schltdl were obtained from the Department of Food and Bioproduct Sciences, University of Saskatchewan (courtesy of Dr. Vladimir Vujanovic). The strains were originally isolated from the Saskatchewan brown soil under durum-pulses-canola rotation system. The inhibition of mycelial growth of these pathogens by biocontrol bacteria was assessed using an *in vitro* dual plate assay (Godebo et al., 2020).

Glycerol stock cultures of *L. capsici* K-Hf-H2, *P. simiae* K-Hf-L9 and *P. agglomerans* PSV1-7 were removed from storage at -80 °C and allowed to thaw at room temperature for approximately 10 min. A loopful of each glycerol stock culture was then streaked on fresh 1/10 Difco Trypticase soy agar (TSA) plates and incubated for 72 h at 25 °C. After incubation, a single colony was streaked along two opposite edges, 1.5 cm away from the periphery of a fresh potato dextrose agar (PDA) plate. Then, a plug (5 mm diameter) of *F. avenaceum* and *F. oxysporum* was taken from a 5 d old PDA culture using a sterile metal corer (5 mm diameter) and placed at the center of the PDA plates (Xu et al., 2014). The plates were incubated in the dark at 23 °C until the mycelia on a negative control plate attained full growth (i.e., until mycelia fully covered the PDA plate). At this time, the assay plates were visually examined for the presence of *Fusarium* mycelial growth inhibition. The mycelial growth was considered "inhibited" when no growth was detected up to or past the point of bacterial growth. Also, additional *Fusarium* mycelial growth inhibition assays were conducted using *L. gummosis* K-Be-H3. *Lysobacter gummosis* K-Be-H3 is an isolate that exhibited strong antagonistic activity against *A. euteiches* mycelial growth but did not demonstrate consistent biocontrol efficacy in suppressing ARR in field pea (Godebo, 2019).

4.4.2 Evaluation of cell-free supernatant for antimicrobial activity

Cell-free supernatants of biocontrol bacteria *L. capsici* K-Hf-H2, *P. simiae* K-Hf-L9, *P. agglomerans* PSV1-7 and *L. gummosis* K-Be-H3 were evaluated for antagonistic activity against mycelial growth of *A. euteiches* (Kaewchomphunuch et al., 2022). First, each biocontrol bacteria were grown in 10 mL of ½ strength Difco Trypticase soy broth (TSB) at 25 °C and 120 rpm for

24 h and the cultures were adjusted to an absorbance value of 1 at OD_{600 nm}. Next, 5 mL of the bacterial suspensions were transferred to 250 mL of fresh ½ strength TSB media and incubated at 25°C and 120 rpm for 14 d. Each day bacterial growth was recorded using OD_{600 nm}, and cell-free supernatants were extracted through centrifugation followed by cell filtering.

Briefly, 10 mL of each broth culture was withdrawn each day and centrifuged at 10,000×g for 2 min, and the resulting supernatant was filtered through Whatman's 0.2 µm filter (Whatman™) according to Hossain et al. (2015). Finally, the cell-free supernatant was evaluated for inhibitory activity towards the radial growth of *A. euteiches* mycelia using the agar well diffusion assay described in the subsequent Section 4.4.3. Additionally, a portion of the supernatant was used to investigate storage and autoclaving stability. For storage stability assessment, the cell-free supernatant was stored at -20°C, 4°C and room temperature (approximately 24 °C) for four months from Jan 1, 2022, to May 2, 2022. The storage (-20°C, 4°C and 24 °C) and autoclaving stability of the cell-free supernatants were determined using an agar well diffusion assay. Cell-free supernatant was deemed stable when it exhibited similar antimicrobial activity and no significant difference compared to the fresh cell-free supernatants.

4.4.3 Agar-well diffusion assay

The agar-well diffusion assay was conducted using fresh PDA plates (Balouiri et al., 2016). Two wells were made along two opposite edges, 1.5 cm away from the plate periphery using a sterile cork borer (5 mm diameter), and 250 µL of the cell-free supernatant was added to each well under aseptic techniques (Bauer et al., 1966). Plates were kept at 4 °C for 30 min to allow the bioactive compounds to diffuse (Martin-Garcia et al., 2022). Next, a plug of the *A. euteiches* mycelia (5 mm diameter) was placed at the center of the assay plate and incubated at 23°C in the dark for 7 d. After the incubation period, assay plates were examined visually for the presence of mycelial growth inhibitory activity. Mycelial growth was considered inhibited when there was no mycelial growth around wells. The negative control consisted of PDA plates inoculated with *A. euteiches* mycelia (5 mm diameter) and wells that received 250 µL of filtered (0.2 µm) ½ strength TSB. The assay was repeated and conducted using CRD in four replicates, and at each sampling time data was collected from four inhibition zones. Finally, analysis of variance (ANOVA) was performed using the SAS general linear models (Proc GLM) procedure (Version 9.3, SAS Institute Inc.; Cary, NC, USA). The means were separated by calculating Fisher's Least Significant Difference (LSD) at a 95% confidence interval.

4.4.4 Biocontrol of root rot complex of field pea and lentil

Two sets of growth chamber experiments were conducted in the College of Agriculture and Bioresources controlled environment facility at the University of Saskatchewan, Canada. Field pea (cv. CDC Meadow; *Pisum sativum* L) and lentil (cv. CDC Proclaim; *Lens culinaris* Medik.) were the test crops, and two different plant-growing media were used. The first media was vermiculite (SUNGRO HORTICULTURE, USA), and the second was a non-sterile clay loam (Dark Brown Chernozem - Ardill Association; 0-to 15-cm depth) collected from the Kernan Crop Research Farm.

Aphanomyces euteiches AE1, SMCD 2241 *F. avenaceum* (Fr.) Sacc and SMCD 2242 *F. oxysporum* Schltdl were used to establish artificial RRC against which the biocontrol efficacy of *L. capsici* K-Hf-H2, *P. simiae* K-Hf-L9 and *P. agglomerans* PSV1-7 were assessed and the entire trial consisted of five treatment combinations (Table 4.1). In addition, plants inoculated with the pathogen(s) alone within the respective treatment group served as a positive control. In contrast, un-inoculated (untreated) plants were negative controls for the entire experiment. Moreover, a summary of the research sequence carried out to investigate the biological control of ARR and RRC in field pea and lentil is diagrammatically represented in Fig. 4.1 below. *A. euteiches* AE1 was obtained from the Department of Plant Science and Crop Development Centre, University of Saskatchewan (courtesy of Dr. Sabine Banniza).

Table 4.1. Root rot pathogens combination, pathogens inoculum concentration and application volume

Pathogen combination	Inoculum concentration	Application per plant	Inoculum ratio (V/V)
A. e	5×10^3 zoospore mL^{-1}	5 mL	1
A. e + F. a	5×10^3 zoospore mL^{-1} + 5×10^3 spore mL^{-1}	10 mL	1:1
A. e + F. o	5×10^3 zoospore mL^{-1} + 5×10^3 spore mL^{-1}	10 mL	1:1
F. a + F. o	5×10^3 zoospore mL^{-1} + 5×10^3 spore mL^{-1}	10 mL	1:1
A. e + F. a + F. o	5×10^3 zoospore mL^{-1} + 5×10^3 spore mL^{-1} + 5×10^3 spore mL^{-1}	15 mL	1:1:1

Where, A. e: *A. euteiches*; F. a: *F. avenaceum*; F. o: *F. oxysporum*.

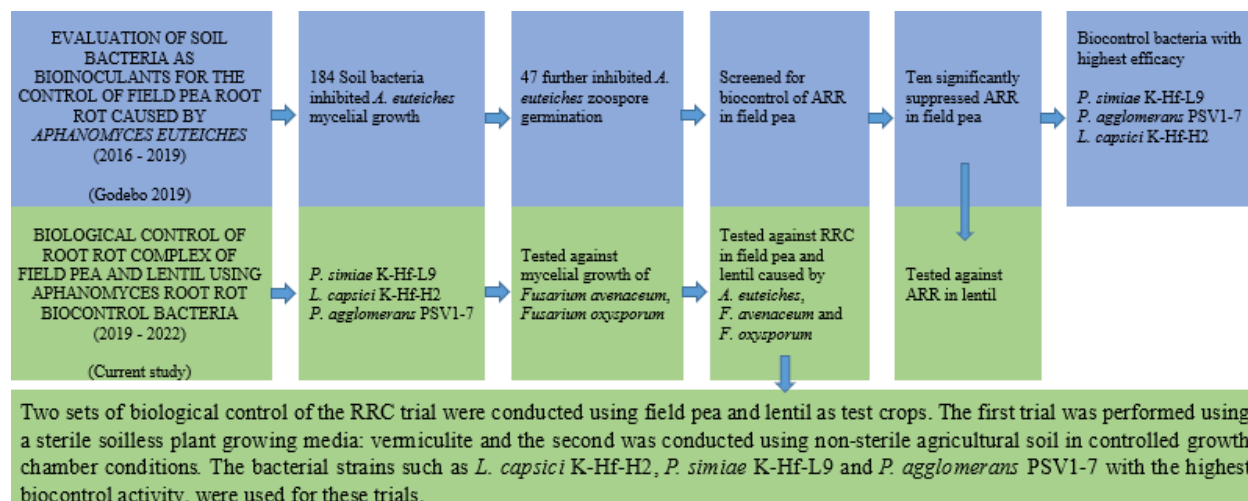


Figure 4.1. Diagrammatic representation of the sequence of research activities carried out in the investigation of biological control of aphanomyces root rot (ARR) and root rot complex (RRC) in field pea and lentil. The blue sections indicate previously conducted study (Godebo, 2019), and the green sections represent the current study.

4.4.5 Biocontrol of root rot complex in vermiculite

4.4.5.1 Experimental design and growth conditions

All the growth chamber experiments were conducted using a completely randomized design with four replicates. The growth chamber room temperature was set to 22 °C day/21 °C night with a day length of 16 h. Light intensity ranged from 300 to 390 $\mu\text{mol}\cdot\text{m}^{-2}\cdot\text{s}^{-1}$. The light bulbs in the room were Phillips T-5 Fluorescence bulb # 835 (ON, Canada). Water holding capacity was determined according to Rowell (1994), and throughout the experiment, the moisture level for each pot was maintained at 80% of the water holding capacity. Plant positions were re-randomized at each watering period throughout the trial to minimize the impact of light, temperature and humidity variations.

4.4.5.2 Seed preparation and planting

Pea (cv. CDC Meadow) and lentil (cv. CDC Proclaim) seeds were obtained from the Crop Development Centre (courtesy of Dr. Tom Warkentin), University of Saskatchewan. The pea and lentil seeds were surface sterilized by soaking in ethanol (65% v/v) for 3 min and sodium hypochlorite (1.2% v/v) for 5 min, followed by ten rinses in sterile tap water (Vincent, 1970). Four surface-sterilized pea and lentil seeds were sown at equal depth (approximately 2.5 cm below the top surface) in 2500 mL pots containing 260 g sterile vermiculite and covered with aluminum foil until germination. Immediately after emergence, the field pea and lentil plants were thinned to two

plants per pot. After the first week of germination, additions of distilled water were alternated with 2/5 strength of Hoagland's nutrient solution every two days (Hoagland and Arnon, 1938).

4.4.5.3 Biocontrol inoculum preparation and application

Biocontrol bacteria, *L. capsici* K-Hf-H2, *P. simiae* K-Hf-L9 and *P. agglomerans* PSV1-7 (Godebo, 2020), were taken from -80 °C storage, allowed to warm to room temperature for approximately 10 min and a loopful was streaked on and cultured on 1/10 TSA plate at room temperature (24 °C) for 72 h. A loopful of a bacterial colony of each strain was transferred to 300 mL ½ strength TSB and cultured on a benchtop shaker at 120 rpm and 24 °C for 72 h. The cell growth was measured in optical density (OD_{600 nm}) using a Thermo Scientific Fluorescence multi-mode microplate reader Varioskan™ LUX (Thermo Scientific, USA). Bacterial suspensions were concentrated by centrifugation (20 min at 5000 rpm), washed three times in 150 mL sterile phosphate-buffered saline (PBS) solution, and re-suspended in sterile tap water (Chlebek et al., 2020; Godebo et al., 2020). The bacterial cell density in the suspension was obtained as an OD value and converted into CFU mL⁻¹ (Chlebek et al., 2020). The inoculum volume was adjusted to a target concentration of 1x10⁸ CFU mL⁻¹. To allow pre-colonization of the root, 6 d after germination, each plant was inoculated with 5 mL of one of the bacterial suspensions at a concentration of 1x10⁸ CFU mL⁻¹ per plant.

4.4.5.4 Pathogen inoculum preparation and application

Aphanomyces euteiches zoospores were produced according to Islam et al. (2007) with modifications as described by the Saskatchewan University Plant Science-Crop, Development Centre (Sivachandra et al., 2020). Briefly, four plugs of *A. euteiches* (5 mm) were taken from mother plates of 5% Corn Meal Agar (CMA) that had been incubated for 3 d to develop a mycelial mat and transferred to CYP agar (CMA + Yeast Extract + Phosphate Buffer) plates on which approximately 15 4-cm-long autoclaved wheat leaves were placed on the surface. These plates were incubated for 4 d at 23 °C under dark conditions. On the fourth day, *A. euteiches* mycelia with the wheat leaves were transferred to 100 mL sterile distilled water in a 250 mL flask. The flasks were covered with tin foil and placed on a benchtop shaker at 110 rpm for 16 h to induce *A. euteiches* zoospores, after which zoospore concentration was adjusted to 0.5 x 10⁴ zoospore mL⁻¹.

The *Fusarium* pathogen inoculums were produced according to the method described by Koch et al. (2020). Strains of *F. avenaceum* and *F. oxysporum* were cultured on PDA plates. Then,

plates with sporulating cultures were flooded with 10 mL of sterile distilled water, and conidia were dislodged by gently scraping the colony surface with a sterile spatula. Next, the suspensions were filtered through cotton gauze, and mycelial fragments were removed. Finally, the concentration of conidial spores of the *Fusarium* pathogen was determined with a hemocytometer. Depending on the number of spores present, the concentration of the resulting suspensions was adjusted to 0.5×10^4 spore mL^{-1} for *F. avenaceum* and *F. oxysporum* (Le et al., 2009; Koch et al., 2020).

Three days after bacterial inoculation, and typically 10 d after seed germination, five different pathogens combinations described in Table 4.1 above were applied by pipetting into the root zone immediately beside the point of plant emergence. The disease suppression efficacy of the three biocontrol bacteria was independently evaluated against the five combinations.

4.4.6 Biocontrol of root rot complex in non-sterile soil

The three bacteria assessed for biocontrol efficacy against RRC in field pea and lentil using vermiculite as a growing medium were further evaluated for biocontrol efficacy in non-sterile field soil (500 g). The soil was a clay loam (Dark Brown Chernozem) collected from the Kernen Crop Research Farm from the top 15 cm of an Ardill Association soil. Initially, non-sterile air-dry field soil (500 g) was sieved through a 2 mm mesh and was placed in 500 mL pots. Next, bringing the soil to 80% water holding capacity through the addition of reverse osmosis water, the pots were covered with aluminum foil to retain moisture and incubated for 10 d on a growth chamber bench before sowing the pea and lentil seeds. Seed preparation, planting, biocontrol and pathogen inoculum preparation and application were accomplished in a manner identical to the sections described above (Sections 4.3.5.1 to 4.3.5.4). Thus, as in the trials using vermiculite as the growth medium, individual replicates in each treatment category contained two plants per pot and pots were arranged in a completely randomized design in four replicates.

4.4.7 Data collection and analysis for the experiment using both vermiculite and field soil

Field pea and lentil plants were grown for 60 days, at which time they were removed from each pot and assessed for the level of disease development and suppression. Initially, the roots were washed, and adhering vermiculite/soil was removed. Then, the level of disease development was assessed and recorded using a 1 to 7 visual scale as described in Chatterton et al. (2019) (Table 4.2). Data were analyzed by nonparametric analysis, where mean ranks were calculated using the

SAS procedures of Proc Rank followed by an analysis of variance with Proc Mixed. Next, the relative impact of each biocontrol bacteria on disease severity or suppression and their confidence interval was calculated using the LD-CI macro (Shah and Madden, 2004). Moreover, ANOVA for shoot dry weight was performed using the SAS general linear models (Proc GLM) procedure (Version 9.3, SAS Institute Inc.; Cary, NC, USA). Finally, the impact of the biocontrol bacteria on shoot dry weight was separated by calculating the LSD at a 95% confidence interval.

Table 4.2. Description of visual rating scale used to assess root rot development and suppression (adapted from Chatterton et al., 2019).

Rating	Lesion description	Root discoloured (%)	Root mass reduction
1	0	0	0
2	Small (0.1–0.2 cm) reddish-brown discolouration at point of seed attachment	0	0
3	Localized root/epicotyl lesions (0.5 to 1 cm) coalescing around ½ of taproot	10–20%	0
4	Lesions encircle tap root/epicotyl	95%	5–10%
5	Extended epicotyl lesions	100%	20–50%
6	Lesions encircling the stem, < 2 cm long	100%	50–80%
7	Lesions > 2 cm, decay of taproot/epicotyl	Dead	Dead

4.4.8 Biocontrol of aphanomyces root rot in lentil

A separate biocontrol assessment of ARR in lentil (CDC Proclaim) was conducted under growth chamber conditions using ten bacteria that previously significantly suppressed ARR in field pea (Godebo, 2019). In the current trial with lentil as the test crop, sterile vermiculite and non-sterile Ardill Association Brown Chernozem soil collected from the top 15 cm agricultural field near Central Butte was used as plant growing media.

The two trials were conducted in the controlled environment facility at the College of Agriculture and Bioresources at the University of Saskatchewan, following the methods described in Sections 4.3.5.1 to 4.3.5.4. Thus, the trials were carried out using a completely randomized design with four replicates. However, the plants were grown for 28 days to be consistent with a previous study (Godebo et al., 2020). Then the plants were removed from each pot, adhering vermiculite or soil was removed, and root rot development/suppression data were collected using a 0-4 visual rating scale as described in Wakelin et al. (2002) and to be consistent with previous

study (Godebo et al., 2019) data collection. Therefore, the disease rating score differs from the one described in Section 4.4.7. Briefly, 0 indicated No symptoms; roots healthy and white; 1 = Initial symptoms of root rot; discolouration, usually a light tan colour, in sections of the root system; 2 = Discolouration of most or all the root system, small watery lesions may be present on the root and around the hypocotyl/epicotyl regions; 3 = Advanced disease symptoms, dwarfing of the plant and yellowing of the lower leaves. Extensive darkening and discolouration of the root system and extensive lesion formation; 4 = root entirely rotted/plant dead.

Finally, the disease scales were analyzed by nonparametric analysis, where mean rank was calculated using Proc Rank followed by analysis of variance with Proc Mixed. Next, the relative impact of each biocontrol bacteria on disease severity or suppression and their confidence interval was calculated using the LD-CI macro (Shah and Madden, 2004).

4.5 Results

4.5.1 *In vitro* inhibition of *Fusarium* pathogens

The four bacteria, *L. capsici* K-Hf-H2, *P. simiae* K-Hf-L9, *P. agglomerans* PSV1-7 and *L. gummosis* K-Be-H3, inhibited the radial growth of a strain of *F. avenaceum* (Fig. 4.2) and *F. oxysporum* (Fig. 4.3). Although all four bacteria showed significant inhibitory activity towards both *Fusarium* strains, *F. avenaceum* mycelial growth was more significantly inhibited. Of the four bacteria, *L. gummosis* K-Be-H3 exhibited the most inhibition, including lysing the mycelia tips and well-grown mycelia structure with an apparent loss of mycelia integrity and alteration of the mycelia tip morphology (Fig. 4.4). However, its inhibitory activity towards *F. oxysporum* mycelial growth was the same as the three biocontrol bacteria.

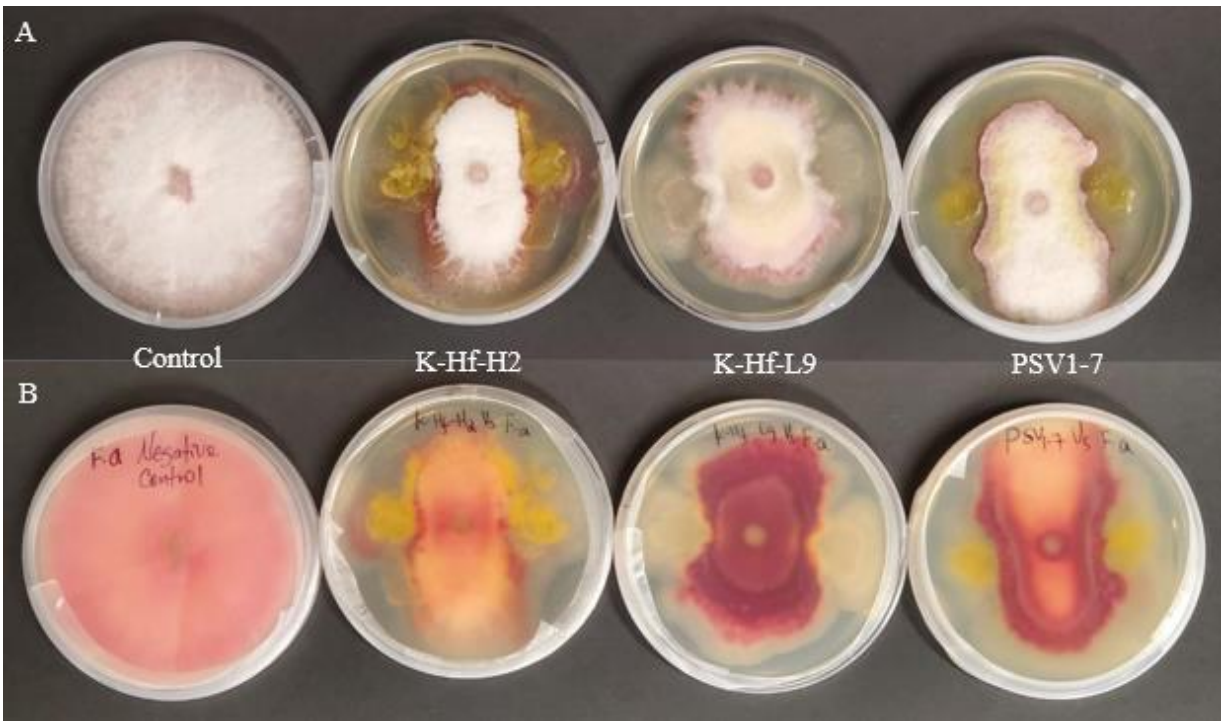


Figure 4.2. Inhibition of *Fusarium avenaceum* mycelial growth on PDA plates. Where, A and B were the top and bottom views of the assay plates, respectively. K-Hf-H2: *Lysobacter capsici*; K-Hf-L9: *Pseudomonas simiae*; PSV1-7: *Pantoea agglomerans*.

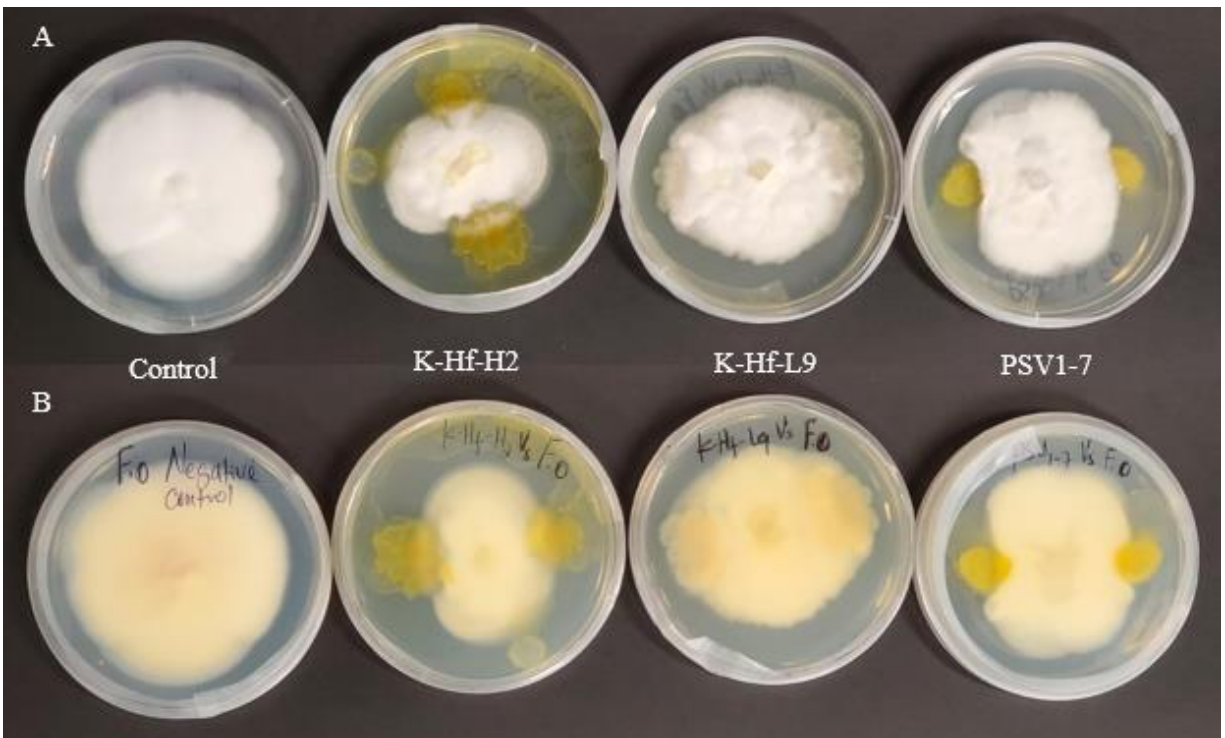


Figure 4.3. Inhibition of *Fusarium oxysporum* mycelial growth on PDA plates. Where, A and B were the top and bottom views of the assay plates, respectively. K-Hf-H2: *Lysobacter capsici*; K-Hf-L9: *Pseudomonas simiae*; PSV1-7: *Pantoea agglomerans*.

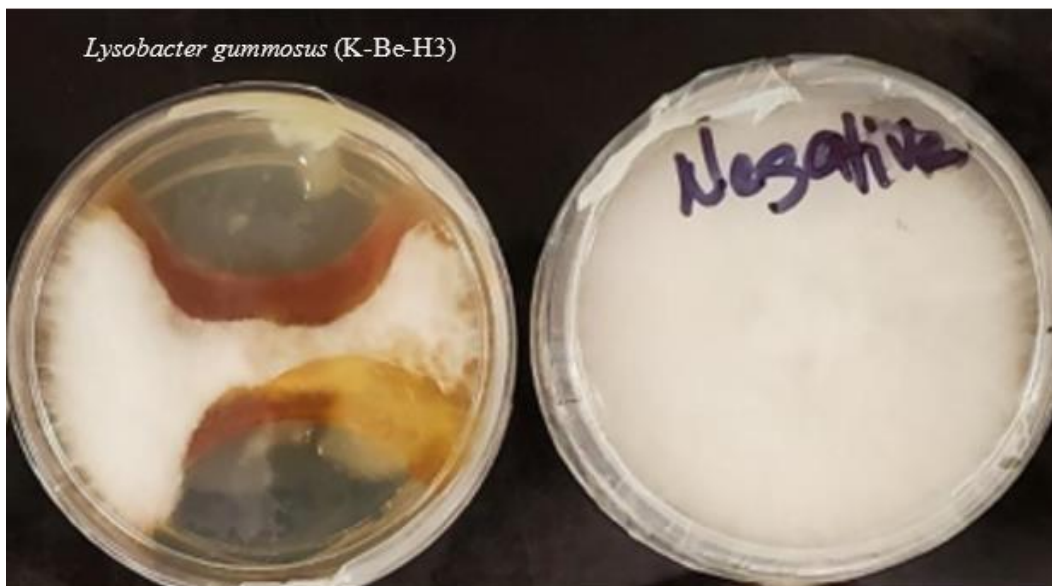


Figure 4.4. Inhibition of *Fusarium avenaceum* mycelial growth on PDA plates by *L. gummosus* K-Be-H3.

4.5.2 Antagonistic activity of cell-free supernatant

The cell-free extracts were assessed for inhibitory activity against *A. euteiches* mycelial growth using the agar well diffusion technique. The *L. capsici* K-Hf-H2 cell-free supernatant inhibited *A. euteiches* mycelial growth (Fig. 4.5 and 4.7). However, the cell-free supernatant obtained from the first six-day culture failed to exhibit inhibitory activity. In comparison, the extract from the 7 to 14 d (stationary to death/decline phase: Fig. 4.6) culture displayed inhibitory activity with a mean zone of inhibition ranging from 2 mm (day seven culture extract) to 8.25 mm (day nine culture extract) (Fig. 4.7). However, no inhibitory activity was observed from *P. simiae* K-Hf-L9, *P. agglomerans* PSV1-7 and *L. gummosus* K-Be-H3 cell-free supernatant.

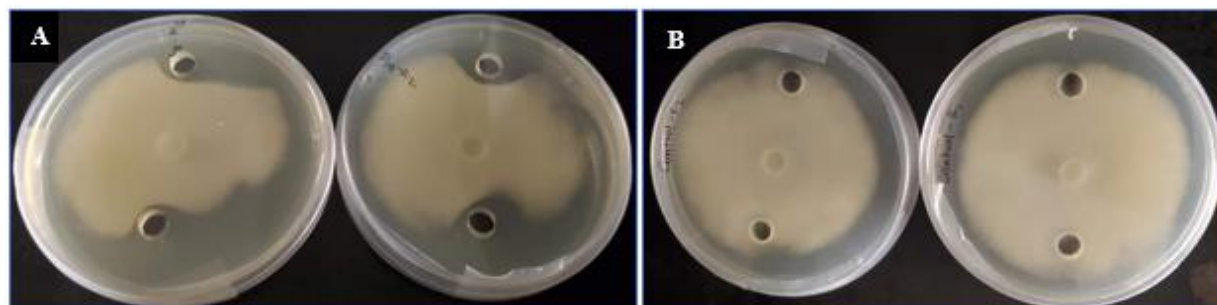


Figure 4.5. Agar-well diffusion assay depicting inhibition of *A. euteiches* mycelia with *L. capsici* K-Hf-H2 cell-free supernatant. A: clearing zone around the wells indicates mycelial growth inhibition. B: negative control plates. The assay was repeated and conducted on a duplicate plate, and data was collected from four inhibition zones each time.

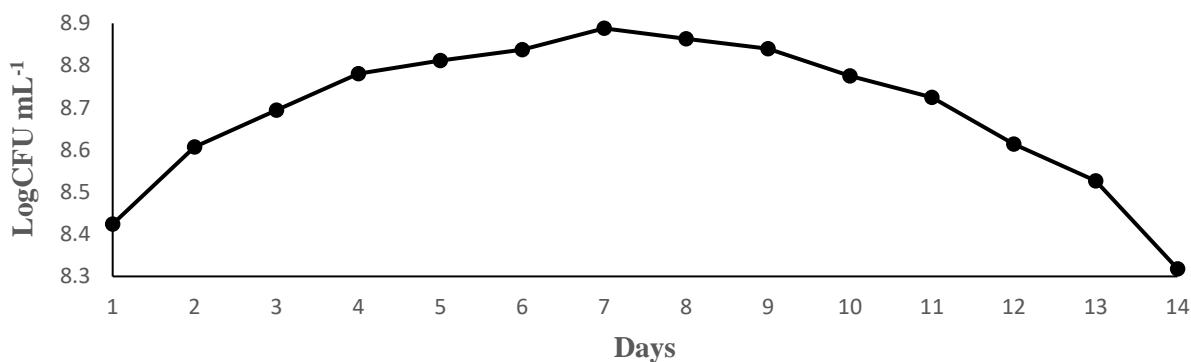


Figure 4.6. Growth curve of *L. capsici* K-Hf-H2. The strain was grown in 250 mL half-strength Difco Trypticase soy broth for 14 days at 24°C and 120 rpm. The bacterial suspension was taken daily, and the optical density at 600 nm was measured. The experiment was repeated, and mean OD values were converted to CFU mL⁻¹ then log CFU mL⁻¹.

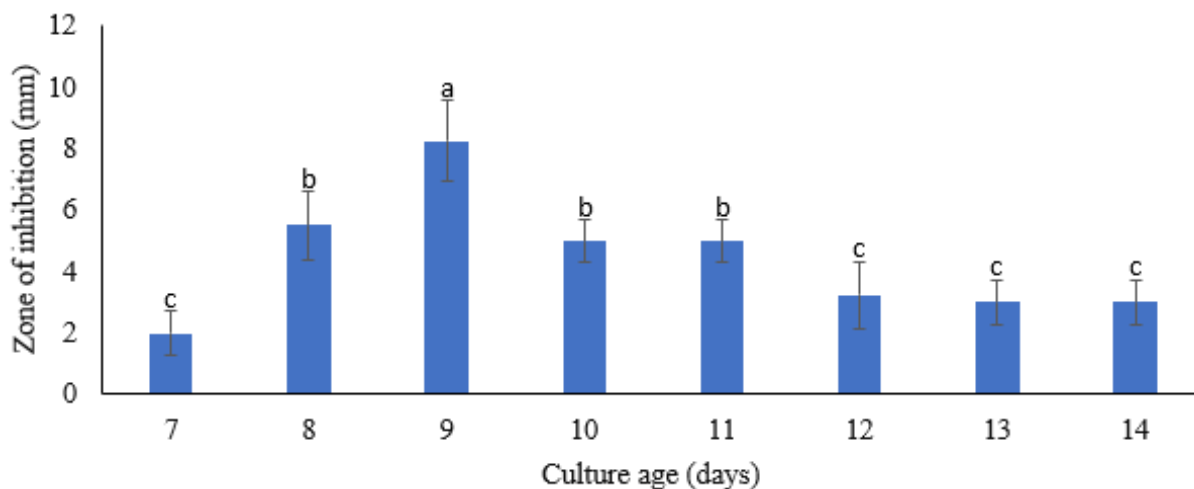


Figure 4.7. Comparison of the zone of inhibition between cell-free supernatant extracted over the 14 d of *L. capsici* K-Hf-H2 growth phase. The days across the X-axis represent the age of the culture at which time cell-free supernatant was extracted. The cell-free supernatant obtained from the first six-day culture did not produce inhibition; thus, no data was displayed. Error bars indicate the mean standard deviation and means with the same letter are not significantly different.

4.5.3 Autoclave and storage stability of cell-free supernatant

The storage and autoclave stability assessment of the *L. capsici* K-Hf-H2 cell-free supernatant indicated that storing at 4°C preserves the inhibitory potential of the bioactive metabolite within the cell-free supernatant (Table 4.3, Fig. 4.8). However, keeping at -20°C and autoclaving the cell-free supernatant inactivated/denatured the bioactive metabolite, as evidenced by the loss of mycelia growth inhibition potential. Although the cell-free supernatant stored at room temperature exhibited some level of mycelial growth inhibition, the extract held at 4°C

produced consistent and identical mycelial growth inhibition to the fresh extract (Table 4.3). The results suggest that the 4°C storage preserved the natural/initial status of the bioactive metabolite. Furthermore, the mycelial growth inhibition from the extract stored at 4°C was localized, and the mycelia tips approaching the wells were inhibited. In contrast, the inhibition from the extract stored at room temperature was widespread and mycelial tips approaching the plate edge were inhibited.

Table 4.3. Storage and autoclave stability of *Lysobacter capsici* K-Hf-H2 cell-free supernatant

Conditions	Culture age (d) ^a							
	7	8	9	10	11	12	13	14
	Mean zone of inhibition (mm) ^b							
Fresh cell-free supernatant	2	5.5	8.25	5	5	3.25	3	3
Room Temperature (24°C)	0	2	3	2	1	0	1	1
4°C	1.75	5	7.25	3.75	4.5	3	1.75	1.75
-20°C	0	0	0	0	0	0	0	0
Autoclaved	0	0	0	0	0	0	0	0

^a Age of the culture, at which time the cell-free supernatant of *Lysobacter capsici* K-Hf-H2 was extracted during the two weeks growth period. The numbers 7-14 represent the age of culture. ^b Mean inhibition zone resulting from cell-free extracts of day 7 to day 14 culture under the three storage and autoclave conditions. The fresh cell-free supernatant from the first six days did not exhibit inhibitory activity; thus, excluded from the storage and autoclave stability assays.

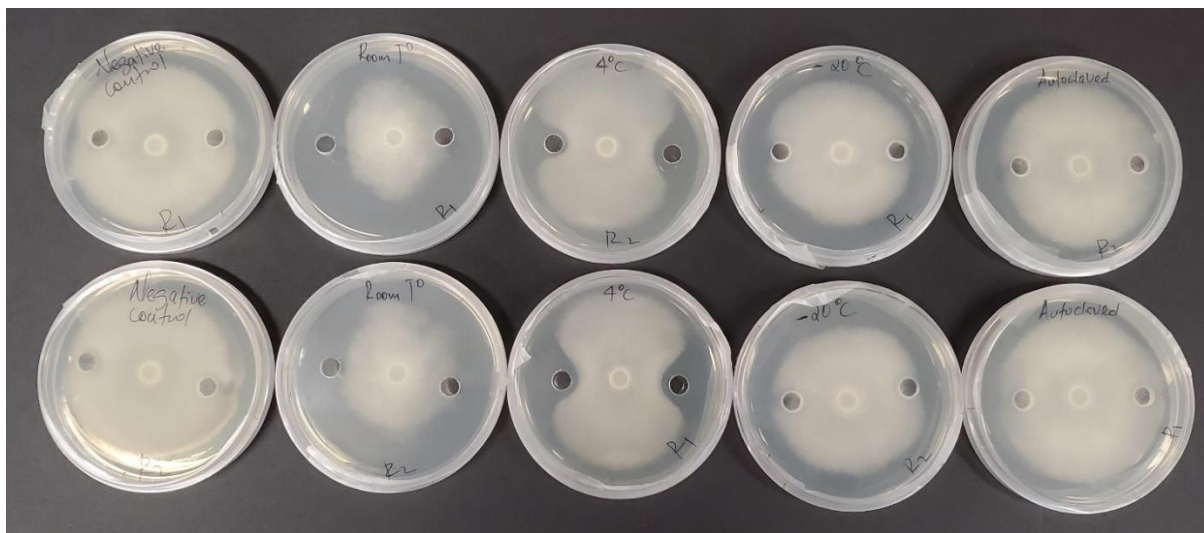


Figure 4.8. Storage and autoclave stability assessment. **Negative control:** wells received 250 µL of filtered half-strength Difco Trypticase soy broth; **Room T°**, **4°C** and **-20°C**: wells received 250 µL of cell-free supernatant stored at room temperature; 4°C and -20°C for four months, respectively. **Autoclaved:** wells received autoclaved 250 µL of cell-free supernatant. A plug of *A. euteiches* mycelia (5 mm diameter) was placed in the center of each plate. The assay was repeated and conducted on a duplicate plate, and data was collected from four interaction zones each time.

4.5.4 Biocontrol of root rot complex in vermiculite

The field pea and lentil plants grown in vermiculite displayed varying root rot symptom levels. The symptoms worsened if *A. euteiches* was co-inoculated with *F. avenaceum* and *F. oxysporum*. Thus, the highest root rot symptom was observed when all three pathogens were co-inoculated (Table 4.4). Therefore, the median disease score (MDS) for field peas was 4 when inoculated with *A. euteiches* alone and 5 when all three pathogens were applied. In contrast, the MDS for the lentils was 4 when inoculated with *A. euteiches* and 6 when inoculated with all three pathogens (Table 4.5). This trend suggests that lentils are likely more susceptible when *A. euteiches* co-occurs with *F. avenaceum* and *F. oxysporum* based on the response trend observed in field pea.

Compared to the positive control treatments, although *P. agglomerans* PSV1-7 exhibited some level of biocontrol efficacy against *A. euteiches* and *F. avenaceum* co-inoculated field pea (Table 4.4); and *A. euteiches*, *F. avenaceum* and *F. oxysporum* co-inoculated lentil (Table 4.5), the biocontrol bacteria did not exhibit disease suppression potential as observed when the plants were grown in non-sterile agricultural soil discussed in the next section (Section 4.5.5).

Table 4.4. Effect of biocontrol bacteria *L. capsici* K-Hf-H2, *P. simiae* K-Hf-L9 and *P. agglomerans* PSV1-7 on root rot severity in field pea grown in vermiculite in growth chamber conditions

Treatment	Pathogen ^a	Median Disease Score ^b	Mean Rank	Relative Effect ^c	95% CI of the RE ^d	
					Lower limit	Upper limit
<i>L. capsici</i> K-Hf-H2	A. e	3	14	0.67	0.44	0.81
<i>P. simiae</i> K-Hf-L9	A. e	2	10	0.48	0.33	0.64
<i>P. agglomerans</i> PSV1-7	A. e	3	10	0.48	0.28	0.7
Negative control	Uninoculated	1	3	0.13	0.1	0.26
Positive control	A. e	4	15	0.74	0.46	0.86
<i>L. capsici</i> K-Hf-H2	A. e + F. a	4	17	0.8	0.69	0.86
<i>P. simiae</i> K-Hf-L9	A. e + F. a	3	9	0.44	0.34	0.56
<i>P. agglomerans</i> PSV1-7	A. e + F. a	3	9	0.4	0.3	0.52
Negative control	Uninoculated	1	3	0.1	.	.
Positive control	A. e + F. a	4	16	0.76	0.53	0.86
<i>L. capsici</i> K-Hf-H2	A. e + F. o	3	13	0.63	0.43	0.77
<i>P. simiae</i> K-Hf-L9	A. e + F. o	3	12	0.59	0.43	0.73
<i>P. agglomerans</i> PSV1-7	A. e + F. o	3	10	0.49	0.27	0.72
Negative control	Uninoculated	1	3	0.1	.	.
Positive control	A. e + F. o	3	14	0.69	0.48	0.82
<i>L. capsici</i> K-Hf-H2	F. a + F. o	3	13	0.66	0.45	0.8
<i>P. simiae</i> K-Hf-L9	F. a + F. o	3	12	0.59	0.4	0.75
<i>P. agglomerans</i> PSV1-7	F. a + F. o	2	3	0.44	0.28	0.62
Negative control	Uninoculated	1	10	0.1	.	.
Positive control	F. a + F. o	3	14	0.71	0.54	0.81
<i>L. capsici</i> K-Hf-H2	A. e + F. a + F. o	5	14	0.66	0.45	0.8
<i>P. simiae</i> K-Hf-L9	A. e + F. a + F. o	5	13	0.63	0.49	0.73
<i>P. agglomerans</i> PSV1-7	A. e + F. a + F. o	4	7	0.3	0.3	0.3
Negative control	Uninoculated	1	3	0.1	.	.
Positive control	A. e + F. a + F. o	5	17	0.81	0.65	0.87

^a Inoculated root rot pathogen: *A. euteiches* (A.e), *F. avenaceum* (F.a) and *F. oxysporum* (F.o); ^b Median disease score based on a 1-7 rating scale: 1 (no disease), 2 (reddish-brown discoloration at point of seed attachment), 3 (Localized root/epicotyl lesions), 4 (Lesions encircle tap root/epicotyl), 5 (Extended epicotyl lesions), 6 (Lesions encircling the stem, < 2 cm long) and 7 (Lesions > 2 cm, decay of taproot/epicotyl). ^c Relative effect on disease severity. ^d 95% confidence intervals of the relative effect.

Table 4.5. Effect of biocontrol bacteria *L. capsici* K-Hf-H2, *P. simiae* K-Hf-L9 and *P. agglomerans* PSV1-7 on root rot severity in lentil grown in vermiculite in growth chamber conditions.

Treatment	Pathogen ^a	Median Disease Score ^b	Mean Rank	Relative Effect ^c	95% CI of the RE ^d	
					Lower limit	Upper limit
<i>L. capsici</i> K-Hf-H2	A. e	3	14	0.69	0.55	0.78
<i>P. simiae</i> K-Hf-L9	A. e	2	8	0.38	0.27	0.51
<i>P. agglomerans</i> PSV1-7	A. e	3	10	0.48	0.37	0.58
Negative control	Uninoculated	1	3	0.1	.	.
Positive control	A. e	4	18	0.86	0.77	0.89
<i>L. capsici</i> K-Hf-H2	A. e + F. a	4	12	0.56	0.39	0.72
<i>P. simiae</i> K-Hf-L9	A. e + F. a	4	11	0.54	0.41	0.65
<i>P. agglomerans</i> PSV1-7	A. e + F. a	4	9	0.4	0.3	0.52
Negative control ^e	Uninoculated	1	3	0.1	.	.
Positive control	A. e + F. a	5	19	0.9	0.70	0.90
<i>L. capsici</i> K-Hf-H2	A. e + F. o	4	13	0.64	0.45	0.78
<i>P. simiae</i> K-Hf-L9	A. e + F. o	4	13	0.61	0.45	0.74
<i>P. agglomerans</i> PSV1-7	A. e + F. o	3	9	0.44	0.22	0.7
Negative control ^e	Uninoculated	1	3	0.1	.	.
Positive control	A. e + F. o	4	15	0.71	0.5	0.83
<i>L. capsici</i> K-Hf-H2	F. a + F. o	3	12	0.56	0.35	0.74
<i>P. simiae</i> K-Hf-L9	F. a + F. o	3	13	0.64	0.46	0.77
<i>P. agglomerans</i> PSV1-7	F. a + F. o	3	12	0.56	0.35	0.74
Negative control	Uninoculated	1	3	0.1	.	.
Positive control	F. a + F. o	3	13	0.64	0.46	0.77
<i>L. capsici</i> K-Hf-H2	A. e + F. a + F. o	5	12	0.57	0.46	0.67
<i>P. simiae</i> K-Hf-L9	A. e + F. a + F. o	6	16	0.76	0.59	0.85
<i>P. agglomerans</i> PSV1-7	A. e + F. a + F. o	4	7	0.31	0.29	0.32
Negative control ^e	Uninoculated	1	3	0.1	.	.
Positive control	A. e + F. a + F. o	6	16	0.76	0.59	0.85

^a Inoculated root rot pathogen: *A. euteiches* (A.e), *F. avenaceum* (F.a) and *F. oxysporum* (F.o); ^b Median disease score based on a 1-7 rating scale: 1 (no disease), 2 (reddish-brown discoloration at point of seed attachment), 3 (Localized root/epicotyl lesions), 4 (Lesions encircle tap root/epicotyl), 5 (Extended epicotyl lesions), 6 (Lesions encircling the stem, < 2 cm long) and 7 (Lesions > 2 cm, decay of taproot/epicotyl). ^c Relative effect on disease severity. ^d 95% confidence intervals of the relative effect. ^e Negative control had the same and lowest exclusive scales; thus, the relative effect was constant.

4.5.5 Biocontrol of root rot complex in non-sterile soil

The biocontrol assessment of RRC indicated that when the three pathogens co-occurred in the soil, the disease burden lead complete death of the affected pea plants compared to when a fewer pathogens were used (Figs. 4.9 and 4.10, Table 4.6).

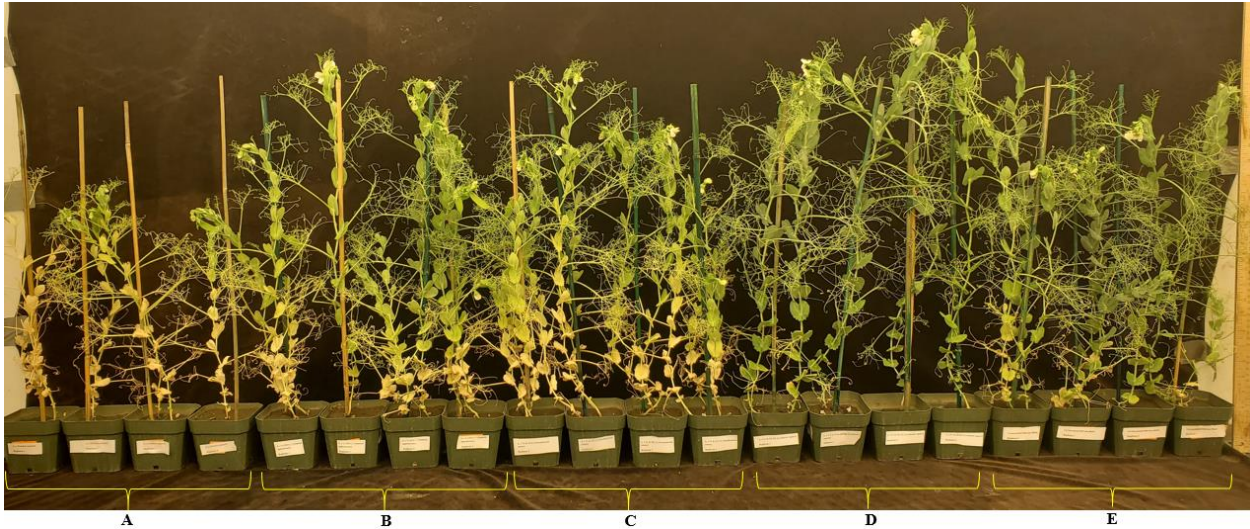


Figure 4.9. Biocontrol assessment of root rot complex in field pea caused by *A. euteiches*. **A:** *A. euteiches*; **B:** *P. simiae* K-Hf-L9 Vs *A. euteiches*; **C:** *P. agglomerans* PSV1-7 Vs *A. euteiches*; **D:** *L. capsici* K-Hf-H2Vs *A. euteiches*; **E:** Un-inoculated. The trials were conducted using a completely randomized design with four replicates.

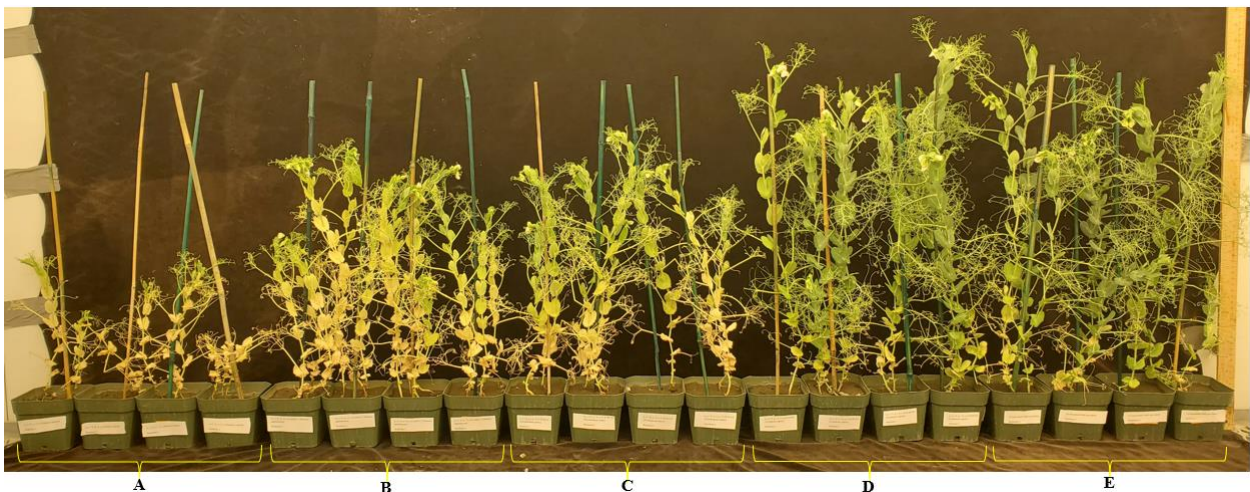


Figure 4.10. Biocontrol assessment of root rot complex in field pea caused by *A. euteiches*, *F. avenaceum* and *F. oxysporum*. **A:** (*A. euteiches* + *F. avenaceum* + *F. oxysporum*). **B:** *P. simiae* K-Hf-L9 Vs (*A. euteiches* + *F. avenaceum* + *F. oxysporum*); **C:** *P. agglomerans* PSV1-7 Vs (*A. euteiches* + *F. avenaceum* + *F. oxysporum*); **D:** *L. capsici* K-Hf-H2 Vs (*A. euteiches* + *F. avenaceum* + *F. oxysporum*); **E:** Un-inoculated. The trials were conducted using a completely randomized design with four replicates.

The biocontrol bacteria *L. capsici* K-Hf-H2, *P. simiae* K-Hf-L9 and *P. agglomerans* PSV1-7 significantly suppressed ARR and ARRC in field pea grown in non-sterile soil (Table 4.6). Of the three biocontrol organisms, *L. capsici* K-Hf-H2 produced the highest biocontrol efficacy with MDS of 3 and a mean rank of 4.9 (CI: 0.16 to 0.33) when tested against all three pathogens. No significant difference was detected with untreated negative control plants (MDS = 3; mean rank: 4.1; CI: 0.13 to 0.32). The overlap of the confidence intervals indicates no significant difference (Table 4.6).

In addition, field pea plants treated with *L. capsici* K-Hf-H2 had significantly higher shoot dry weights in the respective treatment combinations (Table 4.7). These findings suggest that *L. capsici* K-Hf-H2 had direct plant growth-promoting activity in addition to suppressing disease.

Table 4.6. Effect of biocontrol bacteria *L. capsici* K-Hf-H2, *P. simiae* K-Hf-L9 and *P. agglomerans* PSV1-7 on root rot severity in field pea grown in non-sterile soil in growth chamber conditions.

Treatment	Pathogen ^a	Median Disease Score ^b	Mean Rank	Relative Effect ^c	95% CI of the RE ^d	
					Lower limit	Upper limit
<i>L. capsici</i> K-Hf-H2	A. e	2	4	0.2	0.12	0.44
<i>P. simiae</i> K-Hf-L9	A. e	3	11	0.5	0.45	0.63
<i>P. agglomerans</i> PSV1-7	A. e	3	13	0.6	0.49	0.71
Negative control	Uninoculated	3	6	0.3	0.18	0.42
Positive control	A. e	5	18	0.9	0.81	0.9
<i>L. capsici</i> K-Hf-H2	A. e + F. a	3	5	0.2	0.16	0.33
<i>P. simiae</i> K-Hf-L9	A. e + F. a	4	13	0.6	0.53	0.67
<i>P. agglomerans</i> PSV1-7	A. e + F. a	4	13	0.6	0.53	0.67
Negative control	Uninoculated	3	4	0.2	0.13	0.32
Positive control	A. e + F. a	6	18	0.9	0.78	0.90
<i>L. capsici</i> K-Hf-H2	A. e + F. o	3	5	0.2	0.14	0.32
<i>P. simiae</i> K-Hf-L9	A. e + F. o	4	13	0.6	0.5	0.69
<i>P. agglomerans</i> PSV1-7	A. e + F. o	5	13	0.6	0.52	0.74
Negative control	Uninoculated	3	5	0.2	0.14	0.32
Positive control	A. e + F. o	5	18	0.9	0.75	0.89
<i>L. capsici</i> K-Hf-H2	F. a + F. o	2	12	0.3	0.18	0.6
<i>P. simiae</i> K-Hf-L9	F. a + F. o	2	16	0.4	0.25	0.61
<i>P. agglomerans</i> PSV1-7	F. a + F. o	2	14	0.3	0.18	0.6
Negative control	Uninoculated	3	17	0.5	0.36	0.69
Positive control	F. a + F. o	4	22	0.9	0.71	0.9
<i>L. capsici</i> K-Hf-H2	A. e + F. a + F. o	3	5	0.2	0.16	0.33
<i>P. simiae</i> K-Hf-L9	A. e + F. a + F. o	4	13	0.6	0.54	0.69
<i>P. agglomerans</i> PSV1-7	A. e + F. a + F. o	4	12	0.6	0.5	0.66
Negative control	Uninoculated	3	4	0.2	0.13	0.32
Positive control	A. e + F. a + F. o	7	18	0.9	0.78	0.90

^a Inoculated root rot pathogen: *A. euteiches* (A.e), *F. avenaceum* (F.a) and *F. oxysporum* (F.o); ^b Median disease score based on a 1-7 rating scale: 1 (no disease), 2 (reddish-brown discoloration at point of seed attachment), 3 (Localized root/epicotyl lesions), 4 (Lesions encircle tap root/epicotyl), 5 (Extended epicotyl lesions), 6 (Lesions encircling the stem, < 2 cm long) and 7 (Lesions > 2 cm, decay of taproot/epicotyl). ^c Relative effect on disease severity. ^d 95% confidence intervals of the relative effect. The trials were conducted using a completely randomized design with four replicates.

Table 4.7. Effect of biocontrol bacterial strains on shoot dry weight of field pea grown in non-sterile soil in growth chamber pot trials

Treatment	Pathogen	Mean shoot dry weight (g) ^a
<i>L. capsici</i> K-Hf-H2	A. e	6.33a
<i>P. simiae</i> K-Hf-L9	A. e	4.74b
<i>P. agglomerans</i> PSV1-7	A. e	4.68b
Negative control	Uninoculated	4.86b
Positive control	A. e	1.66c
<i>L. capsici</i> K-Hf-H2	A. e + F. a	6.04a
<i>P. simiae</i> K-Hf-L9	A. e + F. a	3.53c
<i>P. agglomerans</i> PSV1-7	A. e + F. a	3.83c
Negative control	Uninoculated	4.86b
Positive control	A. e + F. a	1.14d
<i>L. capsici</i> K-Hf-H2	A. e + F. o	5.83a
<i>P. simiae</i> K-Hf-L9	A. e + F. o	3.88bc
<i>P. agglomerans</i> PSV1-7	A. e + F. o	4.08b
Negative control	Uninoculated	4.86b
Positive control	A. e + F. o	1.74d
<i>L. capsici</i> K-Hf-H2	F. a + F. o	5.64a
<i>P. simiae</i> K-Hf-L9	F. a + F. o	4.20b
<i>P. agglomerans</i> PSV1-7	F. a + F. o	4.40b
Negative control	Uninoculated	4.86ab
Positive control	F. a + F. o	1.82c
<i>L. capsici</i> K-Hf-H2	A. e + F. a + F. o	5.75a
<i>P. simiae</i> K-Hf-L9	A. e + F. a + F. o	3.71c
<i>P. agglomerans</i> PSV1-7	A. e + F. a + F. o	3.64c
Negative control	Uninoculated	4.86b
Positive control	A. e + F. a + F. o	0.70d

^a Means were obtained from an individual trial, with four replicates per treatment. Each replicate consisted of a single pot, with two plants per pot. Means followed by the same letter within a column in the respective treatment category are not significantly different.

Similarly, the biocontrol assessment of RRC in lentil indicated that the co-occurrence of the three pathogens resulted in a severe root rot burden leading to complete death of the plant compared to when a low pathogen number is present (Figs. 4.11 and 4.12).



Figure 4.11. Biological control of root rots in lentils due to *Aphanomyces euteiches* (A. e) by biocontrol bacteria *Lysobacter capsici* K-Hf-H2, *Pseudomonas simiae* K-Hf-L9 and *Pantoea agglomerans* PSV1-7. Negative control: un-inoculated; positive control: (A. e) inoculated. The trials were conducted using a completely randomized design with four replicates.



Figure 4.12. Biological control of root rots in lentils due to *Aphanomyces euteiches* (A. e), *Fusarium avenaceum* (F. a) and *Fusarium oxysporum* (F. o) by biocontrol bacteria *Lysobacter capsici* K-Hf-H2, *Pseudomonas simiae* K-Hf-L9 and *Pantoea agglomerans* PSV1-7. Negative control: un-inoculated; positive control: (A. e + F. a + F. o) inoculated. The trials were conducted using a completely randomized design with four replicates.

All three biocontrol bacteria suppressed ARR development in lentil (Table 4.8) compared to the positive control treatment. Of the three bacteria, *L. capsici* K-Hf-H2 suppressed ARR in lentil to the greater degree (MDS = 2; mean rank = 5.3; CI: 0.18 to 0.33), and no significant difference

was detected between this biocontrol treatment and the untreated negative control lentil plants (MDS = 2; mean rank = 3.8; CI 0.12 to 0.29). The overlap of CI indicates no significant difference (Table 4.8). Although *L. capsici* K-Hf-H2 exhibited the highest biocontrol efficacy in all biocontrol assessment combinations, its biocontrol efficacy significantly decreased as the number of co-inoculated pathogens increased. Thus, the lowest biocontrol efficacy was recorded when all three pathogens co-occurred (Fig. 4.13; Table 4.8).

Even if the root rot severity increased as the number of co-inoculated pathogens increased, the root rot severity was higher when *A. euteiches* was present with *F. avenaceum* and/or *F. oxysporum* than without *A. euteiches*. For example, the MDS was 5 when lentil plants were co-inoculated with *F. avenaceum* and *F. oxysporum*. In contrast, the MDS increased to 6 and 7 when the lentil plants were co-inoculated with *A. euteiches* and *F. avenaceum* and *A. euteiches* and *F. oxysporum*, respectively (Table 4.8). These suggest that *A. euteiches* is the most virulent and aggressive pathogen compared to either *F. avenaceum* or *F. oxysporum*.

The findings of the shoot dry weight corresponded to the respective root rot severity level in each treatment. Thus, lentil plants inoculated with *L. capsici* K-Hf-H2 had significantly higher shoot dry weight than those treated with *P. simiae* K-Hf-L9 and *P. agglomerans* PSV1-7 and the respective positive control treatments throughout the experiment (Table 4.9). Moreover, within the ARR biocontrol assessment treatment category (Table 4.9), no significant difference was detected between the shoot dry weight of *L. capsici* K-Hf-H2 treated and untreated negative control lentil plants.

The untreated negative control field pea and lentil plants grown in non-sterile soil exhibited root rot symptoms with MDS of 3 and 2, respectively (Tables 4.6 and 4.8). Where 2 refers to the development of small reddish-brown discolouration at a point of seed attachment, and 3 describes the presence of localized rot or epicotyl lesion around the tap root. These observations suggest that the soil used also had a root rot-causing pathogen.

Table 4.8. Effect of biocontrol bacteria *L. capsici* K-Hf-H2, *P. simiae* K-Hf-L9 and *P. agglomerans* PSV1-7 on root rot severity in lentil grown in non-sterile soil in growth chamber conditions.

Treatment	Pathogen ^a	Median Disease Score ^b	Mean Rank	Relative Effect ^c	95% CI of the RE ^d	
					Lower limit	Upper limit
<i>L. capsici</i> K-Hf-H2	A. e	2	5	0.24	0.18	0.33
<i>P. simiae</i> K-Hf-L9	A. e	5	14	0.66	0.55	0.75
<i>P. agglomerans</i> PSV1-7	A. e	4	12	0.56	0.48	0.63
Negative control	Uninoculated	2	4	0.16	0.12	0.29
Positive control	A. e	6	18	0.88	0.77	0.9
<i>L. capsici</i> K-Hf-H2	A. e + F. a	3	7	0.3	0.3	0.3
<i>P. simiae</i> K-Hf-L9	A. e + F. a	6	14	0.66	0.49	0.78
<i>P. agglomerans</i> PSV1-7	A. e + F. a	6	14	0.66	0.49	0.78
Negative control ^e	Uninoculated	2	3	0.1	.	.
Positive control	A. e + F. a	6	16	0.78	0.58	0.86
<i>L. capsici</i> K-Hf-H2	A. e + F. o	3	7	0.33	0.27	0.39
<i>P. simiae</i> K-Hf-L9	A. e + F. o	6	13	0.63	0.51	0.73
<i>P. agglomerans</i> PSV1-7	A. e + F. o	6	13	0.62	0.48	0.73
Negative control	Uninoculated	2	3	0.1	.	.
Positive control	A. e + F. o	7	17	0.83	0.67	0.88
<i>L. capsici</i> K-Hf-H2	F. a + F. o	1	5	0.23	0.17	0.32
<i>P. simiae</i> K-Hf-L9	F. a + F. o	4	13	0.63	0.47	0.76
<i>P. agglomerans</i> PSV1-7	F. a + F. o	4	14	0.66	0.5	0.77
Negative control	Uninoculated	2	4	0.17	0.12	0.29
Positive control	F. a + F. o	5	17	0.81	0.63	0.88
<i>L. capsici</i> K-Hf-H2	A. e + F. a + F. o	5	7	0.3	0.3	0.3
<i>P. simiae</i> K-Hf-L9	A. e + F. a + F. o	6	12	0.59	0.47	0.69
<i>P. agglomerans</i> PSV1-7	A. e + F. a + F. o	7	15	0.73	0.56	0.83
Negative control	Uninoculated	2	3	0.1	.	.
Positive control	A. e + F. a + F. o	7	16	0.78	0.56	0.87

^a Inoculated root rot pathogen: *A. euteiches* (A.e), *F. avenaceum* (F.a) and *F. oxysporum* (F.o); ^b Median disease score (MDS) based on a 1-7 rating scale: 1 (no disease), 2 (reddish-brown discolouration at point of seed attachment), 3 (Localized root/epicotyl lesions), 4 (Lesions encircle tap root/epicotyl), 5 (Extended epicotyl lesions), 6 (Lesions encircling the stem, < 2 cm long) and 7 (Lesions > 2 cm, decay of taproot/epicotyl). ^c Relative effect on disease severity. ^d 95% confidence intervals of the relative effect. ^e Negative control had the same and smallest exclusive scales, thus, the relative effect was constant. The trials were conducted using a completely randomized design with four replicates.

Table 4.9. Effect of biocontrol bacterial strains on shoot dry weight of lentil grown in non-sterile soil in growth chamber pot trials

Treatment	Pathogen	Mean shoot dry weight (g) ^a
<i>L. capsici</i> K-Hf-H2	A. e	2.28a
<i>P. simiae</i> K-Hf-L9	A. e	1.17b
<i>P. agglomerans</i> PSV1-7	A. e	0.98b
Negative control	Uninoculated	2.33a
Positive control	A. e	0.74b
<i>L. capsici</i> K-Hf-H2	A. e + F. a	1.38b
<i>P. simiae</i> K-Hf-L9	A. e + F. a	0.96bc
<i>P. agglomerans</i> PSV1-7	A. e + F. a	0.81c
Negative control	Uninoculated	2.33a
Positive control	A. e + F. a	0.46c
<i>L. capsici</i> K-Hf-H2	A. e + F. o	1.08b
<i>P. simiae</i> K-Hf-L9	A. e + F. o	0.79bc
<i>P. agglomerans</i> PSV1-7	A. e + F. o	1.14b
Negative control	Uninoculated	2.33a
Positive control	A. e + F. o	0.50c
<i>L. capsici</i> K-Hf-H2	F. a + F. o	1.87ab
<i>P. simiae</i> K-Hf-L9	F. a + F. o	1.40bc
<i>P. agglomerans</i> PSV1-7	F. a + F. o	1.02cd
Negative control	Uninoculated	2.33a
Positive control	F. a + F. o	0.78d
<i>L. capsici</i> K-Hf-H2	A. e + F. a + F. o	1.25b
<i>P. simiae</i> K-Hf-L9	A. e + F. a + F. o	0.64cd
<i>P. agglomerans</i> PSV1-7	A. e + F. a + F. o	1.02bc
Negative control	Uninoculated	2.33a
Positive control	A. e + F. a + F. o	0.48d

^a Means were obtained from an individual trial, with four replicates per treatment. Each replicate consisted of a single pot, with two plants per pot. Means followed by the same letter within a column in the respective treatment category are not significantly different.

4.5.6 Biocontrol of aphanomyces root rot in lentil

During a separate biocontrol assessment of ARR in lentils using ten antagonistic bacteria, the strains showed some biocontrol efficacy in both growth media (Tables 4.10 and 4.11). Most strains, however, exhibited higher efficacy in non-sterile agricultural soil than vermiculite,

including *L. gummosus* K-Be-H3, a strain with a highest antagonistic activity towards the mycelial growth of *A. euteiches* (Godebo, 2019) and *Fusarium avenaceum* strain (Fig. 4.4). However, statistically, the *L. gummosus* K-Be-H3 efficacy was not different from the efficacy of *P. simiae* K-Hf-L9, *L. capsici* K-Hf-H2, *R. lemnae* PSV1-9, *B. cereus* K-CB2-6, and *L. antibioticus* K-CB2-4 (Table 4.11).

Table 4.10. Effect of biocontrol bacteria against aphanomyces root rot severity in lentil grown in vermiculite in growth chamber conditions.

Treatment	Pathogen	Median Disease Score ^a	Mean Rank	Relative Effect ^b	95% CI of the RE ^c	
					Lower limit	Upper limit
<i>L. capsici</i> K-Hf-H2	<i>A. euteiches</i>	1	63	0.65	0.52	0.76
<i>P. simiae</i> K-Hf-L9	<i>A. euteiches</i>	0	27	0.28	0.18	0.41
<i>P. agglomerans</i> PSV1-7	<i>A. euteiches</i>	0	33	0.34	0.21	0.5
<i>L. gummosus</i> K-Be-H3	<i>A. euteiches</i>	1	69	0.71	0.67	0.75
<i>L. antibioticus</i> K-CB2-4	<i>A. euteiches</i>	0	39	0.4	0.25	0.58
<i>B. cereus</i> K-CB2-6	<i>A. euteiches</i>	1	57	0.59	0.43	0.73
<i>R. lemnae</i> PCV1-13	<i>A. euteiches</i>	1	57	0.59	0.43	0.73
<i>R. lemnae</i> PSV1-9	<i>A. euteiches</i>	1	57	0.59	0.43	0.73
<i>S. plymuthica</i> DR1-2	<i>A. euteiches</i>	1	57	0.59	0.43	0.73
<i>S. paradoxus</i> K-CB1-1	<i>A. euteiches</i>	0	33	0.34	0.21	0.5
Negative control	Uninoculated	0	21	0.21	0.18	0.26
Positive control	<i>A. euteiches</i>	1	69	0.71	0.67	0.75

^a Median disease score based on a 0-4 rating scale: 0 = No symptoms; roots healthy; 1 = Initial symptoms of root rot; discolouration. Light tan colour in sections of the root system; 2 = Discolouration of most or all the root system, small watery lesions may be present on the root and around the hypocotyl/epicotyl regions; 3 = Advanced disease symptoms, dwarfing of the plant and yellowing of the lower leaves. Extensive darkening and discolouration of the root system and extensive lesion formation; 4 = root entirely rotted / plant dead. ^b Relative effect on disease severity. ^c 95% confidence intervals of the relative effect.

Table 4.11. Effect of biocontrol bacteria against aphanomyces root rot severity in lentil grown in non-sterile soil in growth chamber conditions.

Treatment	Pathogen	Median Disease Score ^a	Mean rank	Relative Effect ^b	95% CI of the RE ^c	
					Lower limit	Upper limit
<i>L. capsici</i> K-Hf-H2	<i>A. euteiches</i>	3	45	0.46	0.32	0.61
<i>P. simiae</i> K-Hf-L9	<i>A. euteiches</i>	2	45	0.46	0.25	0.69
<i>P. agglomerans</i> PSV1-7	<i>A. euteiches</i>	4	79	0.82	0.69	0.89
<i>L. gummosus</i> K-Be-H3	<i>A. euteiches</i>	2	25	0.25	0.17	0.36
<i>L. antibioticus</i> K-CB2-4	<i>A. euteiches</i>	2	31	0.32	0.2	0.48
<i>B. cereus</i> K-CB2-6	<i>A. euteiches</i>	2	37	0.38	0.19	0.63
<i>R. lemnae</i> PCV1-13	<i>A. euteiches</i>	3	52	0.52	0.41	0.63
<i>R. lemnae</i> PSV1-9	<i>A. euteiches</i>	2	41	0.44	0.27	0.63
<i>S. plymuthica</i> DR1-2	<i>A. euteiches</i>	3	56	0.58	0.51	0.64
<i>S. paradoxus</i> K-CB1-1	<i>A. euteiches</i>	4	72	0.74	0.61	0.83
Negative control	Uninoculated	4	37	0.38	0.23	0.57
Positive control	<i>A. euteiches</i>	3	64	0.66	0.55	0.75

^a Median disease score based on a 0-4 rating scale: 0 = No symptoms; roots healthy; 1 = Initial symptoms of root rot; discolouration. Light tan colour in sections of the root system; 2 = Discolouration of most or all the root system, small watery lesions may be present on the root and around the hypocotyl/epicotyl regions; 3 = Advanced disease symptoms, dwarfing of the plant and yellowing of the lower leaves. Extensive darkening and discolouration of the root system and extensive lesion formation; 4 = root entirely rotted / plant dead. ^b Relative effect on disease severity. ^c 95% confidence intervals of the relative effect.

4.6 Discussion

The increased risk of yield loss in field pea and lentil due to RRC and the focus on sustainable production has resulted in many efforts to isolate and identify soil-associated bacteria conferring resistance against RRC pathogens. In sustainable agriculture, such an approach is becoming a sound alternative for managing plant disease and improving crop productivity (Ramamoorthy et al., 2001). In the current study, the bacterial strains *L. capsici* K-Hf-H2, *P. simiae* K-Hf-L9 and *P. agglomerans* PSV1-7 with the highest biocontrol efficacy against ARR and an additional strain, *L. gummosis* K-Be-H3 (Godebo et al., 2020) were assessed for biocontrol activity against root rot complex pathogens often associated with *A. euteiches*.

L. capsici K-Hf-H2, *P. simiae* K-Hf-L9, *P. agglomerans* PSV1-7 and *L. gummosis* K-Be-H3 inhibited the mycelial growth of *F. avenaceum*, and *F. oxysporum* strains in *in vitro* dual plate screenings at different efficacy levels (Figs. 4.2, 4.3 and 4.4), suggesting broad spectrum activity.

In addition, the difference in antagonistic activity indicates variations in inhibitory potential among the bacterial strains. Given the common occurrence of *A. euteiches* with *F. avenaceum* and *F. oxysporum* in field pea and lentil fields across western Canada, the identification of biocontrol bacteria with a broad spectrum of activities has potential promise and practical significance. Similarly, various biocontrol agents with varying levels of biocontrol capacity were commercialized as biocontrol agents for other plant pathogens. For instance, registered broad-spectrum biocontrol agents include Kodiak (*Bacillus subtilis* GB03) for *Rhizoctonia* spp., *Fusarium* spp., and *Aspergillus* spp.; Integral (*B. subtilis* MBI 600) for *Rhizoctonia* spp. and *Fusarium* spp.; and Serenade (*B. subtilis* QST 713) for *Botrytis* spp., *Sclerotinia* spp., *Xanthomonas* spp., and *Erwinia* spp. (Liu et al., 2017). These *Bacillus subtilis* species are now named as *Bacillus velezensis* (Dunlap et al., 2016).

The agar well diffusion assay demonstrated that the cell-free supernatant from *L. capsici* K-Hf-H2 inhibits the growth of *A. euteiches*, and the production of inhibitory metabolites was dependent on the bacterial growth phase (Figs. 4.5, 4.6 and 4.7). Studies have demonstrated that microbes undergo specific physiological responses during their growth cycle (Lag phase, log phase, stationary phase and death/decline phase) (Robador et al., 2018). During the stationary phase, where the nutrients are depleted and metabolic waste products accumulate, the microbial cells produce secondary metabolites in the culture (fermenting media) after microbial growth is completed (Nigam and Singh, 2014). Therefore, the inhibition of *A. euteiches* mycelia by the cell-free supernatant obtained from day 7 to day 14 culture suggests the bioactive molecules were secondary metabolites. Moreover, the growth period from 7 to 14 d on the growth curve of *L. capsici* K-Hf-H2 (Fig. 6) represents the stationary to the death/decline phase.

Lysobacter species are well-known for producing a variety of extracellular bioactive metabolites and antimicrobial compounds, including antibiotics, enzymes and other compounds against different pathogenic organisms (Reichenbach, 2006; Gómez et al., 2015). In fact, the genus obtained the name "Lysobacter" due to its ability to lyse these organisms and literally means the "lysing rod" (Christensen and Cook, 1978; Brescia et al., 2020). Therefore, this finding lays a foundation for future studies aiming at exploring the efficacy of *L. capsici* K-Hf-H2 cell-free supernatant or its bioactive chemical to control ARR. On the other hand, the inability to detect inhibitory metabolites from the *P. simiae* K-Hf-L9, *P. agglomerans* PSV1-7 and *L. gummosis* K-

Be-H3 cell-free supernatant indicates the need for future optimized and strain-specific fermentation media.

The result from the storage and autoclave stability assay indicated that storage conditions significantly influenced the antagonistic nature of the cell-free supernatant. Of the four conditions (i.e., room temperature: 24°C; 4°C, -20°C and autoclaving), the cell-free supernatant stored at 4°C for four months preserved inhibitory potential and thus was deemed stable at 4°C (Table 4.3; Fig. 4.8). This finding is consistent with the finding by Md Sidek et al. (2018). Md Sidek et al. (2018) investigated the stability of cell-free inhibitory substance produced by *Pediococcus acidilactici* kp10 and found that during a one-month storage period, the crude extract of *P. acidilactici* Kp10 was only stable at 4°C and lost its activity at -20°C and -80°C.

The growth chamber trials assessed the potential for biological control of RRC in field pea and lentils caused by *A. euteiches*, *F. avenaceum* and *F. oxysporum* using ARR biocontrol bacteria identified in a study conducted by Godebo et al. (2020). The trials utilized vermiculite and non-sterile agricultural soil as a plant-growing media for each crop and investigated the biocontrol bacteria of *L. capsici* K-Hf-H2, *P. simiae* K-Hf-L9 and *P. agglomerans* PSV1-7. Although some level of biocontrol efficacy was observed when using vermiculite, the efficacy levels were inconsistent and highly reduced compared to those observed using non-sterile agricultural soil. This observation is consistent with previous study findings (Godebo, 2019). Thus, it suggests that vermiculite might not be an appropriate growth medium for such biocontrol assessment studies. However, it has higher water retention potential (Safronovitz, 2011), a condition root rot pathogens prefer most; therefore, it is most likely suited to conduct other inoculation experiments, such as investigating root rot symptom severity.

In the growth chamber study conducted using non-sterile agricultural soil, the biocontrol bacteria significantly reduced root rot severity compared to the positive control in both field pea and lentil (Tables 4.6 and 4.8). However, the strains exhibited higher efficacy in the field pea than the lentil in all treatment combinations. Moreover, of the three biocontrol bacteria investigated against ARR and RRC, *L. capsici* K-Hf-H2 significantly reduced disease severity in both field pea and lentil compared to the control (Figs. 4.9, 4.10, 4.11 and 4.12). Other researchers also reported similar findings. For instance, Liu et al. (2019) identified *L. capsici* NF87–2 that showed a broad spectrum of biocontrol activity against phytopathogens such as *F. oxysporum*, *R. solani*, *Alternaria*

brassicae, *Sclerotinia sclerotiorum*, *Botrytis cinerea* and *Colletotrichum gloeosporioides*. Another study by Ji et al. (2008) identified *L. antibioticus* that inhibited the growth of various phytopathogenic bacteria and fungi and suppressed bacterial leaf blight in rice. These studies demonstrated the broad-spectrum activity of the bacteria belonging to the genus *Lysobacter*. Therefore, *Lysobacter* species are multi-functional bacteria with great significance and potential applications in agriculture to prevent destructive diseases like RRC (Hsieh et al., 2005; Gómez et al., 2015). For these reasons, *Lysobacter* is regarded as a potential biocontrol agent (Lin et al., 2021).

The findings of this study were consistent with reports for other groups of bacteria (Xu and Kim, 2014). For example, Xu and Kim (2014) investigated the efficacy of seven *Paenibacillus* strains against fusarium crown and root rot in tomato under greenhouse conditions and reported that all tested strains significantly reduced disease severity and promoted growth compared to the control. In the current study, *L. capsici* K-Hf-H2 was identified as capable of promoting growth in field pea in non-sterile soil compared with untreated negative control plants during the growth chamber trial. Thus, a significant shoot dry weight increase was recorded, with a maximum increase of 56.5% in field pea treated with *L. capsici* K-Hf-H2 and *A. euteiches* (Table 4.7). Several studies have reported similar findings that biocontrol bacteria also engage in direct plant growth promoting activity, providing holistic benefits, including improved disease resistance and productivity. For example, Puopolo et al. (2010) identified *L. capsici* PG4 that inhibited *F. oxysporum* f. sp. lycopersi, *F. oxysporum* f. sp. radicle-lycopersici and *R. solani* and drastically reduced the incidence of tomato crown and root rot which ultimately led to a marked increase in plant fresh weight in greenhouse studies. Furthermore, Márquez et al. (2020) reported that a *Bacillus* strain promoted growth and inhibited the propagation of necrotic spots in paper plants caused by *F. solani*. On the other hand, the increased shoot dry weight could be associated with the *L. capsici* K-Hf-H2 simply suppressing those native pathogens which appeared to cause root rot disease in the negative (untreated) control plants.

Lysobacter gummosus K-Be-H3 demonstrated strong antagonistic activity in inhibiting both *A. euteiches* and *F. avenaceum* mycelial growth (Fig. 4.4). In addition, although low efficacy was observed in suppressing ARR in field pea (Godebo et al., 2020), of ten bacterial strains tested, *L. gummosus* K-Be-H3 strain demonstrated significant suppression of ARR in lentil (Table 4.11).

These findings indicate that *L. gummosus* K-Be-H3 has biocontrol potential and suggest the need for future studies that aim to utilize its natural broad-spectrum antimicrobial weapon.

During both growth chamber trials using vermiculite and non-sterile agricultural soil, the root rot severity was higher as the number of co-inoculated pathogens increased (Tables 4.4, 4.5, 4.6 and 4.8). This could be attributed to a synergistic interaction between the pathogens investigated in this study. The synergistic interaction of pathogens towards both field pea and lentil can lead to the breakdown of resistance against one pathogen and can intensify disease, as observed for several other multi-species pathosystems of pea and lentil (Basler 1981; Peters and Grau 2002; Tiwari et al. 2018; Willsey et al. 2018; Zitnick-Anderson et al. 2018). Moreover, the root rot severity was higher in lentil (Table 4.8) than in field pea (Table 4.6) when *A. euteiches* and *F. avenaceum* were co-inoculated. This indicates that lentil is more susceptible than field pea when *A. euteiches* co-occurs with the *F. avenaceum*. This could be attributed to the more aggressive nature of *F. avenaceum* when in contact with lentil than pea, as stated in Bogdan (2019). Therefore, biocontrol bacteria like *L. capsici* K-Hf-H2, with a broad spectrum of activity, present unique potential.

4.7 Conclusions

This study identified that biocontrol bacteria, *L. capsici* K-Hf-H2, *P. simiae* K-Hf-L9, *P. agglomerans* PSV1-7 and *L. gummosis* K-Be-H3, harbour a broad spectrum of antimicrobial activity, which inhibited the mycelial growth of strains of *F. avenaceum* and *F. oxysporum* in *in vitro* dual plate screenings. The *in vivo* results demonstrated that RRC in field pea and lentil can be suppressed more significantly by *L. capsici* K-Hf-H2 biocontrol bacteria compared with *P. simiae* K-Hf-L9 and *P. agglomerans* PSV1-7. Variation in antagonistic potential in inhibiting *A. euteiches*, *F. avenaceum* and *F. oxysporum* mycelial growth and biocontrol efficacy against RRC suggest the possible variation in the biocontrol mechanism.

In addition to the absence of effective management strategies against RRC, which urges the need for continued research, the application of biocontrol bacteria represents a sustainable agriculture technology. Therefore, future studies should assess the biocontrol efficacy of *L. capsici* K-Hf-H2 under field conditions. Moreover, including other variables such as inoculation rate, application frequency, and co-inoculation of *L. capsici* K-Hf-H2 with the other biocontrol bacteria may increase biocontrol fitness and consequently increase plant health and productivity.

It is well documented that most soil bacteria with antagonistic activity under laboratory conditions exhibit low or no biocontrol efficacy when tested in both growth chamber and field conditions, as indicated in a meta-analysis review (Chapter Three). However, the fact that this study was a continuation of research from an initial study (2016 to 2019) that identified 184 isolates antagonistic to *A. euteiches* (Godebo, 2019) and now focused on a few strains shows the extensive work accomplished. Moreover, it suggests the potential promise in controlling ARR and RRC. Furthermore, the study has gone through the milestones essential in discovering effective biocontrol agents, including whole-genome sequencing and identification of biocontrol-related gene and gene clusters discussed in the following chapter (Chapter Five). Therefore, it is now critical to investigate the biocontrol potential of *L. capsici* K-Hf-H2 under field conditions.

5. WHOLE-GENOME ANALYSIS OF BACTERIAL ISOLATES WITH BIOCONTROL POTENTIAL TOWARDS APHANOMYCES ROOT ROT IN FIELD PEA AND LENTIL CAUSED BY *APHANOMYCES EUTEICHES*^{1,2}

5.1 Preface

In Chapter four, three ARR biocontrol bacteria, *L. capsici* K-Hf-H2, *P. simiae* K-Hf-L9 and *P. agglomerans* PSV1-7 that suppressed RRC in field pea and lentil caused by strains of *A. euteiches*, *F. avenaceum* and *F. oxysporum* under controlled growth chamber conditions were identified. Moreover, *L. capsici* K-Hf-H2 was not only the most effective biocontrol agent against RRC in both field pea and lentil but also resulted in increased shoot dry weight in field pea compared to untreated negative control plants. However, mechanism(s) by which biocontrol bacteria suppressed disease development is unknown. Therefore, to elucidate biocontrol mechanisms, it is necessary to first sequence the complete genome of the biocontrol bacteria and conduct a whole genome analysis using bioinformatics tools, followed by general functional experiments under laboratory conditions. Thus, this chapter describes the complete genomes of the biocontrol bacteria that were sequenced, annotated, and comparatively analyzed. Additionally, experiments in which the biocontrol bacteria were examined for siderophores production, proteolytic and cellulolytic activity, and desiccation tolerance are described.

¹The whole-genome shotgun project for *L. capsici* K-Hf-H2, *P. simiae* K-Hf-L9, *P. agglomerans* PSV1-7 and *L. gummosus* K-Be-H3 has been deposited in GenBank and accessible using the accession numbers CP090945.1, CP066169.2, CP091189.1 and CP091194.1, respectively.

² The genomic sequence of *P. simiae* K-Hf-L9 is published in ASM Journals (Microbiology Resource Announcements) as Godebo, A. T., MacKenzie, K. D., Walley, F. L., Germida, J. J., & Yost, C. K. (2021). Complete Genome Sequence of a *Pseudomonas simiae* Strain with Biocontrol Potential against *Aphanomyces* Root Rot. *Microbiology Resource Announcements*, 10(18), e00222-21. DOI: [10.1128/MRA.00222-21](https://doi.org/10.1128/MRA.00222-21)

5.2 Abstract

Microbial biocontrol agents protect crops through direct and indirect mechanisms, including the production of antimicrobial secondary metabolites, induction of local and systemic resistance within the plant and competition for space and nutrients. Therefore, whole genome sequence analysis and laboratory-based functional experiments were conducted to determine potential genetic determinants and biocontrol mechanisms responsible for controlling ARR and RRC in field pea and lentil. The complete genome sequence analysis revealed that *L. capsici* K-Hf-H2, *P. simiae* K-Hf-L9 and *P. agglomerans* PSV1-7, harbour genes potentially involved in the biocontrol of ARR and RRC, including genes predicted to code for the production of antibiotics, lytic enzymes and siderophores. In the *L. capsici* K-Hf-H2 genome, biosynthetic gene clusters (BGCs) encoding for heat stable antifungal factor (HSAF), cellulase (endoglucanase), chitinase, metalloendopeptidase (extracellular zinc proteases), aminopeptidases and siderophores were detected. In the *P. simiae* K-Hf-L9 genome, gene and gene clusters involved in chitin metabolism and TldE-TldD proteolytic activity were detected. However, a significant portion of the *P. simiae* K-Hf-L9 genome was found to encode fluorescent siderophores, known as pyoverdine. The *P. agglomerans* PSV1-7 genome also harbours genes essential for the biological control of plant pathogens, including gene clusters involved in chitin and N-acetylglucosamine utilization and several other genes encoding for iron acquisition and metabolism via siderophores-mediated mechanisms. Comparative genome analysis indicated that even though the biocontrol bacteria share large genomic regions when compared with type strains, multiple genomic areas specific to each of the biocontrol strains were detected. The AntiSMASH pipeline was used to identify various BGCs representing DNA sequences responsible for producing different secondary metabolites known to be involved in biological control of ARR and RRC. Siderophore production and proteolytic activity assays indicated that strains K-Hf-H2, K-Hf-L9, and PSV1-7 produce siderophores and degrade protein. Cellulolytic activity showed that K-Hf-H2 and K-Hf-L9 hydrolyze cellulose, whereas PSV1-7 did not exhibit visually detectable cellulolytic activity. Collectively, these results demonstrated that *L. capsici* K-Hf-H2, *P. simiae* K-Hf-L9 and *P. agglomerans* PSV1-7 have gene and gene clusters that potentially involve in the suppression of ARR and RRC. Moreover, the laboratory-based assays supported the genome analysis findings. Therefore, further functional genomic experiments that aim to determine the dominant biocontrol

mechanism, for example, one that generates mutants lacking a specific biocontrol trait, followed by *in vitro* and *in vivo* confirmatory investigations, need to be conducted.

5.3 Introduction

Microbial whole-genome sequencing is an excellent tool for the biological characterization of the genetic features of an isolated microorganism, including bacterial species with biocontrol potential (Jiang et al., 2022). This technology is now broadly accessible due to a decrease in instrument and consumables costs, and it is now available in many laboratories to execute their internal genome sequencing projects (Finotello et al., 2012; Quail et al., 2012). Oxford Nanopore sequencing is one technology that generates reads sufficiently long to be of great use in *de novo* assembly (Koren and Phillippy, 2015). Therefore, the long-read data from the Oxford Nanopore MinION is commonly used to assemble complete bacterial genomes to accurately reconstruct gene order and orientation without using data from other sequencing technologies (Loman et al., 2015).

Lysobacter capsici, *Pseudomonas simiae*, and *Pantoea agglomerans* are multi-functional Gram-negative bacteria that have been reported to have various applications in agriculture, including biocontrol of plant pathogens (Hsieh et al., 2005; Gómez et al., 2015). Elucidating microbial genomes is essential for understanding biocontrol mechanisms (Luo et al., 2018). For example, several researchers identified genes responsible for bioactive secondary metabolites in *L. capsici*, *P. species* and *P. agglomerans* (Cho et al., 2015; Puopolo et al., 2016; Shariati et al., 2017) by using complete genome sequencing data. Moreover, genome comparison among the genomes of *L. capsici* AZ78, *Stenotrophomonas malthophilia* K729a and *Xanthomonas campestris* pv. *campestris* ATCC33913 showed that *L. capsici* AZ78 genome contained genes involved in the production of antibiotics and siderophores (Puopolo et al., 2016). Furthermore, a study by Loper et al. (2012) identified genes involved in antibiotic and siderophore production via genome comparison among *Pseudomonas fluorescens* strains. Similarly, research by Shariati et al. (2017) identified sets of genes responsible for antibiotics and the production of siderophores in closely related strains of *P. agglomerans*. Therefore, these findings suggest that *Lysobacter*, *Pseudomonas* and *Pantoea* species contain genes encoding for traits potentially involved in the suppression of plant pathogenic microorganisms.

As discussed in Chapter 4, *L. capsici* K-Hf-H2, *P. simiae* K-Hf-L9 and *P. agglomerans* PSV1-7 were identified as effective biocontrol agents against ARR and RRC in field pea and lentil

under growth chamber conditions. Thus, it is important to understand the mechanisms by which biocontrol was achieved. One approach is using molecular tools and bioinformatics resources such as high-throughput DNA sequencing, genome annotations and comparisons. Information from these analyses can help identify potential biocontrol mechanisms behind *in vitro* pathogen inhibition and *in vivo* disease symptom suppression. Therefore, the overall objective of the study presented in this Chapter was to characterize the genetic features of *L. capsici* K-Hf-H2, *P. simiae* K-Hf-L9 and *P. agglomerans* PSV1-7 using whole-genome sequence analysis and identify potential biocontrol mechanisms. The specific objectives included: (I) sequencing the whole genome of these biocontrol bacteria; (II) comparing the genetic features of these bacteria with other characterized strains of the same species; (III) identifying genomic regions (genes and gene cluster) potentially involved in the suppression of ARR and RRC; and (IV) assessing functional and physiological activities under laboratory conditions. To accomplish these objectives, the study in this Chapter was developed based on the following hypothesis:

Biocontrol bacteria, *L. capsici* K-Hf-H2, *P. simiae* K-Hf-L9 and *P. agglomerans* PSV1-7, harbour specific sets of genes responsible for biocontrol activity against *A. euteiches*, *F. avenaceum* and *F. oxysporum*.

Laboratory-based functional and physiological experiments were used to provide evidence of potential biocontrol mechanisms identified using comparative genome analysis.

5.4 Materials and methods

5.4.1 Strain activation and DNA extraction

Lysobacter capsici K-Hf-H2, *P. simiae* K-Hf-L9, *P. agglomerans* PSV1-7 and *L. gummosus* K-Be-H3 were sub-cultured from frozen stock (50% glycerol, in -80°C storage) on Luria Broth (LB) agar plates (Fig. 5.1) and grown at 28°C for 24 h. Next, a loop of an isolated colony was transferred to $\frac{1}{2}$ strength TSB and incubated on a benchtop shaker at 28°C for 24 h. Then, genomic DNA was extracted using the FastDNA Spin kit (MP Biomedicals) according to the manufacturer's instructions.

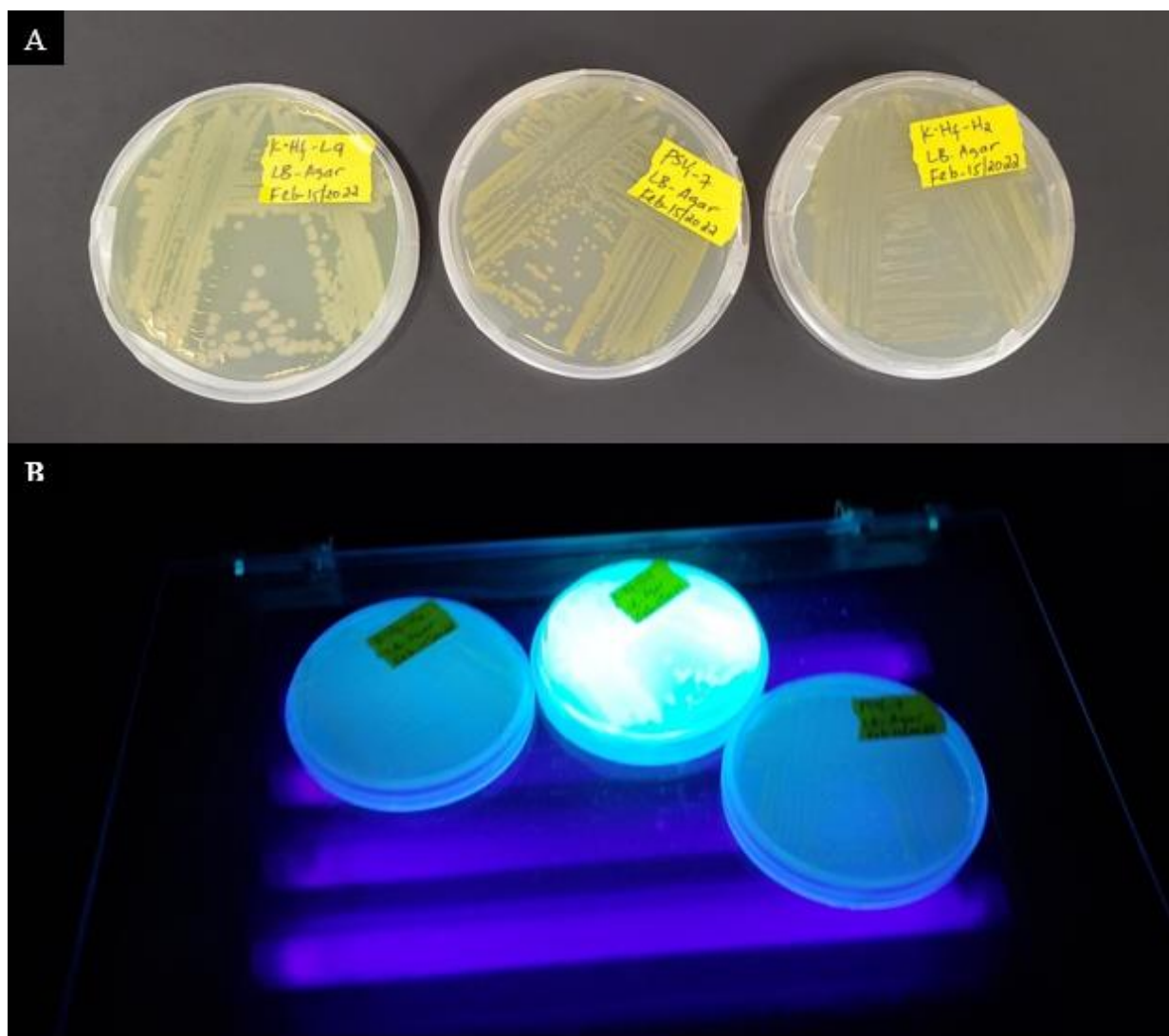


Figure 5.1. Biocontrol bacteria *L. capsici* K-Hf-H2, *P. simiae* K-Hf-L9, and *P. agglomerans* PSV1-7 on Luria Broth agar plate (Figure 5.1A). Biocontrol bacteria *P. simiae* strain K-Hf-L9 (Figure 5.1B, the middle plate) exhibited fluorescence under UV light. Based on the 16S rRNA sequence, this strain was previously classified and reported as *P. fluorescens* K-Hf-L9 (Godebo, 2019). However, average nucleotide identity (ANI) suggested that the strain was more related to *P. simiae* than *P. fluorescens*.

5.4.2 Whole-genome sequencing and assembly

The genomic DNA sample of *L. capsici* K-Hf-H2, *P. agglomerans* PSV1-7 and *L. gummosus* K-Be-H3 were sent to Genome Quebec (Montréal, Canada, www.genomequebec.com) for whole-genome sequencing and assembly. There the whole genome of *L. capsici* K-Hf-H2, *P. agglomerans* PSV1-7 and *L. gummosus* K-Be-H3 were sequenced and assembled using PacBio Sequel sequencing technology and GS De Novo Assembler, respectively. Using the genomic DNA extracted in Section 5.4.1, the complete genome sequencing of *P. simiae* K-Hf-L9 was performed

at the University of Regina. Briefly, the genomic DNA of *P. simiae* K-Hf-L9 was sheared using a g-TUBE (Covaris, Woburn, MA, USA) and a centrifugation protocol yielding an average DNA fragment size of approximately 8,000 bases (Eppendorf 5424 centrifuge and two 30-s centrifugations at $2,000 \times g$). Then a Nanopore library was prepared and sequenced using a MinION Mk1B device. Finally, MinION DNA sequencing data were evaluated using NanoPlot version 1.27.0 (De Coster et al., 2018).

5.4.3 Whole-genome annotation and comparative analysis

The whole-genome sequences of *L. capsici* K-Hf-H2, *P. simiae* K-Hf-L9, *P. agglomerans* PSV1-7 and *L. gummosus* K-Be-H3 were annotated with the Rapid Annotation Subsystem Technology (RAST) Web server version 2.0 (Aziz et al., 2008; Overbeek et al., 2014) and NCBI Prokaryotic Genome Annotation Pipeline (PGAP) version 5.3 (Tatusova et al., 2016). During RAST annotation, the classic RAST defaults were used (i.e., annotation scheme: classic RAST; gene caller: RAST; FIGfam version: Release70; automatically fix errors: yes; backfill gaps: yes).

Following genome annotations, the genomes of *L. capsici* K-Hf-H2, *P. simiae* K-Hf-L9, *P. agglomerans* PSV1-7, and *L. gummosus* K-Be-H3 were individually compared with complete genomes sequences of publicly available type strains as described in Puopolo et al. (2016) and Luo et al. (2018). First, the bacterial strains selected for these comparisons were retrieved from DDBJ/EMBL/GenBank database using their accession number. Then, their genomic information was utilized for comparative analysis using BRIG (Alikhan et al., 2011) and EDGAR (Efficient Database framework for comparative Genome Analysis using BLAST score Ratios) (Blom et al., 2016). Finally, visual comparison maps were generated in both genomic ring via BRIG and Venn-diagram via EDGAR version 3.0.

BLAST Ring Image Generator displays similarity between a reference genome and sets of query sequences and generates images depicting matches calculated from the reference sequence. Thus, sequences absent or sequences having an identity ratio lower than a defined cut-off value (50% identity ratio in this study) corresponding to the reference sequences were indicated by a gap. However, BRIG cannot display regions absent from the reference genome but present in the query sequences; thus, the Venn diagram was used to determine the number of shared and unique genes among each biocontrol bacterial strain and those selected for comparisons in the respective group via EDGAR version 3.0. EDGAR is a software platform for bacterial genome analysis

maintained at Justus-Liebig-University, Giessen. It was developed to support comparative gene content analyses combined with visual result representation (Yu et al., 2017; Dieckmann et al., 2021).

5.4.4 Detection of antibiotic resistance genes

The whole genome sequences of *L. capsici* K-Hf-H2, *P. simiae* K-Hf-L9, *P. agglomerans* PSV1-7 and *L. gummosus* K-Be-H3 were submitted to the comprehensive antibiotic resistance database (CARD; <https://card.mcmaster.ca>) to detect the presence of clinically relevant antimicrobial resistance (AMR) genes (Alock et al., 2020). The AMR genes were detected using the "Perfect" and "Strict" algorithms integrated within the CARD.

5.4.5 Phylogenetic analysis

The 16S rRNA gene sequences for *L. capsici* K-Hf-H2, *P. simiae* K-Hf-L9, *P. agglomerans* PSV1-7, and *L. gummosus* K-Be-H3 were obtained from Godebo (2019) data archives. In contrast, the 16S rRNA gene sequences of known-type strains selected for the comparison were collected from the GenBank database. Finally, a phylogenetic tree for *L. capsici* K-Hf-H2, *P. simiae* K-Hf-L9, *P. agglomerans* PSV1-7 and *L. gummosus* K-Be-H3 was generated using MEGAX (Kumar et al., 2018). Initially, the sequences were aligned using ClustalW, and the trees were generated using the Neighbour-Joining method (Saitou and Nei, 1987). Then, the evolutionary distances were computed using Kimura's two-parameter model (Kimura, 1980). Bootstrap values (1000 replicates) higher than 70 were shown next to the branches (Felsenstein, 1985).

5.4.6 Identification of secondary metabolite regions

Identification of secondary metabolite regions in *L. capsici* K-Hf-H2, *P. simiae* K-Hf-L9, *P. agglomerans* PSV1-7 and *L. gummosus* K-Be-H3 genomes was performed using AntiSMASH (antibiotics and Secondary Metabolite Analysis Shell). AntiSMASH is a comprehensive pipeline that identifies biosynthetic loci covering the range of known secondary metabolite compound classes. Some of these include polyketides, aminoglycosides, bacteriocins, and siderophores. AntiSMASH aligns identified regions at the gene cluster level to their nearest relatives from a database containing all other known gene clusters and integrates or cross-links all previously available secondary-metabolite-specific gene analysis methods in one interactive view (Medema et al., 2011).

5.4.7 Laboratory investigation of functional activities

Strains *L. capsici* K-Hf-H2, *P. simiae* K-Hf-L9 and *P. agglomerans* PSV1-7 were evaluated for functional activities on microbial culture media under laboratory conditions. The functional and physiological activities tested in this study include production of siderophores, protein hydrolysis, cellulolytic activity and desiccation resistance.

5.4.7.1 Siderophores production capacity

Lysobacter capsici K-Hf-H2, *P. simiae* K-Hf-L9 and *P. agglomerans* PSV1-7 were evaluated for siderophores production on Chrome Azurol S (CAS) media using the method described in Alexander and Zuberer (1991) and Reza (2017). Briefly, a loop full of a fresh colony of each strain was inoculated at the center of the CAS plate in a circular motion in three replicates. Then, the plates were incubated at 25 °C for 7 d. Finally, the experiment was repeated, and siderophore production was determined based on the presence of an orange halo around the bacteria colony.

5.4.7.2 Protein hydrolysis activity

Lysobacter capsici K-Hf-H2, *P. simiae* K-Hf-L9 and *P. agglomerans* PSV1-7 were evaluated for proteolytic activity using skimmed milk agar (SMA) media. The SMA media was prepared with the composition of 10 g L⁻¹ skimmed milk powder, 1 g L⁻¹ glucose, 1 g L⁻¹ yeast extract, g L⁻¹ K₂HPO₄ 1, g L⁻¹ KH₂PO₄ 0.5, 0.1 g L⁻¹ MgSO₄ and 20 g L⁻¹ agar as described by Salarizadeh et al. (2014).

A loop full of a fresh colony of each strain was inoculated at the center of the SMA plate in a circular motion in three replicates. The plates were incubated at 25 °C for 5 d. Three replicates of SMA plates that received 20 µL of filter-sterilized Trypsin (150 USP units mg⁻¹) enzyme solution were included as a positive test control. The trypsin enzyme solution was prepared by dissolving 0.1 g of Trypsin (150 USP units mg⁻¹) in 10 mL of sterile distilled water.

The agar-well diffusion method discussed in Section 4.4.3 was used to assess the proteolytic activity of cell-free supernatants extracted from broth cultures of each isolate. The strains were cultured in ½ strength TSB at 110 rpm and 28°C for 72 h. After incubation, the culture was centrifuged at 5000 rpm for 15 min. The resulting supernatant was filtered, and 250 µL of each isolate cell-free supernatant was applied to each well. Three replicates of SMA plates with wells that received 50 µL of filter-sterilized the trypsin enzyme solution were included as a positive

control. Finally, the plates were incubated at 25 °C for 5 d, and the presence of hydrolysis or disillumination ring around each colony and well visually confirmed proteolytic activity.

5.4.7.3 Cellulose hydrolysis capacity

Lysobacter capsici K-Hf-H2, *P. simiae* K-Hf-L9 and *P. agglomerans* PSV1-7 were evaluated for cellulolytic activity using cellulose-Congo red agar media as described in Gupta et al. (2012). Briefly, the cellulose-Congo-red agar media was prepared with the following combination: KH₂PO₄ (0.5 g), MgSO₄ (0.25 g), cellulose (2 g), agar (15 g), Congo-Red (0.2 g), and gelatin (2 g); distilled water 1L and at pH 6.8–7.2. Then, a loop full of fresh colonies of each strain was inoculated at the center of cellulose-Congo-red agar media, and the plates were incubated at 25 °C for 5 d. Finally, the cellulolytic activity was determined based on the discoloration of the Congo-Red (Lu et al., 2004).

5.4.7.4 Desiccation tolerance assay

Lysobacter capsici K-Hf-H2, *P. simiae* K-Hf-L9 and *P. agglomerans* PSV1-7 were assessed for desiccation tolerance using the filtration method described by Gilbert et al. (2007) and Vanderlinde et al. (2010). Briefly, bacteria were grown in ½ strength TSB to the late log phase as measured by OD_(600 nm) and diluted to 1/10 in sterile water to a total volume of 50 mL. Next, the diluted culture was filtered according to the manufacturer's specifications with a Millipore Vacuum Manifold (Millipore Inc., Bedford, MA) (Fig. 5.2.) using Microfil Filtration Funnels and S-Pak 0.45-mm Type HA membranes (Millipore Inc.). Membranes were then cut in half and transferred to an empty Petri dish (dry) and a water-agar plate (12.5 g agar L⁻¹) (wet) and stored at room temperature and humidity for 24 h. Next, membranes were transferred to 2 mL tubes containing 1.5 mL of distilled water and vortexed at speed 8 for 15 minutes to remove cells from the membrane and re-suspend. Finally, the number of viable bacteria was determined following the spread plate technique, and the percent survival (PS) was calculated as described below (Equ. 5.1).

$$PS = (CFU_{mL^{-1}}_{(air)}/CFU_{mL^{-1}}_{(water)}) * 100 \quad (\text{Eq. 5.1})$$



Figure 5.2. Cell-filtration using Millipore Vacuum Manifold (Millipore Inc., Bedford, MA), Microfil Filtration Funnels and S-Pak 0.45-mm Type HA membranes (Millipore Inc.). An accu-jet ® pro pipette controller was used to remove air through the nozzles of each filter flask and aid the filtration.

5.5 Results

5.5.1 Genomic features

The *L. capsici* K-Hf-H2 genome has a consensus length of 6 017 450 bp with an average G+C content of 66.5% assembled in 1 contig. A total of 5 006 genes were predicted in the *L. capsici* K-Hf-H2 genome, of which 4 625 were total-coding genes and from the total-coding genes 4 545 were predicted to be protein-coding sequences. Furthermore, 6 rRNA and 51 tRNA coding genes were predicted in the *L. capsici* K-Hf-H2 genome (Table 5.1).

The *P. simiae* K-Hf-L9 genome has a consensus length of 6 199 521 bp with a G+C content of 60.28% assembled in 1 contig. A total of 5 679 genes were predicted in the *P. simiae* K-Hf-L9 genome, of which 5 587 were total-coding genes and from the total coding 5 425 were predicted to be protein-coding sequences. Furthermore, 19 rRNA and 69 tRNA coding genes were predicted in the *P. simiae* K-Hf-L9 genome (Table 5.1).

The *P. agglomerans* PSV1-7 genome has a consensus length of 4 053 926 bp with an average G+C content of 54.8% assembled in 5 contigs, representing 1 chromosome and 4 separate plasmids. A total of 4 733 genes were predicted in the *P. agglomerans* PSV1-7 genome, of which 4 625 total-coding genes and from the total-coding genes 4 545 were protein-coding sequences. Moreover, 22 rRNA and 77 tRNA coding genes were predicted in the *P. agglomerans* PSV1-7 genome (Table 5.1).

The *L. gummosus* K-Be-H3 genome has a consensus length of 6 017 450 bp with an average G+C content of 66.5% assembled in 1 contig. A total of 5 004 genes were predicted in the *L. gummosus* K-Be-H3 genome, of which 4 943 were total-coding and from the total-coding 4 861 were protein-coding sequences. Furthermore, 6 rRNA and 51 tRNA coding genes were predicted in the *L. gummosus* K-Be-H3 genome (Table 5.1).

PlasmidFinder version 1.3 did not detect any plasmid in the *L. capsici* K-Hf-H2, *P. simiae* K-Hf-L9 and *L. gummosus* K-Be-H3 genomes. However, it detected four plasmids in the *P. agglomerans* PSV1-7 genome. The plasmids have circular DNA with a consensus length of 621 667 bp, 179 440 bp, 122 140 bp and 51 994 bp (Table 5.1).

Table 5.1. Summary of the *Lysobacter capsici* K-Hf-H2, *Pseudomonas simiae* K-Hf-L9, *Pantoea agglomerans* PSV1-7 and *Lysobacter gummosus* K-Be-H3 genome characteristics

Characteristics	Value(s)			
	K-Hf-H2	K-Hf-L9	PSV1-7	K-Be-H3
No. of contigs (chromosome, plasmid)	1	1	1, 4	1
Genome size (bp)	6 017 450	6 199 521	4 053 926	6 017 450
G+C content (%)	66.5	60.28	54.8	66.5
Total no. of genes	5 006	5 679	4 733	5 004
Total no. of CDSs ^a	4 945	5 587	4 625	4 943
No. of CDSs with protein	4 855	5 425	4 545	4 861
No. of RNA genes	61	92	108	61
No. of complete rRNAs (5S, 16S, 23S)	2, 2, 2	7, 6, 6	8, 7, 7	2, 2, 2
No. of tRNAs	51	69	77	51
No. of noncoding RNAs	4	4	9	4
Total no. of pseudogenes	83	162	80	82
Total no. plasmid	0	0	4	0
Plasmid 1 Size (bp)	0	0	621667	0
Plasmid 2 Size (bp)	0	0	179440	0
Plasmid 3 Size (bp)	0	0	122140	0
Plasmid 4 Size (bp)	0	0	51994	0

^a CDSs, coding sequences. The 4733 genes predicted in the *Pantoea agglomerans* PSV1-7 genome comprises all the genes across the five replicons (i.e., chromosome and 4 plasmids).

5.5.2 Genome annotation

Genome annotation using RAST revealed that from the total number of proteins encoded in the genomes of the *L. capsici* K-Hf-H2, 38% were assigned in subsystem categories, whereas 62% could not be assigned (Fig. 5.3). Similarly, 53%, 59% and 38% of the protein-encoding genes in *P. simiae* K-Hf-L9, *P. agglomerans* PSV1-7 and *L. gummosus* K-Be-H3 genomes were assigned to subsystem categories, respectively (Figs. 5.4, 5.5 and 5.6). In contrast, 47%, 41% and 62% of the protein-encoding genes in *P. simiae* K-Hf-L9, *P. agglomerans* PSV1-7 and *L. gummosus* K-Be-H3 genomes could not be assigned in the subsystem categories. The most abundant subsystem feature counts were Carbohydrates (*L. capsici* K-Hf-H2: 286 counts; *P. simiae* K-Hf-L9: 515 counts; *P. agglomerans* PSV1-7: 466 counts; *L. gummosus* K-Be-H3: 284 counts), Amino Acids and Derivatives (*L. capsici* K-Hf-H2: 401 counts; *P. simiae* K-Hf-L9: 739 counts; *P. agglomerans* PSV1-7: 389 counts; *L. gummosus* K-Be-H3: 399 counts) and Protein Metabolism (*L. capsici* K-Hf-H2: 268 counts; 268 counts; *P. simiae* K-Hf-L9: 299 counts; *P. agglomerans* PSV1-7: 262 counts; *L. gummosus* K-Be-H3) (Figs. 5.3 to 5.6).

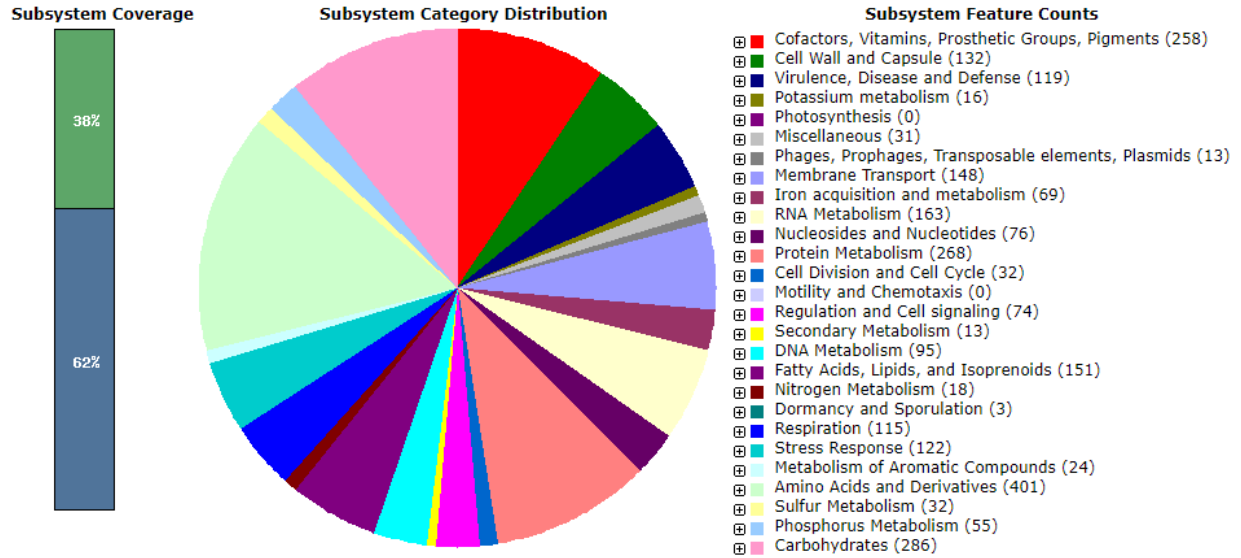


Figure 5.3. Analysis of the protein-encoding genes (pegs) of the *Lysobacter capsici* K-Hf-H2 whole-genome sequence assigned to subsystem categories based on the RAST version 2.0 server. The bar on the left presents the percentage of pegs assigned to subsystems (green) and the pegs that could not be placed into any subsystem (blue). The pie chart in the center depicts the subsystem category distribution. The coloured categories on the right indicate the subsystem feature counts.

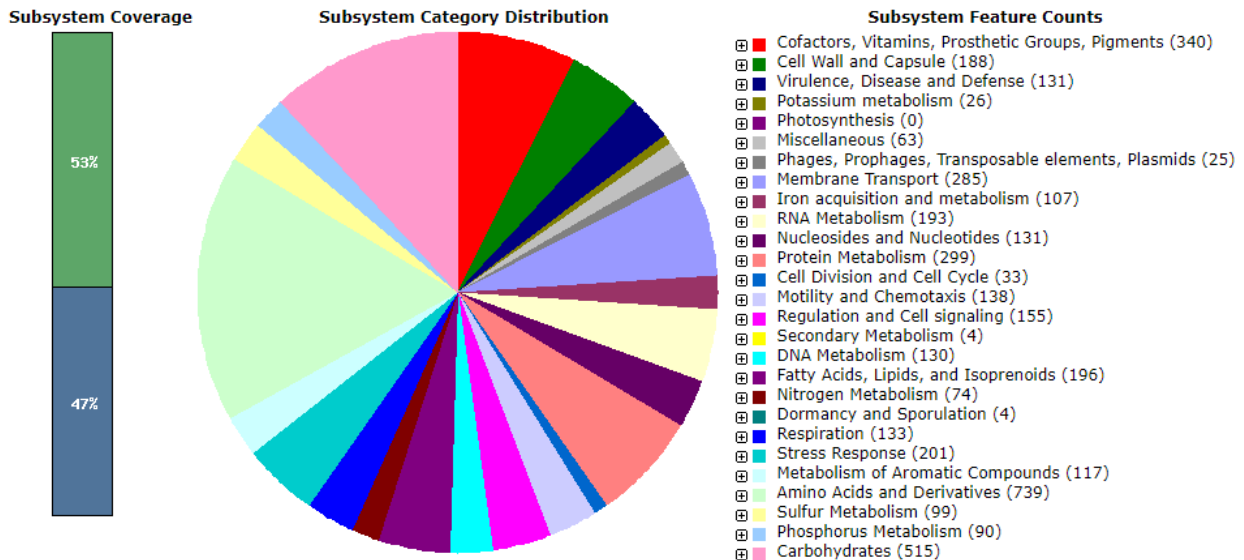


Figure 5.4. Analysis of the protein-encoding genes (pegs) of the *Pseudomonas simiae* K-Hf-L9 whole-genome sequence assigned to subsystem categories based on the RAST version 2.0 server. The bar on the left presents the percentage of pegs assigned to subsystems (green) and the pegs that could not be placed into any subsystem (blue). The pie chart in the center depicts the subsystem category distribution. The coloured categories on the right indicate the subsystem feature counts.

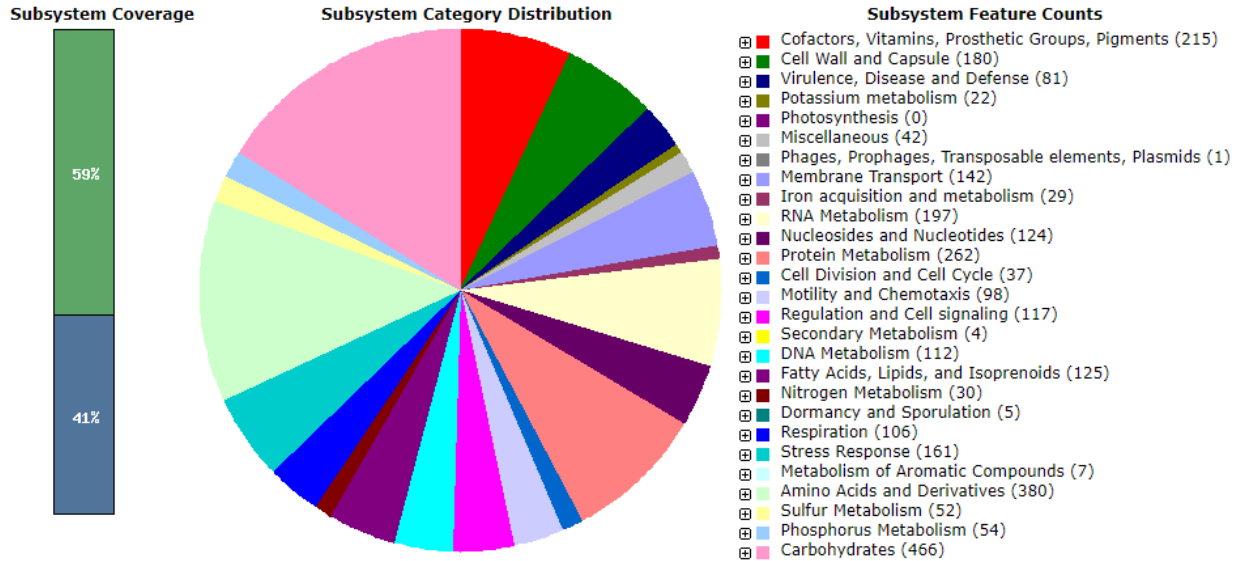


Figure 5.5. Analysis of the protein-encoding genes (pegs) of the *Pantoea agglomerans* PSV1-7 whole-genome sequence assigned to subsystem categories based on the RAST version 2.0 server. The bar on the left presents the percentage of pegs assigned to subsystems (green) and the pegs that could not be placed into any subsystem (blue). The pie chart in the center depicts the subsystem category distribution. The coloured categories on the right indicate the subsystem feature counts.

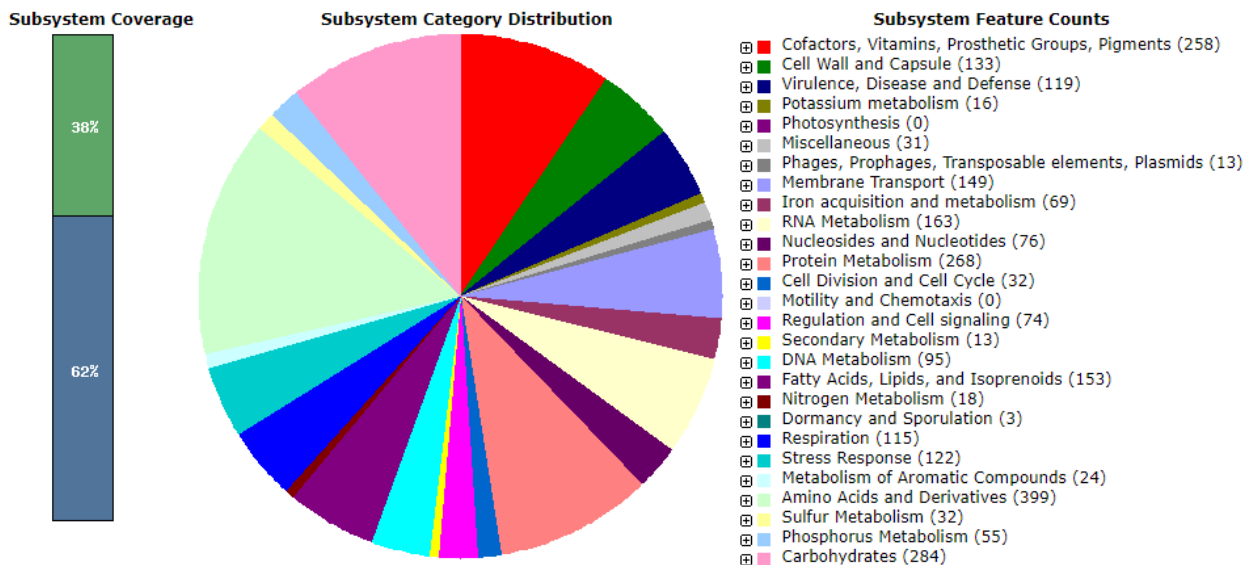


Figure 5.6. Analysis of the protein-encoding genes (pegs) of the *Lysobacter gummosus* K-Be-H3 whole-genome sequence assigned to subsystem categories based on the RAST version 2.0 server. The bar on the left presents the percentage of pegs assigned to subsystems (green) and the pegs that could not be placed into any subsystem (blue). The pie chart in the center depicts the subsystem category distribution. The coloured categories on the right indicate the subsystem feature counts.

Given the biocontrol activity of the four bacteria, preliminary analysis revealed that strains harbour several genes and BGCs important for biological control of plant pathogens (Tables C.1

to C.3). For example, in *L. capsici* K-Hf-H2 there were one gene encoding HSAF, three genes encoding endoglucanase EC 3.2.1.4, four genes encoding chitinase EC 3.2.1.14, five genes encoding extracellular zinc protease EC 3.4.24.25 and EC 3.4.24.26, and four genes encoding aminopeptidases EC 3.4.11 (Table C.1). The Enzyme Commission (EC) number indicates the numerical classification scheme for enzymes based on their catalyzed chemical reactions (Ryu et al., 2019). Moreover, four genes involved in auxin biosynthesis, a key regulator of plant growth and development, were detected (Table C.1).

The detected genes and BGCs encoding for various lytic enzymes were homologous to gene and gene clusters found in other bacteria. For example, in *L. capsici* K-Hf-H2, the lysyl metalloendopeptidase EC 3.4.24 encoding for extracellular zinc protease EC 3.4.24.25 and EC 3.4.24.26, chitinase EC 3.2.1.14, and endoglucanase EC 3.2.1.4 were homologous to the ones detected in *Streptomyces coelicolor* A3, *Streptomyces griseus* subsp. *griseus* NBRC 13350, *Streptosporangium roseum* and *Saccharopolyspora erythraea* NRRL 2338 (Figs. 5.7 to 5.9).

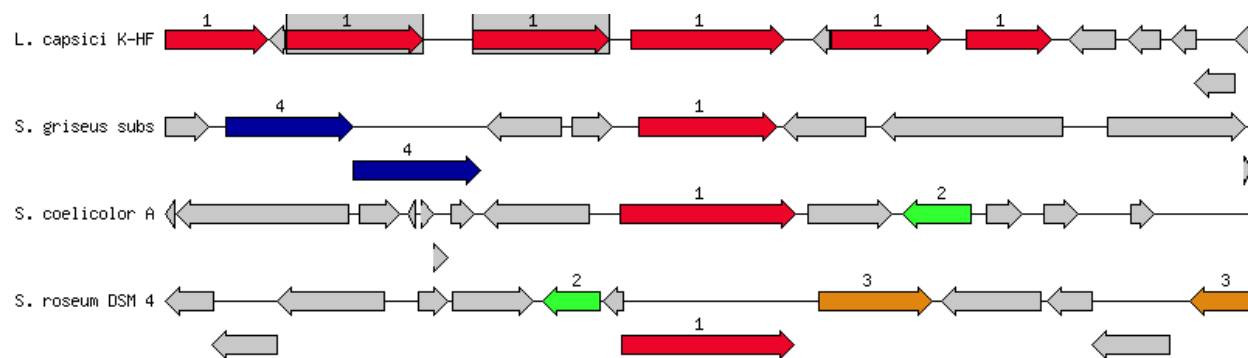


Figure 5.7. Annotation overview for K-Hf-H2.peg.1000 in *L. capsici* K-HF-H2 encoding for extracellular zinc protease (EC 3.4.24.25) and (EC 3.4.24.26). The chromosomal region of the focus gene (top) was compared with bacterial strains of *Streptomyces griseus*, *S. coelicolor* and *Streptosporangium roseum*. The graphic is centred on the focus gene, which is red and numbered 1. Sets of genes with a similar sequence are grouped with the same number and colour. The figure shows a cluster of extracellular zinc proteases in the K-HF-H2 genome.

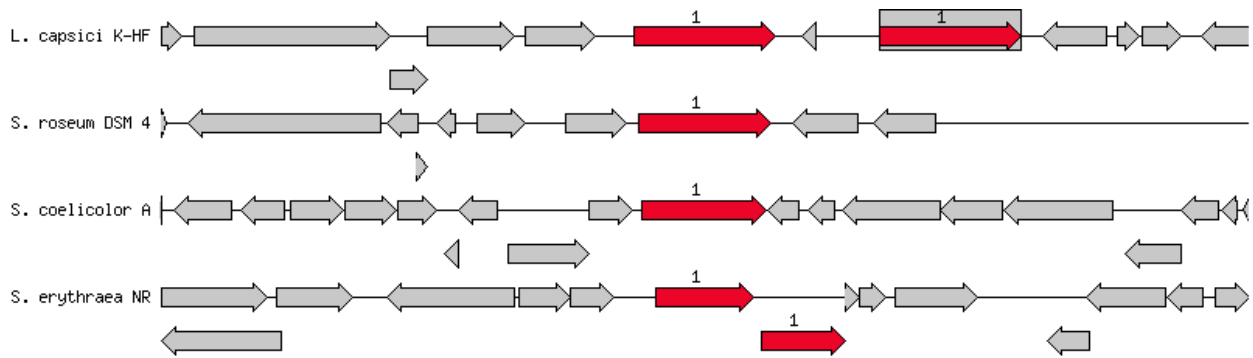


Figure 5.8. Annotation overview for K-Hf-H2.peg.3466 in *L. capsici* K-HF-H2 encoding for chitinase EC 3.2.1.14. The chromosomal region of the focus gene (top) was compared with bacterial strains of *Streptosporangium roseum*, *Streptomyces coelicolor* and *Saccharopolyspora erythraea* organisms. The graphic is centered on the focus gene, which is red and numbered 1. Sets of genes with similar sequence are grouped with the same number and color.

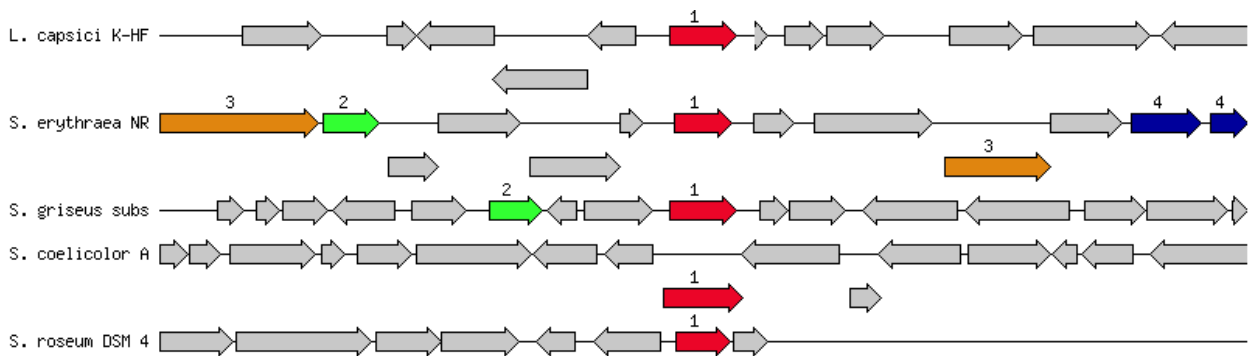


Figure 5.9. Annotation overview for K-Hf-H2.peg.855 in *L. capsici* K-HF-H2 encoding for endoglucanase EC 3.2.1.4. The chromosomal region of the focus gene (top) was compared with bacterial strains of *Saccharopolyspora erythraea*, *Streptomyces griseus*, *Streptosporangium roseum* and *Streptomyces coelicolor*. The graphic is centred on the focus gene, which is red and numbered 1. Sets of genes with a similar sequence are grouped with the same number and colour.

Similarly, gene and gene clusters encoding traits potentially involved in the biological control of root rot pathogens were detected in the *P. simiae* K-Hf-L9 genome (Table C.2). Particularly, six genes that catabolize the chitin and its monomer, N-acetylglucosamine, EC 3.5.1.25, EC 2.7.1.69 and EC 3.5.99.6; and five genes responsible for the TldE-TldD proteolytic activity were detected (Table C.2). These genes and gene clusters were found to be a similarity to ones detected in other bacteria as indicated in Figs. 5.10 and 5.11. In addition, a significant portion of the genome was found to encode for fluorescent siderophores known as pyoverdine (Table C.2).

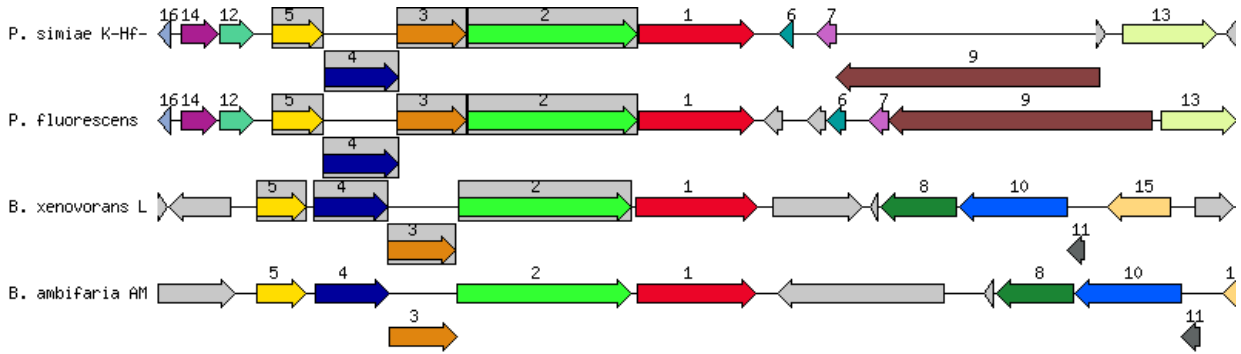


Figure 5.10. Annotation overview for K-Hf-L9,peg.4600 in *P. simiae* K-Hf-L9 encoding for N-acetylglucosamine utilizing genes: EC 3.5.1.25, EC 2.7.1.69 and EC 3.5.99.6. The chromosomal region of the focus gene (top) was compared with bacterial strains of *Pseudomonas fluorescens*, *Burkholderia xenovorans*, and *B. ambifaria*. The graphic is centred on the focus gene, which is red and numbered 1. Sets of genes with a similar sequence are grouped with the same number and colour.

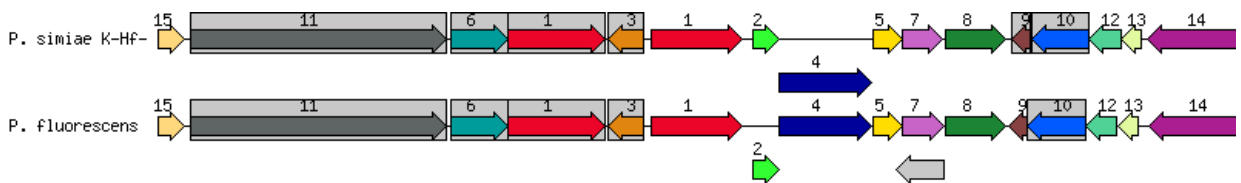


Figure 5.11. Annotation overview for K-Hf-L9,peg.846 and K-Hf-L9,peg.848 in *P. simiae* K-Hf-L9 encoding for TldE-TldD proteolytic complex genes. The chromosomal region of the focus gene (top) was compared with *P. fluorescens* SBW25. The graphic is centred on the focus gene, which is red and numbered 1. Sets of genes with a similar sequence are grouped with the same number and colour.

Similar to the other biocontrol bacteria described above, *P. agglomerans* PSV1-7 also harbour genes essential for the biological control of plant pathogens (Table C.3). For example, six genes involved in chitin and N-acetylglucosamine utilization, three genes responsible for the TldE-TldD proteolytic activity, and several other genes encoding for iron acquisition and metabolism via siderophores mediated mechanisms were detected in *P. agglomerans* PSV1-7 (Table C.2). Moreover, these genes were similar to genes detected in other bacteria. For example, the genes encoding for TldD protein, part of the TldE-TldD proteolytic complex, was homologous to the one found in *Escherichia coli* K 12 (Fig. 5.12).

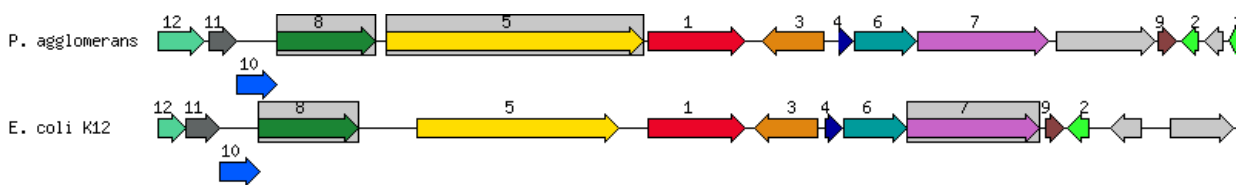


Figure 5.12. Annotation overview for PSV1,peg.969 in *P. agglomerans* PSV 1-7 encoding for TldD protein, part of TldE/TldD proteolytic complex. The chromosomal region of the focus gene (top) was

compared with *Escherichia Coli* K 12. The graphic is centred on the focus gene, which is red and numbered 1. Sets of genes with a similar sequence are grouped with the same number and colour.

5.5.3 Genome comparison

The *L. capsici* K-Hf-H2 genome was compared with complete genome sequence of four publicly available type strains such as *L. capsici* AZ78, *L. capsici* 55, *L. capsici* KNU-14 and *L. capsici* NF87_2. The analysis revealed that the whole genome of these five strains ranges from 6 017 450 to 6 391 889 bp, with G+C content ranging from 66.5 to 66.8%. Moreover, the CDSs ranged from 4 945 to 5 258 (Table 5.2).

Table 5.2. Summary of genomic features of *Lysobacter capsici* K-Hf-H2, *Lysobacter capsici* AZ78, *Lysobacter capsici* 55, *Lysobacter capsici* KNU-14 and *Lysobacter capsici* NF87_2

Genomic features	K-Hf-H2	AZ78	55	KNU-14	NF87_2
No. of contigs (chromosome)	1	1	1	1	1
Genome size (bp)	6 017 450	6 270 417	6 391 889	6 270 417	6 315 468
G+C content (%)	66.5	66.7	66.6	66.8	66.8
Total no. of genes	5 006	5 086	5 320	5 086	5 294
Total no. of CDSs ^a	4 945	5 024	5 258	5 024	5 231
No. of CDSs with protein	4 855	4 956	5 177	4 956	5 195
No. of RNA genes	61	62	62	62	63
No. of complete rRNAs (5S, 16S, 23S)	2, 2, 2	2, 2, 2	2,2,2	2,2,2	2,2,2
No. of tRNAs	51	52	52	52	53
No. of noncoding RNAs	4	4	4	4	4
Total no. of pseudogenes	83	68	81	68	36
Total no. plasmid	0	0	0	0	0

^aCDSs, coding sequences

BRIG generated a visual map of genome comparison among *L. capsici* K-Hf-H2, *L. capsici* AZ78, *L. capsici* 55, *L. capsici* KNU-14 and *L. capsici* NF87_2. BRIG detected the presence of genes unique to *L. capsici* K-Hf-H2, as indicated by the gaps (Fig 5.13). Moreover, the analysis of shared and unique genes among the *L. capsici* K-Hf-H2 genome and the four related type strains indicated that strains shared a core genome of 3 543 orthologs and *L. capsici* K-Hf-H2 contained 906 unique genes (Fig. 5.14).

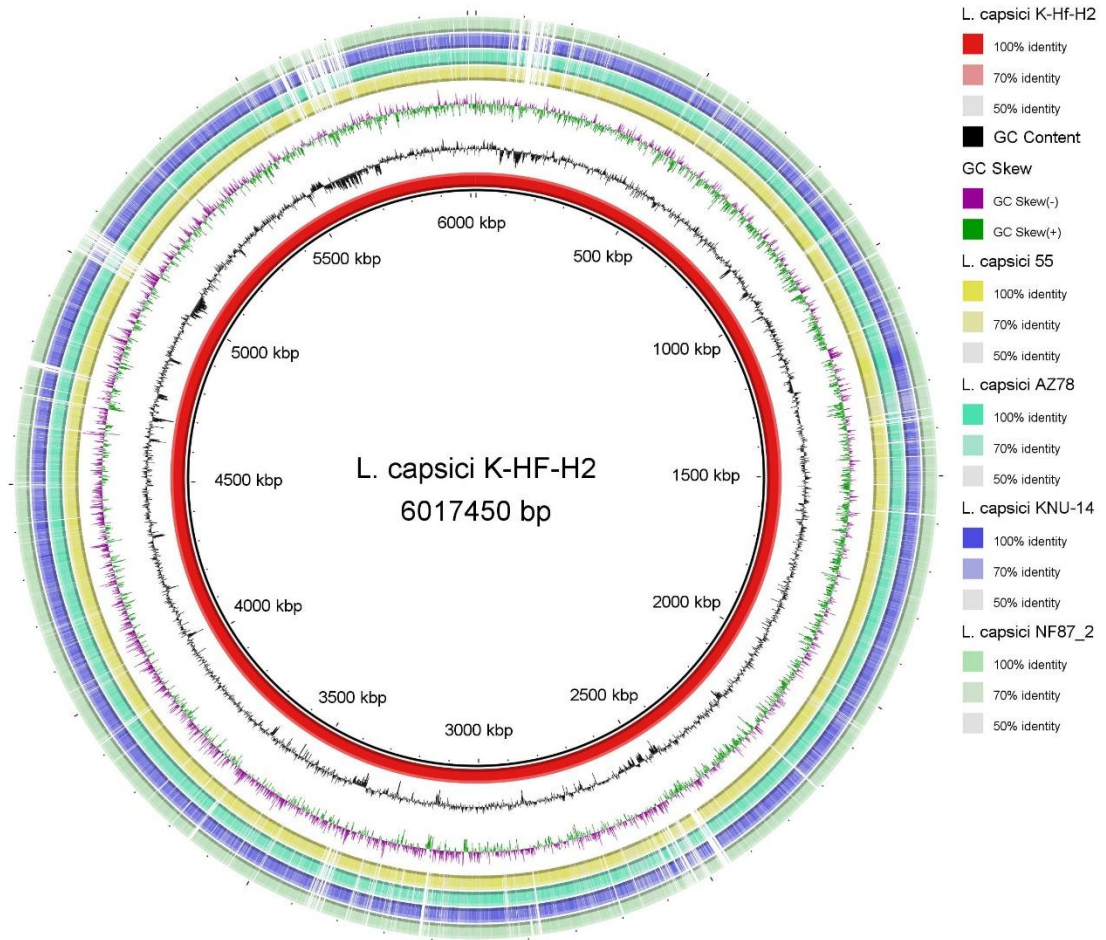
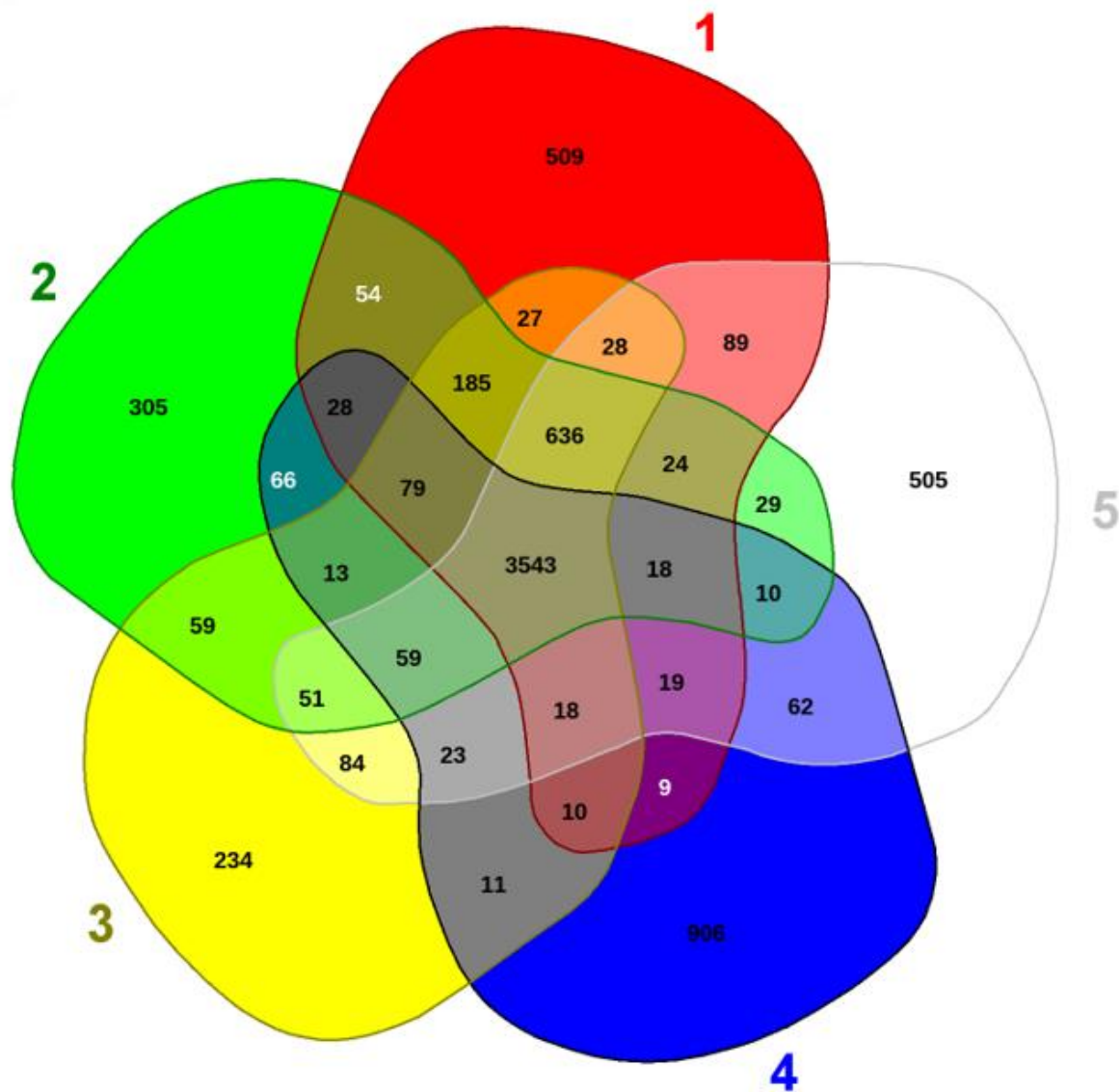


Figure 5.13. Graphical visualization of the BLAST comparisons of the *Lysobacter capsici* K-Hf-H2 genome with genomes of four type strains, *L. capsici* 55, *L. capsici* AZ78, *L. capsici* KNU-14 and *L. capsici* NF87_2. The order of the rings: Ring 1. *L. capsici* K-Hf-H2; Ring 2. GC Content; Ring 3. GC Skew; Ring 4. *L. capsici* 55, Ring 5. *L. capsici* AZ78, Ring 6. *L. capsici* KNU-14 and Ring 7. *L. capsici* NF87_2. The darker regions indicate the presence of multiple hits corresponding to the portion of the *L. capsici* K-Hf-H2 genome sequence. In contrast, gaps indicate the absence of sequences with less than a 50% identity ratio to the *L. capsici* K-Hf-H2 genome sequence. The graph was generated by BRIG 0.95.



1. *Lysobacter capsici* AZ78 [accession number: JAJA02000003]
2. *Lysobacter capsici* 55 [accession number: NZ_CP011130]
3. *Lysobacter capsici* KNU-14 [accession number: NZ_CP023465]
4. *Lysobacter capsici* K-Hf-H2 [accession number: NZ_CP090945]
5. *Lysobacter capsici* NF87-2 [accession number: NZ_CP076103]

Figure 5.14. Venn Diagram showing the number of shared and genome-specific gene families among *Lysobacter capsici* K-Hf-H2 and the four type strains *L. capsici* 55, *L. capsici* AZ78, *L. capsici* KNU-14 and *L. capsici* NF87_2. The diagram was generated using EDGAR version 3.0.

The *P. simiae* K-Hf-L9 genome was compared with the complete genome sequence of two publicly available type strains, *P. simiae* PCL1751 and WCS417. The analysis revealed that the whole

genome of the three strains ranges from 6143950 to 6199521 bp with G+C content ranging in small margin (60.3 to 60.4%). Moreover, the CDSs ranged from 5575 to 5615 (Table 5.3).

Table 5.3. Summary of genomic features of *Pseudomonas simiae* K-Hf-L9, *Pseudomonas simiae* PCL1751 and *Pseudomonas simiae* WCS417

Genomic features	K-Hf-L9	PCL1751	WCS417
No. of contigs (chromosome)	1	1	1
Genome size (bp)	6 199 521	6 143 950	6 169 071
G+C content (%)	60.3	60.4	60.3
Total no. of genes	5 679	5 668	5 692
Total no. of CDSs ^a	5 587	5 575	5 615
No. of CDSs with protein	5 425	5 507	5 534
No. of RNA genes	92	93	77
No. of complete rRNAs (5S, 16S, 23S)	7, 6, 6	7,6,6	4,2,3
No. of tRNAs	69	68	64
No. of noncoding RNAs	4	4	4
Total no. of pseudogenes	162	68	81
Total no. plasmid	0	0	0

^a CDSs, coding sequences

Genome comparison using BRIG detected the presence of genes unique to *P. simiae* K-Hf-L9 compared with the complete genome sequence of *P. simiae* PCL1751 and *P. simiae* WCS417 (Fig 5.15). Moreover, the three strains shared a core genome of 5107 orthologs, and *P. simiae* K-Hf-L9 contained 252 unique genes (Fig. 5.16).

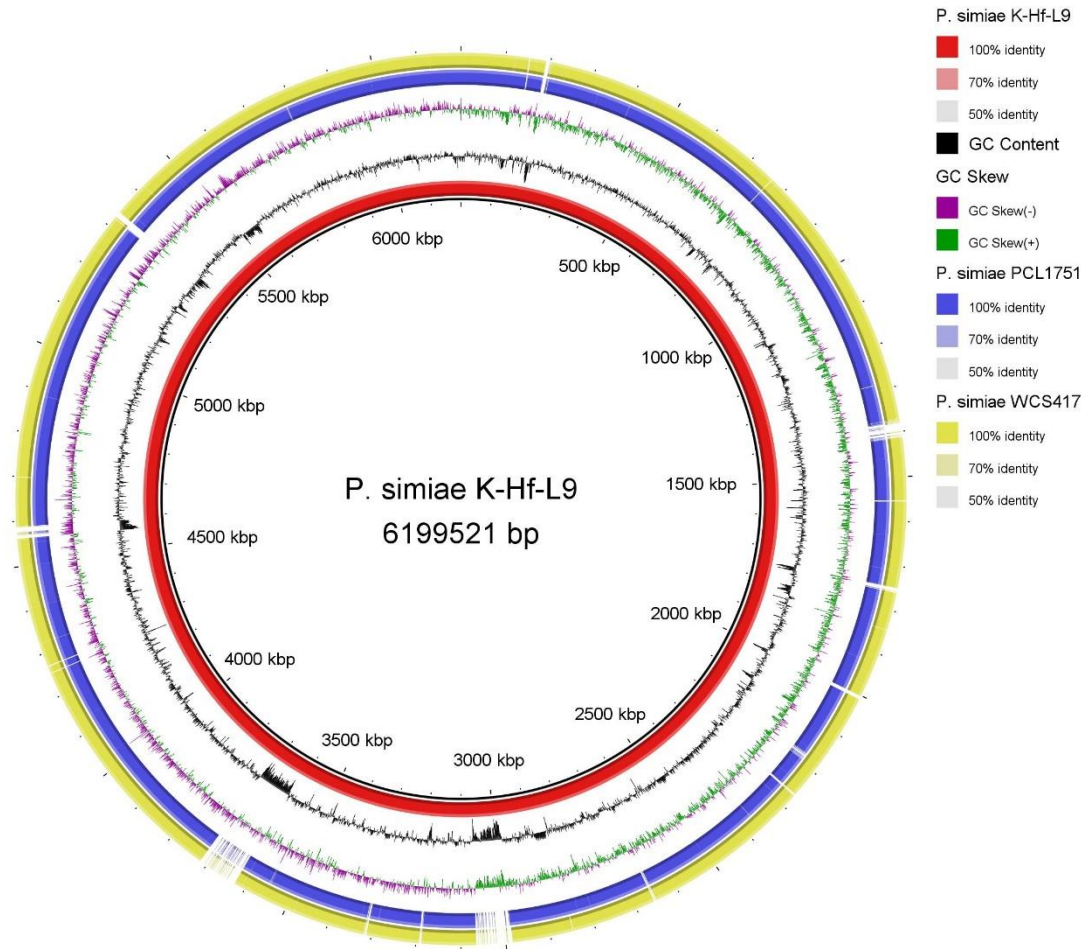
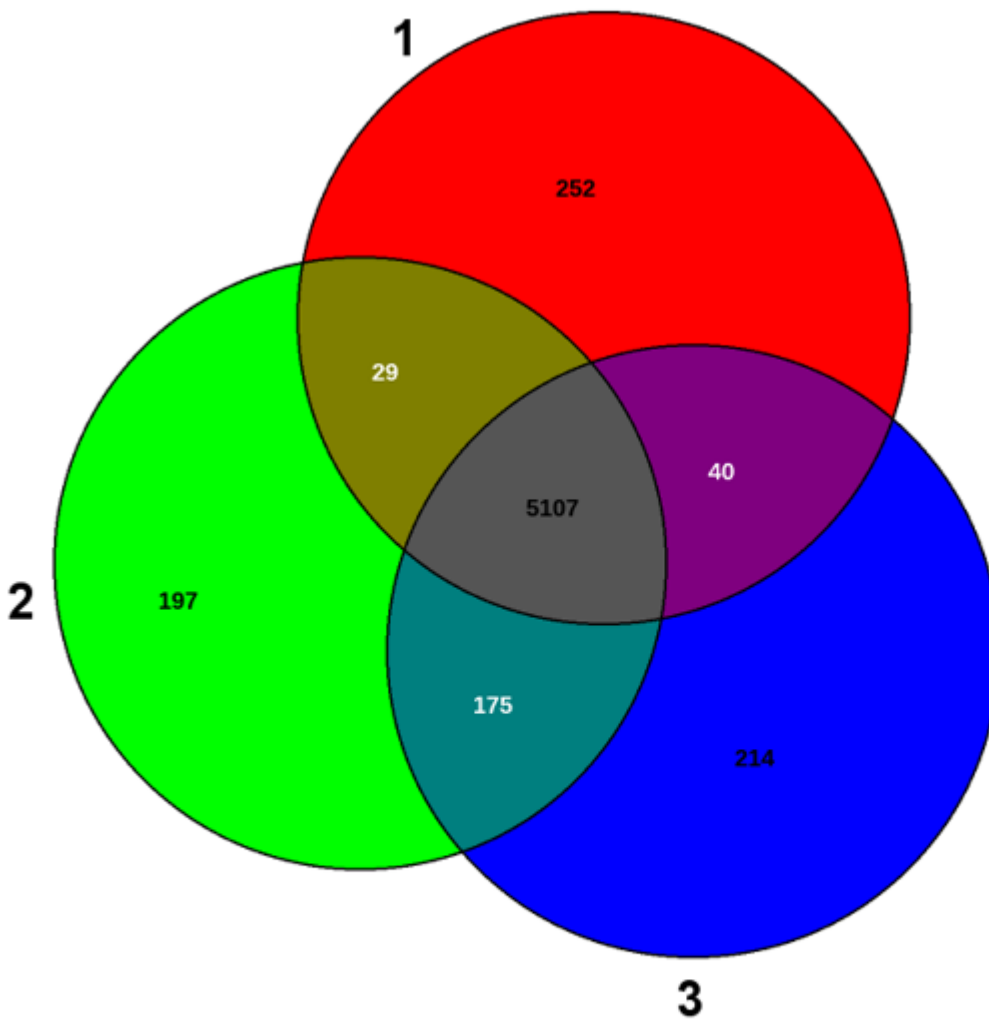


Figure 5.15. Graphical visualization of the BLAST comparisons of the *Pseudomonas simiae* K-Hf-L9 genome with genomes of two type strains, *Pseudomonas simiae* PCL1751 and *Pseudomonas simiae* WCS417. The order of the rings: Ring 1. *P. simiae* K-Hf-L9; Ring 2. GC Content; Ring 3. GC Skew; Ring 4. *P. simiae* PCL1751 and Ring 5. *P. simiae* WCS417. The darker regions indicate the presence of multiple hits corresponding to the portion of the *P. simiae* K-Hf-L9 genome sequence. In contrast, gaps indicate the absence of sequences with less than a 50% identity ratio to the *P. simiae* K-Hf-L9 genome sequence. The graph was generated by BRIG 0.95.



1: *Pseudomonas simiae* K-Hf-L9 [accession number: NZ_CP066169]

2: *Pseudomonas simiae* PCL1751 [accession number: NZ_CP010896]

3: *Pseudomonas simiae* WCS417 [accession number: NZ_CP007637]

Figure 5.16. Venn Diagram showing the number of shared and genome-specific gene families among *Pseudomonas simiae* K-Hf-L9, *Pseudomonas simiae* PCL1751 and *Pseudomonas simiae* WCS417. The diagram was generated using EDGAR version 3.0.

The *P. agglomerans* PSV1-7 complete genome sequence was compared with the complete genome sequence of two publicly available type strains, *P. agglomerans* UAEU18 and *P. agglomerans* ZJU23. The analysis revealed that the complete genome size of the three strains ranges from 4 040 629 to 4 151 813 bp, with G+C content ranging from 54.8 to 55.5%. Moreover, the CDSs ranged from 4 360 to 4 625 (Table 5.4). Unlike the genome comparison described above, 3-4 plasmids with sizes ranging from 1 405 to 621 667 bp were detected in the *P. agglomerans* strains (Table 5.5).

Table 5.4. Summary of genomic features of *Pantoea agglomerans* PSV1-7, *Pantoea agglomerans* UAEU18 and *Pantoea agglomerans* ZJU23

Genomic features	PSV1-7	UAEU18	ZJU23
No. of contigs (chromosome, plasmid)	5	5	4
Genome size (bp)	4 053 926	4 040 629	4 151 813
G+C content (%)	54.8	55.5	55.5
Total no. of genes	4 733	4477	4 680
Total no. of CDSs ^a	4 625	4 360	4 570
No. of CDSs with protein	4 545	4 281	4 513
No. of RNA genes	108	117	110
No. of complete rRNAs (5S, 16S, 23S)	8, 7, 7	8,7,7	8, 7, 7
No. of tRNAs	77	80	77
No. of noncoding RNAs	9	15	11
Total no. of pseudogenes	80	79	57
Total no. plasmid	4	4	3
Plasmid 1 Size (bp)	621 667	513 383	567 588
Plasmid 2 Size (bp)	179 440	184 488	170 989
Plasmid 3 Size (bp)	122 140	86 850	170 877
Plasmid 4 Size (bp)	51 994	1 405	

^a CDSs, coding sequences

Genome comparison using BRIG detected the presence of genes unique to *P. agglomerans* PSV1-7 compared with the complete genome sequence of *P. agglomerans* UAEU18 and *P. agglomerans* ZJU23 (Fig 5.17). Moreover, the three strains shared a core genome of 3854 orthologs, and *P. agglomerans* PSV1-7 contained 442 unique genes (Fig. 5.18).

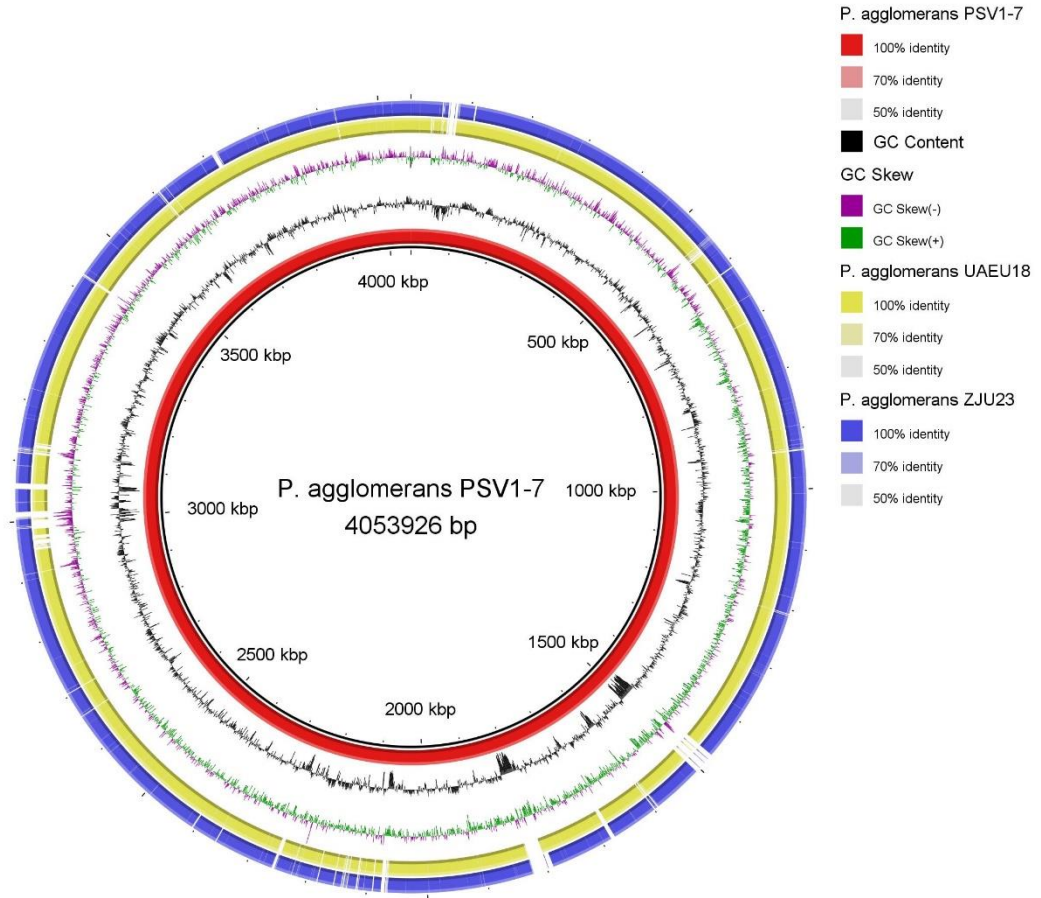
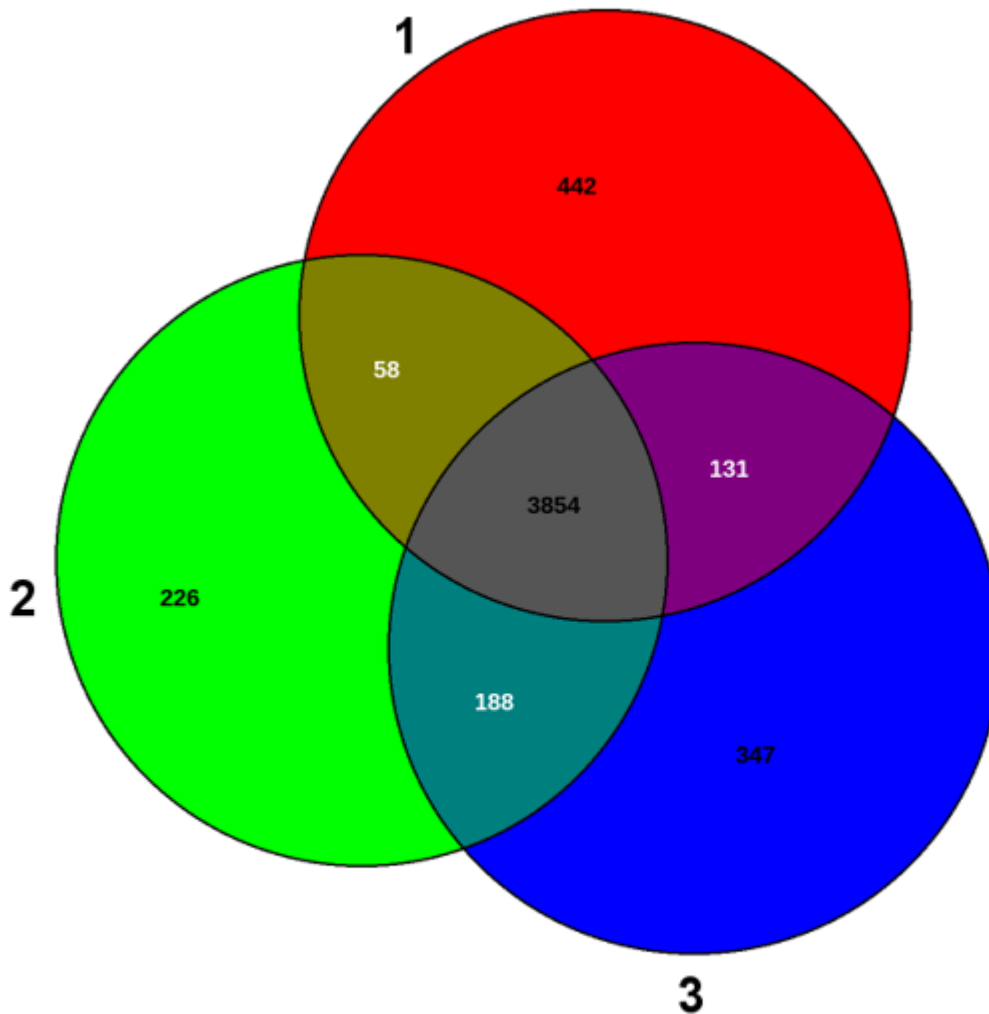


Figure 5.17. Graphical visualization of the BLAST comparisons of the *Pantoea agglomerans* PSV1-7 chromosome with chromosomes of two type strains, *Pantoea agglomerans* UAEU18 and *Pantoea agglomerans* ZJU23. The order of the rings: Ring 1. *P. agglomerans* PSV1-7; Ring 2. GC Content; Ring 3. GC Skew; Ring 4. *P. agglomerans* UAEU18 and Ring 5 *P. agglomerans* ZJU23. The darker regions indicate the presence of multiple hits corresponding to the portion of the *P. agglomerans* PSV1-7 genome sequence. In contrast, gaps indicate the absence of sequences with less than a 50% identity ratio to the *P. agglomerans* PSV1-7 genome sequence. The graph was generating by BRIG 0.95.



1: *Pantoea agglomerans* PSV1-7 [accession number: NZ_CP091189]

2: *Pantoea agglomerans* UAEU18 [accession number: NZ_CP048033]

3: *Pantoea agglomerans* ZJU23 [accession number: NZ_CP068440]

Figure 5.18. Venn Diagram showing the number of shared and genome-specific gene families among *Pantoea agglomerans* PSV1-7, *Pantoea agglomerans* UAEU18 and *Pantoea agglomerans* ZJU23. The diagram was generated using EDGAR version 3.0.

Comparison of the *L. gummosus* K-Be-H3 genome with two publicly available *L. gummosus* type strains (10.1.1 and 3.2.110) indicated that the three strains have a relatively small difference in various parameters of genomic feature (Table 5.5). For example, their genome size ranged from 6 017 450 to 6 056 618 bp with a G+C content of 66.5%. Moreover, their predicted CDSs ranged from 4 943 to 4 985 (Table 5.5).

Table 5.5. Summary of genomic features of *Lysobacter gummosus* K-Be-H3, *Lysobacter gummosus* 10.1.1 and *Lysobacter gummosus* 3.2.11

Genomic features	K-Be-H3	10.1.1	3.2.11
No. of contigs (chromosome)	1	1	1
Genome size (bp)	6 017 450	6 056 609	6 056 618
G+C content (%)	66.5	66.5	66.5
Total no. of genes	5 004	5 038	5 046
Total no. of CDSs ^a	4 943	4 977	4 985
No. of CDSs with protein	4 861	4 894	4 906
No. of RNA genes	61	61	61
No. of complete rRNAs (5S, 16S, 23S)	2, 2, 2	2,2,2	2,2,2
No. of tRNAs	51	51	51
No. of noncoding RNAs	4	4	4
Total no. of pseudogenes	82	83	79
Total no. plasmid	0	0	0

^aCDSs, coding sequences

Although *L. gummosus* K-Be-H3, *L. gummosus* 10.1.1 and 3.2.110 were identified to have similar genomic features, the comparative genome analysis using BRIG detected the presence of genes unique to strain K-Be-H3 (Fig. 5.19). Moreover, the three *L. gummosus* strains shared a core genome of 4 524 orthologs, and *L. gummosus* K-Be-H3 contained 327 unique genes (Fig. 5.20).

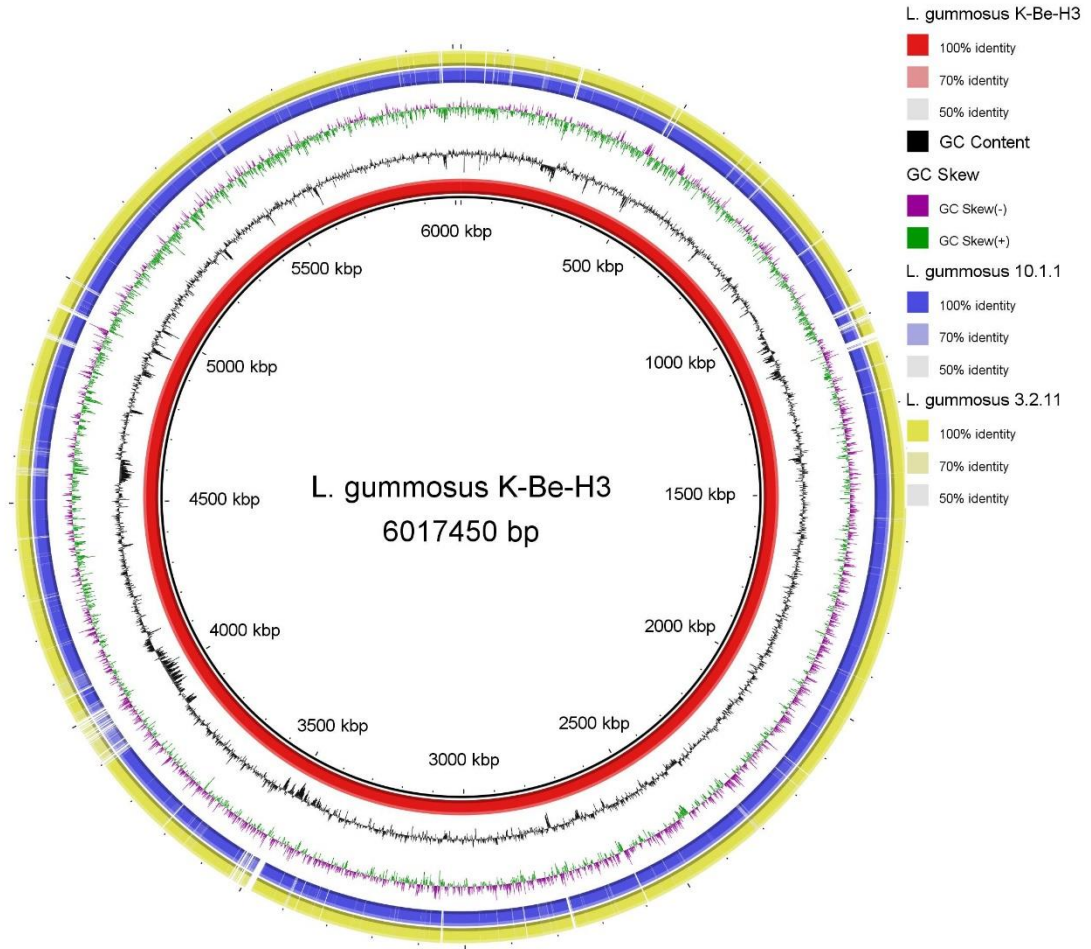
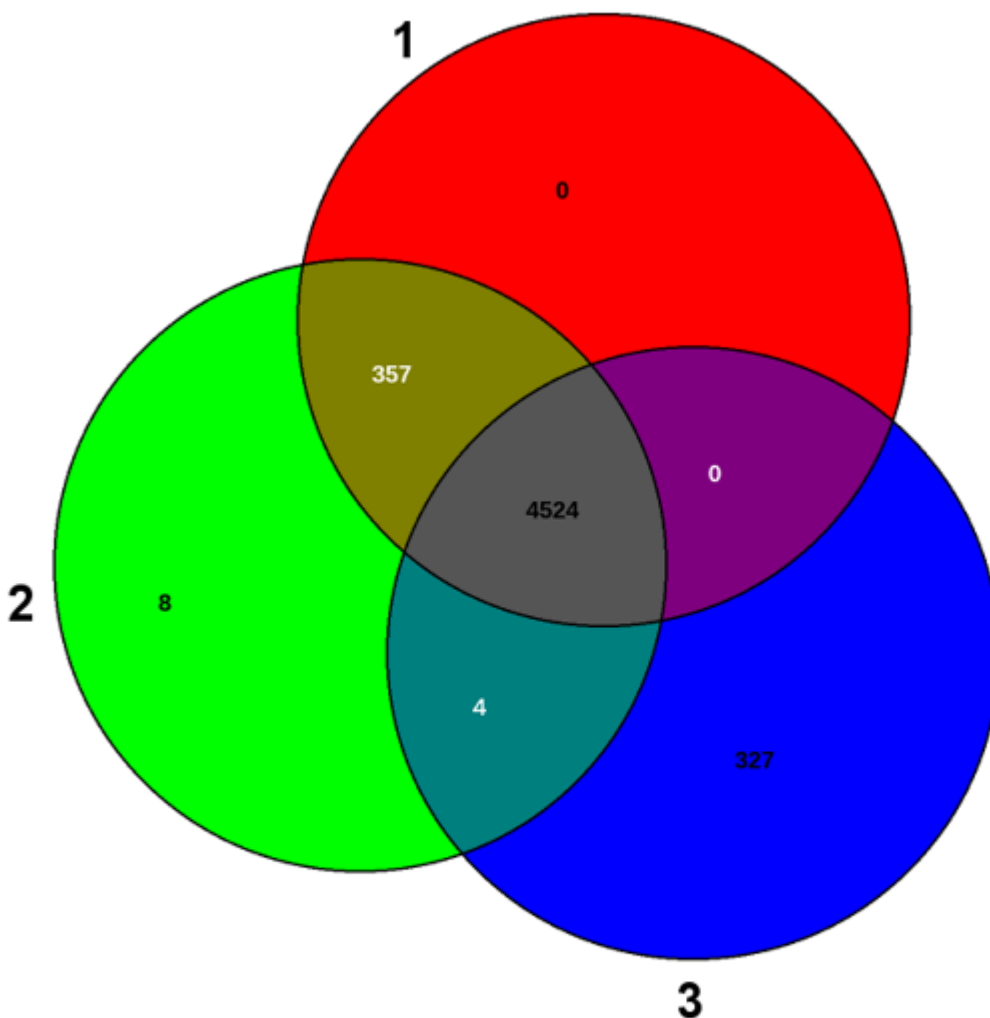


Figure 5.19. Graphical visualization of the BLAST comparisons of the *Lysobacter gummosus* K-Be-H3 genome with genomes of two type strains, *Lysobacter gummosus* 10.1.1 and *Lysobacter gummosus* 3.2.11. The order of the rings: Ring 1. *Lysobacter gummosus* K-Be-H3; Ring 2. GC Content; Ring 3. GC Skew; Ring 4. *Lysobacter gummosus* 10.1.1 and Ring 5. *Lysobacter gummosus* 3.2.11. The darker regions indicate the presence of multiple hits corresponding to the portion of the *Lysobacter gummosus* K-Be-H3 genome sequence. In contrast, gaps indicate the absence of sequences with less than a 50% identity ratio to the *Lysobacter gummosus* K-Be-H3 genome sequence. The graph was generating by BRIG 0.95.



1: *Lysobacter gummosus* 10.1.1 [accession number: NZ_CP093547]

2: *Lysobacter gummosus* 3.2.11 [accession number: NZ_CP011131]

3: *Lysobacter gummosus* K-Be-H3 [accession number: NZ_CP091194]

Figure 5.20. Venn Diagram showing the number of shared and genome-specific gene families among *Lysobacter gummosus* K-Be-H3, *Lysobacter gummosus* 10.1.1, and *Lysobacter gummosus* 3.2.11. The diagram was generated using EDGAR version 3.0.

5.5.4 Antibiotics resistance genes

Several different kinds of antibiotic resistance genes were detected in the genomes of the biocontrol bacteria with a varying level of percent identity to target sequences of those known for other bacteria (Tables 5.6 to 5.8). For example, five antibiotic resistance genes, two copies of *adeF*, *qacG*, *qacJ* and *vanY* gene, were identified in the *L. capsici* K-Hf-H2 genome with percent identity ranging from 32.85 to 61 % (Table 5.6). Similarly, five antibiotic resistance genes were detected

in the *P. simiae* K-Kf-L9 genome, with percent identity ranging from 38.5 to 72.1 (Table 5.7). In contrast, ten antibiotic-resistance genes were detected in the *P. agglomerans* PSV1-7 genome. Compared with *L. capsici* K-Hf-H2 and *P. simiae* K-Kf-L9, a high number of antibiotic resistance genes were detected in the *P. agglomerans* PSV1-7, and the majority had a higher percentage identity, providing stronger prediction (Table 5.8).

Table 5.6. Antibiotic resistance genes in *L. capsici* K-Hf-H2 and *L. gummosus* K-Be-H3 genome using CARD database

Antibiotic resistance ontology	Antimicrobial resistance gene family	Drug class	Resistance mechanism	Proportion of region matched (%)
adeF	Resistance-nodulation-cell division (RND) antibiotic efflux pump	Fluoroquinolone antibiotic, tetracycline antibiotic	Antibiotic efflux	60.4
adeF	Resistance-nodulation-cell division (RND) antibiotic efflux pump	Fluoroquinolone antibiotic, tetracycline antibiotic	Antibiotic efflux	61
qacG	Small multidrug resistance (SMR) antibiotic efflux pump	Disinfecting agents and antiseptics	Antibiotic efflux	42.31
qacJ	Small multidrug resistance (SMR) antibiotic efflux pump	Disinfecting agents and antiseptics	Antibiotic efflux	41.18
vanY gene in vanM cluster	vanY, glycopeptide resistance gene cluster	Glycopeptide antibiotic	Antibiotic target alteration	32.85

Table 5.7. Antibiotic resistance genes in *P. simiae* K-Kf-L9 genome using CARD database.

Antibiotic resistance ontology	Antimicrobial resistance gene family	Drug class	Resistance mechanism	Proportion of region matched (%)
vanG	Glycopeptide resistance gene cluster, Van ligase	Glycopeptide antibiotic	Antibiotic target alteration	38.5
adeF	Resistance-nodulation-cell division (RND) antibiotic efflux pump	Fluoroquinolone antibiotic, tetracycline antibiotic	Antibiotic efflux	41.81
<i>Pseudomonas aeruginosa</i> soxR	ATP-binding cassette (ABC) antibiotic efflux pump, major facilitator superfamily (MFS) antibiotic efflux pump, resistance-nodulation-cell division (RND) antibiotic efflux pump	Fluoroquinolone antibiotic, cephalosporin, glycylcycline, penam, tetracycline antibiotic, rifamycin antibiotic, phenicol antibiotic, disinfecting agents and antiseptics	Antibiotic target alteration, antibiotic efflux	70.42
<i>Acinetobacter baumannii</i> AbaQ	Major facilitator superfamily (MFS) antibiotic efflux pump	Fluoroquinolone antibiotic	Antibiotic efflux	72.1
adeF	Resistance-nodulation-cell division (RND) antibiotic efflux pump	Fluoroquinolone antibiotic, tetracycline antibiotic	Antibiotic efflux	67.08

Table 5.8. Antibiotic resistance genes in *P. agglomerans* PSV1-7 genome using CARD database.

Antibiotic resistance ontology	Antimicrobial resistance gene family	Drug class	Resistance mechanism	Proportion of region matched (%)
CRP (C-reactive protein)	Resistance-nodulation-cell division (RND) antibiotic efflux pump	Macrolide antibiotic, fluoroquinolone antibiotic, penam	Antibiotic efflux	98.57
rsmA	Resistance-nodulation-cell division (RND) antibiotic efflux pump	Fluoroquinolone antibiotic, diaminopyrimidine antibiotic, phenicol antibiotic	Antibiotic efflux	89.66
<i>Klebsiella pneumoniae</i> KpnH	Major facilitator superfamily (MFS) antibiotic efflux pump	Macrolide antibiotic, fluoroquinolone antibiotic, aminoglycoside antibiotic, carbapenem, cephalosporin, penam, peptide antibiotic, penem	Antibiotic efflux	88.21
<i>Klebsiella pneumoniae</i> KpnF	Major facilitator superfamily (MFS) antibiotic efflux pump	Macrolide antibiotic, aminoglycoside antibiotic, cephalosporin, tetracycline antibiotic, peptide antibiotic, rifamycin antibiotic, disinfecting agents and antiseptics	Antibiotic efflux	75.73
adeF	Resistance-nodulation-cell division (RND) antibiotic efflux pump	Fluoroquinolone antibiotic, tetracycline antibiotic	Antibiotic efflux	60.8
adeF	Resistance-nodulation-cell division (RND) antibiotic efflux pump	Fluoroquinolone antibiotic, tetracycline antibiotic	Antibiotic efflux	42.06
<i>Escherichia coli</i> EF-Tu mutants conferring resistance to Pulvomycin	Elfamycin resistant EF-Tu	Elfamycin antibiotic	Antibiotic target alteration	89.82
<i>Morganella morganii</i> gyrB conferring	Fluoroquinolone resistant gyrB	Fluoroquinolone antibiotic	Antibiotic target alteration	80.72

resistance to fluoroquinolones				
Escherichia coli EF-Tu mutants conferring resistance to Pulvomycin	Elfamycin resistant EF-Tu	Elfamycin antibiotic	Antibiotic target alteration	91.09
Haemophilus influenzae PBP3 conferring resistance to beta-lactam antibiotics	Penicillin-binding protein mutations conferring resistance to beta-lactam antibiotics	Cephalosporin, cephamycin, penam	Antibiotic target alteration	53.19

5.5.5 Phylogenetic analysis

The phylogenetic analysis conducted based on the 16S rRNA gene sequence showed the genetic relationship of the biocontrol bacteria with representative species selected in each genus (Fig. 5.21 to 5.23). For example, the phylogenetic analysis among the *Lysobacter* species showed that *L. capsici* strain 10.4.5 [accession number: FN357197.1] and *L. capsici* strain 6.2.3 [accession number: FN357196.1] were found to be the closest type strains with clade bootstrap value of 99.9% (Fig. 5.21). On the other hand, the most immediate strain of *L. gummosus* K-Be-H3 was *L. gummosus* (Fig. 5.21).

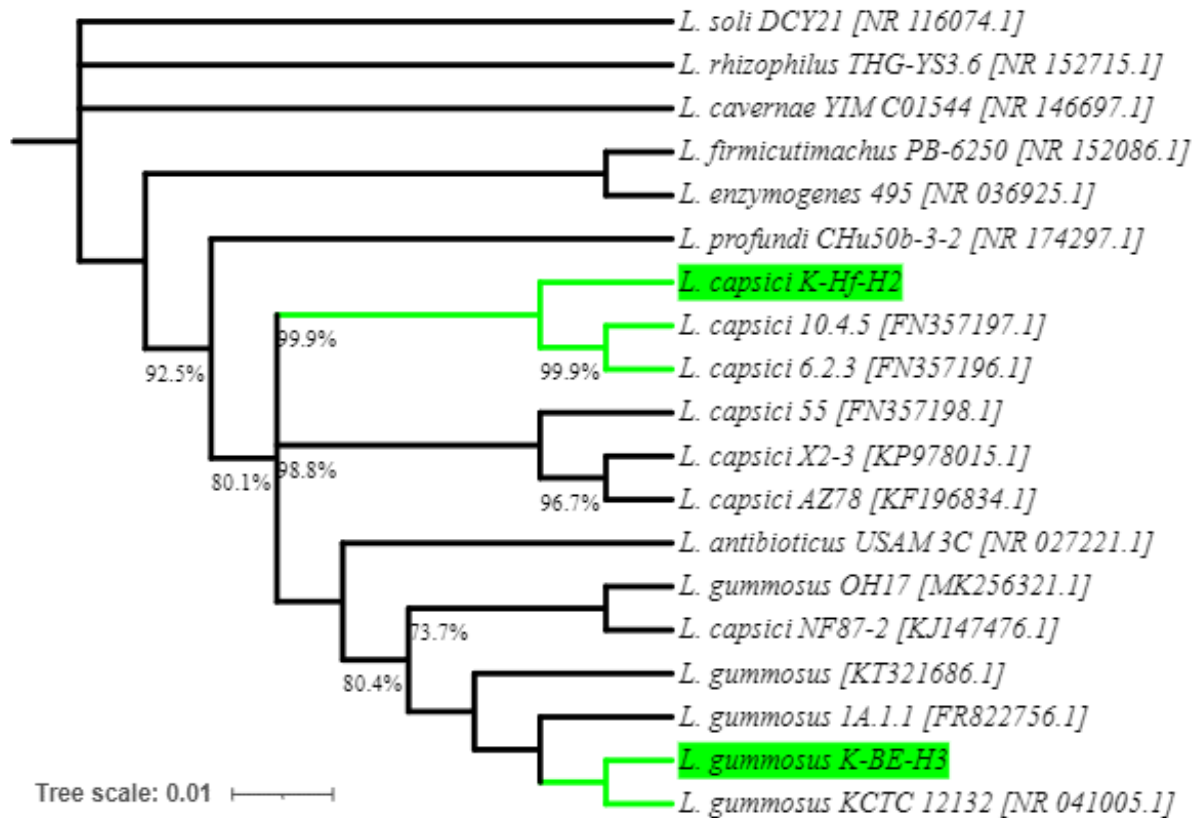


Figure 5.21. Phylogenetic tree showing the relationships among *L. capsici* K-Hf-H2, *L. gummosus* K-BE-H3 and members of the genus *Lysobacter*. The tree was inferred based on their 16S rRNA gene sequences data collected from the GenBank database. The sequences were aligned by ClustalW, and the product was used to generate a phylogenetic tree using the Neighbor-Joining method (Saitou and Nei, 1987). The evolutionary distances were computed using Kimura's two-parameter model (Kimura, 1980). The sequences' accession numbers are provided in parentheses. Numbers at the nodes indicate bootstrap values, >70%, from 1000 data replication (Felsenstein, 1985). The phylogenetic analyses were performed using MEGAX (Kumar et al., 2018).

The phylogenetic analysis for *P. simiae* K-Hf-L9 and selected members from its genus showed that strain K-Hf-L9 was clustered together *P. simiae* strain OLi [accession number: NR 042392.1] with clade bootstrap value of 100%. Compared to the *Lysobacter* species, species within the *Pseudomonas* have higher relatedness even if the selected members have different species name (Fig. 5.22).

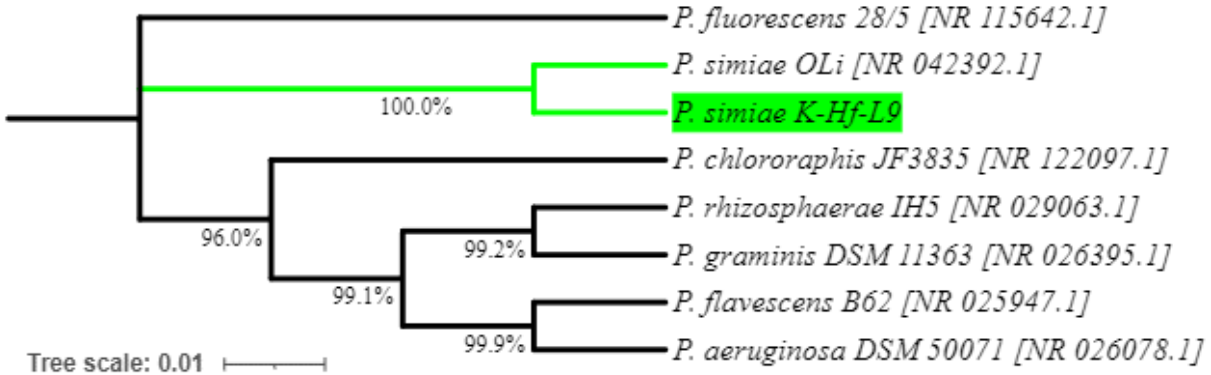


Figure 5.22. Phylogenetic tree showing the relationships between *Pseudomonas simiae* K-Hf-L9 and members of the genus *Pseudomonas*. The tree was inferred based on their 16S rRNA gene sequences data collected from the GenBank database. The sequences were aligned by ClustalW, and the product was used to generate a phylogenetic tree using the Neighbor-Joining method (Saitou and Nei, 1987). The evolutionary distances were computed using Kimura's two-parameter model (Kimura, 1980). The sequences' accession numbers are provided in parentheses. Numbers at the nodes indicate bootstrap values, >70%, from 1000 replication of the data (Felsenstein, 1985). The phylogenetic analyses were carried out using MEGAX (Kumar et al., 2018).

The phylogenetic analysis for *P. agglomerans* PSV 1-7 and selected members of its genus showed that strain PSV 1-7 was clustered together *P. agglomerans* UAEU18 [accession number: NR CP048033], *P. agglomerans* ZJU23 [accession number: NR CP068440] and *P. agglomerans* C410P1 [accession number: NR CP016889] with clade bootstrap value of 100% (Fig. 5.23).

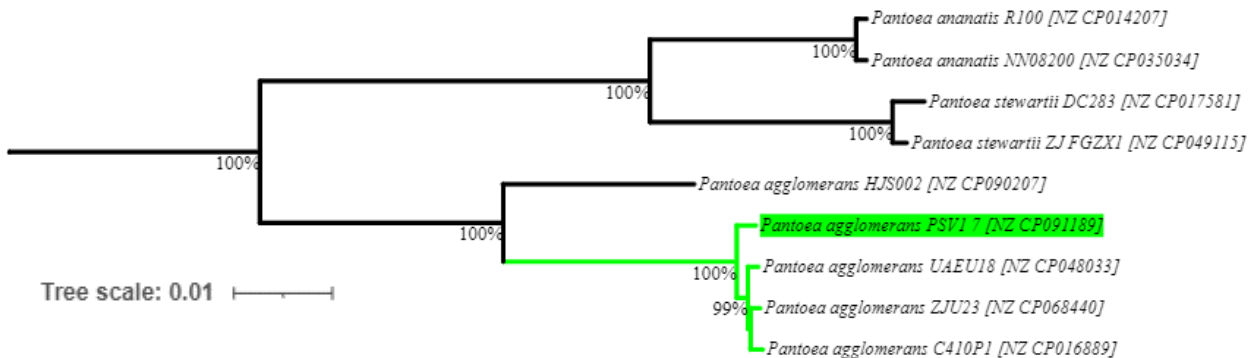


Figure 5.23. Phylogenetic tree showing the relationships between *Pantoea agglomerans* PSV1-7 and members of the genus *Pantoea*. The tree was inferred based on their 16S rRNA gene sequences data collected from the GenBank database. The sequences were aligned by ClustalW, and the product was used to generate a phylogenetic tree using the Neighbor-Joining method (Saitou and Nei, 1987). The evolutionary distances were computed using Kimura's two-parameter model (Kimura, 1980). The sequences' accession numbers are provided in parentheses. Numbers at the nodes indicate bootstrap values, >70%, from 1000 replication of the data (Felsenstein, 1985). The phylogenetic analyses were carried out using MEGAX (Kumar et al., 2018).

5.5.6 Identification of secondary metabolite regions

The AntiSMASH pipeline identified various BGCs within the whole genome sequences of the biocontrol bacteria, representing DNA sequences responsible for the production of different kinds of secondary metabolites (Tables 5.9 to 5.11). According to the AntiSMASH output, some of these secondary metabolites were identified as ribosomally synthesized, and others were described as non-ribosomally synthesized secondary metabolites.

AntiSMASH output for *L. capsici* K-Hf-H2 and *L. gummosus* K-Be-H3 detected 14 regions encoding for secondary metabolites with percent similarity ranging from 1% to 100%. Secondary metabolites encoding regions with percent similarity score of 50 and more are listed in Tables 5.9 and 5.10. Among the identified secondary metabolites, the HSAF encoding region was identified to score 100% similarity in both strains.

Table 5.9. Secondary metabolites biosynthetic gene clusters in *L. capsici* K-Hf-H2

Antibiotics name	Type	Position	Similarity
Rhizomide A / rhizomide B / rhizomide C	NRPS ^a	547558 - 600397	100%
Heat-stable antifungal factor	NRPS-PKS ^b	1783466 - 1832936	100%
Xanthoferrin	Siderophore	3916541 - 3931298	85%
Sodorifen	Lanthipeptide class-ii	5484772 - 5579103	50%
Xanthomonadin I	Arylpolyene	5898931 - 5940136	57%

^aNRPS: non-ribosomal peptide synthetases; ^bNRPS-T1PKS: hybrid NRPS-PKS biosynthetic gene cluster (PKS: Polyketide synthase)

Table 5.10. Secondary metabolites biosynthetic gene clusters in *L. gummosus* K-Be-H3

Antibiotics name	Type	Position	Similarity
Heat-stable antifungal factor	NRPS-PKS ^a	1774439 - 1823909	100%
rhizomide A / rhizomide B / rhizomide C	NRPS ^b	3006978 - 3059817	100%
Xanthomonadin I	Arylpolyene	3684589 - 3725794	57%
Sodorifen	Lanthipeptide class-ii	4045622 - 4139953	50%
Xanthoferrin	Siderophore	5693427 - 5708184	85%

^aNRPS-PKS: hybrid NRPS-PKS biosynthetic gene cluster (PKS: Polyketide synthase); ^bNRPS: non-ribosomal peptide synthetases

Further analysis of the HSAF, a secondary metabolite active against microbial sphingolipid synthesis, a structure required for the polarized growth of mycelia, the genomic region was found to be similar to the HSAF biosynthetic gene cluster from *L. enzymogenes* (Yu et al., 2007). Moreover, a sphingolipid metabolism map using the Kyoto Encyclopedia of Genes and Genomes

(KEGG) database indicated that the *L. capsici* K-Hf-H2 and *L. gummosus* K-Be-H3 genome has a total of 8 genes that interfere with the sphingolipid biosynthesis at three junctions as indicated in the green background in Fig. 5.24. Of these eight genes, for example, in *L. capsici* K-Hf-H2, three were beta-galactosidase EC 3.2.1.23 K-Hf-H2.peg.2824, K-Hf-H2.peg.2826 and K-Hf-H2.peg.4307; four were alpha-galactosidase EC 3.2.1.22 K-Hf-H2.peg.2151, K-Hf-H2.peg.2815, K-Hf-H2.peg.4298 and K-Hf-H2.peg.4300 and one gene was exo-alpha-sialidase EC 3.2.1.18 K-Hf-H2.peg.3941.

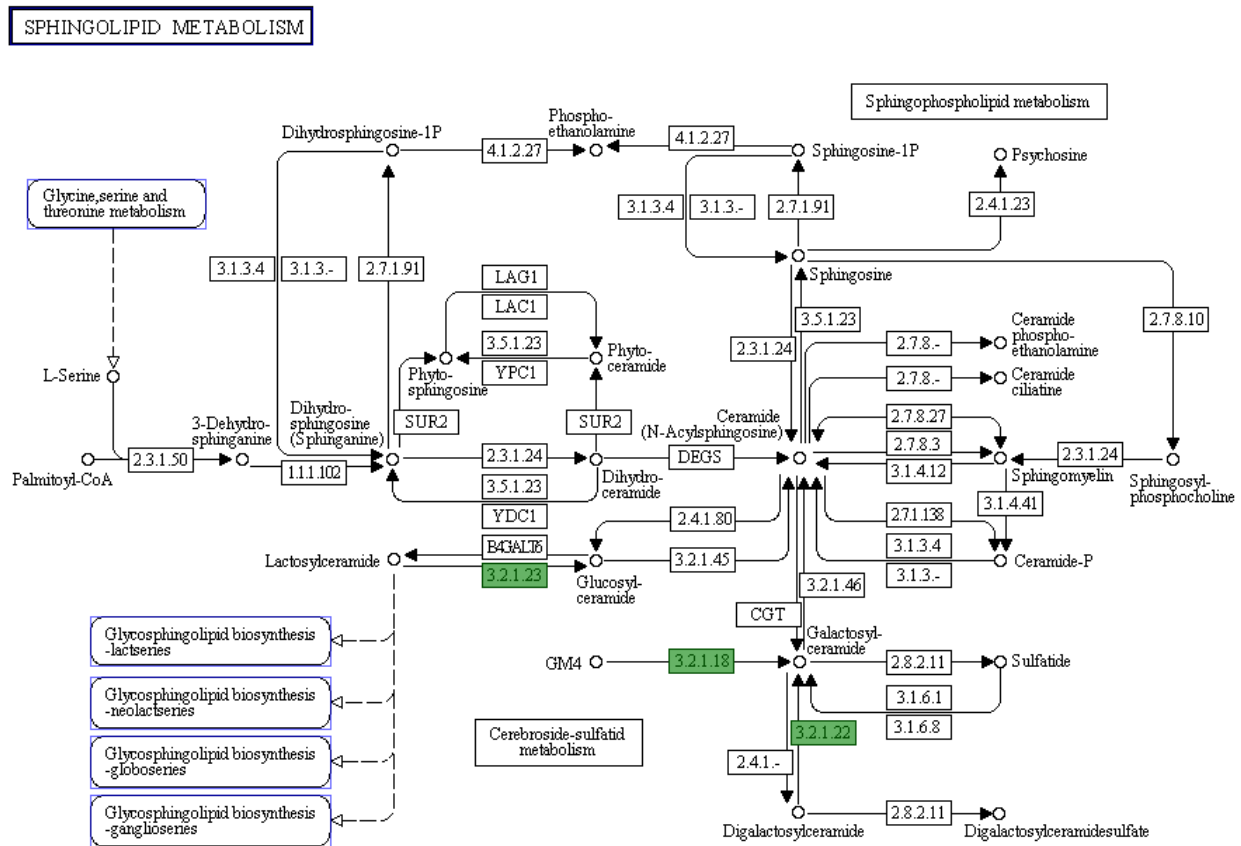


Figure 5.24. KEGG map showing sphingolipid synthesis for fungi. *Lysobacter capsici* K-HF-H2 interfere with the biosynthesis of sphingolipid via eight genes at three targets indicated by green background in the synthesis pathway. These eight genes are three beta-galactosidase (EC 3.2.1.23) K-Hf-H2.peg.2824, K-Hf-H2.peg.2826 and K-Hf-H2.peg.4307; four alpha-galactosidase (EC 3.2.1.22) K-Hf-H2.peg.2151, K-Hf-H2.peg.2815, K-Hf-H2.peg.4298 and K-Hf-H2.peg.4300 and one exo-alpha-sialidase (EC 3.2.1.18) K-Hf-H2.peg.3941.

AntiSMASH output for *P. simiae* K-Hf-L9 detected 12 regions (five unknown) encoding for secondary metabolites with percent similarity score less than 50%; thus, data is not presented as these regions are less likely to be secondary metabolite encoding regions.

AntiSMASH output for *P. agglomerans* PSV1-7 detected 7 regions (one unknown), including two gene clusters on plasmid 1, that encode for secondary metabolites with percent similarity ranging from 13% to 100%. Secondary metabolites encoding regions with percent similarity score of 50 and more are listed in Tables 5.11. Among the identified secondary metabolites, the Desferrioxamine E (siderophores) and carotenoid encoding regions were identified to score 100% similarity (Table 5.11). Moreover, aryl polyenes were the other region with a significant matching hit that has a percent similarity of 95. Although four plasmids were detected in *P. agglomerans* PSV1-7, only plasmid 1 with size of 621 667 bp was detected to carry a secondary metabolite encoding region (Table 5.11).

Table 5.11. Secondary metabolites biosynthetic gene clusters in *P. agglomerans* PSV1-7

Chromosome			
Antibiotics name	Type	Position	Similarity
Aryl polyenes	Arylpolyene hserlactone	3175489 - 3235329	94%
Plasmid 1, size 621,667 bp			
Desferrioxamine E	Siderophore	281601 - 293955	100%
Carotenoid	Terpene	482741 - 506302	100%

5.5.7 Laboratory investigation of functional activities

5.5.7.1 Siderophores production capacity

The siderophore production assessment indicated that the biocontrol bacteria, *L. capsici* K-Hf-H2, *P. simiae* K-Hf-L9 and *P. agglomerans* PSV1-7, can chelate iron through siderophore production as detected by the presence of orange halos around the bacterial colony on the CAS media (Fig. 5.25). *Pseudomonas simiae* K-Hf-L9 started the halo zone formation after 24 h of incubation, whereas the other *L. capsici* K-Hf-H2 and *P. agglomerans* PSV1-7 did not show any sign of halo zone formation until 72 h of incubation.

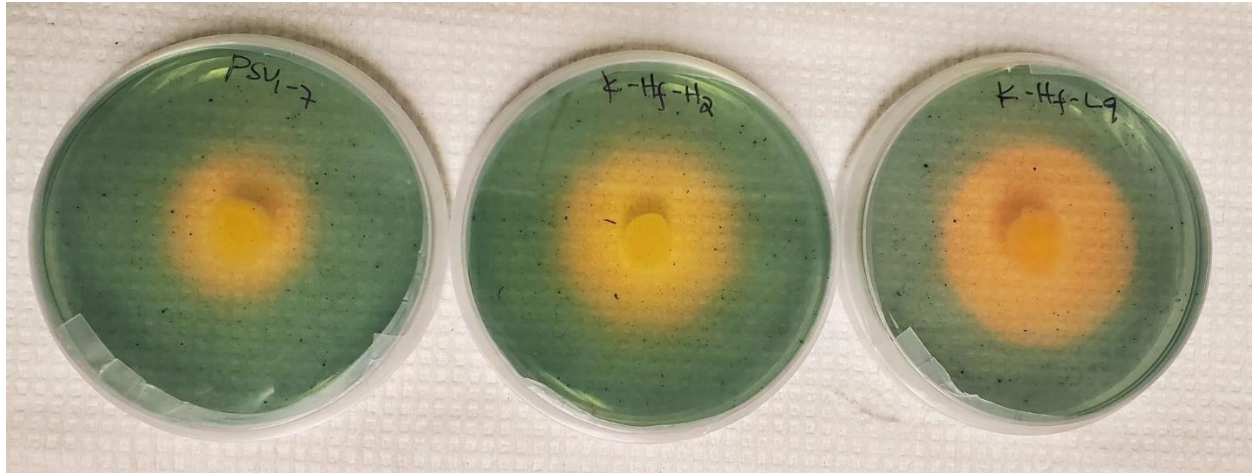


Figure 5.25. Siderophore production by *Pantoea agglomerans* PSV1-7, *Lysobacter capsici* K-Hf-H2 and *Pseudomonas simiae* K-Hf-L9 on Chrome Azurol S (CAS). The orange halo zones around the colony indicate siderophore production. The plates were incubated at 25 °C for 7 d.

5.5.7.2 Protein hydrolysis activity

The biocontrol bacteria exhibited proteolytic activity on SMA media as detected by an area of protein dissolution ring around the bacterial colony (Figs. 5.26 to 5.28) and wells (Fig. 5.26B). Trypsin enzyme solution used as a positive control also resulted in a similar protein hydrolysis ring on SMA media with and without wells (Fig. 5.29). However, the biocontrol bacteria showed varying proteolytic activity.

Lysobacter capsici K-Hf-H2 showed proteolytic activity within 48 h of incubation. In contrast, *P. simiae* K-Hf-L9 and *P. agglomerans* PSV1-7 exhibited proteolytic activity within 72 h and 96 h of incubation, respectively. Moreover, the cell-free supernatant of *L. capsici* K-Hf-H2 showed protein hydrolysis activity within 24 h of incubation (Fig. 5.26B). However, the cell-free supernatant *P. simiae* K-Hf-L9 (Fig 5.27B) and *P. agglomerans* PSV1-7 (Fig. 5.28B) did not produce proteolytic activity.

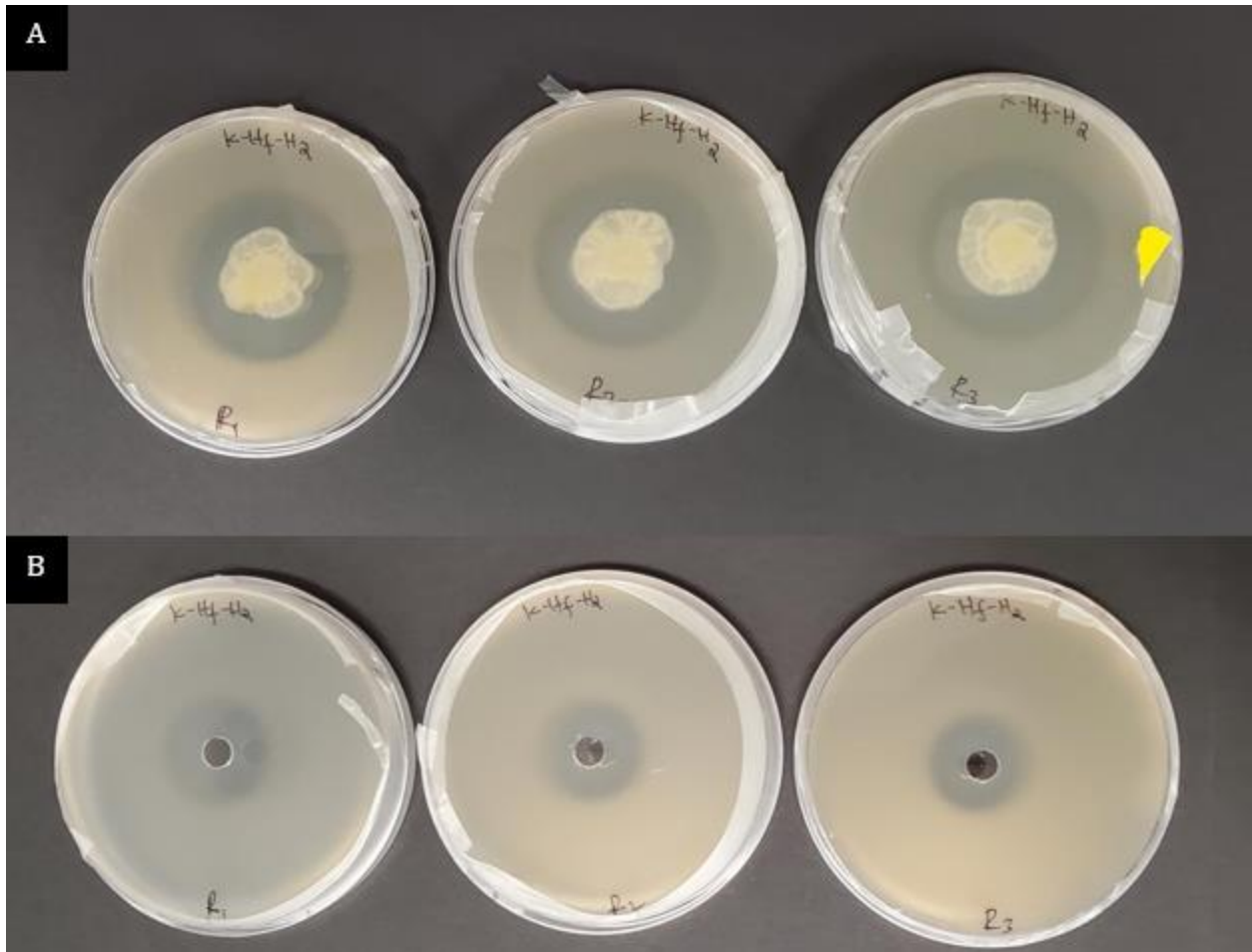


Figure 5.26. Protein hydrolysis by *Lysobacter capsici* K-Hf-H2. Clearing zones around the colonies (A) and wells (B) indicate protein hydrolysis on skimmed milk agar (SMA) plates. The plates were incubated at 25 °C for 5 d.

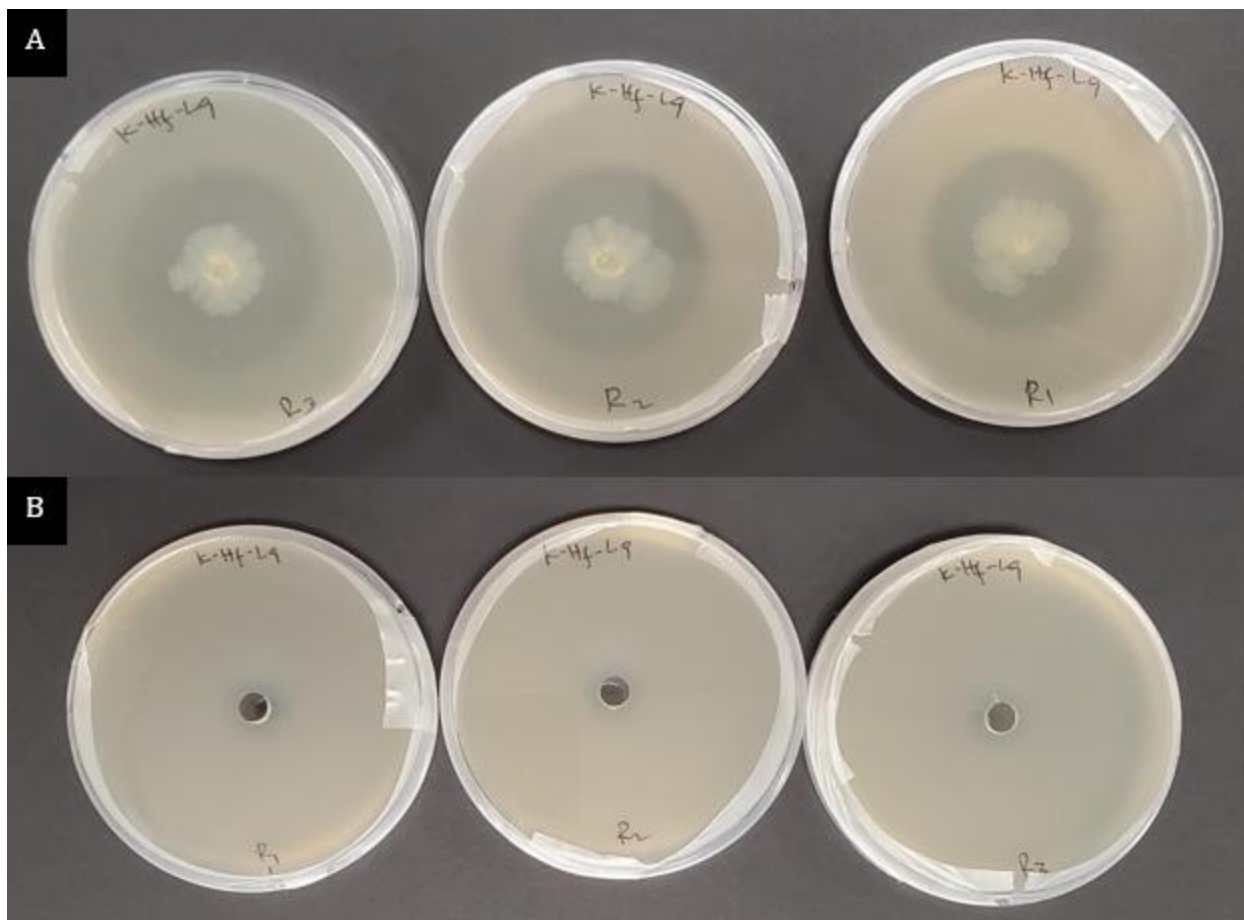


Figure 5.27. Protein hydrolysis by *Pseudomonas simiae* K-Hf-L9. Clearing zones around the colonies (A) indicate protein hydrolysis on skimmed milk agar (SMA) plates. The plates were incubated at 25 °C for 5 d. However, the cell-free supernatant of *P. simiae* K-Hf-L9 did not produce visually detectable protein hydrolysis around the wells (B) within 7 d of incubation at 25 °C.

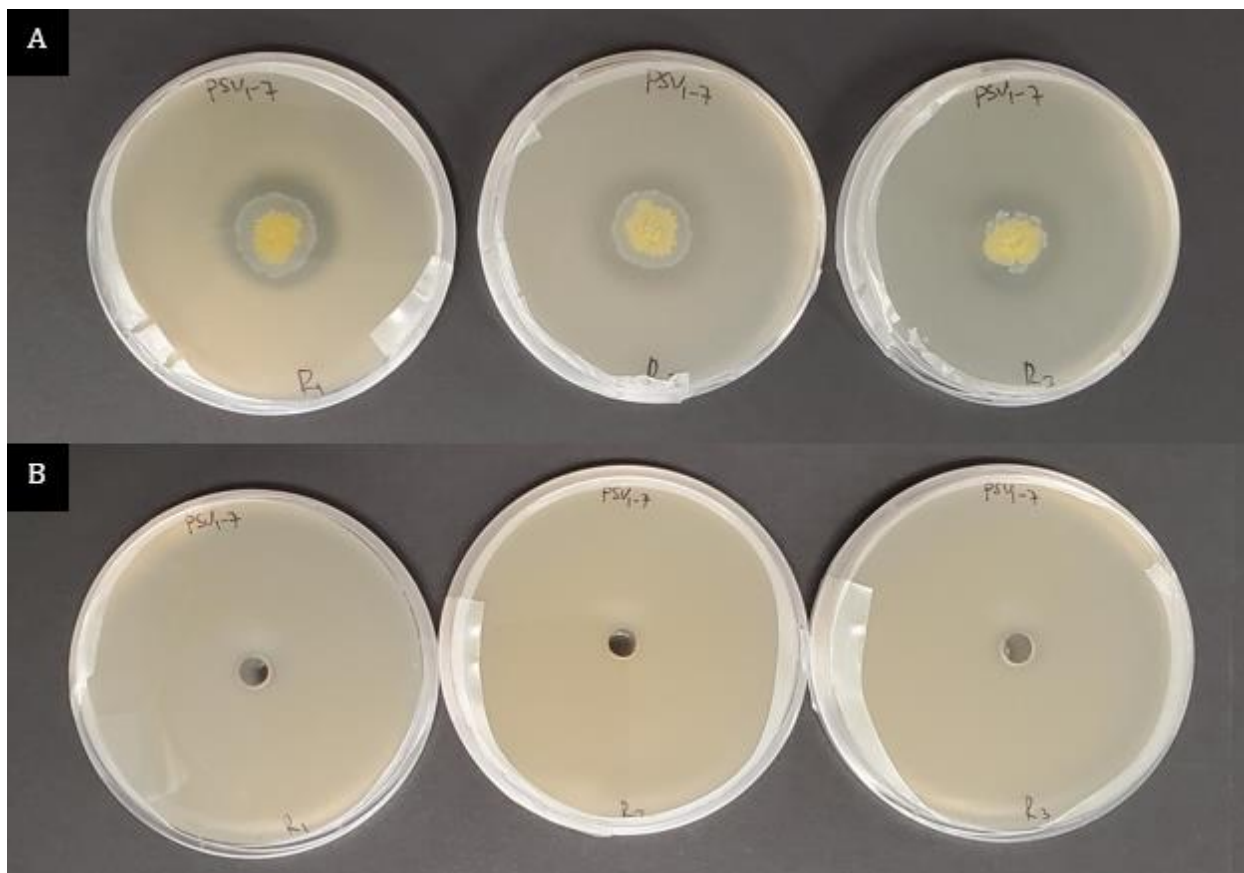


Figure 5.28. Protein hydrolysis by *Pantoea agglomerans* PSV1-7. Clearing zones around the colonies (A) indicate protein hydrolysis on skimmed milk agar (SMA) plates. The plates were incubated at 25 °C for 5 d. However, the cell-free supernatant of *Pantoea agglomerans* PSV1-7 did not produce visually detectable protein hydrolysis around the wells (B) within 7 d of incubation at 25 °C.

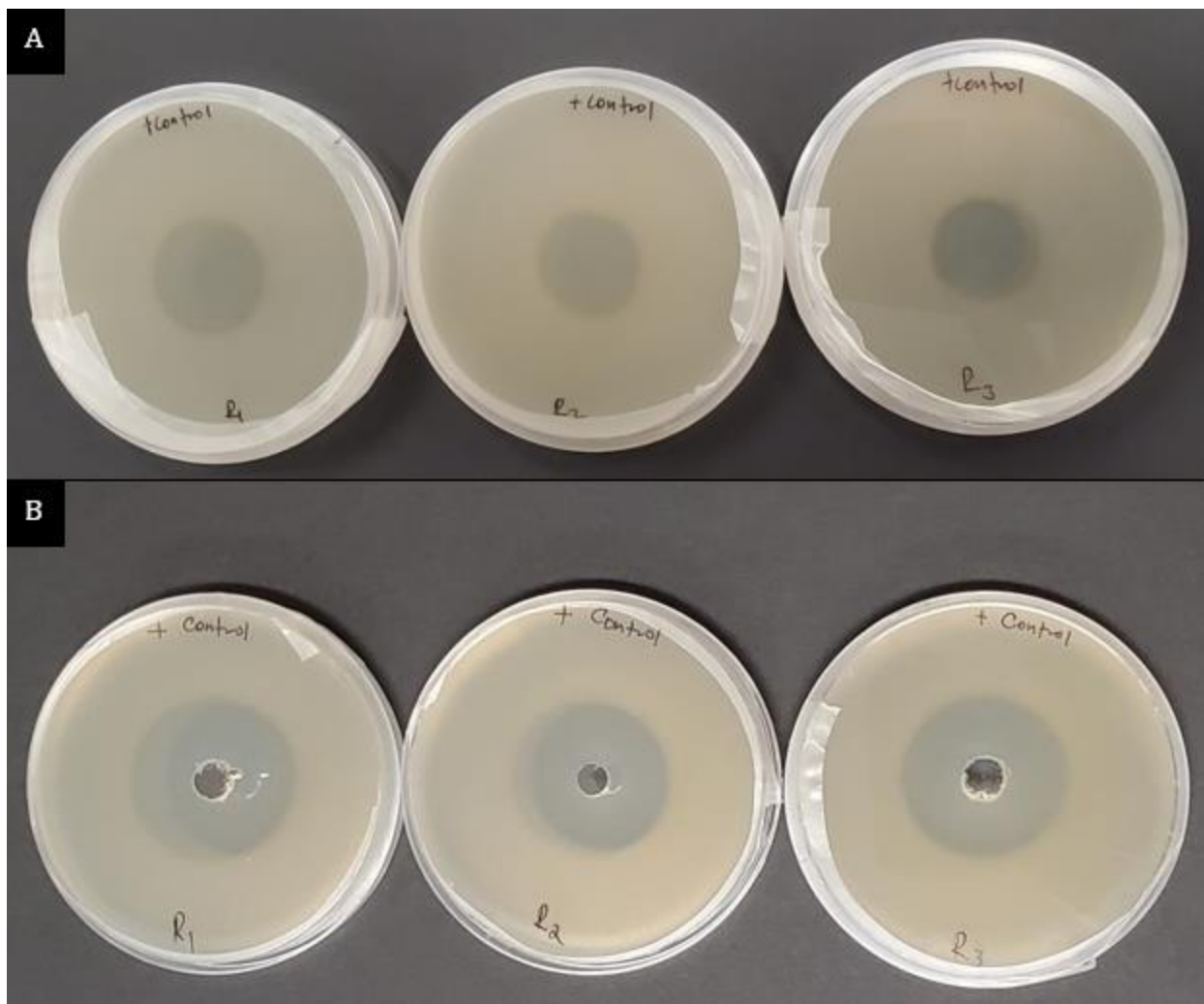


Figure 5.29. Protein hydrolysis positive controls. (A): skimmed milk agar plates that received 20 μL of filter-sterilized Trypsin (150 USP units mg^{-1}) enzyme solution; (B): skimmed milk agar plates with wells that received filter-sterilized 50 μL of the trypsin enzyme solution. The clearing zones in the center of the plates indicate protein hydrolysis by the enzyme trypsin. The plates were incubated at 25 $^{\circ}\text{C}$ for 5 d.

5.5.7.3 Cellulose hydrolysis capacity

The cellulose hydrolysis experiment indicated that *P. simiae* K-Hf-L9 and *L. capsici* K-Hf-H2 exhibited cellulolytic activity on cellulose-Congo-red agar media as shown by a clearing zone around the bacterial colony (Figs. 5.30 and 5.31). However, cellulolytic activity was not observed on the cellulose-Congo-red agar media inoculated with *P. agglomerans* PSV1-7.

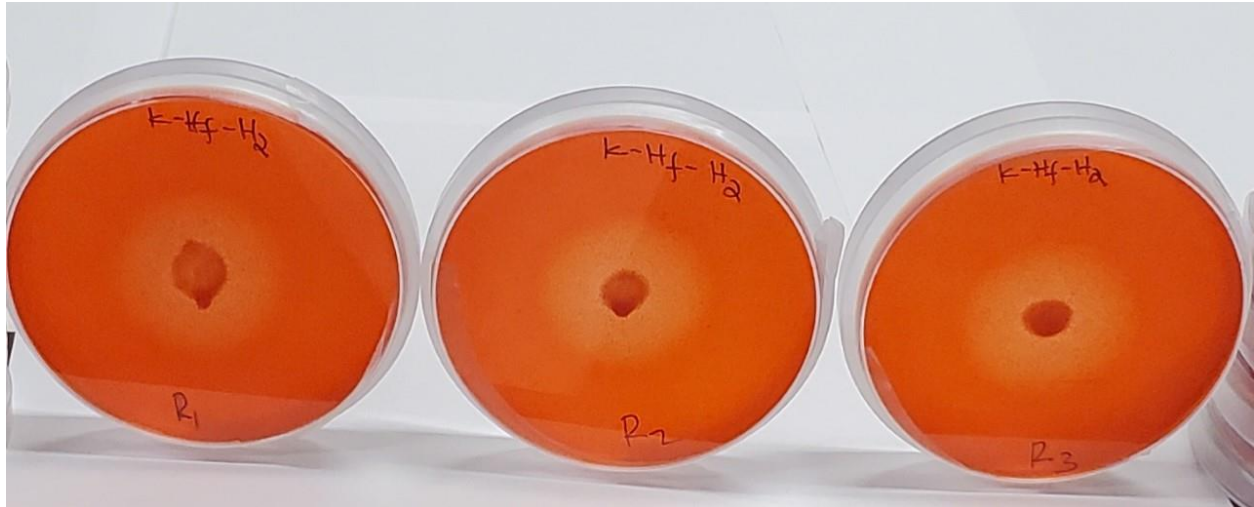


Figure 5.30. Cellulose hydrolysis capacity of *Lysobacter capsici* K-Hf-H2 on cellulose-Congo-red agar media. Clearing zones around the colony indicate hydrolysis of cellulose. The plates were incubated at 25 °C for 5 d.

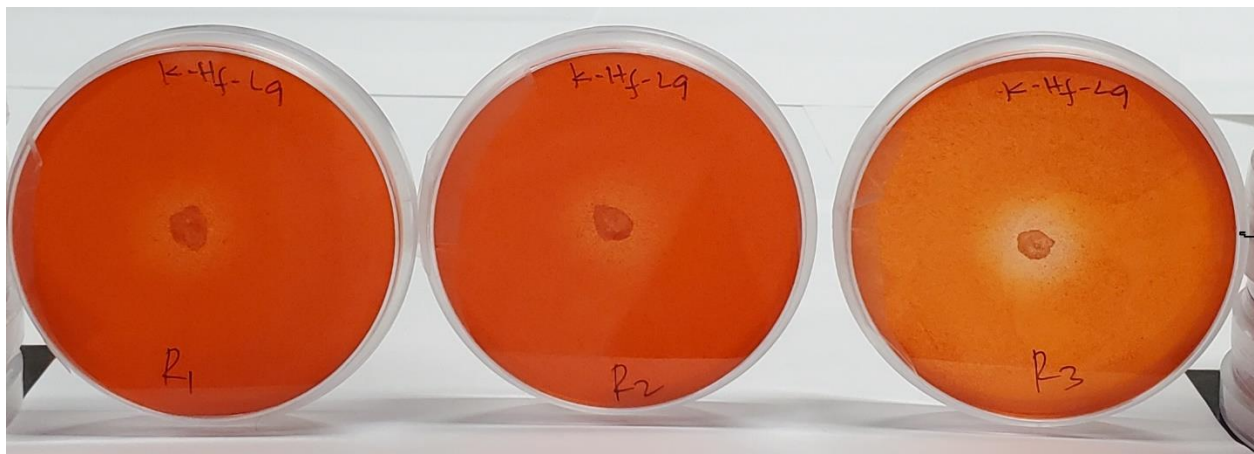


Figure 5.31. Cellulose hydrolysis capacity of *Pseudomonas simiae* K-Hf-L9 on cellulose-Congo-red agar media. Clearing zones around the colony indicate hydrolysis of cellulose. The plates were incubated at 25 °C for 5 d.

5.5.7.4 Desiccation tolerance

A desiccation tolerance assay was performed to determine the sensitivity of biocontrol bacteria to low water availability. The assay identified that biocontrol bacteria *L. capsici* K-Hf-H2 and *P. simiae* K-Hf-L9 were significantly reduced in desiccation tolerance compared with *P. agglomerans* PSV1-7 (Fig. 5.32), indicating that the two biocontrol bacteria are more sensitive to decreased water availability.

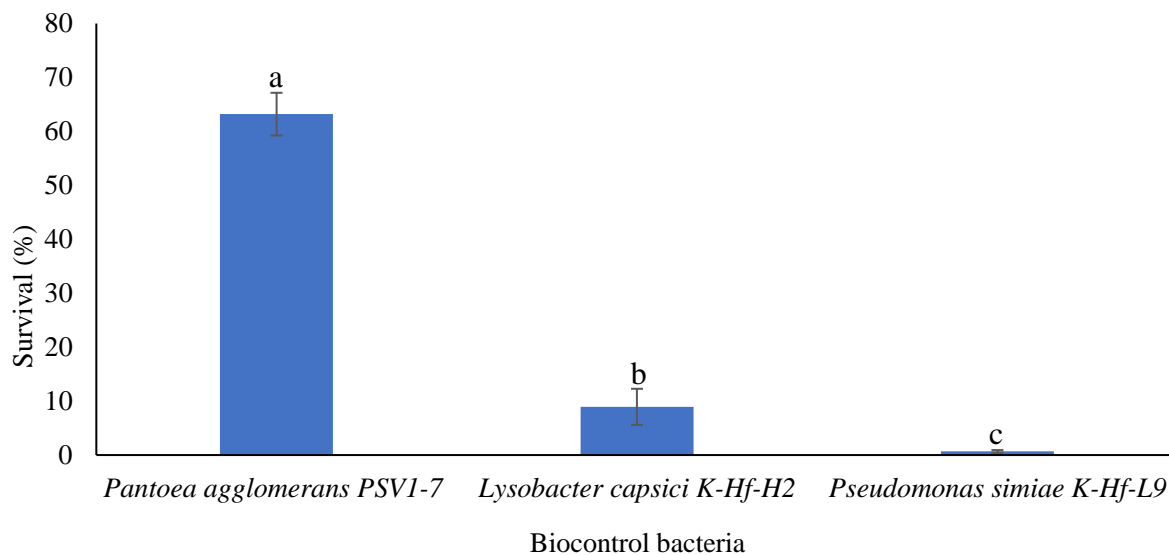


Figure 5.32. Desiccation tolerance of biocontrol bacteria. The reported values are mean percent survival obtained from three independent experiments. Membranes were cut in half and transferred to an empty Petri dish (dry) and a water-agar plate (12.5 g agar L⁻¹) (wet) and stored at room temperature and humidity for 24 h. Error bars indicate standard deviation. The percent survival of the biocontrol bacteria was significantly different and means represented with a different letter indicate significant difference.

5.6 Discussion

Developing effective biological control agents against phytopathogens is a knowledge-intensive strategy that has become an integral component of pest and pathogen management (Jeffers and Chong, 2021). Biological control methods not only play an essential role in replacing chemical fungicides but are also viewed as an environmentally sustainable alternative. Recently, a study by Godebo (2019) identified *L. capsici* K-Hf-H2, *P. simiae* K-Hf-L9 and *P. agglomerans* PSV1-7 as effective biocontrol agents of ARR in field pea in growth chamber conditions. Further investigations against RRC in field pea and lentil caused by strains of *A. euteiches*, *F. avenaceum* and *F. oxysporum* demonstrated that these biocontrol agents suppressed disease symptoms in planta, with *L. capsici* K-Hf-H2 being the most effective as discussed in Chapter 4. However, information regarding the genomic profiles and biological characteristics of these biocontrol bacteria were needed to explore possible biocontrol mechanisms and ultimately aid their registration as biological control agents of ARR and RRC of field pea and lentil in Canada. Therefore, the genomes of the *L. capsici* K-Hf-H2, *P. simiae* K-Hf-L9 and *P. agglomerans* PSV1-7 and an additional strain, *L. gummosus* K-Be-H3, a strain that significantly suppressed ARR in

lentil were sequenced using the PacBio and Nanopore sequencing technology and their complete genomes were analyzed using various bioinformatics tools. The PacBio sequencing technology was preferred for its longer reads and associated advantage during assembly, which is more likely to result in a closed genome than, for example, Illumina (Xie et al., 2020). On the other hand, nanopore sequencing was used due to its inexpensive sample preparation that requires minimal chemistries or enzyme-dependent amplification to generate high-quality data (Branton et al., 2008).

Complete genome sequence annotation and comparison highlighted significant similarities and differences between the biocontrol bacteria and similar bacteria selected for genome analysis and comparison. The comparative analysis revealed high diversity between *L. capsici* K-Hf-H2, *P. simiae* K-Hf-L9, *P. agglomerans* PSV1-7, *L. gummosus* K-Be-H3 and the similar bacteria selected for genome analysis and comparison (Figs 5.3 to 5.20). Moreover, several genes and gene clusters encoding various activities potentially involved in the suppression of ARR and RRC were detected (Tables 5.9 to 5.11). These findings were consistent with similar studies (Puopolo et al., 2016; Shariati et al., 2017; Montes-Osuna et al., 2021; Xu et al., 2022). For example, Puopolo et al. (2016) conducted a comparative analysis between *L. capsici* AZ78 and two other related bacteria. They showed the three strains had high diversity, and strain AZ78 harbours a significant gene pool essential for the biocontrol of plant pathogens. Similarly, Xu et al. (2022) performed a comparative genome analysis of two *L. enzymogenes* strains (CX03 and CX06) with different biocontrol capacities and other *Lysobacter* species. *Lysobacter enzymogenes* CX03 was reported to display a broad spectrum of antibacterial activity, whereas *L. enzymogenes* CX06 displayed a broad spectrum of antagonistic activities against various fungi and oomycetes (Xu et al., 2022), suggesting strain-specific variabilities. In line with this, the *L. capsici* K-Hf-H2 and *L. gummosus* K-Be-H3 strains identified as biocontrol agents of ARR displayed varying antagonistic and biocontrol potential towards ARR in field pea and lentil (Godebo, 2019; and Chapter four). Although *L. gummosus* K-Be-H3 exhibited strong antagonistic activity against *A. euteiches* during *in vitro* assay, that level of efficacy was not observed when tested against ARR in field pea grown in non-sterile soil under growth chamber condition (Godebo, 2019) and thus this strain was not selected as a candidate for RRC assessed in this Ph.D. study. However, the strain was investigated against ARR in lentil along with nine other bacteria. During this time, *L. gummosus* K-Be-H3

significantly suppressed disease development, suggesting *L. gummosus* K-Be-H3 was more effective in lentil than field pea.

Members of the *Lysobacter* species are known to produce various kinds of antibiotics and lytic enzymes (Gómez et al., 2015; Hashizume et al., 2016; Brescia et al., 2021). In addition, many exhibit a broad spectrum of antimicrobial and biocontrol activities against phytopathogenic bacteria, fungi and oomycetes (Xu et al., 2022). Accordingly, several genes and gene clusters encoding for biosynthetic traits that are potentially involved in antagonistic interaction with *A. euteiches*, *F. avenaceum*, *F. oxysporum* and other fungal pathogens were detected in *L. capsici* K-Hf-H2 and *L. gummosus* K-Be-H3 genome, highlighting the strains' biocontrol properties (Table C.1). Of these, the metalloendopeptidases that are associated with the release of extracellular zinc protease are a notable example as these enzymes lyse cell walls of oomycetes and fungi. Similarly, Puopolo et al. (2016) reported an extracellular zinc protease and other lytic enzymes capable of degrading cellulose, chitin, and laminarin as the primary mechanism by which *L. capsici* AZ78 inhibits plant pathogens. Moreover, other studies indicate that *Lysobacter* species produce various extracellular enzymes with lytic potential against the cell wall components of phytopathogens (Kobayashi and Yuen, 2007; Hayward et al., 2010). In agreement with this, my study also revealed that *L. capsici* K-Hf-H2 and *L. gummosus* K-Be-H3 genomes harbour an array of genes and gene clusters encoding for lytic enzymes capable of degrading cellulose, chitin, and proteins (Table C.1).

Lysobacter species are well-recognized as capable of producing a variety of extracellular enzymes, including chitinases, endonucleases and proteases (Zhang et al., 2001; Gökçen et al., 2014; Gómez et al., 2015). Chitinolytic activity was reported as one of the primary mechanisms by which, for example, *L. enzymogenes* C3 inhibit fungal pathogen via conidial deformation and abnormal germ tube growth (Zhang and Yuen, 2000). Similarly, during *in vitro* assay in my study, both *L. capsici* K-Hf-H2 and *L. gummosus* K-Be-H3 significantly inhibited mycelial growth of *F. avenaceum* and *L. gummosus* K-Be-H3, resulting in a significant alteration of mycelia growth morphology suggesting chitinolytic activity similar to that in *L. enzymogenes* C3. *Lysobacter* species are also known to produce extracellular β -1, 3-glucanases with cellulolytic activity (Palumbo et al., 2005). Palumbo et al. (2005) generated mutants lacking extracellular β -1, 3-glucanases encoding genes (three *gluABC* genes). Their results indicated the mutant strain's inhibitory potential against *Pythium* damping-off and *Bipolaris* leaf spot was reduced, suggesting

the loss of cellulolytic mechanism in the mutant strain. *Pythium* is an oomycete pathogen like *Aphanomyces*, and its cell wall structure is composed of cellulose instead of chitin in fungi. Thus, identifying genes encoding for extracellular β -1,3-glucanases in *L. capsici* K-Hf-H2 and *L. gummosus* K-Be-H3 indicates the potential utilization of cellulolytic activity in suppressing ARR. Moreover, even though *Lysobacter* species are known for various lytic enzymes, their protein hydrolysis capacity attracted the most attention mainly for its application in industrial processes (Gökçen et al., 2014). In this study, for example, *L. capsici* K-Hf-H2 tested positive for proteolytic (Fig. 5.26) and cellulolytic activity (Fig. 5.30). My findings support the strain's genomic profile, which suggests their involvement in the suppression of ARR and RRC.

Intriguingly, the AntiSMASH pipeline detected biosynthetic gene cluster encoding for HSAF with 100 percent similarity with one detected in *L. enzymogenes* OH11 (Yu et al., 2007). Although several studies have reported HSAF as a novel and forerunner of future biological pesticides (Li et al., 2006; Kobayashi and Yuen, 2005), information regarding factors affecting its production, such as pH, temperature, rotation speed and fermentation media and time are not well described. However, studies by Yu et al. (2007) and Tang et al. (2018) indicated that HSAF is a colourless powder produced under nutrient-limiting conditions and has a melting point greater than 300°C. Furthermore, in my study, the cell-free supernatant stability assay indicated that *L. capsici* K-Hf-H2 cell-free supernatant was stable only at 4°C, and the inhibitory potential was lost when autoclaved as well as stored at 24°C. These observations suggest the active metabolite in the crude extract was not heat stable but rather other lytic enzymes(s), likely protease (Mong Thu and Krasaekoopt, 2016). This could be attributed to the culture media used to grow the bacteria. As stated above, HSAF is produced under nutrient-limiting conditions (Yu et al., 2007; Tang et al., 2018); however, the culture media used to grow the bacteria for cell-free supernatant extraction was rich in nutrients ($\frac{1}{2}$ strength TSB, Section 4.4.2). Given the various reports supporting the HSAF as the forerunner of future biological pesticides, and the identification of biosynthetic gene cluster in the *Lysobacter* strains with their novel mechanism of action, that is, the metabolite targets the sphingolipid type required for the radial growth of fungal mycelia (Fig. 5.24) and structure (Fig. 5.33) lays a foundation for a follow-up study to explain its role in the suppression of ARR and RRC.

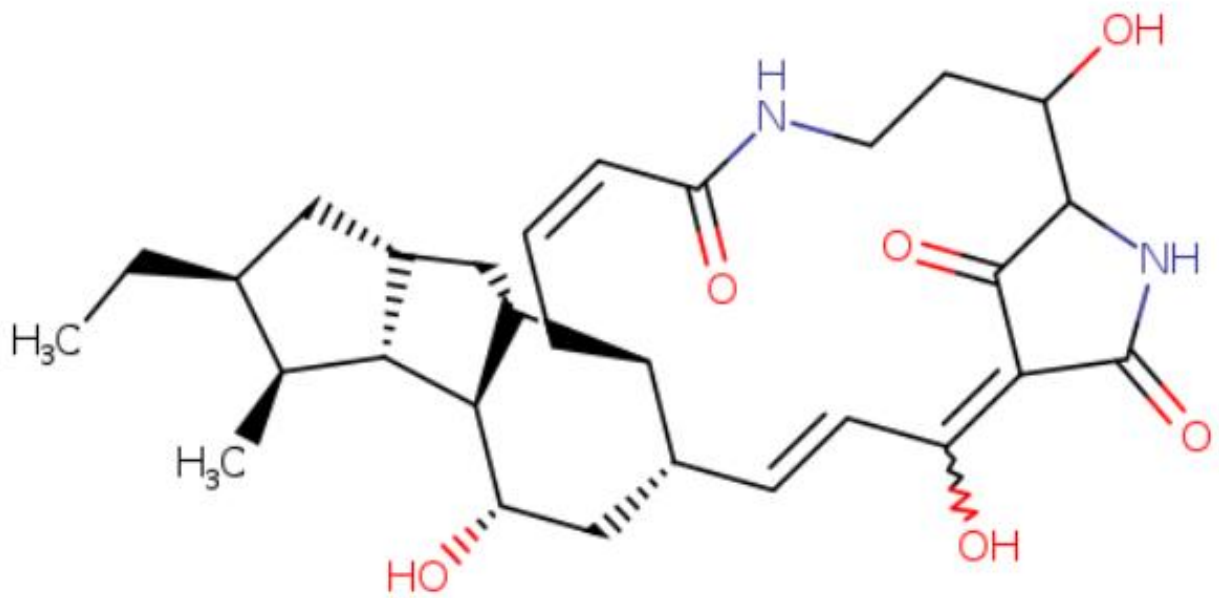


Figure 5.33. Chemical structure of HSAF (Yu et al., 2007)

Although biocontrol bacteria are reported to utilize several mechanisms of action, such as antibiosis, competition for nutrients and colonization, parasitism, interfering with the mechanisms of pathogenesis and induction of local or systemic resistance to suppress disease symptoms in plants (Bardin et al., 2015; Mishra et al., 2018; Niu et al., 2020), the conditions that affect these mechanisms and make them switch from one to another are unclear (Bardin et al., 2015). However, *Lysobacter* species are reported to exert multiple mechanisms of action, and this attribute is important as it diminishes the occurrence of resistant populations of plant-pathogenic microorganisms (Puopolo et al., 2018). Accordingly, *L. capsici* K-Hf-H2 was not only identified as harbouring an extensive array of genes and gene clusters with potential lytic capacity against plant pathogens but also able to inhibit the growth of *A. euteiches*, *F. avenaceum* and *F. oxysporum* *in vitro* assays and suppress RRC in field pea and lentil in growth chamber conditions. My genome analyses findings were supported by the laboratory-based functional experiments, which identified *L. capsici* K-Hf-H2 as capable of chelating iron through siderophore production (Fig. 5.25), proteolytic and cellulolytic activity via the release of lytic enzymes (Figs. 5.26 and 5.30). This broad-spectrum activity of *L. capsici* K-Hf-H2 is consistent with the result observed for *L. enzymogenes* CX03 and *L. enzymogenes* C3 (Giesler and Yuen, 1998; Yuen et al., 2003;

Kobayashi et al., 2005; Xu et al., 2022). *Lysobacter enzymogenes* CX03 was reported to show broad-spectrum antagonistic activity toward plant-pathogenic bacteria and controlled black rot on cabbage (Xu et al., 2022). In contrast, *L. enzymogenes* C3 was able to suppress fungal and oomycete plant diseases that collectively cause root rot complex in field pea and lentil such as *R. solani* (Giesler and Yuen, 1998), *F. graminearum* (Yuen et al., 2003) and *P. ultimum* (Kobayashi et al., 2005). Thus, the main antifungal factor in *L. enzymogenes* C3 was reported to be HSAF (Yu et al., 2007; Xu et al., 2022).

AntiSMASH analysis also found a biosynthetic gene cluster encoding for Rhizomide A / rhizomide B / rhizomide C with 100 % matching identity in both *L. capsici* K-Hf-H2 and *L. gummosus* K-Be-H3. Rhizomide A / rhizomide B / rhizomide C is a secondary metabolite with antibacterial, immunosuppressive and antitumor activities. For example, Wang et al. (2018) reported Rhizomide A's antitumor activity against several human tumour cells lines, biocontrol activity against cucumber downy mildew and antagonistic activity against *Staphylococcus aureus* and *Bacillus subtilis* in *in vitro* assays. These suggest that the members of the *Lysobacter* genus have a wide range of applications, including human health.

Xanthoferrin is a siderophore-type secondary metabolite that AntiSMASH detected in *L. capsici* K-Hf-H2 and *L. gummosus* K-Be-H3, which play a vital role in iron competition with other microorganisms. For example, in *in vitro* functional experiments, *L. capsici* K-Hf-H2 exhibited iron-chelating potential on the CAS plate (Fig. 5.25). Furthermore, this iron-chelating capacity was related to the biocontrol attributes of *Lysobacter* species (de Bruijn et al., 2015). This finding was consistent with Ko et al. (2011), Puopolo et al. (2016) and Chen et al. (2020), who stated *L. antibioticus* HS124, *L. capsici* AZ78, and *L. enzymogenes* LE16 were able to chelate iron via a different type of siderophores, respectively.

Xanthomonadin is a membrane-bound yellow pigment common in *Xanthomonas* and *Lysobacter* species (He et al., 2020; Xu et al., 2022) and first reported from phytopathogenic bacteria *Xanthomonas* spp. (Rajagopal et al., 1997). Although its significance during pathogenesis is unknown, reports indicate it plays a role in protection against photodamage (Poplawsky et al., 2000). Therefore, this suggests the need for further analysis of the Xanthomonadin encoding gene to verify its role in the biological control of ARR and RRC.

Sodorifen is another interesting secondary metabolite detected in both *L. capsici* K-Hf-H2 and *L. gummosus* K-Be-H3 (Tables 5.9 and 5.10). It was homologous to the sodorifen found in *Serratia plymuthica* species (Domik et al., 2016), a root-associated bacteria that suppress fungal plant disease via direct interaction with pathogens and inducing resistance in the host plant (Müller et al., 2009). Reports indicate that Sodorifen is a novel and unique volatile secondary metabolite with a chemical formula of C₁₆H₂₆ (Domik et al., 2016).

Further genome analysis was conducted using the CARD database to detect antibiotic-resistance genes in the biocontrol bacteria genome. The CARD is a manually curated resource containing high-quality reference data on the molecular basis of AMR, emphasizing the genes, proteins, and mutations involved in clinically relevant AMR (Jia et al., 2017). The analysis indicated antibiotics resistance genes, such as *adeF* (two copies), *qacG*, *qacJ* and *vanY* gene in the *vanM* cluster, were identified in *L. capsici* K-Hf-H2 and *L. gummosus* K-Be-H3 genome (Table 5.6). The *adeF*, *adeG* and *adeH* genes were initially reported to encode a resistance-nodulation-cell division pump responsible for the enhanced resistance of *Acinetobacter baumannii* to multiple antibiotics (Coyne et al., 2010). However, the *adeG* and *adeH* genes cotranscribed with *adeF* were not detected in the *Lysobacter* strains. Therefore, the antibiotic resistance gene *adeF* alone does not confer phenotypic resistance and is similarly described in Zhao et al. (2019). Thus, the *Lysobacter* strains are not a safety concern for *adeF* alone. The *qac* genes, *qacG* and *qacJ*, are named after quaternary ammonium compounds (one of their primary substrates); their practical significance is for resistance to antiseptics (Jaglic et al., 2012). The *vanY* is one of the seven genes (*vanR*, *vanS*, *vanH*, *vanA*, *vanX*, *vanY*, and *vanZ*) in the *vanA* gene cluster required for the phenotypic expression of vancomycin resistant (Ligozzi et al., 1998). Since only one of the seven genes was detected in the *Lysobacter* strains, there is a high probability that the antibiotic resistance gene *vanY* alone does not confer phenotypic resistance. Moreover, my analysis indicated that the *qacG* and *qacJ* genes and the *vanY* gene in the *vanM* cluster have less than a 50% identity score, suggesting that they likely are not specific antibiotic-resistance genes (Table 5.6). Therefore, these *Lysobacter* strains are not a safety concern. However, further investigation is required to verify this claim.

Pseudomonas simiae K-Hf-L9 and *P. agglomerans* PSV1-7 were the other biocontrol bacteria that significantly suppressed ARR in field pea and lentil, although their efficacy was less when tested against RRC. Furthermore, these biocontrol bacteria significantly inhibited the

mycelial growth of the root rot complex pathogen *F. avenaceum* and *F. oxysporum* during *in vitro* assays (Figs. 4.2 and 4.3), suggesting that the strains also have a broad spectrum of activity. The *P. simiae* K-Hf-L9 and *P. agglomerans* PSV1-7 complete genome analyses indicated that the strains contain genes encoding for various traits potentially involved in biological control of ARR and RRC (Tables C.2 and C.3). For example, genes encoding for siderophore production (Pyoverdine in K-Hf-L9; Enterobactin in PSV1-7), chitin utilization and several other protein degrading enzymes were detected (Tables C.2 and C.3). Moreover, the laboratory-based functional experiment revealed that the two bacteria were also positive for siderophores production and protein hydrolysis (Figs 5.25, 5.28 and 5.29). Furthermore, the AntiSMASH pipeline found 12 and 7 BGCs in *P. simiae* K-Hf-L9 and *P. agglomerans* PSV1-7, respectively (Tables 5.11 and 5.12). The genome analysis finding supported by the laboratory-based investigation indicates that these two biocontrol bacteria potentially utilize multiple mechanisms to suppress ARR and RRC in field pea and lentil. These findings were consistent with Berendsen et al. (2015) and Stringlis et al. (2018), who reported 11 BGCs in *P. simiae* strain WCS417, enabling the strain to outcompete neighbouring microbes. It was reported that although *P. simiae* strains contain genes encoding for putative antibacterial activity (bactericidal proteins and bacteriocins) (Pieterse et al., 2021), the antagonistic and biocontrol potential is believed to be mainly through siderophore-mediated competition for iron (Berendsen et al., 2015). Similarly, in my study, in the siderophores production assessment, compared to *P. agglomerans* PSV1-7 and *L. capsici* K-Hf-H2, the production of the siderophore by *P. simiae* K-Hf-L9 was observed within 24 h of incubation in comparison to PSV1-7 and K-Hf-H2 that needed 72 h, suggesting that *P. simiae* K-Hf-L9 requires less lag-phase to start siderophores production or the siderophores type in K-Hf-L9 strain has a higher affinity.

The primary mechanism by which strains of *P. agglomerans* suppress plant disease has been reported to be via competitive exclusion (occupation of sites otherwise colonized by the pathogen) and the production of antibiotics which target pathogens (Wright et al., 2001; Vanneste et al., 2001; Pusey et al., 2011; Sammer et al., 2012; Kamber et al., 2012; Smith et al., 2013). As stated above, the *P. agglomerans* PSV1-7 genome harbours genes that play a role in the competitive occupation of biological niches. For example, genes encoding for chitin and protein degradation (Table C.3) and BGCs encoding for siderophore, Desferrioxamine E (Yamanaka et al., 2005) were detected in *P. agglomerans* PSV1-7 (Table 5.11), suggesting the use of lytic enzymes and siderophores

mediated biocontrol activity in suppressing ARR and RRC. Similarly, Haidar et al. (2021) and Thissera et al. (2020) showed the *P. agglomerans* S1 and *P. agglomerans* Pa biocontrol mechanism to be a combination of antifungal activity, induction of resistance and siderophores production.

The CARD database detected five antibiotic-resistance genes in *P. simiae* K-Hf-L9. In addition to the *vanG* and *adeF* genes discussed above for *Lysobacter* species, which have less than a 50% identity score and likely are not specific antibiotic-resistance genes, the two other antibiotic resistance genes detected in *P. simiae* K-Hf-L9 were *Pseudomonas aeruginosa* *soxR* and *Acinetobacter baumannii* *AbaQ* (Table 5.7). The SoxR is a transcriptional regulator that controls oxidative stress response in *Pseudomonas aeruginosa* and *Escherichia coli* along with its partner SoxS (Palma et al., 2005). Thus, the *SoxR* is not a safety concern, and SoxS was not detected in *P. simiae* K-Hf-L9. In contrast, *AbaQ* is reported to be mainly involved in removing quinolone-type drugs in *A. baumannii* (Pérez-Varela et al., 2018). Furthermore, Pérez-Varela et al. (2018) conducted antimicrobial susceptibilities in two mutants of *A. baumannii* lacking the *AbaQ* gene. Their results indicated that the *AbaQ* mutants were up to 32-fold susceptible to quinolone-type antibiotics such as ciprofloxacin, levofloxacin, and nalidixic acid. However, the mutants and the wild types were equally susceptible to various drug classes (Pérez-Varela et al., 2018). Therefore, although the *AbaQ* gene is susceptible to multiple antibiotics, its resistance to quinolone-type drugs may pose a safety concern on *P. simiae* K-Hf-L9 utilization. Therefore, further experiments, for example, whether the *AbaQ* gene in *P. simiae* K-Hf-L9 confers phenotypic resistance to quinolone-type drugs, need to be conducted. Another study could be to determine whether deletion of the *AbaQ* gene alters antimicrobial susceptibilities of *P. simiae* K-Hf-L9.

In contrast, ten antibiotic-resistance genes were found in the *P. agglomerans* PSV1-7 (Table 5.8). Not only two-fold antibiotic resistance genes were detected in *P. agglomerans* PSV1-7 compared to strains of *Lysobacter* and *P. simiae*, but also the majority had a higher identity match to a reference gene in the CARD database, providing stronger prediction. For example, two copies of *Escherichia coli* EF-Tu mutants with a high matching identity conferring resistance to Pulvomycin (an inhibitor of protein biosynthesis) were found in *P. agglomerans* PSV1-7 (Table 5.8). Therefore, further experiments need to be conducted to determine whether the antibiotic resistance genes in *P. agglomerans* PSV1-7 confer phenotypic resistance. No phenotypic resistance expression means less safety concern, and such a finding will aid the registration of the strain as a commercial biocontrol agent.

5.7 Conclusions

This study identified that the ARR and RRC biocontrol bacteria studied here harbour genes and BGCs encoding for antibiotics, lytic enzymes, and other bioactive molecules such as various classes of siderophores. These findings are consistent with the observations of *in vitro* and *in vivo* broad-spectrum activity of the biocontrol bacteria. Moreover, the laboratory-based siderophore production, proteolytic and cellulolytic activity experiments also supported the genome analysis findings.

Among the biocontrol bacteria tested, the *Lysobacter* strains harboured genes encoding various traits important for suppressing ARR and RRC. Moreover, although few antibiotic-resistance genes were found, none appeared to be a safety concern. Thus, their approval for large-scale field-based experiments or to make them commercially available for use against ARR and RRC is expected to be less complicated.

Lysobacter capsici K-Hf-H2 was the most effective biocontrol agent that significantly suppressed RRC in field pea and lentil caused by *A. euteiches*, *F. avenaceum* and *F. oxysporum*. Although the merits of specialists versus generalists in the concept of biocontrol efficacy are debatable, given the occurrence of *A. euteiches* as a complex together with other root rot-causing pathogens, the identification of RRC biocontrol bacterium presents a great opportunity. However, a future study should also assess the impact of the biocontrol bacteria on *Rhizobium* strains that form a symbiotic association with field pea and lentil.

6. SYNTHESIS AND CONCLUSIONS

Root rot complex of field pea and lentil is caused by several fungal and fungus-like organisms, including *A. euteiches*, *F. avenaceum* and *F. oxysporum*. In recent years this root rot complex has been abundant across western Canada at a destructive level (Bogdan, 2019). On the other hand, management strategies against RRC and its component pathogens are still inadequate. Several researchers (Heungens and Parke, 2001; Hossain et al., 2014; Lagerlöf et al., 2020) have examined the potential for biological control of ARR in multi-step processes that include isolation of inhibitory organisms, lab assays, growth chamber assays, and field trials. Recently I identified *L. capsici* K-Hf-H2, *P. simiae* K-Hf-L9 and *P. agglomerans* PSV1-7 as potential biocontrol agents against ARR in field pea under controlled growth chamber conditions (Godebo, 2019). However, the interaction of *A. euteiches* with other root rot pathogens (i.e., as found in the RRC) was not investigated and thus is the focus of my Ph.D. research.

The overall goal of my Ph.D. research was to examine factors affecting the potential use of biocontrol agents for ARR, assess these potential biological agents for control of RRC in field pea and lentil, and elucidate potential mechanisms by which biocontrol of RRC was achieved. A comprehensive meta-analysis review examined what we know about using biological control agents against ARR and identified key factors affecting success of such agents (Chapter 3). The meta-analysis findings in Chapter 3 suggested the need to investigate the ARR biocontrol bacteria *L. capsici* K-Hf-H2, *P. simiae* K-Hf-L9 and *P. agglomerans* PSV1-7 for their potential to control RRC in field pea and lentil caused by interactions between *A. euteiches*, *F. avenaceum* and *F. oxysporum* (Chapter 4). The biocontrol activity of select bacterial strains was assessed using sterile vermiculite and non-sterile agricultural soil as a plant-growing media under growth chamber conditions. In addition, 10 bacteria that significantly suppressed ARR in field pea (Godebo, 2019) were evaluated for biocontrol efficacy against ARR in lentil in growth chamber conditions. This led to *L. gummosus* K-Be-H3 being identified as the most effective bacterial strain (Chapter 4). Based on these findings, the whole genomes of *L. capsici* K-Hf-H2, *P. simiae* K-Hf-L9, *P. agglomerans* PSV1-7, and *L. gummosus* K-Be-H3 were sequenced, annotated, and comparatively analyzed using bioinformatics tools (Chapter 5). These strains were also assessed for siderophore production, proteolytic and cellulolytic activity and desiccation tolerance under laboratory conditions, as discussed in Chapter 5.

6.1 Summary of findings

Field pea and lentil are important economic crops for western Canadian farmers, mainly for export (Chatterton et al., 2019). However, in recent years, the production of these crops has been under severe threat due to ARR and RRC pathogens that severely damage roots, leading infected plants to wilt and die prematurely (Banniza et al., 2013; Chatterton et al., 2015; Gossen et al., 2016). My study demonstrated the potential of bacterial biocontrol agents as an alternative approach to mitigate the loss of productivity due to ARR and RRC in field pea and lentil.

In Chapter 3, the effectiveness of biocontrol agents in relation to type of biocontrol agent, richness, application method, type of study and reporting system-oriented moderator variables were assessed using a meta-analysis review. My results not only revealed the potential promise for biological control of ARR but also provided insight into the current state of the science of biological control of ARR. In addition, although several researchers have examined the biological control of ARR in multi-step processes, my study was the first quantitative review. My results showed significant positive outcomes for ARR suppression even when the summary effect value was adjusted for missing studies assumed to represent publication bias. Comparatively, more significant suppression was achieved in growth chamber trials than in field-based experiments suggesting the need for more field trials to demonstrate (or explain) the efficacy level observed under growth chamber conditions. The occurrence of more than one pathogen as part of a disease complex under field conditions is one of the long lists of factors affecting the efficacy of biocontrol agents (Parke et al., 1991; Xue, 2003; Hughes and Grau, 2013). Therefore, identifying ARR biocontrol bacteria with biocontrol activity towards pathogens that collectively cause RRC in field pea and lentil is very important.

In Chapter 4, I investigated the potential for biological control of RRC in field pea and lentil caused by *A. euteiches*, *F. avenaceum* and *F. oxysporum* using *L. capsici* K-Hf-H2, *P. simiae* K-Hf-L9 and *P. agglomerans* PSV1-7 under growth chamber conditions. My results revealed that the strains had a broad spectrum of inhibitory activity against mycelial growth of pathogens during *in vitro* assays, and *L. capsici* K-Hf-H2 was the most effective in controlling RRC in field pea and lentil in controlled growth chamber conditions. Given the occurrence of *A. euteiches* as a complex with other root rot-causing pathogens, identifying biocontrol agents effective against RRC is needed in order to effectively use biocontrol agents as commercial products. My results agree with several other studies that indicate *Lysobacter* strains exert a broad spectrum of biocontrol activity

against various phytopathogens (de Bruijn et al., 2015; Puopolo et al., 2016). My study evaluating 10 strains for biological control of ARR in lentil identified *L. gummosus* K-Be-H3 as the most effective bacterium.

The results in Chapter 4 demonstrated the need to understand the mechanisms by which *L. capsici* K-Hf-H2, *P. simiae* K-Hf-L9, *P. agglomerans* PSV1-7 and *L. gummosus* K-Be-H3 acted as biocontrol agents. Therefore, in Chapter 5, I conducted a complete genome analysis using bioinformatics tools, followed by general functional experiments under laboratory conditions. The complete genomes of *L. capsici* K-Hf-H2, *P. simiae* K-Hf-L9, *P. agglomerans* PSV1-7 and *L. gummosus* K-Be-H3 were sequenced, annotated, and comparatively analyzed. In addition, the biocontrol bacteria were investigated for siderophores production, proteolytic and cellulolytic activity, and desiccation tolerance. Although my results are limited in providing conclusive evidence regarding the disease suppression and the mechanism(s) of action (i.e., cause and effect relationship), my results revealed that the biocontrol bacteria harbour an array of genes and gene clusters encoding for biosynthetic traits that potentially contribute to antagonistic interactions with phytopathogens. Based on the literature, bacterial biocontrol agents with a broad spectrum of activity exhibit a range of mechanisms such as antagonism (e.g., production of antibiotics, volatile compounds, or enzymes), competition (e.g., for space and nutrient), parasitism, or the induction of local or systemic resistance (Bardin et al., 2015; Mishra et al., 2018; Niu et al., 2020).

In Chapter 5, I also found evidence that the biocontrol bacteria can chelate iron through siderophore production and hydrolyze protein and cellulose via proteolytic and cellulolytic activity, respectively. These findings supported the genome analysis, which identified genes encoding for different siderophores types such as Vibrioferrin and Xanthoferrin in *L. capsici* K-Hf-H2, Pyoverdine in *P. simiae* K-Hf-L9 and Enterobactin in *P. agglomerans* PSV1-7 genome. The proteolytic assay finding is another example that supported the genome analysis, which, for example, detected an extracellular zinc protease in *L. capsici* K-Hf-H2, Metalloproteases in *P. simiae* K-Hf-L9, and *P. agglomerans* PSV1-7 genomes that potentially involved in protein degradation. In addition, extracellular zinc protease and lytic enzymes capable of degrading cell wall components of fungi and oomycetes have been reported as potential biocontrol mechanisms involved in suppressing root rot pathogens (Puopolo et al., 2016).

Chapters 3, 4 and 5 findings suggest the potential for biological control of ARR and RRC in field pea and lentil using soil bacteria with traits antagonistic to phytopathogens. Interestingly, during my meta-analysis review, I found that using consortia of bacteria had greater disease suppression efficacy than a single organism inoculation (Chapter 3), suggesting the potential use of *L. capsici* K-Hf-H2, *P. simiae* K-Hf-L9, *P. agglomerans* PSV1-7 and *L. gummosus* K-Be-H3 for mixed application to prevent ARR and RRC via synergistic or additive effects. *Lysobacter* species, strains of *P. simiae* and *P. agglomerans* were reported to be effective biocontrol agents against several plant pathogens, including pathogens, causing RRC in field pea and lentil (Pandolfi et al., 2010; Godebo, 2019; Liu et al., 2019). For example, *L. capsici* NF87-2 showed a broad spectrum of biocontrol activity against *F. oxysporum*, *R. solani*, *Alternaria brassicae*, *Sclerotinia sclerotiorum*, *Botrytis cinerea* and *Colletotrichum gloeosporioides* (Liu et al., 2019). Similarly, *P. simiae* WCS417 suppressed fusarium wilt via siderophore-mediated competition (Duijff et al., 1993; Van Peer et al., 1990), and *P. agglomerans* inhibited *F. graminearum*, the causative agent of fusarium head blight in oats, maize, wheat, and barley (Pandolfi et al., 2010). I also found that the cell-free supernatant from *L. capsici* K-Hf-H2 inhibits the growth of *A. euteiches* mycelia (Chapter 4). The production of inhibitory metabolites depended on the bacterium growth phase, as only the supernatant obtained from the late stationary to death/decline phase demonstrated inhibitory potential (Chapter 4). Furthermore, my results revealed that the inhibition activity of the supernatant was stable for four months when stored at 4°C. Microorganisms demonstrate physiological responses due to changes in the surrounding environment during their growth cycle (Robador et al., 2018). One such response is the production of secondary metabolite when nutrients are depleted, and metabolic wastes are accumulated in the fermenting media (Nigam and Singh, 2014). My result offered additional insight for future investigations on the possibility of utilizing active secondary metabolites to control ARR and RRC rather than a live biocontrol agent itself.

In Chapter 5, I further analyzed the biocontrol bacteria genome for BGCs encoding for secondary metabolite. The result detected several BGCs encoding various classes of secondary metabolites potentially involved in the suppression of ARR and RRC in field pea and lentil. For example, the HSAF and Xanthoferrin in *L. capsici* K-Hf-H-2 and *L. gummosus* K-Be-H3, and Desferrioxamine E in *P. agglomerans* PSV1-7 are notable examples of the BGCs that potentially participate in the suppression of ARR and RRC in field pea and lentil. Moreover, in Chapter 5, I performed additional genome analyses to detect antibiotic-resistance genes. Although the analyses

detected antibiotics resistance genes in the biocontrol bacteria genome, based on literature (Ligozzi et al., 1998; Jaglic et al., 2012; Zhao et al., 2019), the genes detected in *L. capsici* K-Hf-H-2 and *L. K-Be-H3* are unlikely to confer phenotypic resistance. Thus, these strains are less likely to be a safety concern due to clinically relevant antibiotic-resistance genes and therefore are suited for potential commercialization.

7. FUTURE RESEARCH

My Ph.D. dissertation is an important contribution to understanding the potential control of ARR and RRC in field pea and lentil using soil bacteria as bioinoculants. My growth chamber studies demonstrated the importance and need to conduct field trials to assess the efficacy of these biocontrol bacteria under field conditions. Such field trials will provide opportunities to assess how biotic variables (such as the presence or absence of ARR and RRC pathogens) and abiotic variables (such as soil type, pH, moisture, nutrient level, salinity and temperature) affect the activity and efficacy of biocontrol agents.

Legumes, including field pea and lentil establish a symbiotic association with *Rhizobium* strains. Therefore, future studies should investigate the impact of the biocontrol bacteria on *Rhizobium* strains that form symbiotic associations with field pea and lentil. These trials should encompass both *in situ* and *in-plant* experiments. The first will provide evidence of direct impact (e.g., impact on bacterium survival), and the second will provide information on the effect of the biocontrol agents on nodule formation.

My findings also suggested mixed application of biocontrol agents for greater efficacy. Therefore, future studies should consider the consortia of biocontrol bacteria against ARR and RRC in field pea and lentil; however, the strains should be evaluated for compatibility. The biocontrol bacteria were evaluated for efficacy using a liquid application (drenching) throughout my investigation. Future studies should consider the impact of other application methods like seed coatings. I found evidence that the cell-free supernatant of *L. capsici* K-Hf-H2 possesses inhibitory potential. Thus, future studies should assess the potential application of cell-free culture extracts to suppress ARR and RRC.

My research presented in this dissertation provided essential details to shed light on the still not fully comprehended mechanistic nature of disease suppression. Even though my study identified genes and gene cluster encoding for biosynthetic traits thought to be expressed in the suppression of ARR and RRC, a future study that explains specific cause-and-effect relationships should be considered. For example, one such study would be generating mutant strains lacking specific genes encoding for specific traits (e.g., HSAF, extracellular zinc protease, or chitinase) in the *Lysobacter* strains and siderophores in *P. simiae* K-Hf-L9 and *P. agglomerans* PSV1-7 and

evaluating the difference in biocontrol potential between the wild and mutant strain. Such functional genomic experiments would provide evidence directly linking genes to disease suppression mechanisms.

Biocontrol agents are constantly tested for potential health risks, and one stream of such evaluation is resistance to antibiotics. My genome analysis detected genes that potentially confer phenotypic resistance to various classes of antibiotics. Therefore, future studies should investigate the antibiotic resistance profile of the biocontrol bacteria under laboratory conditions. Such a study can be expanded to the extent of exciting resistance encoding genes and evaluating the mutant strains. Also, the strains could be screened for known virulence genes.

Lastly, future studies, mainly the field-based trials investigating the biological control of ARR and RRC, should involve industrial partners experienced in developing a large quantity of biocontrol inoculum. Such collaboration offers an opportunity for knowledge transfer and facilitates realizing the ultimate goal: effective control of ARR and RRC in field pea and lentil.

8. REFERENCE

- Abdel-Kader, M. M., S. El-Mougy, N., Aly, M. De., & L., L. (2012). Different approaches of bio-control agents for controlling root rot incidence of some vegetables under greenhouse conditions. *International Journal of Agriculture and Forestry*, 2(1), 115–127. <https://doi.org/10.5923/j.ijaf.20120201.18>
- Abril, J. F., & Castellano, S. (2019). Genome annotation. In *Encyclopedia of Bioinformatics and Computational Biology*. Ranganathan, S., Gribskov, M., & Schönbach, C. (Eds.), Elsevier: Amsterdam, The Netherlands (pp. 195–209). <https://doi.org/10.1016/B978-0-12-809633-8.20226-4>
- Adewale, B. A. (2020). Will long-read sequencing technologies replace short-read sequencing technologies in the next 10 years? *African Journal of Laboratory Medicine*, 9(1), 5. <https://doi.org/10.4102/ajlm.v9i1.1340>
- Alcock, B. P., Raphenya, A. R., Lau, T. T. Y., Tsang, K. K., Bouchard, M., Edalatmand, A., Huynh, W., Nguyen, A. L. V., Cheng, A. A., Liu, S., Min, S. Y., Miroshnichenko, A., Tran, H. K., Werfalli, R. E., Nasir, J. A., Oloni, M., Speicher, D. J., Florescu, A., Singh, B., ... McArthur, A. G. (2019). CARD 2020: Antibiotic resistome surveillance with the comprehensive antibiotic resistance database. *Nucleic Acids Research*, gkz935. <https://doi.org/10.1093/nar/gkz935>
- Alexander, D. B., & Zuberer, D. A. (1991). Use of chrome azurol S reagents to evaluate siderophore production by rhizosphere bacteria. *Biology and Fertility of Soils*, 12(1), 39–45. <https://doi.org/10.1007/BF00369386>
- Alikhan, N. F., Petty, N. K., Ben Zakour, N. L., & Beatson, S. A. (2011). BLAST ring image generator (BRIG): Simple prokaryote genome comparisons. *BMC Genomics*, 12(1), 402. <https://doi.org/10.1186/1471-2164-12-402>
- Allen, M. (2017). *The sage encyclopedia of communication research methods*. SAGE Publications, Inc. <https://doi.org/10.4135/9781483381411>
- Altermann, E., Tegetmeyer, H. E., & Chanyi, R. M. (2022). The evolution of bacterial genome assemblies—Where do we need to go next? *Microbiome Research Reports*, 1(2), 15. <https://doi.org/10.20517/mrr.2022.02>
- An, F., Li, H., Diao, Z., & Lv, J. (2019). The soil bacterial community in cropland is vulnerable to Cd contamination in winter rather than in summer. *Environmental Science and Pollution Research*, 26(1), 114–125. <https://doi.org/10.1007/s11356-018-3531-8>
- Andrews, J. H., & Harris, R. F. (2000). The ecology and biogeography of microorganisms on plant surfaces. *Annual Review of Phytopathology*, 38(1), 145–180. <https://doi.org/10.1146/annurev.phyto.38.1.145>

- Aziz, R. K., Bartels, D., Best, A. A., DeJongh, M., Disz, T., Edwards, R. A., Formsma, K., Gerdes, S., Glass, E. M., Kubal, M., Meyer, F., Olsen, G. J., Olson, R., Osterman, A. L., Overbeek, R. A., McNeil, L. K., Paarmann, D., Paczian, T., Parrello, B., ... Zagnitko, O. (2008). The rast server: Rapid annotations using subsystems technology. *BMC Genomics*, *9*(1), 75. <https://doi.org/10.1186/1471-2164-9-75>
- Bakker, P. A. H. M., Berendsen, R. L., Doornbos, R. F., Wintermans, P. C. A., & Pieterse, C. M. J. (2013). The rhizosphere revisited: Root microbiomics. *Frontiers in Plant Science*, *4*. <https://doi.org/10.3389/fpls.2013.00165>
- Balouiri, M., Sadiki, M., & Ibsouda, S. K. (2016). Methods for in vitro evaluating antimicrobial activity: A review. *Journal of Pharmaceutical Analysis*, *6*(2), 71–79. <https://doi.org/10.1016/j.jpha.2015.11.005>
- Banniza, S., Bhadauria, V., Peluola, C. O., Armstrong-Cho, C., & Morrall, R. A. A. (2013). First report of *Aphanomyces euteiches* in Saskatchewan. *Canadian Plant Disease Survey*, *93*, 163-164.
- Bardin, M., Ajouz, S., Comby, M., Lopez-Ferber, M., Graillet, B., Siegwart, M., & Nicot, P. C. (2015). Is the efficacy of biological control against plant diseases likely to be more durable than that of chemical pesticides? *Frontiers in Plant Science*, *6*. <https://doi.org/10.3389/fpls.2015.00566>
- Basler, F. (1981). Weeds and their control. *Lentils. Common Wealth Agricultural Bureaux (Farnham Royal)*, *143*, 154.
- Bauer, A. W., Kirby, W. M. M., Sherris, J. C., & Turck, M. (1966). Antibiotic susceptibility testing by a single high content disk method. *American Journal of Clinical Pathology*, *45*, 492-496.
- Ben Khedher, M., Ghedira, K., Rolain, J.-M., Ruimy, R., & Croce, O. (2022). Application and challenge of 3rd generation sequencing for clinical bacterial studies. *International Journal of Molecular Sciences*, *23*(3), 1395. <https://doi.org/10.3390/ijms23031395>
- Berendsen, R. L., van Verk, M. C., Stringlis, I. A., Zamioudis, C., Tommassen, J., Pieterse, C. M. J., & Bakker, P. A. H. M. (2015). Unearthing the genomes of plant-beneficial *Pseudomonas* model strains WCS358, WCS374 and WCS417. *BMC Genomics*, *16*(1), 539. <https://doi.org/10.1186/s12864-015-1632-z>
- Bergman, K. A., Arends, J. P., & Schölvinc, E. H. (2007). *Pantoea agglomerans* septicemia in three newborn infants. *Pediatric Infectious Disease Journal*, *26*(5), 453–454. <https://doi.org/10.1097/01.inf.0000261200.83869.92>
- Blom, J., Kreis, J., Spänig, S., Juhre, T., Bertelli, C., Ernst, C., & Goesmann, A. (2016). EDGAR 2.0: An enhanced software platform for comparative gene content analyses. *Nucleic Acids Research*, *44*(W1), W22–W28. <https://doi.org/10.1093/nar/gkw255>

- Bodah, E. T. (2017). Root rot diseases in plants: a review of common causal agents and management strategies. *Agricultural Research & Technology Open Access Journal*, 5(3), 555661. <https://doi.org/10.19080/ARTOAJ.2017.04.555661>
- Bogdan, J. 2019. Fusarium Root Rot in Pulse Crops. https://saskpulse.com/files/technical_documents/191115_Fusarium_RR_in_Pulses-compressed.pdf Pulse Knowledge, 1-7. Retrieved July 11, 2022.
- Bonaterra, A., Camps, J., & Montesinos, E. (2005). Osmotically induced trehalose and glycine betaine accumulation improves tolerance to desiccation, survival and efficacy of the postharvest biocontrol agent *Pantoea agglomerans* EPS125. *FEMS Microbiology Letters*, 250(1), 1–8. <https://doi.org/10.1016/j.femsle.2005.06.028>
- Bonaterra, A., Mari, M., Casalini, L., & Montesinos, E. (2003). Biological control of *Monilinia laxa* and *Rhizopus stolonifer* in postharvest of stone fruit by *Pantoea agglomerans* EPS125 and putative mechanisms of antagonism. *International Journal of Food Microbiology*, 84(1), 93–104. [https://doi.org/10.1016/S0168-1605\(02\)00403-8](https://doi.org/10.1016/S0168-1605(02)00403-8)
- Borenstein, M., Hedges, L., Higgins, J., & Rothstein, H. (2013). Comprehensive meta-analysis version 3 [software] Biostat. *Englewood, NJ*. <http://www.meta-analysis.com>
- Brady, C. L., Venter, S. N., Cleenwerck, I., Vandemeulebroecke, K., De Vos, P., & Coutinho, T. A. (2010). Transfer of *Pantoea citrea*, *Pantoea punctata* and *Pantoea terrea* to the genus *Tatumella* emend. As *Tatumella citrea* comb. Nov., *Tatumella punctata* comb. Nov. and *Tatumella terrea* comb. Nov. and description of *Tatumella morbirosei* sp. Nov. *International Journal of Systematic and Evolutionary Microbiology*, 60(3), 484–494. <https://doi.org/10.1099/ijs.0.012070-0>
- Branton, D., Deamer, D. W., Marziali, A., Bayley, H., Benner, S. A., Butler, T., Di Ventra, M., Garaj, S., Hibbs, A., Huang, X., Jovanovich, S. B., Krstic, P. S., Lindsay, S., Ling, X. S., Mastrangelo, C. H., Meller, A., Oliver, J. S., Pershin, Y. V., Ramsey, J. M., ... Schloss, J. A. (2008). The potential and challenges of nanopore sequencing. *Nature Biotechnology*, 26(10), 1146–1153. <https://doi.org/10.1038/nbt.1495>
- Braun-Kiewnick, A., Jacobsen, B. J., & Sands, D. C. (2000). Biological control of *Pseudomonas syringae* pv. *Syringae*, the causal agent of basal kernel blight of barley, by antagonistic *Pantoea agglomerans*. *Phytopathology*, 90(4), 368–375. <https://doi.org/10.1094/PHYTO.2000.90.4.368>
- Brescia, F., Pertot, I., & Puopolo, G. (2020). *Lysobacter*. In *Beneficial Microbes in Agro-Ecology* (pp. 313–338). Elsevier. <https://doi.org/10.1016/B978-0-12-823414-3.00016-2>
- Brescia, F., Vlassi, A., Bejarano, A., Seidl, B., Marchetti-Deschmann, M., Schuhmacher, R., & Puopolo, G. (2021). Characterisation of the antibiotic profile of *Lysobacter capsici* AZ78, an effective biological control agent of plant pathogenic microorganisms. *Microorganisms*, 9(6), 1320. <https://doi.org/10.3390/microorganisms9061320>

- Bristow, S. M., Bolland, M. J., MacLennan, G. S., Avenell, A., Grey, A., Gamble, G. D., & Reid, I. R. (2013). Calcium supplements and cancer risk: A meta-analysis of randomised controlled trials. *British Journal of Nutrition*, *110*(8), 1384–1393. <https://doi.org/10.1017/S0007114513001050>
- Brown, B. J., & Leff, L. G. (1996). Comparison of fatty acid methyl ester analysis with the use of api 20e and nft strips for identification of aquatic bacteria. *Applied and Environmental Microbiology*, *62*(6), 2183–2185. <https://doi.org/10.1128/aem.62.6.2183-2185.1996>
- Bubici, G., Kaushal, M., Prigigallo, M. I., Gómez-Lama Cabanás, C., & Mercado-Blanco, J. (2019). Biological control agents against fusarium wilt of banana. *Frontiers in Microbiology*, *10*, 616. <https://doi.org/10.3389/fmicb.2019.00616>
- Caliz, J., Vila, X., Martí, E., Sierra, J., Nordgren, J., Lindgren, P.-E., Bañeras, L., & Montserrat, G. (2011). The microbiota of an unpolluted calcareous soil faces up chlorophenols: Evidences of resistant strains with potential for bioremediation. *Chemosphere*, *83*(2), 104–116. <https://doi.org/10.1016/j.chemosphere.2011.01.016>
- Chaiharn, M., Chunnhaleuchanon, S., & Lumyong, S. (2009). Screening siderophore producing bacteria as potential biological control agent for fungal rice pathogens in Thailand. *World Journal of Microbiology and Biotechnology*, *25*(11), 1919–1928. <https://doi.org/10.1007/s11274-009-0090-7>
- Chandrasekaran, M., Subramanian, D., Yoon, E., Kwon, T., & Chun, S.-C. (2016). Meta-analysis reveals that the genus pseudomonas can be a better choice of biological control agent against bacterial wilt disease caused by *Ralstonia solanacearum*. *The Plant Pathology Journal*, *32*(3), 216–227. <https://doi.org/10.5423/PPJ.OA.11.2015.0235>
- Chatterton, S., Shirliffe, S., Banniza, S., Larney, F., Hrapovic, L., Bowness, R., de Gooijer, H., Lupwayi, N., Beres, B., & Larsen J. (2016). Root rot in peas and lentils in western Canada. https://saskpulse.com/files/general/170418_Root_Rot_Brochure_v7_LR1.pdf, 1-12. Retrieved October 18, 2021.
- Chatterton, S., Harding, M. W., Bowness, R., McLaren, D. L., Banniza, S., & Gossen, B. D. (2019). Importance and causal agents of root rot on field pea and lentil on the Canadian prairies, 2014–2017. *Canadian Journal of Plant Pathology*, *41*(1), 98–114. <https://doi.org/10.1080/07060661.2018.1547792>
- Chatterton, S., Harding, M., Bowness, R., Strydhorst, S., Cleland, C., Storzynsky, Q., Dubitz, T., Nielsen, J., & Olson, M. (2015). Survey of root rot in Alberta field pea in 2014. *Canadian Plant Disease Survey*, *95*, 170-172.
- Chen, D. M., Yang, H. J., Huang, J. G., & Yuan, L. (2020). *Lysobacter enzymogenes* le16 autolysates have potential as biocontrol agents—*Lysobacter* sp. Autolysates as biofungicide. *Journal of Applied Microbiology*, *129*(6), 1684–1692. <https://doi.org/10.1111/jam.14752>

- Chernin, L., Ismailov, Z., Haran, S., & Chet, I. (1995). Chitinolytic *Enterobacter agglomerans* antagonistic to fungal plant pathogens. *Applied and Environmental Microbiology*, *61*(5), 1720–1726. <https://doi.org/10.1128/aem.61.5.1720-1726.1995>
- Chlebek, D., Pinski, A., Żur, J., Michalska, J., & Hupert-Kocurek, K. (2020). Genome mining and evaluation of the biocontrol potential of *Pseudomonas fluorescens* brz63, a new endophyte of oilseed rape (*Brassica napus* L.) against fungal pathogens. *International Journal of Molecular Sciences*, *21*(22), 8740. <https://doi.org/10.3390/ijms21228740>
- Cho, S. T., Chang, H.-H., Egamberdieva, D., Kamilova, F., Lugtenberg, B., & Kuo, C. H. (2015). Genome analysis of *Pseudomonas fluorescens* pcl1751: A rhizobacterium that controls root diseases and alleviates salt stress for its plant host. *PLOS ONE*, *10*(10), e0140231. <https://doi.org/10.1371/journal.pone.0140231>
- Christensen, P., & Cook, F. D. (1978). *Lysobacter*, a new genus of nonfruiting, gliding bacteria with a high base ratio. *International Journal of Systematic Bacteriology*, *28*(3), 367–393. <https://doi.org/10.1099/00207713-28-3-367>
- Chukeatirote, E., Phueaouan, T., & Piwkam, A. (2018). Screening of rhizosphere soil bacteria for biocontrol of *Lasiodiplodia theobromae*. *Agriculture and Natural Resources*, *52*(4), 325–329. <https://doi.org/10.1016/j.anres.2018.10.009>
- Cole, B. J., Feltcher, M. E., Waters, R. J., Wetmore, K. M., Mucyn, T. S., Ryan, E. M., Wang, G., Ul-Hasan, S., McDonald, M., Yoshikuni, Y., Malmstrom, R. R., Deutschbauer, A. M., Dangl, J. L., & Visel, A. (2017). Genome-wide identification of bacterial plant colonization genes. *PLOS Biology*, *15*(9), e2002860. <https://doi.org/10.1371/journal.pbio.2002860>
- Conner, R. L., Chang, K. F., Hwang, S. F., Warkentin, T. D., & McRae, K. B. (2013). Assessment of tolerance for reducing yield losses in field pea caused by aphanomyces root rot. *Canadian Journal of Plant Science*, *93*(3), 473–482. <https://doi.org/10.4141/cjps2012-183>
- Conrath, U., Beckers, G. J. M., Langenbach, C. J. G., & Jaskiewicz, M. R. (2015). Priming for enhanced defense. *Annual Review of Phytopathology*, *53*(1), 97–119. <https://doi.org/10.1146/annurev-phyto-080614-120132>
- Cornforth, D. M., Popat, R., McNally, L., Gurney, J., Scott-Phillips, T. C., Ivens, A., Diggle, S. P., & Brown, S. P. (2014). Combinatorial quorum sensing allows bacteria to resolve their social and physical environment. *Proceedings of the National Academy of Sciences*, *111*(11), 4280–4284. <https://doi.org/10.1073/pnas.1319175111>
- Coyne, S., Rosenfeld, N., Lambert, T., Courvalin, P., & Périchon, B. (2010). Overexpression of resistance-nodulation-cell division pump adefgh confers multidrug resistance in *Acinetobacter baumannii*. *Antimicrobial Agents and Chemotherapy*, *54*(10), 4389–4393. <https://doi.org/10.1128/AAC.00155-10>
- Cruz, A. T., Cazacu, A. C., & Allen, C. H. (2007). *Pantoea agglomerans*, a plant pathogen causing human disease. *Journal of Clinical Microbiology*, *45*(6), 1989–1992. <https://doi.org/10.1128/JCM.00632-07>

- de Bruijn, I., Cheng, X., de Jager, V., Expósito, R. G., Watrous, J., Patel, N., Postma, J., Dorrestein, P. C., Kobayashi, D., & Raaijmakers, J. M. (2015). Comparative genomics and metabolic profiling of the genus *Lysobacter*. *BMC Genomics*, *16*(1), 991. <https://doi.org/10.1186/s12864-015-2191-z>
- De Coster, W., D’Hert, S., Schultz, D. T., Cruets, M., & Van Broeckhoven, C. (2018). NanoPack: Visualizing and processing long-read sequencing data. *Bioinformatics*, *34*(15), 2666–2669. <https://doi.org/10.1093/bioinformatics/bty149>
- de Sá, P. H. C. G., Guimarães, L. C., das Graças, D. A., de Oliveira Veras, A. A., Barh, D., Azevedo, V., da Costa da Silva, A. L., & Ramos, R. T. J. (2018). Next-generation sequencing and data analysis. In *Omics Technologies and Bio-Engineering* (pp. 191–207). Elsevier. <https://doi.org/10.1016/B978-0-12-804659-3.00011-7>
- Dieckmann, M. A., Beyvers, S., Nkouamedjo-Fankep, R. C., Hanel, P. H. G., Jelonek, L., Blom, J., & Goesmann, A. (2021). EDGAR3.0: Comparative genomics and phylogenomics on a scalable infrastructure. *Nucleic Acids Research*, *49*(W1), W185–W192. <https://doi.org/10.1093/nar/gkab341>
- Domik, D., Magnus, N., & Piechulla, B. (2016). Analysis of a new cluster of genes involved in the synthesis of the unique volatile organic compound sodorifen of *Serratia plymuthica* 4Rx13. *FEMS Microbiology Letters*, *363*(14), fnw139. <https://doi.org/10.1093/femsle/fnw139>
- Duijff, B. J., Gianinazzi-Pearson, V., & Lemanceau, P. (1997). Involvement of the outer membrane lipopolysaccharides in the endophytic colonization of tomato roots by biocontrol *Pseudomonas fluorescens* strain WCS417r. *New Phytologist*, *135*(2), 325–334. <https://doi.org/10.1046/j.1469-8137.1997.00646.x>
- Duijff, B. J., Meijer, J. W., Bakker, P. A. H. M., & Schippers, B. (1993). Siderophore-mediated competition for iron and induced resistance in the suppression of fusarium wilt of carnation by fluorescent *Pseudomonas* spp. *Netherlands Journal of Plant Pathology*, *99*(5–6), 277–289. <https://doi.org/10.1007/BF01974309>
- Dunlap, C. A., Kim, S.-J., Kwon, S.-W., & Rooney, A. P. (2016). *Bacillus velezensis* is not a later heterotypic synonym of *Bacillus amyloliquefaciens*; *Bacillus methylotrophicus*, *Bacillus amyloliquefaciens* subsp. *Plantarum* and ‘*Bacillus oryzicola*’ are later heterotypic synonyms of *Bacillus velezensis* based on phylogenomics. *International Journal of Systematic and Evolutionary Microbiology*, *66*(3), 1212–1217. <https://doi.org/10.1099/ijsem.0.000858>
- ECODA, (2022). ECODA: eastern Canada oilseeds development alliance. <https://www.ecodainc.ca/pulses/>. Retrieved July 2, 2022.
- Edwards, D. J., & Holt, K. E. (2013). Beginner’s guide to comparative bacterial genome analysis using next-generation sequence data. *Microbial Informatics and Experimentation*, *3*(1), 2. <https://doi.org/10.1186/2042-5783-3-2>
- Eilenberg, J., Hajek, A., & Lomer, C. (2001). Suggestions for unifying the terminology in biological control. *BioControl*, *46*(4), 387–400. <https://doi.org/10.1023/A:1014193329979>

- Ejigu, G. F., & Jung, J. (2020). Review on the computational genome annotation of sequences obtained by next-generation sequencing. *Biology*, 9(9), 295. <https://doi.org/10.3390/biology9090295>
- Elad, Y., & Stewart, A. (2007). Microbial control of *Botrytis* spp. In Y. Elad, B. Williamson, P. Tudzynski, & N. Delen (Eds.), *Botrytis: Biology, Pathology and Control* (pp. 223–241). Springer Netherlands. https://doi.org/10.1007/978-1-4020-2626-3_13
- El-Mougy, N. S., & Abdel-Kader, M. M. (2019). Biocontrol measures against onion basal rot incidence under natural field conditions. *Journal of Plant Pathology*, 101(3), 579–586. <https://doi.org/10.1007/s42161-018-00237-8>
- Felsenstein, J. (1985). Phylogenies and the comparative method. *The American Naturalist*, 125(1), 1–15. <https://doi.org/10.1086/284325>
- Finotello, F., Lavezzo, E., Fontana, P., Peruzzo, D., Albiero, A., Barzon, L., Falda, M., Di Camillo, B., & Toppo, S. (2012). Comparative analysis of algorithms for whole-genome assembly of pyrosequencing data. *Briefings in Bioinformatics*, 13(3), 269–280. <https://doi.org/10.1093/bib/bbr063>
- Fischbach, M., & Voigt, C. A. (2010). Prokaryotic gene clusters: A rich toolbox for synthetic biology. *Biotechnology Journal*, 5(12), 1277–1296. <https://doi.org/10.1002/biot.201000181>
- Francés, J., Bonaterra, A., Moreno, M. C., Cabrefiga, J., Badosa, E., & Montesinos, E. (2006). Pathogen aggressiveness and postharvest biocontrol efficiency in *Pantoea agglomerans*. *Postharvest Biology and Technology*, 39(3), 299–307. <https://doi.org/10.1016/j.postharvbio.2005.11.002>
- Francis, C. A., Obratsova, A. Y., & Tebo, B. M. (2000). Dissimilatory metal reduction by the facultative anaerobe *Pantoea agglomerans* sp1. *Applied and Environmental Microbiology*, 66(2), 543–548. <https://doi.org/10.1128/AEM.66.2.543-548.2000>
- Frankowski, J., Lorito, M., Scala, F., Schmid, R., Berg, G., & Bahl, H. (2001). Purification and properties of two chitinolytic enzymes of *Serratia plymuthica* HRO-C48. *Archives of Microbiology*, 176(6), 421–426. <https://doi.org/10.1007/s002030100347>
- Gao, J., Sasse, J., Lewald, K. M., Zhalnina, K., Cornmesser, L. T., Duncombe, T. A., Yoshikuni, Y., Vogel, J. P., Firestone, M. K., & Northen, T. R. (2018). Ecosystem fabrication (Ecofab) protocols for the construction of laboratory ecosystems designed to study plant-microbe interactions. *Journal of Visualized Experiments*, 134, 57170. <https://doi.org/10.3791/57170>
- Gaulin, E., Jacquet, C., Bottin, A., & Dumas, B. (2007). Root rot disease of legumes caused by *Aphanomyces euteiches*. *Molecular Plant Pathology*, 8(5), 539–548. <https://doi.org/10.1111/j.1364-3703.2007.00413.x>
- Gaulin, E., Pel, M. J. C., Camborde, L., San-Clemente, H., Courbier, S., Dupouy, M.-A., Lengellé, J., Veyssiere, M., Le Ru, A., Grandjean, F., Cordaux, R., Moumen, B., Gilbert, C., Cano, L. M., Aury, J.-M., Guy, J., Wincker, P., Bouchez, O., Klopp, C., & Dumas, B. (2018).

- Genomics analysis of *Aphanomyces* spp. Identifies a new class of oomycete effector associated with host adaptation. *BMC Biology*, *16*(1), 43. <https://doi.org/10.1186/s12915-018-0508-5>
- Geere, I. W. (1977). *Enterobacter agglomerans*: the clinically important plant pathogen. *Canadian Medical Association Journal*, *116*(5), 517.
- Genus *Lysobacter* (2022). <https://lpsn.dsmz.de/search?word=lysobacter>. Retrieved September 15, 2022
- Genus *Pantoea* (2022). <https://www.bacterio.net/genus/pantoea>. Retrieved September 20, 2022.
- Ghirardi, S., Dessaint, F., Mazurier, S., Corberand, T., Raaijmakers, J. M., Meyer, J. M., Dessaux, Y., & Lemanceau, P. (2012). Identification of traits shared by rhizosphere-competent strains of *fluorescent pseudomonads*. *Microbial Ecology*, *64*(3), 725–737. <https://doi.org/10.1007/s00248-012-0065-3>
- Ghorbanpour, M., Omidvari, M., Abbaszadeh-Dahaji, P., Omidvar, R., & Kariman, K. (2018). Mechanisms underlying the protective effects of beneficial fungi against plant diseases. *Biological Control*, *117*, 147–157. <https://doi.org/10.1016/j.biocontrol.2017.11.006>
- Giesler, L. J., & Yuen, G. Y. (1998). Evaluation of *Stenotrophomonas maltophilia* strain C3 for biocontrol of brown patch disease. *Crop Protection*, *17*(6), 509–513. [https://doi.org/10.1016/S0261-2194\(98\)00049-0](https://doi.org/10.1016/S0261-2194(98)00049-0)
- Giguere, D. (2022). Applications of nanopore DNA sequencing for improved genome assembly. *Electronic Thesis and Dissertation Repository*. <https://ir.lib.uwo.ca/etd/8437>
- Gilbert, K. B., Vanderlinde, E. M., & Yost, C. K. (2007). Mutagenesis of the carboxy terminal protease CtpA decreases desiccation tolerance in *Rhizobium leguminosarum*. *FEMS Microbiology Letters*, *272*(1), 65–74. <https://doi.org/10.1111/j.1574-6968.2007.00735.x>
- Glare, T., Caradus, J., Gelernter, W., Jackson, T., Keyhani, N., Köhl, J., Marrone, P., Morin, L., & Stewart, A. (2012). Have biopesticides come of age? *Trends in Biotechnology*, *30*(5), 250–258. <https://doi.org/10.1016/j.tibtech.2012.01.003>
- Glick, B. R. (2012). Plant growth-promoting bacteria: Mechanisms and applications. *Scientifica*, *2012*, 1–15. <https://doi.org/10.6064/2012/963401>
- Godebo, A. T. (2019). Evaluation of soil bacteria as bioinoculants for the control of field pea root rot caused by *Aphanomyces euteiches* [Thesis, University of Saskatchewan], 1-142. <http://hdl.handle.net/10388/11939>
- Godebo, A. T., Germida, J. J., & Walley, F. L. (2020). Isolation, identification, and assessment of soil bacteria as biocontrol agents of pea root rot caused by *Aphanomyces euteiches*. *Canadian Journal of Soil Science*, *100*(3), 206–216. <https://doi.org/10.1139/cjss-2019-0133>

- Godebo, A. T., MacKenzie, K. D., Walley, F. L., Germida, J. J., & Yost, C. K. (2021). Complete genome sequence of a *Pseudomonas simiae* strain with biocontrol potential against aphanomyces root rot. *Microbiology Resource Announcements*, *10*(18), e00222-21. <https://doi.org/10.1128/MRA.00222-21>
- Godebo, A. T., Wee, N. M. J., Yost, C. K., Walley, F. L., & Germida, J. J. (2022). A meta-analysis to determine the state of biological control of aphanomyces root rot. *Frontiers in Molecular Biosciences*, *8*, 777042. <https://doi.org/10.3389/fmolb.2021.777042>
- Gökçen, A., Vilcinskas, A., & Wiesner, J. (2014). Biofilm-degrading enzymes from *Lysobacter gummosus*. *Virulence*, *5*(3), 378–387. <https://doi.org/10.4161/viru.27919>
- Gómez Expósito, R., Postma, J., Raaijmakers, J. M., & De Bruijn, I. (2015). Diversity and activity of *Lysobacter* species from disease suppressive soils. *Frontiers in Microbiology*, *6*. <https://doi.org/10.3389/fmicb.2015.01243>
- Gómez-Lama Cabanás, C., Wentzien, N. M., Zorrilla-Fontanesi, Y., Valverde-Corredor, A., Fernández-González, A. J., Fernández-López, M., & Mercado-Blanco, J. (2022). Impacts of the biocontrol strain *Pseudomonas simiae* picf7 on the banana holobiont: Alteration of root microbial co-occurrence networks and effect on host defense responses. *Frontiers in Microbiology*, *13*, 809126. <https://doi.org/10.3389/fmicb.2022.809126>
- Gonzalez-Garcia, L., Guevara-Barrientos, D., Lozano-Arce, D., Gil, J., Díaz-Riaño, J., Duarte, E., Andrade, G., Bojacá, J. C., Hoyos, M. C., Chavarro, C., Guayazan, N., Chica, L. A., Buitrago Acosta, M. C., Bautista, E., Trujillo, M., & Duitama, J. (2022). *New algorithms for accurate and efficient de-novo genome assembly from long DNA sequencing reads* [Preprint]. *Bioinformatics*. <https://doi.org/10.1101/2022.08.30.505891>
- Gossen, B. D., Conner, R. L., Chang, K.-F., Pasche, J. S., McLaren, D. L., Henriquez, M. A., Chatterton, S., & Hwang, S.-F. (2016). Identifying and managing root rot of pulses on the northern great plains. *Plant Disease*, *100*(10), 1965–1978. <https://doi.org/10.1094/PDIS-02-16-0184-FE>
- Graupner, P. R., Thornburgh, S., Mathieson, J. T., Chapin, E. L., Kemmitt, G. M., Brown, J. M., & Snipes, C. E. (1997). Dihydromaltophilin; a novel fungicidal tetramic acid containing metabolite from *Streptomyces* sp. *The Journal of Antibiotics*, *50*(12), 1014–1019. <https://doi.org/10.7164/antibiotics.50.1014>
- Grimont, P. A. D., & Grimont, F. (2005). *Bergey's Manual of Systematic Bacteriology: Volume Two: The Proteobacteria, Part B-The Gammaproteobacteria. Volume 2.*
- Grover, M., Bodhankar, S., Sharma, A., Sharma, P., Singh, J., & Nain, L. (2021). PGPR mediated alterations in root traits: way toward sustainable crop production. *Frontiers in Sustainable Food Systems*, *4*, 618230.
- Guetsky, R., Shtienberg, D., Elad, Y., & Dinoor, A. (2001). Combining biocontrol agents to reduce the variability of biological control. *Phytopathology*, *91*(7), 621–627. <https://doi.org/10.1094/PHYTO.2001.91.7.621>

- Guide to Crop Protection. (2021). Chemical management of weeds, plant diseases and insects. <https://www.saskatchewan.ca/business/agriculture-natural-resources-and-industry/agribusiness-farmers-and-ranchers/crops-and-irrigation/crop-guides-and-publications/guide-to-crop-protection>. Retrieved September 4, 2021.
- Gupta, P., Samant, K., & Sahu, A. (2012). Isolation of cellulose-degrading bacteria and determination of their cellulolytic potential. *International Journal of Microbiology*, 2012, 1–5. <https://doi.org/10.1155/2012/578925>
- Hackl, S. T., Harbig, T. A., & Nieselt, K. (2022). *Technical report on best practices for hybrid and long read de novo assembly of bacterial genomes utilizing Illumina and Oxford Nanopore Technologies reads* [Preprint]. Bioinformatics. <https://doi.org/10.1101/2022.10.25.513682>
- Haidar, R., Yacoub, A., Roudet, J., Fermaud, M., & Rey, P. (2021). Application methods and modes of action of *Pantoea agglomerans* and *Paenibacillus* sp., to control the grapevine trunk disease-pathogen, *Neofusicoccum parvum*. *OENO One*, 55(3), 1-16. <https://hal.inrae.fr/hal-03297061>
- Han, D. Y., Coplin, D. L., Bauer, W. D., & Hoitink, H. A. J. (2000). A rapid bioassay for screening rhizosphere microorganisms for their ability to induce systemic resistance. *Phytopathology*, 90(4), 327–332. <https://doi.org/10.1094/PHYTO.2000.90.4.327>
- Harbola, A., Negi, D., Manchanda, M., & Kesharwani, R. K. (2022). Bioinformatics and biological data mining. In *Bioinformatics* (pp. 457–471). Elsevier. <https://doi.org/10.1016/B978-0-323-89775-4.00019-5>
- Hashizume, H., Hirose, S., Sawa, R., Muraoka, Y., Ikeda, D., Naganawa, H., & Igarashi, M. (2004). Tripropeptins, novel antimicrobial agents produced by *Lysobacter* sp. ii. Structure elucidation. *The Journal of Antibiotics*, 57(1), 52–58. <https://doi.org/10.7164/antibiotics.57.52>
- Hayward, A. C., Fegan, N., Fegan, M., & Stirling, G. R. (2010). *Stenotrophomonas* and *Lysobacter*: Ubiquitous plant-associated gamma- proteobacteria of developing significance in applied microbiology. *Journal of Applied Microbiology*, 108(3), 756–770. <https://doi.org/10.1111/j.1365-2672.2009.04471.x>
- He, Y.-W., Cao, X.-Q., & Poplawsky, A. R. (2020). Chemical structure, biological roles, biosynthesis and regulation of the yellow xanthomonadin pigments in the phytopathogenic genus *xanthomonas*. *Molecular Plant-Microbe Interactions*, 33(5), 705–714. <https://doi.org/10.1094/MPMI-11-19-0326-CR>
- Health Canada PMRA. (2009). Registration decision *Pantoea agglomerans* strain E325 https://publications.gc.ca/collections/collection_2009/arla-pmra/H113-25-2009-6E.pdf, 1-10. Retrieved September 10, 2022.
- Heimpel, G. E., & Mills, N. J. (2017). *Biological control: Ecology and applications* (1st ed.). Cambridge University Press, 380. <https://doi.org/10.1017/9781139029117>

- Heungens, K., & Parke, J. L. (2001). Postinfection biological control of oomycete pathogens of pea by *burkholderia cepacia* ammdr1. *Phytopathology*, 91(4), 383–391. <https://doi.org/10.1094/PHYTO.2001.91.4.383>
- Hoagland, D. R., & Arnon, D. I. (1938). The water-culture method for growing plants without soil. *California Agricultural Experiment Station Circulation*, 347, 32. <http://hdl.handle.net/2027/uc2.ark:/13960/t51g1sb8j>
- Hossain, M. J., Ran, C., Liu, K., Ryu, C. M., Rasmussen-Ivey, C. R., Williams, M. A., Hassan, M. K., Choi, S.-K., Jeong, H., Newman, M., Kloepper, J. W., & Liles, M. R. (2015). Deciphering the conserved genetic loci implicated in plant disease control through comparative genomics of *Bacillus amyloliquefaciens* subsp. Plantarum. *Frontiers in Plant Science*, 6. <https://doi.org/10.3389/fpls.2015.00631>
- Hossain, S., Bergkvist, G., Berglund, K., Glinwood, R., Kabouw, P., Mårtensson, A., & Persson, P. (2014). Concentration- and time-dependent effects of isothiocyanates produced from brassicaceae shoot tissues on the pea root rot pathogen *Aphanomyces euteiches*. *Journal of Agricultural and Food Chemistry*, 62(20), 4584–4591. <https://doi.org/10.1021/jf501776c>
- Hossain, Z., Wang, X., Hamel, C., Knight, J. D., Morrison, M. J., & Gan, Y. (2016). Biological nitrogen fixation by pulse crops on the semiarid Canadian Prairie. *Canadian Journal of Plant Science*, CJPS-2016-0185. <https://doi.org/10.1139/CJPS-2016-0185>
- Hsieh, C., Tsai, M. J., Hsu, T. H., Chang, D. M., & Lo, C. T. (2005). Medium optimization for polysaccharide production of *Cordyceps sinensis*. *Applied Biochemistry and Biotechnology*, 120(2), 145–158. <https://doi.org/10.1385/ABAB:120:2:145>
- Hu, T., Chitnis, N., Monos, D., & Dinh, A. (2021). Next-generation sequencing technologies: An overview. *Human Immunology*, 82(11), 801–811. <https://doi.org/10.1016/j.humimm.2021.02.012>
- Hughes, T. J., & Grau, C. R. (2007). *Aphanomyces* root rot or common root rot of legumes. *The Plant Health Instructor*. <https://doi.org/10.1094/PHI-I-2007-0418-01>
- Iacovelli, R., Alesini, D., Palazzo, A., Trenta, P., Santoni, M., De Marchis, L., Cascinu, S., Naso, G., & Cortesi, E. (2014). Targeted therapies and complete responses in first line treatment of metastatic renal cell carcinoma. A meta-analysis of published trials. *Cancer Treatment Reviews*, 40(2), 271–275. <https://doi.org/10.1016/j.ctrv.2013.09.003>
- Ishimaru, C. A., Klos, E. J., & Brubaker, R. R. (1988). Multiple antibiotic production by *Erwinia herbicola*. *Phytopathology*, 78(6), 746-750.
- Jaglic, Z., & Cervinkova, D. (2012). Genetic basis of resistance to quaternary ammonium compounds - the qac genes and their role: A review. *Veterinárni Medicína*, 57(6), 275–281. <https://doi.org/10.17221/6013-VETMED>

- Jeffers, A., & Chong, J. H. (2021). Biological control strategies in integrated pest management (IPM) programs. <https://lpress.clemson.edu/publication/biological-control-strategies-in-integrated-pest-management-ipm-programs/>.
- Ji, G.-H., Wei, L.-F., He, Y.-Q., Wu, Y.-P., & Bai, X.-H. (2008). Biological control of rice bacterial blight by *Lysobacter antibioticus* strain 13-1. *Biological Control*, *45*(3), 288–296. <https://doi.org/10.1016/j.biocontrol.2008.01.004>
- Jia, B., Raphenya, A. R., Alcock, B., Waglechner, N., Guo, P., Tsang, K. K., Lago, B. A., Dave, B. M., Pereira, S., Sharma, A. N., Doshi, S., Courtot, M., Lo, R., Williams, L. E., Frye, J. G., Elsayegh, T., Sardar, D., Westman, E. L., Pawlowski, A. C., ... McArthur, A. G. (2017). CARD 2017: Expansion and model-centric curation of the comprehensive antibiotic resistance database. *Nucleic Acids Research*, *45*(D1), D566–D573. <https://doi.org/10.1093/nar/gkw1004>
- Jiang, L., Seo, J., Peng, Y., Jeon, D., Park, S. J., Kim, C. Y., Kim, P. I., Kim, C. H., Lee, J. H., & Lee, J. (2023). Genome insights into the plant growth-promoting bacterium *Saccharibacillus brassicae* ATSA2T. *AMB Express*, *13*(1), 9. <https://doi.org/10.1186/s13568-023-01514-1>
- Johnson, K. B., & Stockwell, V. O. (1998). Management of fire blight: a case study in microbial ecology. *Annual Review of Phytopathology*, *36*(1), 227-248.
- Joshi, S., & Satyanarayana, T. (2013). Characteristics and applications of a recombinant alkaline serine protease from a novel bacterium *Bacillus lehensis*. *Bioresource Technology*, *131*, 76–85. <https://doi.org/10.1016/j.biortech.2012.12.124>
- Kaewchomphunuch, T., Charoenpichitnunt, T., Thongbaiyai, V., Ngamwongsatit, N., & Kaeoket, K. (2022). Cell-free culture supernatants of *Lactobacillus* spp. and *Pediococcus* spp. Inhibit growth of pathogenic *Escherichia coli* isolated from pigs in Thailand. *BMC Veterinary Research*, *18*(1), 60. <https://doi.org/10.1186/s12917-022-03140-8>
- Kaewsalong, N., Songkumarn, P., Duangmal, K., & Dethoup, T. (2019). Synergistic effects of combinations of novel strains of *Trichoderma* species and *Coscinium fenestratum* extract in controlling rice dirty panicle. *Journal of Plant Pathology*, *101*(2), 367–372. <https://doi.org/10.1007/s42161-018-0191-y>
- Kamber, T., Lansdell, T. A., Stockwell, V. O., Ishimaru, C. A., Smits, T. H. M., & Duffy, B. (2012). Characterization of the biosynthetic operon for the antibacterial peptide herbicolin in *Pantoea vagans* biocontrol strain c9-1 and incidence in *Pantoea* species. *Applied and Environmental Microbiology*, *78*(12), 4412–4419. <https://doi.org/10.1128/AEM.07351-11>
- Kammonen, J. I., Smolander, O.-P., Paulin, L., Pereira, P. A. B., Laine, P., Koskinen, P., Jernvall, J., & Auvinen, P. (2019). Gapfinisher: A reliable gap filling pipeline for sspace-longread scaffold output. *PLOS ONE*, *14*(9), e0216885. <https://doi.org/10.1371/journal.pone.0216885>
- Kannan, C., Divya, M., Rekha, G., Barbadikar, K. M., Maruthi, P., Hajira, S. K., & Sundaram, R. M. (2022). Whole genome sequencing data of native isolates of *Bacillus* and *Trichoderma*

- having potential biocontrol and plant growth promotion activities in rice. *Data in Brief*, 41, 107923. <https://doi.org/10.1016/j.dib.2022.107923>
- Kempf, H. J., & Wolf, G. (1989). *Erwinia herbicola* as a biocontrol agent of *Fusarium culmorum* and *Puccinia recondita* f. sp. tritici on wheat. *Phytopathology*, 79(9), 990-994.
- Kim, S. Y., Lee, S. Y., Weon, H.-Y., Sang, M. K., & Song, J. (2017). Complete genome sequence of *Bacillus velezensis* M75, a biocontrol agent against fungal plant pathogens, isolated from cotton waste. *Journal of Biotechnology*, 241, 112–115. <https://doi.org/10.1016/j.jbiotec.2016.11.023>
- Kimura, M. (1980). A simple method for estimating evolutionary rates of base substitutions through comparative studies of nucleotide sequences. *Journal of Molecular Evolution*, 16(2), 111–120. <https://doi.org/10.1007/BF01731581>
- King, E. B. (1993). Biocontrol of aphanomyces root rot and pythium damping-off by *Pseudomonas cepacia* ammd on four pea cultivars. *Plant Disease*, 77(12), 1185. <https://doi.org/10.1094/PD-77-1185>
- Ko, H. S., Jin, R.-D., Krishnan, H. B., Lee, S.-B., & Kim, K.-Y. (2009). Biocontrol ability of *Lysobacter antibioticus* hs124 against phytophthora blight is mediated by the production of 4-hydroxyphenylacetic acid and several lytic enzymes. *Current Microbiology*, 59(6), 608–615. <https://doi.org/10.1007/s00284-009-9481-0>
- Ko, H. S., Tindwa, H., Jin, R. D., Lee, Y. S., Hong, S. H., Hyun, H.-N., Nam, Y., & Kim, K.-Y. (2011). Investigation of Siderophore production and Antifungal activity against *Phytophthora capsici* as related to Iron (Iii) nutrition by *Lysobacter antibioticus* HS124. *Korean Journal of Soil Science and Fertilizer*, 44(4), 650–656. <https://doi.org/10.7745/KJSSF.2011.44.4.650>
- Kobayashi, D. Y., & Yuen, G. Y. (2005). The role of *clp* -regulated factors in antagonism against *Magnaporthe poae* and biological control of summer patch disease of Kentucky bluegrass by *Lysobacter enzymogenes* C3. *Canadian Journal of Microbiology*, 51(8), 719–723. <https://doi.org/10.1139/w05-056>
- Kobayashi, D. Y., & Yuen, G. Y. (2007). The potential of *Lysobacter* spp. As bacterial biological control agents for plant diseases. *CABI Reviews*, 2007. <https://doi.org/10.1079/PAVSNNR20072007>
- Kobayashi, D. Y., Reedy, R. M., Palumbo, J. D., Zhou, J.-M., & Yuen, G. Y. (2005). A *clp* gene homologue belonging to the *crp* gene family globally regulates lytic enzyme production, antimicrobial activity, and biological control activity expressed by *Lysobacter enzymogenes* strain c3. *Applied and Environmental Microbiology*, 71(1), 261–269. <https://doi.org/10.1128/AEM.71.1.261-269.2005>
- Koch, E., Zink, P., Pfeiffer, T., von Galen, A., Linkies, A., Drechsel, J., & Birr, T. (2020). Artificial inoculation methods for testing microorganisms as control agents of seed- and soil-borne

- Fusarium-seedling blight of maize. *Journal of Plant Diseases and Protection*, 127(6), 883–893. <https://doi.org/10.1007/s41348-020-00350-w>
- Köhl, J., Kolnaar, R., & Ravensberg, W. J. (2019). Mode of action of microbial biological control agents against plant diseases: Relevance beyond efficacy. *Frontiers in Plant Science*, 10, 845. <https://doi.org/10.3389/fpls.2019.00845>
- Koren, S., & Phillippy, A. M. (2015). One chromosome, one contig: Complete microbial genomes from long-read sequencing and assembly. *Current Opinion in Microbiology*, 23, 110–120. <https://doi.org/10.1016/j.mib.2014.11.014>
- Koricheva, J., & Gurevitch, J. (2014). Uses and misuses of meta-analysis in plant ecology. *Journal of Ecology*, 102(4), 828–844. <https://doi.org/10.1111/1365-2745.12224>
- Kratz, A., Greenberg, D., Barki, Y., Cohen, E., & Lifshitz, M. (2003). *Pantoea agglomerans* as a cause of septic arthritis after palm tree thorn injury; Case report and literature review. *Archives of Disease in Childhood*, 88(6), 542–544. <https://doi.org/10.1136/adc.88.6.542>
- Kumar, S., Stecher, G., Li, M., Knyaz, C., & Tamura, K. (2018). Mega x: Molecular evolutionary genetics analysis across computing platforms. *Molecular Biology and Evolution*, 35(6), 1547–1549. <https://doi.org/10.1093/molbev/msy096>
- Lagerlöf, J., Ayuke, F., Heyman, F., & Meijer, J. (2020). Effects of biocontrol bacteria and earthworms on *Aphanomyces euteiches* root-rot and growth of peas (*Pisum sativum*) studied in a pot experiment. *Acta Agriculturae Scandinavica, Section B — Soil & Plant Science*, 70(5), 427–436. <https://doi.org/10.1080/09064710.2020.1761995>
- Lahlali, R., Ezrari, S., Radouane, N., Kenfaoui, J., Esmael, Q., El Hamss, H., Belabess, Z., & Barka, E. A. (2022). Biological control of plant pathogens: A global perspective. *Microorganisms*, 10(3), 596. <https://doi.org/10.3390/microorganisms10030596>
- Laitinen, S., Linnainmaa, M., Laitinen, J., Kiviranta, H., Reiman, M., & Liesivuori, J. (1999). Endotoxins and IgG antibodies as indicators of occupational exposure to the microbial contaminants of metal-working fluids. *International Archives of Occupational and Environmental Health*, 72(7), 443–450. <https://doi.org/10.1007/s004200050397>
- Lamers, J. G., Schippers, B., & Geels, F. P. (1988). Soil-borne diseases of wheat in the Netherlands and results of seed bacterization with *Pseudomonads* against *Gaeumannomyces graminis* var. *tritici*, associated with disease resistance. *Cereal breeding related to integrated cereal production*, 134-139.
- Le May, C., Potage, G., Andrivon, D., Tivoli, B., & Outreman, Y. (2009). Plant disease complex: Antagonism and synergism between pathogens of the Ascochyta blight complex on pea: co-occurrence effects on plant pathogens. *Journal of Phytopathology*, 157(11–12), 715–721. <https://doi.org/10.1111/j.1439-0434.2009.01546.x>

- Li, H., Li, H., Bai, Y., Wang, J., Nie, M., Li, B., & Xiao, M. (2011). The use of *Pseudomonas fluorescens* P13 to control sclerotinia stem rot (*Sclerotinia sclerotiorum*) of oilseed rape. *The Journal of Microbiology*, *49*(6), 884–889. <https://doi.org/10.1007/s12275-011-1261-4>
- Li, J., Liu, K., Zhang, J., Huang, L., Coulter, J. A., Woodburn, T., Li, L., & Gan, Y. (2018). Soil–plant indices help explain legume response to crop rotation in a semiarid environment. *Frontiers in Plant Science*, *9*, 1488. <https://doi.org/10.3389/fpls.2018.01488>
- Li, N., Islam, M. T., & Kang, S. (2019). Secreted metabolite-mediated interactions between rhizosphere bacteria and *Trichoderma* biocontrol agents. *PLOS ONE*, *14*(12), e0227228. <https://doi.org/10.1371/journal.pone.0227228>
- Li, S., Du, L., Yuen, G., & Harris, S. D. (2006). Distinct ceramide synthases regulate polarized growth in the filamentous fungus *Aspergillus nidulans*. *Molecular Biology of the Cell*, *17*(3), 1218–1227. <https://doi.org/10.1091/mbc.e05-06-0533>
- Ligozzi, M., Lo Cascio, G., & Fontana, R. (1998). *Vana* gene cluster in a vancomycin-resistant clinical isolate of *Bacillus circulans*. *Antimicrobial Agents and Chemotherapy*, *42*(8), 2055–2059. <https://doi.org/10.1128/AAC.42.8.2055>
- Lin, L., Xu, K., Shen, D., Chou, S., Gomelsky, M., & Qian, G. (2021). Antifungal weapons of *Lysobacter*, a mighty biocontrol agent. *Environmental Microbiology*, *23*(10), 5704–5715. <https://doi.org/10.1111/1462-2920.15674>
- Lindow, S. E., & Brandl, M. T. (2003). Microbiology of the phyllosphere. *Applied and Environmental Microbiology*, *69*(4), 1875–1883. <https://doi.org/10.1128/AEM.69.4.1875-1883.2003>
- Liu, K., Newman, M., McInroy, J. A., Hu, C.-H., & Kloepper, J. W. (2017). Selection and assessment of plant growth-promoting rhizobacteria for biological control of multiple plant diseases. *Phytopathology*®, *107*(8), 928–936. <https://doi.org/10.1094/PHYTO-02-17-0051-R>
- Liu, L., Zhang, S., Luo, M., & Wang, G. (2015). Genomic information of the arsenic-resistant bacterium *Lysobacter arseniciresistens* type strain ZS79T and comparison of *Lysobacter* draft genomes. *Standards in Genomic Sciences*, *10*(1), 88. <https://doi.org/10.1186/s40793-015-0070-5>
- Liu, Y., Qiao, J., Liu, Y., Liang, X., Zhou, Y., & Liu, J. (2019). Characterization of *Lysobacter capsici* strain NF87–2 and its biocontrol activities against phytopathogens. *European Journal of Plant Pathology*, *155*(3), 859–869. <https://doi.org/10.1007/s10658-019-01817-9>
- Loman, N. J., Quick, J., & Simpson, J. T. (2015). A complete bacterial genome assembled *de novo* using only nanopore sequencing data. *Nature Methods*, *12*(8), 733–735. <https://doi.org/10.1038/nmeth.3444>

- Lood, C., Correa Rojo, A., Sinar, D., Verkinderen, E., Lavigne, R., & Noort, V. van. (2022). SASpector: Analysis of missing genomic regions in draft genomes of prokaryotes. *Bioinformatics*, 38(10), 2920–2921. <https://doi.org/10.1093/bioinformatics/btac208>
- Loper, J. E., & Gross, H. (2007). Genomic analysis of antifungal metabolite production by *Pseudomonas fluorescens* Pf-5. In P. A. H. M. Bakker, J. M. Raaijmakers, G. Bloemberg, M. Höfte, P. Lemanceau, & B. M. Cooke (Eds.), *New Perspectives and Approaches in Plant Growth-Promoting Rhizobacteria Research* (pp. 265–278). Springer Netherlands. https://doi.org/10.1007/978-1-4020-6776-1_4
- Loper, J. E., Hassan, K. A., Mavrodi, D. V., Davis, E. W., Lim, C. K., Shaffer, B. T., Elbourne, L. D. H., Stockwell, V. O., Hartney, S. L., Breakwell, K., Henkels, M. D., Tetu, S. G., Rangel, L. I., Kidarsa, T. A., Wilson, N. L., van de Mortel, J. E., Song, C., Blumhagen, R., Radune, D., ... Paulsen, I. T. (2012). Comparative genomics of plant-associated *Pseudomonas* spp.: Insights into diversity and inheritance of traits involved in multitrophic interactions. *PLoS Genetics*, 8(7), e1002784. <https://doi.org/10.1371/journal.pgen.1002784>
- Lou, L., Qian, G., Xie, Y., Hang, J., Chen, H., Zaleta-Rivera, K., Li, Y., Shen, Y., Dussault, P. H., Liu, F., & Du, L. (2011). Biosynthesis of hsaf, a tetramic acid-containing macrolactam from *Lysobacter enzymogenes*. *Journal of the American Chemical Society*, 133(4), 643–645. <https://doi.org/10.1021/ja105732c>
- Lu, H., Giordano, F., & Ning, Z. (2016). Oxford nanopore minion sequencing and genome assembly. *Genomics, Proteomics & Bioinformatics*, 14(5), 265–279. <https://doi.org/10.1016/j.gpb.2016.05.004>
- Lu, W.-J., Wang, H.-T., Nie, Y.-F., Wang, Z.-C., Huang, D.-Y., Qiu, X.-Y., & Chen, J.-C. (2004). Effect of inoculating flower stalks and vegetable waste with ligno-cellulolytic microorganisms on the composting process. *Journal of Environmental Science and Health, Part B- Pesticides, Food Contaminants, and Agricultural Wastes*, 39(5–6), 871–887. <https://doi.org/10.1081/LESB-200030896>
- Lueder, M. R., Cer, R. Z., Patrick, M., Voegtly, L. J., Long, K. A., Rice, G. K., & Bishop-Lilly, K. A. (2021). Manual annotation studio (Mas): A collaborative platform for manual functional annotation of viral and microbial genomes. *BMC Genomics*, 22(1), 733. <https://doi.org/10.1186/s12864-021-08029-8>
- Luo, G., Shi, Z., & Wang, G. (2012). *Lysobacter arseniciresistens* sp. Nov., an arsenite-resistant bacterium isolated from iron-mined soil. *International Journal of Systematic and Evolutionary Microbiology*, 62(Pt_7), 1659–1665. <https://doi.org/10.1099/ijs.0.034405-0>
- Luo, Y., Cheng, Y., Yi, J., Zhang, Z., Luo, Q., Zhang, D., & Li, Y. (2018). Complete genome sequence of industrial biocontrol strain *paenibacillus polymyxa* hy96-2 and further analysis of its biocontrol mechanism. *Frontiers in Microbiology*, 9, 1520. <https://doi.org/10.3389/fmicb.2018.01520>

- Luo, Y., Huang, H., Liang, J., Wang, M., Lu, L., Shao, Z., Cobb, R. E., & Zhao, H. (2013). Activation and characterization of a cryptic polycyclic tetramate macrolactam biosynthetic gene cluster. *Nature Communications*, *4*(1), 2894. <https://doi.org/10.1038/ncomms3894>
- Lynch, T., Petkau, A., Knox, N., Graham, M., & Van Domselaar, G. (2016). A primer on infectious disease bacterial genomics. *Clinical Microbiology Reviews*, *29*(4), 881–913. <https://doi.org/10.1128/CMR.00001-16>
- Ma, W., Penrose, D. M., & Glick, B. R. (2002). Strategies used by rhizobia to lower plant ethylene levels and increase nodulation. *Canadian Journal of Microbiology*, *48*(11), 947–954. <https://doi.org/10.1139/w02-100>
- Madden, L. V., & Paul, P. A. (2011). Meta-analysis for evidence synthesis in plant pathology: An overview. *Phytopathology*, *101*(1), 16–30. <https://doi.org/10.1094/PHYTO-03-10-0069>
- Margesin, R., Zhang, D.-C., Albuquerque, L., Froufe, H. J. C., Egas, C., & da Costa, M. S. (2018). *Lysobacter silvestris* sp. Nov., isolated from alpine forest soil, and reclassification of *Luteimonas tolerans* as *Lysobacter tolerans* comb. Nov. *International Journal of Systematic and Evolutionary Microbiology*, *68*(5), 1571–1577. <https://doi.org/10.1099/ijsem.0.002710>
- Marian, M., & Shimizu, M. (2019). Improving performance of microbial biocontrol agents against plant diseases. *Journal of General Plant Pathology*, *85*(5), 329–336. <https://doi.org/10.1007/s10327-019-00866-6>
- Mark, G. L., Morrissey, J. P., Higgins, P., & O’Gara, F. (2006). Molecular-based strategies to exploit *Pseudomonas* biocontrol strains for environmental biotechnology applications: Molecular-based strategies to exploit *Pseudomonas* strains. *FEMS Microbiology Ecology*, *56*(2), 167–177. <https://doi.org/10.1111/j.1574-6941.2006.00056.x>
- Márquez, R., Blanco, E. L., & Aranguren, Y. (2020). *Bacillus* strain selection with plant growth-promoting mechanisms as potential elicitors of systemic resistance to gray mold in pepper plants. *Saudi Journal of Biological Sciences*, *27*(8), 1913–1922. <https://doi.org/10.1016/j.sjbs.2020.06.015>
- Martínez-García, P. M., Ruano-Rosa, D., Schilirò, E., Prieto, P., Ramos, C., Rodríguez-Palenzuela, P., & Mercado-Blanco, J. (2015). Complete genome sequence of *Pseudomonas fluorescens* strain PICF7, an indigenous root endophyte from olive (*Olea europaea* L.) and effective biocontrol agent against *Verticillium dahliae*. *Standards in Genomic Sciences*, *10*(1), 10. <https://doi.org/10.1186/1944-3277-10-10>
- Martín-García, B., De Montijo-Prieto, S., Jiménez-Valera, M., Carrasco-Pancorbo, A., Ruiz-Bravo, A., Verardo, V., & Gómez-Caravaca, A. M. (2022). Comparative extraction of phenolic compounds from olive leaves using a sonotrode and an ultrasonic bath and the evaluation of both antioxidant and antimicrobial activity. *Antioxidants*, *11*(3), 558. <https://doi.org/10.3390/antiox11030558>

- Mazurier, S., Corberand, T., Lemanceau, P., & Raaijmakers, J. M. (2009). Phenazine antibiotics produced by *fluorescent Pseudomonads* contribute to natural soil suppressiveness to Fusarium wilt. *The ISME Journal*, 3(8), 977–991. <https://doi.org/10.1038/ismej.2009.33>
- McDonald, B. A., & Linde, C. (2002). Pathogen population genetics, evolutionary potential, and durable resistance. *Annual Review of Phytopathology*, 40(1), 349–379. <https://doi.org/10.1146/annurev.phyto.40.120501.101443>
- McLaren, D. L. Hausermann, D.J. Henriquez, M.A. Chang, K.F. & Kerley, T.J. (2015). Field pea diseases in Manitoba in 2014. *Canadian plant disease survey*. 95:173-175.
- Md Sidek, N. L., Halim, M., Tan, J. S., Abbasiliasi, S., Mustafa, S., & Ariff, A. B. (2018). Stability of bacteriocin-like inhibitory substance (Blis) produced by *Pediococcus acidilactici* kp10 at different extreme conditions. *BioMed Research International*, 2018, 1–11. <https://doi.org/10.1155/2018/5973484>
- Medema, M. H., Blin, K., Cimermancic, P., de Jager, V., Zakrzewski, P., Fischbach, M. A., Weber, T., Takano, E., & Breitling, R. (2011). Antismash: Rapid identification, annotation and analysis of secondary metabolite biosynthesis gene clusters in bacterial and fungal genome sequences. *Nucleic Acids Research*, 39(suppl_2), W339–W346. <https://doi.org/10.1093/nar/gkr466>
- Meers, P. R., Liu, C., Chen, R., Bartos, W., Davis, J., Dziedzic, N., ... & Wang, S. (2018). Vesicular delivery of the antifungal antibiotics of *Lysobacter enzymogenes* C3. *Applied and Environmental Microbiology*, 84(20), e01353-18. <https://doi.org/10.1128/AEM.01353-18>
- Miess, H., van Trappen, S., Cleenwerck, I., De Vos, P., & Gross, H. (2016). Reclassification of *Pseudomonas* sp. PB-6250T as *Lysobacter firmicutimachus* sp. Nov. *International Journal of Systematic and Evolutionary Microbiology*, 66(10), 4162–4166. <https://doi.org/10.1099/ijsem.0.001329>
- Miller, J. R., Zhou, P., Mudge, J., Gurtowski, J., Lee, H., Ramaraj, T., Walenz, B. P., Liu, J., Stupar, R. M., Denny, R., Song, L., Singh, N., Maron, L. G., McCouch, S. R., McCombie, W. R., Schatz, M. C., Tiffin, P., Young, N. D., & Silverstein, K. A. T. (2017). Hybrid assembly with long and short reads improves discovery of gene family expansions. *BMC Genomics*, 18(1), 541. <https://doi.org/10.1186/s12864-017-3927-8>
- Mishra, R. K., Bohra, A., Kamaal, N., Kumar, K., Gandhi, K., Gk, S., Saabale, P. R., Sij, S. N., Sarma, B. K., Kumar, D., Mishra, M., Srivastava, D. K., & Singh, N. P. (2018). Utilization of biopesticides as sustainable solutions for management of pests in legume crops: Achievements and prospects. *Egyptian Journal of Biological Pest Control*, 28(1), 3. <https://doi.org/10.1186/s41938-017-0004-1>
- Mong Thu, T. T., & Krasaekoopt, W. (2016). Encapsulation of protease from *Aspergillus oryzae* and lipase from *Thermomyces lanuginosus* using alginate and different copolymer types. *Agriculture and Natural Resources*, 50(3), 155–161. <https://doi.org/10.1016/j.anres.2016.06.002>

- Montes-Osuna, N., Gómez-Lama Cabanás, C., Valverde-Corredor, A., Berendsen, R. L., Prieto, P., & Mercado-Blanco, J. (2021). Assessing the involvement of selected phenotypes of *Pseudomonas simiae* picf7 in olive root colonization and biological control of verticillium dahliae. *Plants*, *10*(2), 412. <https://doi.org/10.3390/plants10020412>
- Moussart, A., Wicker, E., Le Delliou, B., Abelard, J.-M., Esnault, R., Lemarchand, E., Rouault, F., Le Guennou, F., Pilet-Nayel, M.-L., Baranger, A., Rouxel, F., & Tivoli, B. (2009). Spatial distribution of *Aphanomyces euteiches* inoculum in a naturally infested pea field. *European Journal of Plant Pathology*, *123*(2), 153–158. <https://doi.org/10.1007/s10658-008-9350-x>
- Muhammad, M. H., Idris, A. L., Fan, X., Guo, Y., Yu, Y., Jin, X., Qiu, J., Guan, X., & Huang, T. (2020). Beyond risk: Bacterial biofilms and their regulating approaches. *Frontiers in Microbiology*, *11*, 928. <https://doi.org/10.3389/fmicb.2020.00928>
- Müller, H., Westendorf, C., Leitner, E., Chernin, L., Riedel, K., Schmidt, S., Eberl, L., & Berg, G. (2009). Quorum-sensing effects in the antagonistic rhizosphere bacterium *Serratia plymuthica* HRO-C48: Biocontrol and quorum sensing in *Serratia plymuthica*. *FEMS Microbiology Ecology*, *67*(3), 468–478. <https://doi.org/10.1111/j.1574-6941.2008.00635.x>
- Narayanasamy, P. (2013). Biological management of diseases of crops: Volume 1: *characteristics of biological control agents*. Springer Netherlands, 673. <https://doi.org/10.1007/978-94-007-6380-7>
- Navarro, F., Sass, M. E., & Nienhuis, J. (2008). Identification and confirmation of quantitative trait loci for root rot resistance in snap bean. *Crop Science*, *48*(3), 962–972. <https://doi.org/10.2135/cropsci2007.02.0113>
- Nel, B., Steinberg, C., Labuschagne, N., & Viljoen, A. (2006). The potential of nonpathogenic *Fusarium oxysporum* and other biological control organisms for suppressing fusarium wilt of banana. *Plant Pathology*, *55*(2), 217–223. <https://doi.org/10.1111/j.1365-3059.2006.01344.x>
- Nguyen, P.-A., Strub, C., Fontana, A., & Schorr-Galindo, S. (2017). Crop molds and mycotoxins: Alternative management using biocontrol. *Biological Control*, *104*, 10–27. <https://doi.org/10.1016/j.biocontrol.2016.10.004>
- Nicot, P. (2011). *Classical and augmentative biological control against diseases and pests: Critical status analysis and review of factors influencing their success*. IOBC/WPRS international organization for biological and integrated control of noxious animals and plants, West Palaearctic Regional Section. http://www.iobc-wprs.org/pub/biological_control_against_diseases_and_pests_2011.pdf
- Nigam, P. S., & Singh, A. (2014). Metabolic pathways | production of secondary metabolites – fungi. In *Encyclopedia of Food Microbiology* (pp. 570–578). Elsevier. <https://doi.org/10.1016/B978-0-12-384730-0.00202-0>
- Niu, B., Wang, W., Yuan, Z., Sederoff, R. R., Sederoff, H., Chiang, V. L., & Borriss, R. (2020). Microbial interactions within multiple-strain biological control agents impact soil-borne

- plant disease. *Frontiers in Microbiology*, *11*, 585404. <https://doi.org/10.3389/fmicb.2020.585404>
- Nunes, C., Usall, J., Teixido, N., Fons, E., & Vinas, I. (2002). Post-harvest biological control by *Pantoea agglomerans* (CPA-2) on Golden Delicious apples. *Journal of Applied Microbiology*, *92*(2), 247–255. <https://doi.org/10.1046/j.1365-2672.2002.01524.x>
- Ojiambo, P. S., & Scherm, H. (2006). Biological and application-oriented factors influencing plant disease suppression by biological control: A meta-analytical review. *Phytopathology*, *96*(11), 1168–1174. <https://doi.org/10.1094/PHYTO-96-1168>
- Olanrewaju, O. S., Glick, B. R., & Babalola, O. O. (2017). Mechanisms of action of plant growth promoting bacteria. *World Journal of Microbiology and Biotechnology*, *33*(11), 197. <https://doi.org/10.1007/s11274-017-2364-9>
- Ortmann, I., & Moerschbacher, B. M. (2006). Spent growth medium of *Pantoea agglomerans* primes wheat suspension cells for augmented accumulation of hydrogen peroxide and enhanced peroxidase activity upon elicitation. *Planta*, *224*(4), 963–970. <https://doi.org/10.1007/s00425-006-0271-7>
- Ortmann, I., Conrath, U., & Moerschbacher, B. M. (2006). Exopolysaccharides of *Pantoea agglomerans* have different priming and eliciting activities in suspension-cultured cells of monocots and dicots. *FEBS Letters*, *580*(18), 4491–4494. <https://doi.org/10.1016/j.febslet.2006.07.025>
- Overbeek, R., Olson, R., Pusch, G. D., Olsen, G. J., Davis, J. J., Disz, T., Edwards, R. A., Gerdes, S., Parrello, B., Shukla, M., Vonstein, V., Wattam, A. R., Xia, F., & Stevens, R. (2014). The seed and the rapid annotation of microbial genomes using subsystems technology (Rast). *Nucleic Acids Research*, *42*(D1), D206–D214. <https://doi.org/10.1093/nar/gkt1226>
- Pal, K. K., Tilak, K. V. B. R., Saxena, A. K., Dey, R., & Singh, C. S. (2000). Antifungal characteristics of a fluorescent *Pseudomonas* strain involved in the biological control of *Rhizoctonia solani*. *Microbiological Research*, *155*(3), 233–242. [https://doi.org/10.1016/S0944-5013\(00\)80038-5](https://doi.org/10.1016/S0944-5013(00)80038-5)
- Palleroni, N. J. (1992). Present situation of the taxonomy of aerobic Pseudomonads. In *Pseudomonas: Molecular Biology and Biotechnology*. Galli E., Silver S., & Witholt B Eds. Washington, DC: American Society for Microbiology; (pp. 105-105).
- Palma, M., Zurita, J., Ferreras, J. A., Worgall, S., Larone, D. H., Shi, L., Campagne, F., & Quadri, L. E. N. (2005). *Pseudomonas aeruginosa* soxr does not conform to the archetypal paradigm for soxr-dependent regulation of the bacterial oxidative stress adaptive response. *Infection and Immunity*, *73*(5), 2958–2966. <https://doi.org/10.1128/IAI.73.5.2958-2966.2005>
- Palmer, M., Steenkamp, E. T., Coetzee, M. P. A., Avontuur, J. R., Chan, W.-Y., van Zyl, E., Blom, J., & Venter, S. N. (2018). Mixta gen. Nov., a new genus in the Erwiniaceae. *International Journal of Systematic and Evolutionary Microbiology*, *68*(4), 1396–1407. <https://doi.org/10.1099/ijsem.0.002540>

- Palmieri, D., Ianiri, G., Del Grosso, C., Barone, G., De Curtis, F., Castoria, R., & Lima, G. (2022). Advances and perspectives in the use of biocontrol agents against fungal plant diseases. *Horticulturae*, 8(7), 577. <https://doi.org/10.3390/horticulturae8070577>
- Palumbo, J. D., Yuen, G. Y., Jochum, C. C., Tatum, K., & Kobayashi, D. Y. (2005). Mutagenesis of β -1,3-glucanase genes in *lysobacter enzymogenes* strain c3 results in reduced biological control activity toward bipolaris leaf spot of tall fescue and pythium damping-off of sugar beet. *Phytopathology*, 95(6), 701–707. <https://doi.org/10.1094/PHTO-95-0701>
- Pandolfi, V., Jorge, E. C., Melo, C. M. R., Albuquerque, A. C. S., & Carrer, H. (2010). Gene expression profile of the plant pathogen *Fusarium graminearum* under the antagonistic effect of *Pantoea agglomerans*. *Genetics and Molecular Research*, 9(3), 1298–1311. <https://doi.org/10.4238/vol9-3gmr828>
- Parke, J. L. (1991). Biological control of pythium damping-off and aphanomyces root rot of peas by application of *Pseudomonas cepacia* or *p. Fluorescens* to seed. *Plant Disease*, 75(10), 987. <https://doi.org/10.1094/PD-75-0987>
- Peer, R., Kuik, A. J., Rattink, H., & Schippers, B. (1990). Control of Fusarium wilt in carnation grown on rockwool by *Pseudomonas sp.* Strain WCS417r and by Fe-EDDHA. *Netherlands Journal of Plant Pathology*, 96(3), 119–132. <https://doi.org/10.1007/BF01974251>
- Pérez-Varela, M., Corral, J., Aranda, J., & Barbé, J. (2018). Functional characterization of abaq, a novel efflux pump mediating quinolone resistance in *Acinetobacter baumannii*. *Antimicrobial Agents and Chemotherapy*, 62(9), e00906-18. <https://doi.org/10.1128/AAC.00906-18>
- Pertot, I., Alabouvette, C., Esteve, E. H., & Franca, S. (2015). Mini-paper—The use of microbial biocontrol agents against soil-borne diseases. *Eip-agri focus group soil-borne diseases*, 1-11. https://ec.europa.eu/eip/agriculture/sites/default/files/8_eip_sbd_mp_biocontrol_final.pdf
- Peter, S. C., Dhanjal, J. K., Malik, V., Radhakrishnan, N., Jayakanthan, M., Sundar, D., ... & Jayakanthan, M. (2019). Encyclopedia of bioinformatics and computational biology. *Ranganathan, S., Grib-skov, M., Nakai, K., Schönbach, C., Eds*, 661-676.
- Peters, R. D., & Grau, C. R. (2002). Inoculation with nonpathogenic *Fusarium solani* increases severity of pea root rot caused by *Aphanomyces euteiches*. *Plant Disease*, 86(4), 411–414. <https://doi.org/10.1094/PDIS.2002.86.4.411>
- Petrillo, C., Castaldi, S., Lanzilli, M., Selci, M., Cordone, A., Giovannelli, D., & Istitato, R. (2021). Genomic and physiological characterization of *Bacilli* isolated from salt-pans with plant growth promoting features. *Frontiers in Microbiology*, 12, 715678. <https://doi.org/10.3389/fmicb.2021.715678>
- Pieterse, C. M. J., Berendsen, R. L., de Jonge, R., Stringlis, I. A., Van Dijken, A. J. H., Van Pelt, J. A., Van Wees, S. C. M., Yu, K., Zamioudis, C., & Bakker, P. A. H. M. (2021).

- Pseudomonas simiae* WCS417: Star track of a model beneficial rhizobacterium. *Plant and Soil*, 461(1–2), 245–263. <https://doi.org/10.1007/s11104-020-04786-9>
- Pieterse, C. M. J., Zamioudis, C., Berendsen, R. L., Weller, D. M., Van Wees, S. C. M., & Bakker, P. A. H. M. (2014). Induced systemic resistance by beneficial microbes. *Annual Review of Phytopathology*, 52(1), 347–375. <https://doi.org/10.1146/annurev-phyto-082712-102340>
- Pieterse, C. M. J., Zamioudis, C., Berendsen, R. L., Weller, D. M., Van Wees, S. C. M., & Bakker, P. A. H. M. (2014). Induced systemic resistance by beneficial microbes. *Annual Review of Phytopathology*, 52(1), 347–375. <https://doi.org/10.1146/annurev-phyto-082712-102340x>
- Poplawsky, A. R., Urban, S. C., & Chun, W. (2000). Biological role of xanthomonadin pigments in *xanthomonas campestris* pv. *Campestris*. *Applied and Environmental Microbiology*, 66(12), 5123–5127. <https://doi.org/10.1128/AEM.66.12.5123-5127.2000>
- Puopolo, G., Raio, A., & Zoina, A. (2010). Identification and characterization of *Lysobacter capsici* strain PG4: a new plant health-promoting rhizobacterium. *Journal of Plant Pathology*, 157-164.
- Puopolo, G., Tomada, S., & Pertot, I. (2018). The impact of the omics era on the knowledge and use of *Lysobacter* species to control phytopathogenic micro-organisms. *Journal of Applied Microbiology*, 124(1), 15–27. <https://doi.org/10.1111/jam.13607>
- Puopolo, G., Tomada, S., Sonogo, P., Moretto, M., Engelen, K., Perazzolli, M., & Pertot, I. (2016). The *Lysobacter capsici* az78 genome has a gene pool enabling it to interact successfully with phytopathogenic microorganisms and environmental factors. *Frontiers in Microbiology*, 7. <https://doi.org/10.3389/fmicb.2016.00096>
- Pusey, P. L., Stockwell, V. O., & Rudell, D. R. (2008). Antibiosis and acidification by *Pantoea agglomerans* strain e325 may contribute to suppression of *Erwinia amylovora*. *Phytopathology*, 98(10), 1136–1143. <https://doi.org/10.1094/PHYTO-98-10-1136>
- Pusey, P. L., Stockwell, V. O., Reardon, C. L., Smits, T. H. M., & Duffy, B. (2011). Antibiosis activity of *Pantoea agglomerans* biocontrol strain e325 against *Erwinia amylovora* on apple flower stigmas. *Phytopathology*, 101(10), 1234–1241. <https://doi.org/10.1094/PHYTO-09-10-0253>
- Quail, M., Smith, M. E., Coupland, P., Otto, T. D., Harris, S. R., Connor, T. R., Bertoni, A., Swerdlow, H. P., & Gu, Y. (2012). A tale of three next generation sequencing platforms: Comparison of Ion torrent, pacific biosciences and illumina MiSeq sequencers. *BMC Genomics*, 13(1), 341. <https://doi.org/10.1186/1471-2164-13-341>
- Quainoo, S., Coolen, J. P. M., van Hijum, S. A. F. T., Huynen, M. A., Melchers, W. J. G., van Schaik, W., & Wertheim, H. F. L. (2017). Whole-genome sequencing of bacterial pathogens: The future of nosocomial outbreak analysis. *Clinical Microbiology Reviews*, 30(4), 1015–1063. <https://doi.org/10.1128/CMR.00016-17>

- Raaijmakers, J. M., & Mazzola, M. (2012). Diversity and natural functions of antibiotics produced by beneficial and plant pathogenic bacteria. *Annual Review of Phytopathology*, *50*(1), 403–424. <https://doi.org/10.1146/annurev-phyto-081211-172908>
- Rajagopal, L., Sundari, C. S., Balasubramanian, D., & Sonti, R. V. (1997). The bacterial pigment xanthomonadin offers protection against photodamage. *FEBS Letters*, *415*(2), 125–128. [https://doi.org/10.1016/S0014-5793\(97\)01109-5](https://doi.org/10.1016/S0014-5793(97)01109-5)
- Reddy, J.D. (2002). Pathogenicity and biological control ability of *Pseudomonas corrugata*. University of Idaho Available from ProQuest Dissertations & Theses Global. <https://www.proquest.com/docview/288068748/previewPDF/3FD631CF52B54CF7PQ/1?accountid=14739>. Retrieved October 14, 2021.
- Reza, M. M. (2017). Assessing the effect of siderophore producing bacteria for the iron nutrition in Lentil and Pea [Thesis dissertation, University of Saskatchewan], 1-130. <http://hdl.handle.net/10388/8147>
- Richardson, E. J., & Watson, M. (2013). The automatic annotation of bacterial genomes. *Briefings in Bioinformatics*, *14*(1), 1–12. <https://doi.org/10.1093/bib/bbs007>
- Risula, D. (2017). Lentils in Saskatchewan. Saskatchewan Ministry of Agriculture. <http://publications.gov.sk.ca/documents/20/86381-c5993bcc-009f-4031-b936-c52c992b9e7d.pdf>. Retrieved July 20, 2022.
- Robador, A., LaRowe, D. E., Finkel, S. E., Amend, J. P., & Neilson, K. H. (2018). Changes in microbial energy metabolism measured by nanocalorimetry during growth phase transitions. *Frontiers in Microbiology*, *9*, 109. <https://doi.org/10.3389/fmicb.2018.00109>
- Robideau, G. (2013). *Systematics and molecular pathogenesis of oomycetes with emphasis on flagellar genes* [Doctor of Philosophy, Carleton University], 1-154. <https://doi.org/10.22215/etd/2013-09733>
- Rocha, I., Ma, Y., Souza-Alonso, P., Vosátka, M., Freitas, H., & Oliveira, R. S. (2019). Seed coating: A tool for delivering beneficial microbes to agricultural crops. *Frontiers in Plant Science*, *10*, 1357. <https://doi.org/10.3389/fpls.2019.01357>
- Rollin-Pinheiro, R., Singh, A., Barreto-Bergter, E., & Del Poeta, M. (2016). Sphingolipids as targets for treatment of fungal infections. *Future Medicinal Chemistry*, *8*(12), 1469–1484. <https://doi.org/10.4155/fmc-2016-0053>
- Romanenko, V. M., & Alimov, D. M. (2000). [Ability of representatives of *Pantoea agglomerans*, as well as *Bacillus subtilis* and some *Pseudomonas* species to suppress the development of phytopathogenic bacteria and micromycetes in regulating plant growth]. *Mikrobiolohichnyi Zhurnal (Kiev, Ukraine: 1993)*, *62*(4), 29–37.
- Rosales, A. M., Vantomme, R., Swings, J., Ley, J., & Mew, T. W. (1993). Identification of some bacteria from paddy antagonistic to several rice fungal pathogens. *Journal of Phytopathology*, *138*(3), 189–208. <https://doi.org/10.1111/j.1439-0434.1993.tb01377.x>

- Rosenberg, M. S. (2000). MetaWin: Statistical software for meta-analysis ([Version] 2.0). Sinauer Associates. <http://library.wur.nl/WebQuery/clc/1730075>
- Rosenberg, M. S., Garrett, K. A., Su, Z., & Bowden, R. L. (2004). Meta-analysis in plant pathology: Synthesizing research results. *Phytopathology*, 94(9), 1013–1017. <https://doi.org/10.1094/PHYTO.2004.94.9.1013>
- Rowell, D. L. (1994). Soil science: methods and applications (p. 345). Harlow: Longman Group.
- Ruocco, M., Woo, S., Vinale, F., Lanzuise, S., & Lorito, M. (2011). Identified difficulties and conditions for field success of biocontrol. 2. Technical aspects: factors of efficacy. *Classical and augmentative biological control against diseases and pests: critical status analysis and review of factors*, 45. <https://hal.inrae.fr/hal-02809014>
- Ryu, J. Y., Kim, H. U., & Lee, S. Y. (2019). Deep learning enables high-quality and high-throughput prediction of enzyme commission numbers. *Proceedings of the National Academy of Sciences*, 116(28), 13996-14001. <https://doi.org/10.1073/pnas.1821905116>
- Safarieskandari, S., Chatterton, S., & Hall, L. M. (2021). Pathogenicity and host range of Fusarium species associated with pea root rot in Alberta, Canada. *Canadian Journal of Plant Pathology*, 43(1), 162-171. <https://doi.org/10.1080/07060661.2020.1730442>
- Safronovitz, B. (2011). Comparing growing media. *Practical Hydroponics and Greenhouses*, (117), 45-50.
- Saitou, N., & Nei, M. (1987). The neighbor-joining method: a new method for reconstructing phylogenetic trees. *Molecular biology and evolution*, 4(4), 406-425. <https://doi.org/10.1093/oxfordjournals.molbev.a040454>
- Salarizadeh, N., Hasannia, S., AKBARI, N. K., & HASSAN, S. R. (2014). Purification and characterization of 50 kDa extracellular metalloprotease from *Serratia* sp. ZF03.
- Samad, A., Brader, G., Pfaffenbichler, N., & Sessitsch, A. (2019). Plant-associated bacteria and the rhizosphere. In *Modern Soil Microbiology* (pp. 163-178). CRC Press.
- Samarzija, D., & Zamberlin, S. (2022). Psychrotrophic Bacteria: *Pseudomonas* spp. *Journal: Encyclopedia of Dairy Sciences*, 375-383.
- Sammer, U. F., Reiher, K., Spiteller, D., Wensing, A., & Völksch, B. (2012). Assessment of the relevance of the antibiotic 2-amino-3-(Oxirane-2,3-dicarboxamido) propanoyl-valine from *Pantoea agglomerans* biological control strains against bacterial plant pathogens. *MicrobiologyOpen*, 1(4), 438–449. <https://doi.org/10.1002/mbo3.43>
- Sanger, F., Nicklen, S., & Coulson, A. R. (1977). DNA sequencing with chain-terminating inhibitors. *Proceedings of the National Academy of Sciences*, 74(12), 5463–5467. <https://doi.org/10.1073/pnas.74.12.5463>

- Saskatchewan Pulse Grower (2017). Root rot in peas and lentils in western Canada. https://saskpulse.com/files/technical_documents/170418_Root_Rot_Brochure_v7_LR1.pdf. Retrieved September 21, 2021.
- Saskatchewan Pulse Growers (2019). Fusarium root rot in pulse crops. https://saskpulse.com/files/newsletters/191205_Fusarium_RR_-_short.pdf. Retrieved July 17, 2022.
- Sauvage, H., Moussart, A., Bois, F., Tivoli, B., Barray, S., & Laval, K. (2007). Development of a molecular method to detect and quantify *Aphanomyces euteiches* in soil. *FEMS Microbiology Letters*, 273(1), 64–69. <https://doi.org/10.1111/j.1574-6968.2007.00784.x>
- Scherlach, K., & Hertweck, C. (2021). Mining and unearthing hidden biosynthetic potential. *Nature Communications*, 12(1), 3864. <https://doi.org/10.1038/s41467-021-24133-5>
- Scott, K., Eyre, M., McDuffee, D., & Dorrance, A. E. (2020). The efficacy of ethaboxam as a soybean seed treatment toward *Phytophthora*, *Phytophthium*, and *Pythium* in ohio. *Plant Disease*, 104(5), 1421–1432. <https://doi.org/10.1094/PDIS-09-19-1818-RE>
- Shah, D. A., & Madden, L. V. (2004). Nonparametric analysis of ordinal data in designed factorial experiments. *Phytopathology*, 94(1), 33–43. <https://doi.org/10.1094/PHYTO.2004.94.1.33>
- Shariati J., V., Malboobi, M. A., Tabrizi, Z., Tavakol, E., Owlia, P., & Safari, M. (2017). Comprehensive genomic analysis of a plant growth-promoting rhizobacterium *Pantoea agglomerans* strain P5. *Scientific Reports*, 7(1), 15610. <https://doi.org/10.1038/s41598-017-15820-9>
- Shrestha, U., Augé, R. M., & Butler, D. M. (2016). A meta-analysis of the impact of anaerobic soil disinfection on pest suppression and yield of horticultural crops. *Frontiers in Plant Science*, 7. <https://doi.org/10.3389/fpls.2016.01254>
- Siddiqui, Z. A. (2006). Pgpr: Prospective biocontrol agents of plant pathogens. In Z. A. Siddiqui (Ed.), *PGPR: Biocontrol and Biofertilization* (pp. 111–142). Springer-Verlag. https://doi.org/10.1007/1-4020-4152-7_4
- Silby, M. W., Winstanley, C., Godfrey, S. A. C., Levy, S. B., & Jackson, R. W. (2011). *Pseudomonas* genomes: Diverse and adaptable. *FEMS Microbiology Reviews*, 35(4), 652–680. <https://doi.org/10.1111/j.1574-6976.2011.00269.x>
- Simmons, C. W., Reddy, A. P., Simmons, B. A., Singer, S. W., & VanderGheynst, J. S. (2014). Effect of inoculum source on the enrichment of microbial communities on two lignocellulosic bioenergy crops under thermophilic and high-solids conditions. *Journal of Applied Microbiology*, 117(4), 1025–1034. <https://doi.org/10.1111/jam.12609>
- Singh, P. P., Shin, Y. C., Park, C. S., & Chung, Y. R. (1999). Biological control of fusarium wilt of cucumber by chitinolytic bacteria. *Phytopathology*®, 89(1), 92–99. <https://doi.org/10.1094/PHYTO.1999.89.1.92>

- Sivachandra Kumar, N. T., Cox, L., Armstrong-Cho, C., & Banniza, S. (2020). Optimization of zoospore production and inoculum concentration of *Aphanomyces euteiches* for resistance screening of pea and lentil. *Canadian Journal of Plant Pathology*, 42(3), 419–428. <https://doi.org/10.1080/07060661.2019.1679888>
- Smith, D. D. N., Kirzinger, M. W. B., & Stavrinides, J. (2013). Draft genome sequence of the antibiotic-producing cystic fibrosis isolate *Pantoea agglomerans* tx10. *Genome Announcements*, 1(5), e00904-13. <https://doi.org/10.1128/genomeA.00904-13>
- Smolińska, U., & Kowalska, B. (2018). Biological control of the soil-borne fungal pathogen *Sclerotinia sclerotiorum* — a review. *Journal of Plant Pathology*, 100(1), 1–12. <https://doi.org/10.1007/s42161-018-0023-0>
- Song, H., Lin, K., Hu, J., & Pang, E. (2018). An updated functional annotation of protein-coding genes in the cucumber genome. *Frontiers in Plant Science*, 9, 325. <https://doi.org/10.3389/fpls.2018.00325>
- Spadaro, D., & Droby, S. (2016). Development of biocontrol products for postharvest diseases of fruit: The importance of elucidating the mechanisms of action of yeast antagonists. *Trends in Food Science & Technology*, 47, 39–49. <https://doi.org/10.1016/j.tifs.2015.11.003>
- Stanier, R. Y., Palleroni, N. J., & Doudoroff, M. (1966). The aerobic Pseudomonads a taxonomic study. *Journal of General Microbiology*, 43(2), 159–271. <https://doi.org/10.1099/00221287-43-2-159>
- Stewart, A. C., Osborne, B., & Read, T. D. (2009). DIYA: A bacterial annotation pipeline for any genomics lab. *Bioinformatics*, 25(7), 962–963. <https://doi.org/10.1093/bioinformatics/btp097>
- Stiling, P., & Cornelissen, T. (2005). What makes a successful biocontrol agent? A meta-analysis of biological control agent performance. *Biological Control*, 34(3), 236–246. <https://doi.org/10.1016/j.biocontrol.2005.02.017>
- Stringlis, I. A., Zhang, H., Pieterse, C. M. J., Bolton, M. D., & de Jonge, R. (2018). Microbial small molecules – weapons of plant subversion. *Natural Product Reports*, 35(5), 410–433. <https://doi.org/10.1039/C7NP00062F>
- Su, Z., Han, S., Fu, Z. Q., Qian, G., & Liu, F. (2018). Heat-stable antifungal factor (Hsaf) biosynthesis in *Lysobacter enzymogenes* is controlled by the interplay of two transcription factors and a diffusible molecule. *Applied and Environmental Microbiology*, 84(3), e01754-17. <https://doi.org/10.1128/AEM.01754-17>
- Sui, Y., Wisniewski, M., Droby, S., Piombo, E., Wu, X., & Yue, J. (2020). Genome sequence, assembly, and characterization of the antagonistic yeast *Candida oleophila* used as a biocontrol agent against post-harvest diseases. *Frontiers in Microbiology*, 11, 295. <https://doi.org/10.3389/fmicb.2020.00295>

- Sullivan, R. F., Holtman, M. A., Zylstra, G. J., White, J. F., & Kobayashi, D. Y. (2003). Taxonomic positioning of two biological control agents for plant diseases as *Lysobacter enzymogenes* based on phylogenetic analysis of 16S rDNA, fatty acid composition and phenotypic characteristics: Plant biocontrol *Lysobacter* strains. *Journal of Applied Microbiology*, *94*(6), 1079–1086. <https://doi.org/10.1046/j.1365-2672.2003.01932.x>
- Takami, H., Toyoda, A., Uchiyama, I., Itoh, T., Takaki, Y., Arai, W., Nishi, S., Kawai, M., Shinya, K., & Ikeda, H. (2017). Complete genome sequence and expression profile of the commercial lytic enzyme producer *Lysobacter enzymogenes* M497-1. *DNA Research*, *dsw055*. <https://doi.org/10.1093/dnares/dsw055>
- Tang, B., Zhao, Y.-C., Shi, X.-M., Xu, H.-Y., Zhao, Y.-Y., Dai, C.-C., & Liu, F.-Q. (2018). Enhanced heat stable antifungal factor production by *Lysobacter enzymogenes* OH11 with cheap feedstocks: Medium optimization and quantitative determination. *Letters in Applied Microbiology*, *66*(5), 439–446. <https://doi.org/10.1111/lam.12870>
- Tatusova, T., DiCuccio, M., Badretdin, A., Chetvernin, V., Nawrocki, E. P., Zaslavsky, L., Lomsadze, A., Pruitt, K. D., Borodovsky, M., & Ostell, J. (2016). NCBI prokaryotic genome annotation pipeline. *Nucleic Acids Research*, *44*(14), 6614–6624. <https://doi.org/10.1093/nar/gkw569>
- Thibaud-Nissen, F. (2022, January). NCBI tools for whole-genome annotation: How you can quickly add high-quality gene annotation to your bacterial and archaeal assemblies. In *Plant and Animal Genome XXIX Conference (January 8-12, 2022)*. PAG.
- Thiruvengadam, R., Gandhi, K., Vaithyanathan, S., Sankarasubramanian, H., Loganathan, K., Lingan, R., Rajagopalan, V. R., Muthurajan, R., Ebenezer Iyadurai, J., & Kuppasami, P. (2022). Complete genome sequence analysis of *Bacillus subtilis* bbv57, a promising biocontrol agent against phytopathogens. *International Journal of Molecular Sciences*, *23*(17), 9732. <https://doi.org/10.3390/ijms23179732>
- Thissera, B., Alhadrami, H. A., Hassan, M. H. A., Hassan, H. M., Behery, F. A., Bawazeer, M., Yaseen, M., Belbahri, L., & Rateb, M. E. (2020). Induction of cryptic antifungal pulicatin derivatives from *Pantoea agglomerans* by microbial co-culture. *Biomolecules*, *10*(2), 268. <https://doi.org/10.3390/biom10020268>
- Tiwari, N., Ahmed, S., Kumar, S., & Sarker, A. (2018). Fusarium wilt: A killer disease of lentil. In T. Askun (Ed.), *Fusarium—Plant Diseases, Pathogen Diversity, Genetic Diversity, Resistance and Molecular Markers*. InTech. <https://doi.org/10.5772/intechopen.72508>
- Ton, J., Pelt, J. A., Loon, L. C., & Pieterse, C. M. J. (2002). The *Arabidopsis* *isr1* locus is required for rhizobacteria-mediated induced systemic resistance against different pathogens. *Plant Biology*, *4*(2), 224–227. <https://doi.org/10.1055/s-2002-25738>
- Top Crop Manager, (2021). New management tools for *Aphanomyces*. <https://www.topcropmanager.com/new-management-tools-for-aphanomyces-21074/> Retrieved September 12, 2021.

- Van der Ent, S., Verhagen, B. W. M., Van Doorn, R., Bakker, D., Verlaan, M. G., Pel, M. J. C., Joosten, R. G., Proveniers, M. C. G., Van Loon, L. C., Ton, J., & Pieterse, C. M. J. (2008). *Myb72* is required in early signaling steps of rhizobacteria-induced systemic resistance in *Arabidopsis*. *Plant Physiology*, *146*(3), 1293–1304. <https://doi.org/10.1104/pp.107.113829>
- van Lenteren, J. C., Bolckmans, K., Köhl, J., Ravensberg, W. J., & Urbaneja, A. (2018). Biological control using invertebrates and microorganisms: Plenty of new opportunities. *BioControl*, *63*(1), 39–59. <https://doi.org/10.1007/s10526-017-9801-4>
- Van Rostenberghe, H., Noraida, R., Wan Pauzi, W. I., Habsah, H., Zeehaida, M., Rosliza, A. R., ... & Maimunah, H. (2006). The clinical picture of neonatal infection with *Pantoea* species. *Japanese Journal of Infectious Diseases*, *59*(2), 120. <https://doi.org/10.1007/s10526-017-9801-4>
- Vanderlinde, E. M., Harrison, J. J., Muszyński, A., Carlson, R. W., Turner, R. J., & Yost, C. K. (2010). Identification of a novel ABC transporter required for desiccation tolerance, and biofilm formation in *Rhizobium leguminosarum* bv. *Viciae* 3841. *FEMS Microbiology Ecology*, *71*(3), 327–340. <https://doi.org/10.1111/j.1574-6941.2009.00824.x>
- Vanneste, J. L., Cornish, D. A., Yu, J., & Voyle, M. D. (2002). The peptide antibiotic produced by *Pantoea agglomerans* eh252 is a microcin. *Acta Horticulturae*, *590*, 285–290. <https://doi.org/10.17660/ActaHortic.2002.590.42>
- Vanneste, J. L., Cornish, D. A., Yu, J., & Voyle, M. D. (2002). The peptide antibiotic produced by *Pantoea agglomerans* eh252 is a microcin. *Acta Horticulturae*, *590*, 285–290. <https://doi.org/10.17660/ActaHortic.2002.590.42>
- Vasilyeva, N. V., Shishkova, N. A., Marinin, L. I., Ledova, L. A., Tsfasman, I. M., Muranova, T. A., Stepnaya, O. A., & Kulaev, I. S. (2014). Lytic peptidase 15 of *Lysobacter* sp. X11 with broad antimicrobial spectrum. *Microbial Physiology*, *24*(1), 59–66. <https://doi.org/10.1159/000356838>
- Verbon, E. H., Liberman, L. M., Zhou, J., Yin, J., Pieterse, C. M. J., Benfey, P. N., Stringlis, I. A., & de Jonge, R. (2022). *Cell-type specific transcriptomics reveals roles for root hairs and endodermal barriers in interaction with beneficial rhizobacterium* [Preprint]. *Plant Biology*. <https://doi.org/10.1101/2022.05.09.491085>
- Vincent, J. M. (1970). A manual for the practical study of root-nodule bacteria. [Published for the International Biological Programme [by] Blackwell Scientific, 164. https://books.google.ca/books?id=dcQcAQAAIAAJ&source=gbs_ViewAPI&redir_esc=y
- Wakelin, S. A., Walter, M., Jaspers, M., & Stewart, A. (2002). Biological control of *Aphanomyces euteiches* root-rot of pea with spore-forming bacteria. *Australasian Plant Pathology*, *31*(4), 401. <https://doi.org/10.1071/AP02051>
- Wang, X., Zhou, H., Chen, H., Jing, X., Zheng, W., Li, R., Sun, T., Liu, J., Fu, J., Huo, L., Li, Y., Shen, Y., Ding, X., Müller, R., Bian, X., & Zhang, Y. (2018). Discovery of recombinases enables genome mining of cryptic biosynthetic gene clusters in *Burkholderiales* species.

Proceedings of the National Academy of Sciences, 115(18).
<https://doi.org/10.1073/pnas.1720941115>

- Wang, Y., Zhao, Y., Bollas, A., Wang, Y., & Au, K. F. (2021). Nanopore sequencing technology, bioinformatics and applications. *Nature Biotechnology*, 39(11), 1348–1365. <https://doi.org/10.1038/s41587-021-01108-x>
- Williamson-Benavides, B. A., & Dhingra, A. (2021). Understanding root rot disease in agricultural crops. *Horticulturae*, 7(2), 33. <https://doi.org/10.3390/horticulturae7020033>
- Willsey, T. L., Chatterton, S., Heynen, M., & Erickson, A. (2018). Detection of interactions between the pea root rot pathogens *Aphanomyces euteiches* and *Fusarium* spp. Using a multiplex qPCR assay. *Plant Pathology*, 67(9), 1912–1923. <https://doi.org/10.1111/ppa.12895>
- Wodzinski, R. S., Umholtz, T. E., Rundle, J. R., & Beer, S. V. (1994). Mechanisms of inhibition of *Erwinia amylovora* by *Erw. Herbicola* *in vitro* and *in vivo*. *Journal of Applied Bacteriology*, 76(1), 22–29. <https://doi.org/10.1111/j.1365-2672.1994.tb04410.x>
- Wright, S. A. I., Zumoff, C. H., Schneider, L., & Beer, S. V. (2001). *Pantoea agglomerans* strain eh318 produces two antibiotics that inhibit *Erwinia amylovora* *in vitro*. *Applied and Environmental Microbiology*, 67(1), 284–292. <https://doi.org/10.1128/AEM.67.1.284-292.2001>
- Wu, L., Chang, K.-F., Conner, R. L., Strelkov, S., Fredua-Agyeman, R., Hwang, S.-F., & Feindel, D. (2018). *Aphanomyces euteiches*: A threat to Canadian field pea production. *Engineering*, 4(4), 542–551. <https://doi.org/10.1016/j.eng.2018.07.006>
- Xie, H., Yang, C., Sun, Y., Igarashi, Y., Jin, T., & Luo, F. (2020). Pacbio long reads improve metagenomic assemblies, gene catalogs, and genome binning. *Frontiers in Genetics*, 11, 516269. <https://doi.org/10.3389/fgene.2020.516269>
- Xie, Y., Wright, S., Shen, Y., & Du, L. (2012). Bioactive natural products from *Lysobacter*. *Natural Product Reports*, 29(11), 1277. <https://doi.org/10.1039/c2np20064c>
- Xu, S. J., & Kim, B. S. (2014). Biocontrol of *Fusarium* crown and root rot and promotion of growth of tomato by *Paenibacillus* strains isolated from soil. *Mycobiology*, 42(2), 158–166. <https://doi.org/10.5941/MYCO.2014.42.2.158>
- Xu, S., Zhang, Z., Xie, X., Shi, Y., Chai, A., Fan, T., Li, B., & Li, L. (2022). Comparative genomics provides insights into the potential biocontrol mechanism of two *Lysobacter enzymogenes* strains with distinct antagonistic activities. *Frontiers in Microbiology*, 13, 966986. <https://doi.org/10.3389/fmicb.2022.966986>
- Xue, A. G. (2003). Efficacy of *Clonostachys rosea* strain ACM941 and fungicide seed treatments for controlling the root rot complex of field pea. *Canadian Journal of Plant Science*, 83(3), 519–524. <https://doi.org/10.4141/P02-078>

- Yamanaka, K., Oikawa, H., Ogawa, H., Hosono, K., Shinmachi, F., Takano, H., Sakuda, S., Beppu, T., & Ueda, K. (2005). Desferrioxamine E produced by *Streptomyces griseus* stimulates growth and development of *Streptomyces tanashiensis*. *Microbiology*, *151*(9), 2899–2905. <https://doi.org/10.1099/mic.0.28139-0>
- Yang, S.-Z., Feng, G.-D., Zhu, H.-H., & Wang, Y.-H. (2015). *Lysobacter mobilis* sp. Nov., isolated from abandoned lead-zinc ore. *International Journal of Systematic and Evolutionary Microbiology*, *65*(Pt 3), 833–837. <https://doi.org/10.1099/ij.s.0.000026>
- Yigit, F., & Dikilitas, M. (2007). Control of fusarium wilt of tomato by combination of *fluorescent Pseudomonas*, non-pathogen *Fusarium* and *Trichoderma harzianum* t-22 in greenhouse conditions. *Plant Pathology Journal*, *6*(2), 159–163. <https://doi.org/10.3923/ppj.2007.159.163>
- Yu, F., Zaleta-Rivera, K., Zhu, X., Huffman, J., Millet, J. C., Harris, S. D., Yuen, G., Li, X.-C., & Du, L. (2007). Structure and biosynthesis of heat-stable antifungal factor (HSAF), a broad-spectrum antimycotic with a novel mode of action. *Antimicrobial Agents and Chemotherapy*, *51*(1), 64–72. <https://doi.org/10.1128/AAC.00931-06>
- Yu, J., Blom, J., Glaeser, S. P., Jaenicke, S., Juhre, T., Rupp, O., Schwengers, O., Spänig, S., & Goesmann, A. (2017). A review of bioinformatics platforms for comparative genomics. Recent developments of the EDGAR 2.0 platform and its utility for taxonomic and phylogenetic studies. *Journal of Biotechnology*, *261*, 2–9. <https://doi.org/10.1016/j.jbiotec.2017.07.010>
- Yu, K., Stringlis, I. A., van Bentum, S., de Jonge, R., Snoek, B. L., Pieterse, C. M. J., Bakker, P. A. H. M., & Berendsen, R. L. (2021). Transcriptome signatures in *Pseudomonas simiae* wcs417 shed light on role of root-secreted coumarins in *Arabidopsis*-mutualist communication. *Microorganisms*, *9*(3), 575. <https://doi.org/10.3390/microorganisms9030575>
- Yuan, S., Wang, L., Wu, K., Shi, J., Wang, M., Yang, X., Shen, Q., & Shen, B. (2014). Evaluation of *Bacillus*-fortified organic fertilizer for controlling tobacco bacterial wilt in greenhouse and field experiments. *Applied Soil Ecology*, *75*, 86–94. <https://doi.org/10.1016/j.apsoil.2013.11.004>
- Yuan, Y., Chung, C. Y.-L., & Chan, T.-F. (2020). Advances in optical mapping for genomic research. *Computational and Structural Biotechnology Journal*, *18*, 2051–2062. <https://doi.org/10.1016/j.csbj.2020.07.018>
- Yuen, G. Y., Broderick, K. C., Jochum, C. C., Chen, C. J., & Caswell-Chen, E. P. (2018). Control of cyst nematodes by *Lysobacter enzymogenes* strain C3 and the role of the antibiotic HSAF in the biological control activity. *Biological Control*, *117*, 158–163. <https://doi.org/10.1016/j.biocontrol.2017.11.007>
- Yuen, G. Y., Jochum, C. C., Osborne, L. E., & Jin, Y. (2003). Biocontrol of Fusarium head blight in wheat by *Lysobacter enzymogenes* C3. *Phytopathology*, *93*, S93.

- Zaid, D. S., Cai, S., Hu, C., Li, Z., & Li, Y. (2022). Comparative genome analysis reveals phylogenetic identity of *Bacillus velezensis* hna3 and genomic insights into its plant growth promotion and biocontrol effects. *Microbiology Spectrum*, *10*(1), e02169-21. <https://doi.org/10.1128/spectrum.02169-21>
- Zhang, J., Du, L., Liu, F., Xu, F., Hu, B., Venturi, V., & Qian, G. (2014). Involvement of both PKS and NRPS in antibacterial activity in *Lysobacter enzymogenes* OH11. *FEMS Microbiology Letters*, *355*(2), 170–176. <https://doi.org/10.1111/1574-6968.12457>
- Zhang, P., Jiang, D., Wang, Y., Yao, X., Luo, Y., & Yang, Z. (2021). Comparison of de novo assembly strategies for bacterial genomes. *International Journal of Molecular Sciences*, *22*(14), 7668. <https://doi.org/10.3390/ijms22147668>
- Zhang, Z., & Yuen, G. Y. (2000). The role of chitinase production by *Stenotrophomonas maltophilia* strain c3 in biological control of *Bipolaris sorokiniana*. *Phytopathology*®, *90*(4), 384–389. <https://doi.org/10.1094/PHTO.2000.90.4.384>
- Zhang, Z., Yuen, G. Y., Sarath, G., & Penheiter, A. R. (2001). Chitinases from the plant disease biocontrol agent, *Stenotrophomonas maltophilia* c3. *Phytopathology*, *91*(2), 204–211. <https://doi.org/10.1094/PHTO.2001.91.2.204>
- Zhao, Y., Cheng, C., Jiang, T., Xu, H., Chen, Y., Ma, Z., Qian, G., & Liu, F. (2019). Control of wheat fusarium head blight by heat-stable antifungal factor (Hsaf) from *Lysobacter enzymogenes*. *Plant Disease*, *103*(6), 1286–1292. <https://doi.org/10.1094/PDIS-09-18-1517-RE>
- Zhao, Y., Wang, J., Chen, J., Zhang, X., Guo, M., & Yu, G. (2020). A literature review of gene function prediction by modeling gene ontology. *Frontiers in Genetics*, *11*, 400. <https://doi.org/10.3389/fgene.2020.00400>
- Zitnick-Anderson, K., Simons, K., & Pasche, J. S. (2018). Detection and qPCR quantification of seven *Fusarium* species associated with the root rot complex in field pea. *Canadian Journal of Plant Pathology*, *40*(2), 261–271. <https://doi.org/10.1080/07060661.2018.1429494>

APPENDIX A CHAPTER 3 SUPPLEMENTAL INFORMATION

Appendix A.1 Articles used for meta-analysis study

- Bazghaleh, N., Prashar, P., Woo, S. and Vandenberg, A., 2020. Effects of Lentil Genotype on the Colonization of Beneficial *Trichoderma* Species and Biocontrol of Aphanomyces Root Rot. *Microorganisms*, 8(9): 1290. Google Scholar
- Bødker, L., Kjølner, R. and Rosendahl, S., 1998. Effect of phosphate and the arbuscular mycorrhizal fungus *Glomus intraradices* on disease severity of root rot of peas (*Pisum sativum*) caused by *Aphanomyces euteiches*. *Mycorrhiza*, 8(3): 169-174. Web of Science®
- Bowers, J.H. and Parke, J.L., 1993. Epidemiology of Pythium damping-off and Aphanomyces root rot of peas after seed treatment with bacterial agents for biological control. *Phytopathology*, 83(12): 1466-1473. Web of Science®
- Dandurand, L.M. and Knudsen, G.R., 1993. Influence of *Pseudomonas fluorescens* on hyphal growth and biocontrol activity of *Trichoderma harzianum* in the spermosphere and rhizosphere of pea. *Phytopathology*, 83(3): 265-270. Google Scholar
- Dandurand, L.M., Mosher, R.D. and Knudsen, G.R., 2000. Combined effects of Brassica napus seed meal and *Trichoderma harzianum* on two soilborne plant pathogens. *Canadian journal of microbiology*, 46(11): 1051-1057. View Record in Scopus
- Godebo, A.T., Germida, J.J. and Walley, F.L., 2020. Isolation, identification, and assessment of soil bacteria as biocontrol agents of pea root rot caused by *Aphanomyces euteiches*. *Canadian Journal of Soil Science*, 100(3): 206-216. Google Scholar
- Heungens, K. and Parke, J.L., 2000. Zoospore homing and infection events: effects of the biocontrol bacterium *Burkholderia cepacia* AMMDR1 on two oomycete pathogens of pea (*Pisum sativum* L.). *Applied and Environmental Microbiology*, 66(12): 5192-5200. Web of Science®
- Heungens, K. and Parke, J.L., 2001. Postinfection biological control of oomycete pathogens of pea by *Burkholderia cepacia* AMMDR1. *Phytopathology*, 91(4): 383-391. Web of Science®
- Heungens, K.K., 1999. Pre-and post-infection interactions between the biocontrol agent *Burkholderia vietnamiensis* AMMDR1 and oomycete pathogens of pea. The University of Wisconsin-Madison. Google scholar
- Hilou, A., Zhang, H., Franken, P. and Hause, B., 2014. Do jasmonates play a role in arbuscular mycorrhiza-induced local bioprotection of *Medicago truncatula* against root rot disease caused by *Aphanomyces euteiches*?. *Mycorrhiza*, 24(1): 45-54. Web of Science®
- Hossain, S., Bergkvist, G., Berglund, K., Glinwood, R., Kabouw, P., Mårtensson, A. and Persson, P., 2014. Concentration-and time-dependent effects of isothiocyanates produced from

- Brassicaceae shoot tissues on the pea root rot pathogen *Aphanomyces euteiches*. *Journal of agricultural and food chemistry*, 62(20): 4584-4591. View Record in Scopus
- Hossain, S., Bergkvist, G., Glinwood, R., Berglund, K., Mårtensson, A., Hallin, S. and Persson, P., 2015. Brassicaceae cover crops reduce aphanomyces pea root rot without suppressing genetic potential of microbial nitrogen cycling. *Plant and Soil*, 392(1): 227-238. View Record in Scopus
- King, E.B. and Parke, J.L., 1993. Biocontrol of *Aphanomyces* root rot and *Pythium* damping-off by *Pseudomonas cepacia* AMMD on four pea cultivars. *Plant Disease*, 77(12): 1185-1188. Google Scholar
- Lagerlöf, J., Ayuke, F., Heyman, F. and Meijer, J., 2020. Effects of biocontrol bacteria and earthworms on *Aphanomyces euteiches* root-rot and growth of peas (*Pisum sativum*) studied in a pot experiment. *Acta Agriculturae Scandinavica, Section B—Soil & Plant Science*, 70(5): 427-436. View Record in Scopus
- Parke, J.L., Rand, R.E., Joy, A.E. and King, E.B., 1991. Biological control of *Pythium* damping-off and *Aphanomyces* root rot of peas by application of *Pseudomonas cepacia* or *P. fluorescens* to seed. *Plant Disease*, 75(10): 987-992. Web of Science®
- Reddy, J.D., 2002. Pathogenicity and biological control ability of *Pseudomonas corrugata*. University of Idaho. Google Scholar
- Slezack, S., Dumas-Gaudot, E., Paynot, M. and Gianinazzi, S., 2000. Is a fully established arbuscular mycorrhizal symbiosis required for bioprotection of *Pisum sativum* roots against *Aphanomyces euteiches*?. *Molecular Plant-Microbe Interactions*, 13(2): 238-241. View Record in Scopus
- Slezack, S., Dumas-Gaudot, E., Rosendahl, S., Kjøller, R., Paynot, M., Negrel, J. and Gianinazzi, S., 1999. Endoproteolytic activities in pea roots inoculated with the arbuscular mycorrhizal fungus *Glomus mosseae* and/or *Aphanomyces euteiches* in relation to bioprotection. *The New Phytologist*, 142(3): 517-529. View Record in Scopus
- Smolinska, U., Knudsen, G.R., Morra, M.J. and Borek, V., 1997. Inhibition of *Aphanomyces euteiches* f. sp. pisi by volatiles produced by hydrolysis of *Brassica napus* seed meal. *Plant disease*, 81(3): 288-292. Google Scholar
- Thygesen, K., Larsen, J. and Bødker, L., 2004. Arbuscular mycorrhizal fungi reduce development of pea root-rot caused by *Aphanomyces euteiches* using oospores as pathogen inoculum. *European Journal of Plant Pathology*, 110(4): 411-419. View Record in Scopus
- Wakelin, S.A., Walter, M., Jaspers, M. and Stewart, A., 2002. Biological control of *Aphanomyces euteiches* root-rot of pea with spore-forming bacteria. *Australasian Plant Pathology*, 31(4): 401-407. View Record in Scopus
- Walter, M., Frampton, C.M.A., Elmer, P.A.G. and Hill, R.A., 1995. Pathogenicity and control using composts of *Aphanomyces euteiches* pea root rot. In *Proceedings of the Forty Eighth*

New Zealand Plant Protection Conference, Angus Inn, Hastings, New Zealand, August 8-10, 1995. New Zealand Plant Protection Society. Google Scholar

Williams-Woodward, J.L., Pflieger, F.L., Fritz, V.A. and Allmaras, R.R., 1997. Green manures of oat, rape and sweet corn for reducing common root rot in pea (*Pisum sativum*) caused by *Aphanomyces euteiches*. Plant and soil, 188(1): 43-48. Google Scholar

Xue, A.G., 2003. Biological control of pathogens causing root rot complex in field pea using *Clonostachys rosea* strain ACM941. Phytopathology, 93(3): 329-335. View Record in Scopus

Table A. 1 Details on publications used in the meta-analysis (162 studies from 24 publication). Treatment means (Xt), Treatment sample size (nt), Control mean (Xc), Control sample size (nc), Treatment mean natural log (ln(Xt)), Control mean natural log (ln(Xc)), Response ratio natural log (lnR), natural log response ratio variance (Var(lnR)). Five moderator variables: Method of application: ((MoA): Suspension = Sus; Seadcoat = SC; Amendment = Ame; Plate assay = PA); Biocontrol agent richness: ((BAR): Single inoculation = SI; Mixed inoculation = MI), Biocontrol agent type: ((BAT): Bacteria = B; Fungus = F; Plant product = PP; Green Manure = GM; Compost = C; Earthworm = EW); Study scope: ((SS): Growth chamber = GC; Field = Field; Laboratory = Lab); and Reporting system: ((RS): Qualitative = Qual; Quantitative = Quan). Note: Sample size refers to the number of replicates used for the experimental analysis.

S/N	Publication	Xt	nt	Xc	nc	(ln(Xt))	(ln(Xc))	(lnR)	(VlnR)	MoA	BAR	BAT	SS	RS
1	Godebo et al. 2020	1.0	8.0	3.0	8.0	0.0	1.1	-1.1	0.3	Sus	SI	B	GC	Qual
2	Godebo et al. 2020	1.8	8.0	3.0	8.0	0.6	1.1	-0.5	0.3	Sus	SI	B	GC	Qual
3	Godebo et al. 2020	1.8	8.0	3.0	8.0	0.6	1.1	-0.5	0.3	Sus	SI	B	GC	Qual
4	Godebo et al. 2020	1.8	8.0	3.0	8.0	0.6	1.1	-0.5	0.3	Sus	SI	B	GC	Qual
5	Godebo et al. 2020	2.0	8.0	3.0	8.0	0.7	1.1	-0.4	0.3	Sus	SI	B	GC	Qual
6	Godebo et al. 2020	2.0	8.0	3.0	8.0	0.7	1.1	-0.4	0.3	Sus	SI	B	GC	Qual
7	Godebo et al. 2020	2.0	8.0	3.0	8.0	0.7	1.1	-0.4	0.3	Sus	SI	B	GC	Qual
8	Godebo et al. 2020	3.0	8.0	3.0	8.0	1.1	1.1	0.0	0.3	Sus	SI	B	GC	Qual
9	Godebo et al. 2020	3.0	8.0	3.0	8.0	1.1	1.1	0.0	0.3	Sus	SI	B	GC	Qual
10	Godebo et al. 2020	3.0	8.0	3.0	8.0	1.1	1.1	0.0	0.3	Sus	SI	B	GC	Qual
11	Godebo et al. 2020	1.5	8.0	3.0	8.0	0.4	1.1	-0.7	0.3	Sus	SI	B	GC	Qual
12	Godebo et al. 2020	1.8	8.0	3.0	8.0	0.6	1.1	-0.5	0.3	Sus	SI	B	GC	Qual
13	Godebo et al. 2020	1.8	8.0	3.0	8.0	0.6	1.1	-0.5	0.3	Sus	SI	B	GC	Qual
14	Godebo et al. 2020	1.8	8.0	3.0	8.0	0.6	1.1	-0.5	0.3	Sus	SI	B	GC	Qual
15	Godebo et al. 2020	2.0	8.0	3.0	8.0	0.7	1.1	-0.4	0.3	Sus	SI	B	GC	Qual
16	Godebo et al. 2020	2.0	8.0	3.0	8.0	0.7	1.1	-0.4	0.3	Sus	SI	B	GC	Qual
17	Godebo et al. 2020	2.5	8.0	3.0	8.0	0.9	1.1	-0.2	0.3	Sus	SI	B	GC	Qual
18	Godebo et al. 2020	3.0	8.0	3.0	8.0	1.1	1.1	0.0	0.3	Sus	SI	B	GC	Qual
19	Godebo et al. 2020	3.0	8.0	3.0	8.0	1.1	1.1	0.0	0.3	Sus	SI	B	GC	Qual
20	Godebo et al. 2020	3.0	8.0	3.0	8.0	1.1	1.1	0.0	0.3	Sus	SI	B	GC	Qual
21	Lagerlöf et akl. 2020	22.2	30.0	52.2	30.0	3.1	4.0	-0.9	0.1	SC	SI	B	GC	Quan
22	Lagerlöf et akl. 2020	1.7	30.0	52.2	30.0	0.5	4.0	-3.4	0.1	n/a	SI	EW	GC	Quan
23	Lagerlöf et akl. 2020	25.8	30.0	52.2	30.0	3.3	4.0	-0.7	0.1	n/a	MI	B+EW	GC	Quan
24	Bazghalel et al. 2020	0.5	3.0	4.4	3.0	-0.7	1.5	-2.2	0.7	PA	SI	F	GC	Quan

25	Hossain et al. 2015	0.3	4.0	0.4	4.0	-1.2	-1.0	-0.2	0.5	Ame	SI	PP	GC	Quan
26	Hossain et al. 2015	0.3	4.0	0.4	4.0	-1.4	-1.0	-0.4	0.5	Ame	SI	PP	GC	Quan
27	Hossain et al. 2015	0.1	4.0	0.4	4.0	-2.3	-1.0	-1.3	0.5	Ame	SI	PP	GC	Quan
28	Hossain et al. 2014	0.9	3.0	1.0	3.0	-0.1	0.0	-0.1	0.7	Ame	SI	PP	GC	Quan
29	Hossain et al. 2014	0.3	3.0	1.0	3.0	-1.4	0.0	-1.4	0.7	Ame	SI	PP	GC	Quan
30	Hossain et al. 2014	1.0	3.0	1.0	3.0	-0.1	0.0	-0.1	0.7	Ame	SI	PP	GC	Quan
31	Hilou 2014	0.0	3.0	0.0	3.0	-6.2	-5.3	-0.9	0.7	Sus	SI	F	GC	Quan
32	Hilou 2014	0.0	3.0	0.0	3.0	-6.9	-5.8	-1.1	0.7	Sus	SI	F	GC	Quan
33	Xue 2003	2.7	42.0	3.5	42.0	1.0	1.3	-0.3	0.0	SC	SI	B	Field	Qual
34	Xue 2003	2.7	42.0	3.5	42.0	1.0	1.3	-0.3	0.0	SC	SI	B	Field	Qual
35	Thygesen et al. 2003	0.6	5.0	1.0	5.0	-0.5	0.0	-0.5	0.4	Sus	SI	F	GC	Qual
36	Thygesen et al. 2003	0.8	5.0	1.0	5.0	-0.3	0.0	-0.3	0.4	Sus	SI	F	GC	Qual
37	Wakelin et al. 2002	1.0	25.0	1.2	25.0	0.0	0.2	-0.2	0.1	SC	SI	B	GC	Qual
38	Wakelin et al. 2002	1.8	25.0	1.2	25.0	0.6	0.2	0.4	0.1	SC	SI	B	GC	Qual
39	Wakelin et al. 2002	1.6	25.0	1.2	25.0	0.5	0.2	0.3	0.1	SC	SI	B	GC	Qual
40	Wakelin et al. 2002	1.4	25.0	1.2	25.0	0.3	0.2	0.2	0.1	SC	SI	B	GC	Qual
41	Wakelin et al. 2002	1.2	25.0	1.2	25.0	0.2	0.2	0.0	0.1	SC	SI	B	GC	Qual
42	Wakelin et al. 2002	1.0	25.0	1.2	25.0	0.0	0.2	-0.2	0.1	SC	SI	B	GC	Qual
43	Wakelin et al. 2002	1.0	25.0	1.2	25.0	0.0	0.2	-0.2	0.1	SC	SI	B	GC	Qual
44	Wakelin et al. 2002	0.8	25.0	1.2	25.0	-0.2	0.2	-0.4	0.1	SC	SI	B	GC	Qual
45	Wakelin et al. 2002	1.4	25.0	1.8	25.0	0.3	0.6	-0.3	0.1	SC	SI	B	GC	Qual
46	Wakelin et al. 2002	1.4	25.0	1.8	25.0	0.3	0.6	-0.3	0.1	SC	SI	B	GC	Qual
47	Wakelin et al. 2002	1.0	25.0	1.8	25.0	0.0	0.6	-0.6	0.1	SC	SI	B	GC	Qual
48	Wakelin et al. 2002	1.0	25.0	1.8	25.0	0.0	0.6	-0.6	0.1	SC	SI	B	GC	Qual
49	Wakelin et al. 2002	0.8	25.0	1.8	25.0	-0.2	0.6	-0.8	0.1	SC	SI	B	GC	Qual
50	Reddy 2002	3.8	90.0	4.0	90.0	1.3	1.4	0.0	0.0	SC	SI	B	GC	Qual
51	Reddy 2002	2.7	90.0	4.0	90.0	1.0	1.4	-0.4	0.0	SC	SI	B	GC	Qual
52	Reddy 2002	1.7	90.0	4.0	90.0	0.5	1.4	-0.9	0.0	SC	SI	B	GC	Qual
53	Reddy 2002	3.0	90.0	4.0	90.0	1.1	1.4	-0.3	0.0	SC	SI	B	GC	Qual
54	Reddy 2002	3.5	90.0	4.0	90.0	1.3	1.4	-0.1	0.0	SC	SI	B	GC	Qual
55	Reddy 2002	3.5	90.0	4.0	90.0	1.2	1.4	-0.1	0.0	SC	SI	B	GC	Qual

56	Reddy 2002	0.5	40.0	1.5	40.0	-0.7	0.4	-1.1	0.1	SC	SI	B	Field	Qual
57	Reddy 2002	0.3	40.0	1.5	40.0	-1.2	0.4	-1.6	0.1	SC	SI	B	Field	Qual
58	Reddy 2002	0.5	40.0	1.5	40.0	-0.7	0.4	-1.1	0.1	SC	SI	B	Field	Qual
59	Reddy 2002	1.0	40.0	1.5	40.0	-0.1	0.4	-0.4	0.1	SC	SI	B	Field	Qual
60	Reddy 2002	0.9	40.0	1.5	40.0	-0.1	0.4	-0.5	0.1	SC	SI	B	Field	Qual
61	Reddy 2002	1.2	40.0	1.2	40.0	0.2	0.2	0.0	0.1	SC	SI	B	Field	Qual
62	Reddy 2002	0.6	40.0	1.2	40.0	-0.5	0.2	-0.7	0.1	SC	SI	B	Field	Qual
63	Reddy 2002	1.5	40.0	1.2	40.0	0.4	0.2	0.2	0.1	SC	SI	B	Field	Qual
64	Reddy 2002	2.5	40.0	1.2	40.0	0.9	0.2	0.7	0.1	SC	SI	B	Field	Qual
65	Reddy 2002	2.9	40.0	1.2	40.0	1.0	0.2	0.8	0.1	SC	SI	B	Field	Qual
66	Reddy 2002	0.5	40.0	1.1	40.0	-0.8	0.1	-0.9	0.1	SC	SI	B	Field	Qual
67	Reddy 2002	0.3	40.0	1.1	40.0	-1.3	0.1	-1.4	0.1	SC	SI	B	Field	Qual
68	Reddy 2002	0.6	40.0	1.1	40.0	-0.6	0.1	-0.7	0.1	SC	SI	B	Field	Qual
69	Reddy 2002	0.6	40.0	1.1	40.0	-0.5	0.1	-0.6	0.1	SC	SI	B	Field	Qual
70	Reddy 2002	0.6	40.0	1.1	40.0	-0.5	0.1	-0.6	0.1	SC	SI	B	Field	Qual
71	Heungens and Parke 2000	0.9	32.0	0.9	32.0	-0.2	-0.1	-0.1	0.1	SC	SI	B	Lab	Quan
72	Heungens and Parke 2000	0.9	32.0	0.9	32.0	-0.1	-0.1	0.0	0.1	SC	SI	B	Lab	Quan
73	Heungens and Parke 2000	1.0	32.0	1.0	32.0	0.0	0.0	0.0	0.1	SC	SI	B	Lab	Quan
74	Heungens and Parke 2000	1.0	32.0	1.0	32.0	0.0	0.0	0.0	0.1	SC	SI	B	Lab	Quan
75	Heungens and Parke 2000	8615.0	20.0	21845.0	20.0	9.1	10.0	-0.9	0.1	SC	SI	B	Lab	Quan
76	Heungens and Parke 2000	20482.0	20.0	21845.0	20.0	9.9	10.0	-0.1	0.1	SC	SI	B	Lab	Quan
77	Heungens and Parke 2000	11947.0	30.0	20513.0	30.0	9.4	9.9	-0.5	0.1	Sus	SI	B	Lab	Quan
78	Heungens and Parke 2000	18080.0	30.0	20513.0	30.0	9.8	9.9	-0.1	0.1	Sus	SI	B	Lab	Quan
79	Slezack et al. 2000	1.9	9.0	3.4	9.0	0.6	1.2	-0.6	0.2	Sus	SI	F	GC	Qual
80	Slezack et al. 2000	3.2	9.0	3.4	9.0	1.2	1.2	-0.1	0.2	Sus	SI	F	GC	Qual
81	Slezack et al. 2000	3.0	9.0	3.0	9.0	1.1	1.1	0.0	0.2	Sus	SI	F	GC	Qual
82	Slezack et al. 2000	3.1	9.0	3.2	9.0	1.1	1.2	0.0	0.2	Sus	SI	F	GC	Qual
83	Slezack et al. 2000	0.1	9.0	0.1	9.0	-3.0	-2.2	-0.7	0.2	Sus	SI	F	GC	Quan
84	Slezack et al. 2000	0.1	9.0	0.1	9.0	-2.2	-2.1	-0.1	0.2	Sus	SI	F	GC	Quan
85	Slezack et al. 2000	0.1	9.0	0.1	9.0	-2.1	-2.2	0.1	0.2	Sus	SI	F	GC	Quan
86	Slezack et al. 2000	0.1	9.0	0.1	9.0	-2.2	-2.1	-0.1	0.2	Sus	SI	F	GC	Quan

87	Dandurand et al. 2000	0.0	10.0	3.1	10.0	-3.3	1.1	-4.4	0.2	SC	SI	F	GC	Qual
88	Dandurand et al. 2000	0.7	10.0	3.1	10.0	-0.4	1.1	-1.5	0.2	SC	SI	PP	GC	Qual
89	Dandurand et al. 2000	0.0	10.0	3.1	10.0	-3.3	1.1	-4.4	0.2	SC	MI	PP+F	GC	Qual
90	Dandurand et al. 2000	3.7	10.0	3.1	10.0	1.3	1.1	0.2	0.2	SC	SI	PP	GC	Qual
91	Dandurand et al. 2000	2.0	10.0	3.1	10.0	0.7	1.1	-0.4	0.2	SC	MI	PP+F	GC	Qual
92	Slezack et al. 1999	3.2	9.0	3.4	9.0	1.2	1.2	-0.1	0.2	Sus	SI	F	Lab	Qual
93	Slezack et al. 1999	1.0	9.0	1.6	9.0	0.0	0.5	-0.5	0.2	Sus	SI	F	Lab	Qual
94	Slezack et al. 1999	1.3	9.0	2.2	9.0	0.3	0.8	-0.5	0.2	Sus	SI	F	Lab	Qual
95	Slezack et al. 1999	2.0	9.0	2.6	9.0	0.7	1.0	-0.3	0.2	Sus	SI	F	Lab	Qual
96	Slezack et al. 1999	2.2	9.0	3.0	9.0	0.8	1.1	-0.3	0.2	Sus	SI	F	Lab	Qual
97	Slezack et al. 1999	0.1	9.0	0.1	9.0	-2.7	-2.5	-0.2	0.2	Sus	SI	F	Lab	Qual
98	Slezack et al. 1999	0.0	9.0	0.0	9.0	-3.4	-3.3	-0.2	0.2	Sus	SI	F	Lab	Qual
99	Slezack et al. 1999	0.0	9.0	0.1	9.0	-3.4	-2.4	-1.1	0.2	Sus	SI	F	Lab	Qual
100	Slezack et al. 1999	0.0	9.0	0.2	9.0	-3.1	-1.9	-1.3	0.2	Sus	SI	F	Lab	Qual
101	Slezack et al. 1999	0.1	9.0	0.2	9.0	-2.6	-1.9	-0.8	0.2	Sus	SI	F	Lab	Qual
102	Heungens 1999	60.3	100.0	57.2	100.0	4.1	4.0	0.1	0.0	SC	SI	B	Lab	Quan
103	Heungens 1999	60.8	100.0	57.2	100.0	4.1	4.0	0.1	0.0	SC	SI	B	Lab	Quan
104	Bodker 1998	0.8	5.0	1.0	5.0	-0.2	0.0	-0.2	0.4	Sus	SI	F	GC	Qual
105	Williams-Woodward et al. 1997	70.0	40.0	30.0	40.0	4.2	3.4	0.8	0.1	Ame	SI	GM	GC	Quan
106	Williams-Woodward et al. 1997	40.0	40.0	14.0	40.0	3.7	2.6	1.0	0.1	Ame	SI	GM	GC	Quan
107	Williams-Woodward et al. 1997	60.0	40.0	30.0	40.0	4.1	3.4	0.7	0.1	Ame	SI	GM	GC	Quan
108	Williams-Woodward et al. 1997	13.0	40.0	14.0	40.0	2.6	2.6	-0.1	0.1	Ame	SI	GM	GC	Quan
109	Williams-Woodward et al. 1997	40.0	40.0	30.0	40.0	3.7	3.4	0.3	0.1	Ame	SI	GM	GC	Quan
110	Williams-Woodward et al. 1997	13.0	40.0	14.0	40.0	2.6	2.6	-0.1	0.1	Ame	SI	GM	GC	Quan
111	Williams-Woodward et al. 1997	10.0	40.0	30.0	40.0	2.3	3.4	-1.1	0.1	Ame	SI	GM	GC	Quan
112	Williams-Woodward et al. 1997	14.0	40.0	14.0	40.0	2.6	2.6	0.0	0.1	Ame	SI	GM	GC	Quan
113	Williams-Woodward et al. 1997	8.0	40.0	30.0	40.0	2.1	3.4	-1.3	0.1	Ame	SI	GM	GC	Quan
114	Williams-Woodward et al. 1997	5.0	40.0	14.0	40.0	1.6	2.6	-1.0	0.1	Ame	SI	GM	GC	Quan
115	Williams-Woodward et al. 1997	4.0	40.0	30.0	40.0	1.4	3.4	-2.0	0.1	Ame	SI	GM	GC	Quan
116	Williams-Woodward et al. 1997	5.0	40.0	14.0	40.0	1.6	2.6	-1.0	0.1	Ame	SI	GM	GC	Quan
117	Williams-Woodward et al. 1997	16.0	40.0	30.0	40.0	2.8	3.4	-0.6	0.1	Ame	SI	GM	GC	Quan

118	Williams-Woodward et al. 1997	15.0	40.0	14.0	40.0	2.7	2.6	0.1	0.1	Ame	SI	GM	GC	Quan
119	Williams-Woodward et al. 1997	11.0	40.0	30.0	40.0	2.4	3.4	-1.0	0.1	Ame	SI	GM	GC	Quan
120	Williams-Woodward et al. 1997	9.0	40.0	14.0	40.0	2.2	2.6	-0.4	0.1	Ame	SI	GM	GC	Quan
121	Smolinska et al. 1997	0.8	60.0	1.6	60.0	-0.2	0.5	-0.7	0.0	Ame	SI	PP	GC	Qual
122	Smolinska et al. 1997	1.2	60.0	1.6	60.0	0.2	0.5	-0.3	0.0	Ame	SI	PP	GC	Qual
123	Smolinska et al. 1997	0.2	50.0	3.9	50.0	-1.6	1.4	-3.0	0.0	Ame	SI	PP	GC	Qual
124	Smolinska et al. 1997	0.9	50.0	3.9	50.0	-0.1	1.4	-1.5	0.0	Ame	SI	PP	GC	Qual
125	Walter et al. 1995	48.0	20.0	93.0	20.0	3.9	4.5	-0.7	0.1	Ame	MI	C	GC	Quan
126	Walter et al. 1995	65.0	20.0	93.0	20.0	4.2	4.5	-0.4	0.1	Ame	MI	C	GC	Quan
127	Walter et al. 1995	100.0	20.0	93.0	20.0	4.6	4.5	0.1	0.1	Ame	SI	C	GC	Quan
128	Walter et al. 1995	95.0	20.0	93.0	20.0	4.6	4.5	0.0	0.1	Ame	SI	C	GC	Quan
129	Walter et al. 1995	100.0	20.0	93.0	20.0	4.6	4.5	0.1	0.1	Ame	MI	C	GC	Quan
130	Walter et al. 1995	60.0	20.0	93.0	20.0	4.1	4.5	-0.4	0.1	Ame	MI	C	GC	Quan
131	Walter et al. 1995	56.0	20.0	93.0	20.0	4.0	4.5	-0.5	0.1	Ame	MI	C	GC	Quan
132	Walter et al. 1995	40.0	20.0	93.0	20.0	3.7	4.5	-0.8	0.1	Ame	MI	C	GC	Quan
133	Walter et al. 1995	95.0	20.0	93.0	20.0	4.6	4.5	0.0	0.1	Ame	SI	C	GC	Quan
134	King and Parke 1993	2.9	210.0	3.0	210.0	1.1	1.1	0.0	0.0	SC	SI	B	Field	Qual
135	King and Parke 1993	2.5	210.0	2.4	210.0	0.9	0.9	0.0	0.0	SC	SI	B	Field	Qual
136	King and Parke 1993	0.1	210.0	0.1	210.0	-2.3	-2.3	0.0	0.0	SC	SI	B	Field	Qual
137	King and Parke 1993	3.1	210.0	3.0	210.0	1.1	1.1	0.0	0.0	SC	SI	B	Field	Qual
138	King and Parke 1993	2.2	210.0	2.4	210.0	0.8	0.9	-0.1	0.0	SC	SI	B	Field	Qual
139	King and Parke 1993	0.2	210.0	0.2	210.0	-1.6	-1.6	0.0	0.0	SC	SI	B	Field	Qual
140	King and Parke 1993	2.1	210.0	2.2	210.0	0.7	0.8	0.0	0.0	SC	SI	B	Field	Qual
141	King and Parke 1993	1.5	210.0	1.6	210.0	0.4	0.5	-0.1	0.0	SC	SI	B	Field	Qual
142	King and Parke 1993	0.1	210.0	0.1	210.0	-2.3	-2.3	0.0	0.0	SC	SI	B	Field	Qual
143	King and Parke 1993	2.7	210.0	3.0	210.0	1.0	1.1	-0.1	0.0	SC	SI	B	Field	Qual
144	King and Parke 1993	2.3	210.0	2.2	210.0	0.8	0.8	0.0	0.0	SC	SI	B	Field	Qual
145	King and Parke 1993	0.2	210.0	0.1	210.0	-1.6	-2.3	0.7	0.0	SC	SI	B	Field	Qual
146	Bowers and Parke 1993	85.9	20.0	84.9	20.0	4.5	4.4	0.0	0.1	SC	SI	B	Field	Qual
147	Bowers and Parke 1993	76.5	20.0	84.9	20.0	4.3	4.4	-0.1	0.1	SC	SI	B	Field	Qual
148	Bowers and Parke 1993	72.7	20.0	84.9	20.0	4.3	4.4	-0.2	0.1	SC	SI	B	Field	Qual

149	Dandurand and Knudsen 1992	0.7	40.0	3.1	40.0	-0.4	1.1	-1.5	0.1	SC	SI	F	GC	Qual
150	Dandurand and Knudsen 1992	1.0	40.0	3.1	40.0	0.0	1.1	-1.1	0.1	SC	MI	F+B	GC	Qual
151	Dandurand and Knudsen 1992	1.1	40.0	3.1	40.0	0.1	1.1	-1.0	0.1	SC	MI	F+B	GC	Qual
152	Dandurand and Knudsen 1992	1.3	40.0	3.1	40.0	0.2	1.1	-0.9	0.1	SC	SI	B	GC	Qual
153	Dandurand and Knudsen 1992	2.9	40.0	3.1	40.0	1.1	1.1	-0.1	0.1	SC	SI	B	GC	Qual
154	Parke et al. 1991	2.9	25.0	3.0	25.0	1.1	1.1	0.0	0.1	SC	SI	B	Field	Qual
155	Parke et al. 1991	2.4	25.0	2.2	25.0	0.9	0.8	0.1	0.1	SC	SI	B	Field	Qual
156	Parke et al. 1991	3.6	25.0	3.8	25.0	1.3	1.3	-0.1	0.1	SC	SI	B	Field	Qual
157	Parke et al. 1991	2.9	25.0	3.0	25.0	1.1	1.1	0.0	0.1	SC	SI	B	Field	Qual
158	Parke et al. 1991	2.1	25.0	2.2	25.0	0.7	0.8	0.0	0.1	SC	SI	B	Field	Qual
159	Parke et al. 1991	3.7	25.0	3.8	25.0	1.3	1.3	0.0	0.1	SC	SI	B	Field	Qual
160	Parke et al. 1991	2.9	25.0	3.0	25.0	1.1	1.1	0.0	0.1	SC	SI	B	Field	Qual
161	Parke et al. 1991	2.5	25.0	2.2	25.0	0.9	0.8	0.1	0.1	SC	SI	B	Field	Qual
162	Parke et al. 1991	3.8	25.0	3.8	25.0	1.3	1.3	0.0	0.1	SC	SI	B	Field	Qual

APPENDIX B CHAPTER 4 SUPPLEMENTAL INFORMATION

Table B. 1 Disease score data for biocontrol assessment of root rot in field pea using vermiculite as a growing media in a growth chamber study

Treatment	Pathogen ^a	Disease level ^b			
		R1	R2	R3	R4
<i>L. capsici</i> K-Hf-H2	A. e	3	4	2	4
<i>P. simiae</i> K-Hf-L9	A. e	2	3	3	2
<i>P. agglomerans</i> PSV1-7	A. e	1	3	2	3
Negative control	Uninoculated	1	1	1	1
Positive control	A. e	4	2	5	3
<i>L. capsici</i> K-Hf-H2	A. e + F. a	4	4	4	4
<i>P. simiae</i> K-Hf-L9	A. e + F. a	3	3	3	4
<i>P. agglomerans</i> PSV1-7	A. e + F. a	3	3	4	3
Negative control	Uninoculated	1	1	1	1
Positive control	A. e + F. a	5	4	4	3
<i>L. capsici</i> K-Hf-H2	A. e + F. o	3	3	4	3
<i>P. simiae</i> K-Hf-L9	A. e + F. o	4	3	3	3
<i>P. agglomerans</i> PSV1-7	A. e + F. o	2	3	3	4
Negative control	Uninoculated	1	1	1	1
Positive control	A. e + F. o	4	4	3	3
<i>L. capsici</i> K-Hf-H2	F. a + F. o	2	3	3	3
<i>P. simiae</i> K-Hf-L9	F. a + F. o	3	2	3	3
<i>P. agglomerans</i> PSV1-7	F. a + F. o	2	2	2	3
Negative control	Uninoculated	1	1	1	1
Positive control	F. a + F. o	3	3	3	3
<i>L. capsici</i> K-Hf-H2	A. e + F. a + F. o	4	4	5	5
<i>P. simiae</i> K-Hf-L9	A. e + F. a + F. o	5	5	5	5
<i>P. agglomerans</i> PSV1-7	A. e + F. a + F. o	4	4	4	4
Negative control	Uninoculated	1	1	1	1
Positive control	A. e + F. a + F. o	5	5	5	5

^a Inoculated root rot pathogen: *A. euteiches* (A.e), *F. avenaceum* (F.a) and *F. oxysporum* (F.o); ^b Disease score based on a 1-7 rating scale: 1 (no disease), 2 (reddish-brown discoloration at point of seed attachment), 3 (Localized root/epicotyl lesions), 4 (Lesions encircle tap root/epicotyl), 5 (Extended epicotyl lesions), 6 (Lesions encircling the stem, < 2 cm long) and 7 (Lesions > 2 cm, decay of taproot/epicotyl).

Table B. 2 Disease score data for biocontrol assessment of root rot in lentil using vermiculite as a growing media in a growth chamber study

Treatment	Pathogen ^a	Disease level ^b			
		R1	R2	R3	R4
<i>L. capsici</i> K-Hf-H2	A. e	4	4	3	4
<i>P. simiae</i> K-Hf-L9	A. e	2	3	3	4
<i>P. agglomerans</i> PSV1-7	A. e	3	3	4	3
Negative control	Uninoculated	1	1	1	1
Positive control	A. e	4	4	4	5
<i>L. capsici</i> K-Hf-H2	A. e + F. a	4	4	4	3
<i>P. simiae</i> K-Hf-L9	A. e + F. a	4	4	4	4
<i>P. agglomerans</i> PSV1-7	A. e + F. a	4	4	4	4
Negative control	Uninoculated	1	1	1	1
Positive control	A. e + F. a	6	5	4	7
<i>L. capsici</i> K-Hf-H2	A. e + F. o	4	4	5	4
<i>P. simiae</i> K-Hf-L9	A. e + F. o	5	4	4	4
<i>P. agglomerans</i> PSV1-7	A. e + F. o	3	3	3	5
Negative control	Uninoculated	1	1	1	1
Positive control	A. e + F. o	4	4	5	5
<i>L. capsici</i> K-Hf-H2	F. a + F. o	4	3	3	2
<i>P. simiae</i> K-Hf-L9	F. a + F. o	3	3	4	3
<i>P. agglomerans</i> PSV1-7	F. a + F. o	3	2	4	3
Negative control	Uninoculated	1	1	1	1
Positive control	F. a + F. o	3	4	3	3
<i>L. capsici</i> K-Hf-H2	A. e + F. a + F. o	5	6	5	5
<i>P. simiae</i> K-Hf-L9	A. e + F. a + F. o	5	6	6	6
<i>P. agglomerans</i> PSV1-7	A. e + F. a + F. o	4	4	5	4
Negative control	Uninoculated	1	1	1	1
Positive control	A. e + F. a + F. o	5	6	6	6

^a Inoculated root rot pathogen: *A. euteiches* (A.e), *F. avenaceum* (F.a) and *F. oxysporum* (F.o); ^b Disease score based on a 1-7 rating scale: 1 (no disease), 2 (reddish-brown discoloration at point of seed attachment), 3 (Localized root/epicotyl lesions), 4 (Lesions encircle tap root/epicotyl), 5 (Extended epicotyl lesions), 6 (Lesions encircling the stem, < 2 cm long) and 7 (Lesions > 2 cm, decay of taproot/epicotyl).

Table B. 3 Disease score data for biocontrol assessment of root rot in field pea using non-sterile agricultural soil as a growing media in a growth chamber study

Treatment	Pathogen ^a	Disease level ^b			
		R1	R2	R3	R4
<i>L. capsici</i> K-Hf-H2	A. e	2	2	2	3
<i>P. simiae</i> K-Hf-L9	A. e	3	3	4	3
<i>P. agglomerans</i> PSV1-7	A. e	3	3	4	4
Negative control	Uninoculated	3	2	3	3
Positive control	A. e	4	5	5	6
<i>L. capsici</i> K-Hf-H2	A. e + F. a	3	3	3	2
<i>P. simiae</i> K-Hf-L9	A. e + F. a	4	4	4	5
<i>P. agglomerans</i> PSV1-7	A. e + F. a	4	4	4	5
Negative control	Uninoculated	3	2	3	3
Positive control	A. e + F. a	6	7	5	7
<i>L. capsici</i> K-Hf-H2	A. e + F. o	3	2	3	3
<i>P. simiae</i> K-Hf-L9	A. e + F. o	5	4	4	5
<i>P. agglomerans</i> PSV1-7	A. e + F. o	5	5	4	4
Negative control	Uninoculated	3	2	3	3
Positive control	A. e + F. o	5	5	6	6
<i>L. capsici</i> K-Hf-H2	F. a + F. o	2	1	2	3
<i>P. simiae</i> K-Hf-L9	F. a + F. o	3	2	2	2
<i>P. agglomerans</i> PSV1-7	F. a + F. o	2	2	1	3
Negative control	Uninoculated	3	2	3	3
Positive control	F. a + F. o	4	5	3	4
<i>L. capsici</i> K-Hf-H2	A. e + F. a + F. o	2	3	3	3
<i>P. simiae</i> K-Hf-L9	A. e + F. a + F. o	4	4	4	5
<i>P. agglomerans</i> PSV1-7	A. e + F. a + F. o	4	4	4	5
Negative control	Uninoculated	3	2	3	3
Positive control	A. e + F. a + F. o	5	7	5	7

^a Inoculated root rot pathogen: *A. euteiches* (A.e), *F. avenaceum* (F.a) and *F. oxysporum* (F.o); ^b Disease score based on a 1-7 rating scale: 1 (no disease), 2 (reddish-brown discoloration at point of seed attachment), 3 (Localized root/epicotyl lesions), 4 (Lesions encircle tap root/epicotyl), 5 (Extended epicotyl lesions), 6 (Lesions encircling the stem, < 2 cm long) and 7 (Lesions > 2 cm, decay of taproot/epicotyl).

Table B. 4 Disease score data for biocontrol assessment of root rot in lentil using non-sterile agricultural soil as a growing media in a growth chamber study

Treatment	Pathogen ^a	Disease level ^b			
		R1	R2	R3	R4
<i>L. capsici</i> K-Hf-H2	A. e	2	3	1	1
<i>P. simiae</i> K-Hf-L9	A. e	4	5	5	6
<i>P. agglomerans</i> PSV1-7	A. e	4	4	6	4
Negative control	Uninoculated	2	1	1	1
Positive control	A. e	6	7	6	6
<i>L. capsici</i> K-Hf-H2	A. e + F. a	3	3	3	3
<i>P. simiae</i> K-Hf-L9	A. e + F. a	7	7	5	6
<i>P. agglomerans</i> PSV1-7	A. e + F. a	7	7	5	6
Negative control	Uninoculated	2	1	1	1
Positive control	A. e + F. a	7	7	6	6
<i>L. capsici</i> K-Hf-H2	A. e + F. o	3	4	5	3
<i>P. simiae</i> K-Hf-L9	A. e + F. o	6	6	6	5
<i>P. agglomerans</i> PSV1-7	A. e + F. o	6	6	6	4
Negative control	Uninoculated	2	1	1	1
Positive control	A. e + F. o	7	7	6	6
<i>L. capsici</i> K-Hf-H2	F. a + F. o	2	1	2	1
<i>P. simiae</i> K-Hf-L9	F. a + F. o	3	4	4	5
<i>P. agglomerans</i> PSV1-7	F. a + F. o	4	4	4	5
Negative control	Uninoculated	2	1	1	1
Positive control	F. a + F. o	4	5	5	5
<i>L. capsici</i> K-Hf-H2	A. e + F. a + F. o	6	5	5	5
<i>P. simiae</i> K-Hf-L9	A. e + F. a + F. o	6	6	7	7
<i>P. agglomerans</i> PSV1-7	A. e + F. a + F. o	7	7	7	6
Negative control	Uninoculated	2	1	1	1
Positive control	A. e + F. a + F. o	7	7	7	6

^a Inoculated root rot pathogen: *A. euteiches* (A.e), *F. avenaceum* (F.a) and *F. oxysporum* (F.o); ^b Disease score based on a 1-7 rating scale: 1 (no disease), 2 (reddish-brown discoloration at point of seed attachment), 3 (Localized root/epicotyl lesions), 4 (Lesions encircle tap root/epicotyl), 5 (Extended epicotyl lesions), 6 (Lesions encircling the stem, < 2 cm long) and 7 (Lesions > 2 cm, decay of taproot/epicotyl).

Table B. 5 Disease score data for biocontrol assessment of aphanomyces root rot in lentil using vermiculite as a growing media in a growth chamber study

Treatment	Pathogen ^a	Disease level ^b			
		R1	R2	R3	R4
Positive control	<i>A. euteiches</i>	1	1	1	1
<i>L. gummosus</i> K-Be-H3	<i>A. euteiches</i>	1	1	1	1
<i>L. capsici</i> K-Hf-H2	<i>A. euteiches</i>	1	1	1	1
<i>B. cereus</i> K-CB2-6	<i>A. euteiches</i>	0	0	1	1
<i>R. lemnae</i> PCV1-13	<i>A. euteiches</i>	1	1	1	1
<i>R. lemnae</i> PSV1-9	<i>A. euteiches</i>	1	1	1	1
<i>S. plymuthica</i> DR1-2	<i>A. euteiches</i>	1	1	1	1
<i>L. antibioticus</i> K-CB2-4	<i>A. euteiches</i>	1	1	1	0
<i>P. agglomerans</i> PSV1-7	<i>A. euteiches</i>	1	1	0	0
<i>S. paradoxus</i> K-CB1-1	<i>A. euteiches</i>	0	0	1	1
<i>P. simiae</i> K-Hf-L9	<i>A. euteiches</i>	1	0	0	0
Negative control	Uninoculated	0	0	0	0

^a Inoculated root rot pathogen: *A. euteiches*; ^b Disease score based on 0-4 rating scale: 0 = No symptoms; roots healthy; 1 = Initial symptoms of root rot; discolouration. Light tan colour in sections of the root system; 2 = Discolouration of most or all the root system, small watery lesions may be present on the root and around the hypocotyl/epicotyl regions; 3 = Advanced disease symptoms, dwarfing of the plant and yellowing of the lower leaves. Extensive darkening and discolouration of the root system and extensive lesion formation; 4 = root entirely rotted / plant dead.

Table B. 6 Disease score data for biocontrol assessment of aphanomyces root rot in lentil using non-sterile agricultural soil as a growing media in a growth chamber study

Treatment	Pathogen ^a	Disease level ^b			
		R1	R2	R3	R4
Positive control	<i>A. euteiches</i>	4	4	3	3
<i>L. gummosus</i> K-Be-H3	<i>A. euteiches</i>	3	2	2	2
<i>L. capsici</i> K-Hf-H2	<i>A. euteiches</i>	2	3	3	3
<i>B. cereus</i> K-CB2-6	<i>A. euteiches</i>	2	2	3	4
<i>R. lemnae</i> PCV1-13	<i>A. euteiches</i>	3	3	3	3
<i>R. lemnae</i> PSV1-9	<i>A. euteiches</i>	3	3	3	2
<i>S. plymuthica</i> DR1-2	<i>A. euteiches</i>	3	3	3	3
<i>L. antibioticus</i> K-CB2-4	<i>A. euteiches</i>	2	3	3	3
<i>P. agglomerans</i> PSV1-7	<i>A. euteiches</i>	4	4	4	4
<i>S. paradoxus</i> K-CB1-1	<i>A. euteiches</i>	4	4	4	4
<i>P. simiae</i> K-Hf-L9	<i>A. euteiches</i>	3	3	3	2
Negative control	Uninoculated	3	3	3	2

^a Inoculated root rot pathogen: *A. euteiches*; ^b Disease score based on 0-4 rating scale: 0 = No symptoms; roots healthy; 1 = Initial symptoms of root rot; discolouration. Light tan colour in sections of the root system; 2 = Discolouration of most or all the root system, small watery lesions may be present on the root and around the hypocotyl/epicotyl regions; 3 = Advanced disease symptoms, dwarfing of the plant and yellowing of the lower leaves. Extensive darkening and discolouration of the root system and extensive lesion formation; 4 = root entirely rotted / plant dead.

```

data Lentil;
input Treat $ rep dis sub;
datalines;

;
run;
proc print data= Lentil;
run;
proc rank data= Lentil out= Lentil;
var dis;
ranks r;
run;
proc mixed data=Lentil anovaf;
title1 '1-way analysis using MIXED, with contrasts of Treatment';
class Treat;
model r = Treat / chisq ;
repeated / type=un(1) group= Treat;
lsmeans Treat / pdiff;
CONTRAST '5-1' Treat -1 1 0 0;
run;
title1 '1-way analysis using macro confidence interval';
%include '/home/u60047030/LD_CI.SAS';
options ls =100 ps= 1000 nodate nocenter nonumber;
%LD_CI(data=Lentil,group=Treat,var=dis, alpha=0.05, subject=sub);
run;

```

Macros for analysis are available from Dr. Edgar Brunner of the University of Gottingen, Germany. Websites: http://www.ams.med.uni-goettingen.de/Projekte/LD/Makros_LD.html or <http://www.ams.med.uni-goettingen.de/de/sof/ld/makros.html>

Figure B. 1 SAS code used to run non-parametric analysis on disease rating scale

APPENDIX C CHAPTER 5 SUPPLEMENTAL INFORMATION

Table C. 1 Protein encoding genes (pegs) of *Lysobacter capsici* K-Hf-H2 assigned to the subsystems category of Iron acquisition and metabolism (Siderophores), Carbohydrate metabolism (Chitin and Cellulose), Protein Degradation and according to the RAST version 2.0 server

Subsystem	Role	Features
Siderophores	Vibrioferrin PvsA	K-Hf-H2.peg.3327
	Vibrioferrin PvsC	K-Hf-H2.peg.3325
	Vibrioferrin PvsB	K-Hf-H2.peg.3326
	Vibrioferrin PvsE	K-Hf-H2.peg.3323
	Vibrioferrin PvsD	K-Hf-H2.peg.3324
Chitin and N-acetylglucosamine utilization	N-acetylglucosamine kinase	K-Hf-H2.peg.4419
	Chitin binding protein	K-Hf-H2.peg.35
	N-acetyl glucosamine NagP	K-Hf-H2.peg.4417
	N-Acetylglucosamine utilization GntR	K-Hf-H2.peg.4462
	Glucosamine-6-phosphate deaminase	K-Hf-H2.peg.4463
	N-acetylglucosamine NagX	K-Hf-H2.peg.890
	N-Acetylglucosamine utilization LacI	K-Hf-H2.peg.4455
	Beta-hexosaminidase	K-Hf-H2.peg.2176, K-Hf-H2.peg.2344, K-Hf-H2.peg.4422
Chitinase (EC 3.2.1.14)	K-Hf-H2.peg.129, K-Hf-H2.peg.2444, K-Hf-H2.peg.2445, K-Hf-H2.peg.3466, K-Hf-H2.peg.3468	
Cellulose utilization	Endoglucanase (EC 3.2.1.4); extracellular b-1,3-glucanases	K-Hf-H2.peg.855, K-Hf-H2.peg.1129, K-Hf-H2.peg.2843
	Alpha-1,2-mannosidase	K-Hf-H2.peg.64, K-Hf-H2.peg.2345, K-Hf-H2.peg.2739
Cyanophycin Metabolism	Cyanophycinase (EC 3.4.15.6)	K-Hf-H2.peg.625, K-Hf-H2.peg.4323
Putative TldE-TldD proteolytic complex	TldE protein	K-Hf-H2.peg.1388
	TldD family protein	K-Hf-H2.peg.2035, K-Hf-H2.peg.2037
	FIG138315: Putative alpha helix protein	K-Hf-H2.peg.1387
	TldD protein	K-Hf-H2.peg.1386
	TldE/PmbA family protein	K-Hf-H2.peg.2036
Protein degradation	Dipeptidyl carboxypeptidase Dcp	K-Hf-H2.peg.1632
	Asp-X dipeptidase	K-Hf-H2.peg.624, K-Hf-H2.peg.4324
	Isoaspartyl dipeptidase (EC 3.4.19.5)	K-Hf-H2.peg.624

	Extracellular zinc protease (EC 3.4.24.25)	K-Hf-H2.peg.414, K-Hf-H2.peg.1000, K-Hf-H2.peg.1958, K-Hf-H2.peg.1960, K-Hf-H2.peg.2429, K-Hf-H2.peg.2431
Metalloendopeptidases (EC 3.4.24.-)	Extracellular zinc protease (EC 3.4.24.26)	K-Hf-H2.peg.414, K-Hf-H2.peg.1000, K-Hf-H2.peg.1958, K-Hf-H2.peg.1960, K-Hf-H2.peg.2429, K-Hf-H2.peg.2431
	Microbial collagenase (EC 3.4.24.3)	K-Hf-H2.peg.998, K-Hf-H2.peg.4170
	Peptidase B (EC 3.4.11.23)	K-Hf-H2.peg.443
Aminopeptidases (EC 3.4.11.-)	Xaa-Pro aminopeptidase (EC 3.4.11.9)	K-Hf-H2.peg.3671
	Cytosol aminopeptidase PepA (EC 3.4.11.1)	K-Hf-H2.peg.696
Metallocoxypeptidases (EC 3.4.17.-)	D-alanyl-D-alanine coxypeptidase (EC 3.4.16.4)	K-Hf-H2.peg.421, K-Hf-H2.peg.2447, K-Hf-H2.peg.3036
Dipeptidases (EC 3.4.13.-)	Xaa-Pro dipeptidase PepQ (EC 3.4.13.9)	K-Hf-H2.peg.3665
Serine endopeptidase (EC 3.4.21.-)	Prolyl endopeptidase (EC 3.4.21.26)	K-Hf-H2.peg.375
	Lysyl endopeptidase (EC 3.4.21.50)	K-Hf-H2.peg.2087, K-Hf-H2.peg.3712
Omega peptidases (EC 3.4.19.-)	Isoaspartyl aminopeptidase (EC 3.4.19.5)	K-Hf-H2.peg.4324
Phosphate metabolism	Alkaline phosphatase (EC 3.1.3.1)	K-Hf-H2.peg.497, K-Hf-H2.peg.499, K-Hf-H2.peg.564, K-Hf-H2.peg.3177, K-Hf-H2.peg.3708, K-Hf-H2.peg.4097
Plant Hormones	Auxin biosynthesis (EC 4.2.1.20)	K-Hf-H2.peg.2488
	Auxin biosynthesis (EC 2.4.2.18)	K-Hf-H2.peg.622
	Auxin biosynthesis (EC 4.2.1.20)	K-Hf-H2.peg.2489
	Auxin biosynthesis (EC 5.3.1.24)	K-Hf-H2.peg.2490

Table C. 2 Protein encoding genes (pegs) of *Pseudomonas simiae* K-Hf-L9 assigned to the subsystems category of Iron acquisition and metabolism (Siderophores), Carbohydrate metabolism (Chitin) and Protein Degradation according to the RAST version 2.0 server.

Subsystem	Role	Features
Siderophore Pyoverdine	Pyoverdine PvdL	K-Hf-L9.peg.3945
	FIG049111: pyoverdin gene cluster	K-Hf-L9.peg.1903
	FpvI	K-Hf-L9.peg.1972, K-Hf-L9.peg.3581
	Pyoverdine PvdF	K-Hf-L9.peg.2287
	Pyoverdine PvdM	K-Hf-L9.peg.2290
	Pyoverdine PvdO	K-Hf-L9.peg.2288
	Pyoverdine	K-Hf-L9.peg.2283
	Pyoverdine PvdD	K-Hf-L9.peg.2284
	Pyoverdine PvdS	K-Hf-L9.peg.3947
	Pyoverdine PvdG	K-Hf-L9.peg.3946
	Pyoverdine PvdA (EC 1.13.12.-)	K-Hf-L9.peg.3580
	Pyoverdine PvdE	K-Hf-L9.peg.2286
	Pyoverdine PvdH (EC 2.6.1.76)	K-Hf-L9.peg.3937
	Pyoverdine PvdP	K-Hf-L9.peg.2291
Pyoverdine PvdN	K-Hf-L9.peg.2289	
Chitin and N-acetylglucosamine utilization	N-acetylglucosamine IIA, IIB, IIC (EC 2.7.1.69)	K-Hf-L9.peg.4600
	Glucosamine-6-phosphate deaminase	K-Hf-L9.peg.4598
	N-acetylglucosamine-6-phosphate deacetylase	K-Hf-L9.peg.4597
Putative TldE-TldD proteolytic complex	TldE protein	K-Hf-L9.peg.848
	FIG138315: alpha helix protein	K-Hf-L9.peg.847
	TldD protein	K-Hf-L9.peg.846
	TldD	K-Hf-L9.peg.5206
	TldE/PmbA	K-Hf-L9.peg.5207
Aminopeptidases (EC 3.4.11.-)	Xaa-Pro aminopeptidase (EC 3.4.11.9)	K-Hf-L9.peg.1922, K-Hf-L9.peg.5401
	Alanine aminopeptidase N (EC 3.4.11.2)	K-Hf-L9.peg.2431
	Cytosol aminopeptidase PepA (EC 3.4.11.1)	K-Hf-L9.peg.1022
Oligopeptidase A	Oligopeptidase A (EC 3.4.24.70)	K-Hf-L9.peg.49
Metalloprotease	Glutamate carboxypeptidase (EC 3.4.17.11)	K-Hf-L9.peg.3203 K-Hf-L9.peg.989, K-Hf-L9.peg.4176, K-Hf-L9.peg.4177, K-Hf-L9.peg.4940
	D-alanyl-D-alanine carboxypeptidase (EC 3.4.16.4)	K-Hf-L9.peg.4936
	Carboxypeptidase (EC 3.4.17.13)	K-Hf-L9.peg.4936

Table C. 3 Protein encoding genes (pegs) of *Pantoea agglomerans* PSV1-7 assigned to the subsystems category of Iron acquisition and metabolism (Siderophores), Carbohydrate metabolism (Chitin) and Protein Degradation according to the RAST version 2.0 server.

Subsystem	Role	Features
Siderophore Enterobactin	Siderophore (EC 1.3.1.28)	PSV1-7.peg.157
	Ferric enterobactin transport FepG (TC 3.A.1.14.2)	PSV1-7.peg.150
	Ferric enterobactin-bindin FepB (TC 3.A.1.14.2)	PSV1-7.peg.153
	Ferric enterobactin transport FepC (TC 3.A.1.14.2)	PSV1-7.peg.149
	2,3-dihydroxybenzoate (EC 2.7.7.58)	PSV1-7.peg.155
	Enterobactin exporter EntS	PSV1-7.peg.152
	Siderophore (EC 5.4.4.2)	PSV1-7.peg.154
	Apo-aryl carrier domain of EntB	PSV1-7.peg.156
	Siderophore (EC 3.3.2.1)	PSV1-7.peg.156
	Ferric enterobactin transport FepD (TC 3.A.1.14.2)	PSV1-7.peg.151
Chitin and N- acetylglucosamine utilization	N-acetylglucosamine- IIA, IIB, IIC (EC 2.7.1.69)	PSV1-7.peg.3187
	Glucosamine-6-phosphate deaminase (EC 3.5.99.6)	PSV1-7.peg.3189
	Beta-hexosaminidase (EC 3.2.1.52)	PSV1-7.peg.113, PSV1-7.peg.3093
	N-acetylglucosamine-6-phosphate deacetylase (EC 3.5.1.25)	PSV1-7.peg.3190
Putative TldE-TldD proteolytic complex	TldE protein	PSV1-7.peg.1027
	FIG138315: alpha helix protein	PSV1-7.peg.1026
	TldD protein	PSV1-7.peg.969
Protein degradation	Oligopeptidase A (EC 3.4.24.70)	PSV1-7.peg.746
	Dipeptidyl carboxypeptidase Dcp (EC 3.4.15.5)	PSV1-7.peg.2347
	Asp-X dipeptidase	PSV1-7.peg.3039
Aminopeptidases (EC 3.4.11.-)	Peptidase B (EC 3.4.11.23)	PSV1-7.peg.1463
	Xaa-Pro aminopeptidase (EC 3.4.11.9)	PSV1-7.peg.1216
	Alanine aminopeptidase N (EC 3.4.11.2)	PSV1-7.peg.2960
	Cytosol aminopeptidase PepA (EC 3.4.11.1)	PSV1-7.peg.91
Metallocooxypep tidases (EC 3.4.17.-)	D-alanyl-D-alanine carboxypeptidase (EC 3.4.16.4)	PSV1-7.peg.144, PSV1-7.peg.1839, PSV1-7.peg.3029, PSV1-7.peg.3214
	Carboxypeptidase (EC 3.4.17.13)	PSV1-7.peg.1323, PSV1-7.peg.2768
	Thermostable carboxypeptidase 1 (EC 3.4.17.19)	PSV1-7.peg.2286
Dipeptidases (EC 3.4.13.-)	Xaa-Pro dipeptidase PepQ (EC 3.4.13.9)	PSV1-7.peg.360
	Peptidase D (EC 3.4.13.3)	PSV1-7.peg.3439
	Peptidase E (EC 3.4.13.21)	PSV1-7.peg.365